ALPHA-INTEGRIN EXPRESSION AND FUNCTION MODIFY CHEMORESISTANCE AND IMMUNOGENICITY OF ACUTE LYMPHOBLASTIC LEUKEMIA

by

Chi-Chao Liu

BMLSc., The University of British Columbia, 2010

A THESIS SUBMITTED IN PARTIAL FULFILLMENT OF

THE REQUIREMENTS FOR THE DEGREE OF

DOCTOR OF PHILOSOPHY

in

THE FACULTY OF GRADUATE AND POSTDOCTORAL STUDIES

(Experimental Medicine)

THE UNIVERSITY OF BRITISH COLUMBIA

(Vancouver)

February 2017

Abstract

The overall survival rate for pediatric Acute Lymphoblastic Leukemia (ALL) is >85%, achieved mainly via multi-agent chemotherapy. However, therapeutic options remain limited for those experiencing relapse, thus understanding the causes for treatment failures remains an important priority. In this thesis, I investigate the underlying mechanisms that allow leukemic cells to escape chemotherapy. Specifically, I evaluate how integrin-mediated cell adhesion promotes tumor cell survival by increased pro-survival signaling, enhanced resistance to chemotherapeutics, and decreased presentation of immunogenic cell death (ICD) markers.

I show that T-lymphoblast adhesion via α4β1-integrin promotes chemoresistance to doxorubicin-induced apoptosis. Expression of α4δ, a tail-truncated α4-integrin with GFFKR as the cytoplasmic motif, promotes chemoresistance in a manner independent of integrin-mediated adhesion. The adhesion-independent chemoresistance is reproduced by expression of Tacδ, a non-integrin transmembrane receptor fused to the cytosolic GFFKR motif. Additionally, the GFFKR motif-mediated chemoresistance is associated with enhanced Akt activation, Ca^{2+} influx, and drug efflux.

GFFKR is a conserved motif found in α-integrins and previously shown to interact with calreticulin, a calcium-binding endoplasmic reticulum chaperone protein. I found that α4-calreticulin interaction was enhanced by cell adhesion, while α4δ-calreticulin interaction occurred in an adhesion-independent manner. Since cell surface calreticulin is a pro-phagocytic marker for cells undergoing ICD, the impact of integrin function on surface calreticulin in lymphoblasts treated with ICD-inducing agents was evaluated. Engagement of integrins via adhesion, or expression of the minimal GFFKR motif as α4δ or Tacδ, was sufficient to reduce the levels of surface calreticulin. Furthermore, surface calreticulin was also reduced for cells co-

treated with a β1-integrin activating antibody. The resulting integrin-mediated decrease in surface calreticulin significantly reduced engulfment of the target lymphoblasts by macrophages.

Calreticulin expression in lymphoblasts was nullified to assess its role in integrin-mediated chemoresistance. Chemosensitivity was partially restored in calreticulin-null Tacδ cells under non-adherent conditions, and in calreticulin-null wildtype cells under adherent conditions. The affect was partly attributed to calreticulin's role as a regulator of Ca^{2+} influx and drug efflux. Calreticulin was also implicated as a mediator of cytokine-dependent STAT proliferative signaling. This thesis provides evidence for integrin function and cell adhesion as a physiological pro-survival mediator for T-lymphoblasts.

Preface

The original hypothesis of this thesis, that the α4-integrin cytoplasmic tail impacts chemoresistance, was formulated by Dr. Chinten James Lim (CJL). I expanded and formulated the final hypothesis under the supervision of CJL.

A version of Chapter 3 has been published: **C.-C. Liu**, P. Leclair, S.Q. Yap, and C.J. Lim. 2013. The membrane-proximal KXGFFKR motif of alpha-integrin mediates chemoresistance. *Mol Cell Biol*. 33:4334-4345. CJL and I formulated the hypothesis and designed the experiments. I performed the experiments. CJL and I conducted the data analysis. Pascal Leclair (PL) and Shyong Quin Yap (SQY) facilitated the studies by making the recombinant protein substrates GST, GST-CS1, and GST-9.11 used for the cell adhesion assays. CJL and I wrote the manuscript.

A version of Chapter 4 has been published: **C.-C. Liu**, P. Leclair, M. Monajemi, L. Sly, G. Reid, and C.J. Lim. 2016. α-Integrin expression and function modulate presentation of cell surface calreticulin. *Cell Death & Disease*. 7:e2268. CJL and I formulated the hypothesis and designed the experiments. I performed the experiments. CJL and I conducted the data analysis and wrote the manuscript. PL made the recombinant protein substrates GST, GST-CS1 and GST-9.11, and the fluorescent conjugation of fibronectin, FITC-Fn. PL conducted the adhesion experiments shown in Figure 4.19. Mahdis Monajemi (MM) and Dr. Laura M. Sly (LMS) contributed murine-derived macrophages. Dr. Gregor S. Reid (GSR) contributed murine expanded patient samples. The primary human T-ALL cells, BD-53 and BD-67, were obtained from the BC Children's Hospital Biobank with ethics approval from the BC Women's and Children's Hospital institutional review board (H12-03216).

For Chapter 5, CJL and I formulated the hypothesis and designed the experiments. I performed the experiments. CJL and I conducted the data analysis.

Schematic illustration shown in Figure 6.2 was by CJL.

Table of Contents

List of Tables

List of Figures

List of Abbreviations

ABL	Abelson murine leukemia viral oncogene homolog 1
ADAM28	ADAM metallopeptidase domain 28
Akt	RAC-alpha serine/threonine-protein kinase
ALL	acute lymphoblastic leukemia
AML	acute myeloid leukemia
ATE1	arginyl-tRNA protein transferase 1
ATP	adenosine triphosphate
APS	ammonium persulfate
B-ALL	B-cell acute lymphoblastic leukemia
BAX	BCL2 associated X, apoptosis regulator
BCR	breakpoint cluster region protein
BiP	binding immunoglobulin protein
BK channel	big potassium channel
bp	base pair
BSA	bovine serum albumin
calcein-AM	calcein-acetoxymethyl ester
CALR	gene encoding calreticulin
CAMDR	cell adhesion mediated drug resistance
CAMKK	Ca^{2+}/calmodulin-dependent protein kinase kinase
CHO	Chinese hamster ovary cells
CIB	calcium and integrin binding protein

CMV	cytomegalovirus
CMV-IRES	cytomegalovirus-internal ribosome entry site
COG	Children's Oncology Group
CRISPR-Cas9	clustered regularly interspaced short palindromic repeats-CRISPR associated protein 9
Crk	CT10 (avian sarcoma virus) regulator of kinase
CRT	calreticulin
CS1	fibronectin connecting segment 1
DAMPs	damage-associated molecular patterns
Doxo	doxorubicin
EC_{50}	half maximal effective concentration
ECD	extracellular domain
ECM	extracellular matrix
EDTA	ethylenediaminetetraacetic acid
EGTA	ethylene glycol-bis(β-aminoethyl ether)-N,N,N',N'-tetraacetic acid
ER	endoplasmic reticulum
ERK	mitogen-activated protein kinase
ERp57	ER protein of 57-kDa
ETV6	E26 (leukemia virus) transformation-specific variant 6
FAK	focal adhesion kinase
FBS	fetal bovine serum
Fluo-4-AM	Fluo-4-acetoxymethyl ester
Fn	fibronectin

Fn9.11	fibronectin repeats 9 to 11
FOV	fields-of-view
GAPDH	glyceraldehyde-3-phosphate dehydrogenase
GFP	green fluorescent protein
gMFI	geometric mean fluorescence intensity
gp96	heat shock protein gp96
GR	glucocorticoid receptor
GSH-sepharose	glutathione sepharose
GST	glutathione *S*-transferase
HMGB1	high mobility group box 1
HSP27	heat shock protein beta-1
HSP70	heat shock protein 70-kDa
HSP90	heat shock protein 90-kDa
ICAM-1	intercellular adhesion molecule 1
ICD	immunogenic cell death
IFNAR	interferon-α/β receptor
IgG	Immunoglobulin G
ILK	integrin linked kinase
IMDM	Iscove's Modified Dulbecco's Medium
IP	immunoprecipitation
IR-dye	infrared dyes
JAK	Janus kinase
JAK2	Janus kinase 2

KDEL	ER retention sequence, Lysine-Aspartic Acid-Glutamic Acid-Leucine
LFA-1	lymphocyte function-associated antigen 1
LPAM-1	lymphocyte Peyer's patch adhesion molecule 1
LRP1	low-density lipoprotein receptor related protein 1
MAdCAM-1	mucosal vascular addressin cell adhesion molecule 1
MEK	mitogen-activated protein kinase kinase
MCSF	macrophage colony-stimulating factor
MDGI	mammary-derived growth inhibitor
MFI	median fluorescent intensity
MPL	myeloproliferative leukemia virus oncogene
MPNs	myeloproliferative neoplasms
MRD	minimal residual disease
MRP1	multidrug resistance-associated protein 1
Mss4	guanine nucleotide exchange factor MSS4
NES	nuclear export signal
NMR	nuclear magnetic resonance
NSG	NOD-scid/IL-2Rγ null
Oxa	oxaliplatin
PBS	phosphate-buffered saline
PCR	polymerase chain reaction
PDI	protein disulfide-isomerase
PDT	photodynamic therapy
PI3K	phosphatidylinositol-4,5-bisphosphate 3-kinase

PKI	protein kinase inhibitor
PS	phosphatidylserine
RanGTP	GTP-binding nuclear protein Ran
RNA	ribonucleic acid
ROS	reactive oxygen species
RPMI	Roswell Park Memorial Institute medium
RUNX1	runt related transcription factor 1
SDS-PAGE	sodium dodecyl sulfate polyacrylamide gel electrophoresis
SIRP-α	tyrosine-protein phosphatase non-receptor type substrate 1
Src	proto-oncogene tyrosine-protein kinase Src
STAT	signal transducer and activator of transcription
T-ALL	T-cell acute lymphoblastic leukemia
THBS	Thrombospondin
TLR2	Toll-like receptor 2
TLR4	Toll-like receptor 4
TMD	transmembrane domain
tRNA	transfer ribonucleic acid
TSP1	thrombospondin 1
type-I PKA	cAMP-dependent protein kinase type I-alpha regulatory subunit
VCAM-1	vascular cell adhesion molecule 1
VLA-4	very late antigen 4
Wnt	protein wnt
14-3-3 zeta	14-3-3 protein zeta

Acknowledgements

I owe particular thanks to Dr. Chinten James Lim, who not only supported my training with his grant for over six years but also provided guidance in my research and an enormous amount of aid in my writings and presentations.

I thank my supervisory committee members: Dr. Catherine Pallen, Dr. Kirk Schultz, and Dr. Gregor Reid, who have spent their valuable time attending my committee meetings, offering constructive advice and evaluating my progress.

I offer my enduring gratitude to my fellow students in the UBC Experimental Medicine program, who have inspired me to continue my work in this field. I also thank Pascal Leclair and Eva Yap who were always there to provide me with experimental materials.

Thanks to the Michael Cuccione Foundation, who provided two years of graduate studentship support and other travel-related awards.

I also thank my fiancée, Shiny Sachdeva for always being there. Ph.D. training is a long process; I thank her for being patient with me.

Special thanks are owed to my parents, Cliff Liu and Nancy Wu, who have supported me throughout my years of education, both morally and financially.

Thank you all very much!

Dedication

Dedicated in memory of my grandfather,

Cheng Xi Liu

Chapter 1: Introduction

1.1 Acute Lymphoblastic Leukemia

Acute Lymphoblastic Leukemia (ALL) is an acute malignancy of the leukocytes, characterized by the overproduction and accumulation of lymphoblasts (Board, 2016; Inaba et al., 2013; Pui et al., 2004). In patients with ALL, lymphoblasts are overproduced in the bone marrow, causing damage and eventual death by inhibiting the production of normal hematopoietic cells in the bone marrow and by metastatic infiltration into other organs (Board, 2016; Inaba et al., 2013; Pui et al., 2004). Although relatively rare in occurrence, ALL can be seen across all adult age groups, with increased incidence in the elderly (Ward et al., 2014). Constituting 25% of all childhood cancers, ALL is the most prevalent form of pediatric malignancy with a peak incidence occurring in ages between 2 to 5 years old (Graubert et al., 2013; Pui et al., 2004; Ward et al., 2014).

ALL can be classified based on the lineage of lymphocytes into T-cell (T-ALL) or B-cell ALL (B-ALL) (Matloub et al., 2004). Approximately 80% of pediatric ALL is B-ALL (also known as precursor B-lineage ALL, or pre-B ALL), with T-ALL constituting the remainder. Generally, children with T-ALL have a poorer prognosis than those with B-ALL and thus require more intense treatments (Matloub et al., 2004).

The symptoms of ALL can include fever and increased risk of infection due to neutropenia, increased tendency to bleed due to thrombocytopenia, and signs of anemia, including pallor, tachycardia, fatigue, and headache (Chessells, 2001; Margolin et al., 1997; Onciu, 2009). All of these are indicative of a reduced production of functional blood cells because overexpansion of malignant lymphoblasts occupies resources in the bone marrow that

are normally used to produce functioning blood cells (Chessells, 2001; Margolin et al., 1997; Onciu, 2009).

Tests and examinations used to detect and diagnose ALL may include patient history, physical exam, differential complete blood count, blood chemistry and bone marrow aspiration (Chessells, 2001; Margolin et al., 1997; Onciu, 2009). Cytogenetic analysis and immunophenotyping can then be used to determine the exact subtype of the ALL such as Philadelphia chromosome or if this ALL belongs to the T or B cell lineage (Chessells, 2001; Margolin et al., 1997; Onciu, 2009). Similarly, spinal tap, chest x-ray, and testicular biopsy can be used to check if ALL has metastasized to these regions (Chessells, 2001; Margolin et al., 1997; Onciu, 2009).

Dramatic improvements in survival have been achieved in the treatment of pediatric ALL over the past few decades; the 5-year survival rate has risen to approximately 90% for children younger than 15 years (Hunger et al., 2012). However, acquired drug resistance remains a key obstacle to the successful treatment of the remaining 10% (Park, 2014). The treatment of patients with relapsed ALL remains unsatisfactory, with suboptimal remission rates and poor long-term overall survival rates ranging from 15-50%, depending on prognosis stratification of the relapsed ALL (Nguyen et al., 2008). Survivors of childhood ALL face a lifetime of health uncertainties, typically as a result of the long lasting side effects of the strong chemotherapeutic regimen (Graubert et al., 2013; Park, 2014). For example, high cumulative doxorubicin dosage required to treat high-risk ALL significantly increases the risk of heart failure in patients (Octavia et al., 2012). Similarly, treatment for ALL may cause infertility and delayed puberty (Pakakasama et al., 2010; Schultz et al., 2014).

There remains an important need to find more effective treatment options with less severe side-effects for childhood ALL. The work outlined in this thesis aims to understand the underlying mechanisms that allow ALL cells to resist chemotherapeutic treatment. Such mechanistic insights may facilitate the design of targeted therapies able to circumvent acquired chemoresistance and lower the toxicity to healthy tissues. This thesis focuses on investigating the function of α-integrins and its impact on chemoresistance and immunogenicity of T-acute lymphoblastic leukemia. All of the experiments described in this thesis were carried out using either established T-ALL cell lines or mouse-expanded T-ALL patient samples.

1.1.1 Treatment of ALL

The intensity of treatment required for favorable outcome varies substantially among subsets of ALL (Board, 2016). A risk-stratified assignment is utilized so that patients with favorable clinical and biological features, indicative of a good prognosis, can be spared from more intensive and toxic treatments, while a more aggressive and potentially more toxic therapeutic approach can be adopted for patients with unfavorable prognosis (Corrigan and Feig, 2004; Howlader et al., 2013; Smith et al., 2014).

Treatment of ALL can be grossly categorized into three phases consisting of remission induction, consolidation and maintenance phases. During the first phase, remission induction, patients receive a high dose of a chemotherapeutic cocktail in an attempt to get rid of as many leukemia cells as possible (Board, 2016). This typically brings the patients into disease remission. Minimal residual disease (MRD), a clinical determination of the percentage of detectable malignant lymphoblasts in a bone marrow aspirate, is also measured to further determine patient prognosis and the risk of relapse (Board, 2016; Borowitz et al., 2008). Typical

treatment regimens include vincristine, dexamethasone, prednisone, 6-mercaptopurine, methotrexate, daunorubicin, doxorubicin, cytarabine, asparaginase, and 6-thioguanine (Board, 2016). Certain ALL study groups, such as the Children's Oncology Group (COG), select different induction regimens based on a subset of pretreatment factors. Factors used by the COG to determine the intensity of induction include immunophenotype, age and white blood cell count (Smith et al., 2014). Generally, patients with B-cell immunophenotype, younger age, and lower white blood cell count have a better prognosis. Importantly, high-risk ALL subtypes such as T-ALL may receive higher dosing of anthracyclines such as doxorubicin or daunorubicin (Board, 2016). Philadelphia chromosome-positive (*BCR/ABL* fusion gene positive) ALL patients may receive imatinib or dasatinib, both of which are BCR/ABL tyrosine kinase inhibitor, as part of the treatment (Aricò et al., 2010; Schultz et al., 2009).

Once complete remission has been achieved, the treatment of ALL enters the second phase, known as consolidation or intensification, where the goal is to eradicate any leukemia cells that remain in the body that may cause a relapse (Board, 2016; Smith et al., 2014). Several cycles of intensive chemotherapy are given over a six- to nine-month period (Board, 2016). This phase of treatment typically includes methotrexate or doxorubicin (Schultz et al., 2007). An allogeneic bone marrow transplant is usually recommended to patients classified as very high risk at this phase (Board, 2016).

Phase three of the treatment is maintenance, where the goal is to maintain a lower dose of chemotherapeutics in the patients' system to eliminate remaining leukemia cells and further minimize the risk of relapse (Board, 2016). Methotrexate, 6-mercaptopurine, vincristine and pulses of steroids are typically used in this phase of treatment (Board, 2016; Sirvent et al., 2011; te Loo et al., 2006).

Sophisticated decision trees have been developed for the treatment of ALL (Board, 2016). The three phases discussed above are a generalization of treatment procedures. Treatment failure at phase 1 or 2 typically results in a shift to more intensive regimens and increased treatment duration. Treatment failure at phase 3 results in the reinitiating of treatment with a more aggressive approach. As the remission rate of lower-risk pediatric ALL such as B-ALL approaches 98%, chemoresistant relapses and high risk ALL such as T-ALL become the biggest hurdle to overcome in the treatment of pediatric ALL (Board, 2016).

1.2 Hallmarks of Cancer

There are ten hallmarks of cancer; each of them distinctive and complementary capabilities that enable tumor growth and metastatic dissemination (Figure 1.1) (Hanahan and Weinberg, 2011). Six of these hallmarks; *sustaining proliferative signaling*, *evading growth suppressors*, *resisting cell death*, *enabling replicative immortality*, *inducing angiogenesis*, and *activating invasion and metastasis*, were originally proposed in Hanahan and Weinberg's 2000 publication (Hanahan and Weinberg, 2000). Two new enabling hallmarks underlie the six originally proposed ones. These are *genome instability and mutation* that increase the chance and rate at which normal cells acquire genetic abnormalities and thus provide the foundation for the emergence of other hallmarks; and *tumor-promoting inflammation* that promotes multiple hallmark functions such as fostering angiogenesis, providing enhanced proliferative signaling and promoting invasiveness (Hanahan and Weinberg, 2011). The 2011 update also added two new emerging hallmarks: *deregulating cellular energetics* and *avoiding immune destruction* (Hanahan and Weinberg, 2011). Deregulating cellular energetics involves the capacity to change cellular metabolism to support abnormal proliferation. Avoiding immune destruction allows the

cancer cells to avoid detection and evade immunological destruction by T cells, B cells, macrophages and natural killer cells (Hanahan and Weinberg, 2011).

As a malignancy of the bone marrow, ALL is no exception — meaning that the tumor exhibits hallmark characteristics such as an unusually active JAK/STAT pathway that gives rise to sustained proliferative signaling (Harvey et al., 2010; Mullighan et al., 2009) and, p53 mutation and telomerase expression which enable the cancer cells to achieve genome instability and replicative immortality (Broccoli et al., 1995; Findley et al., 1997; Imai et al., 2004; Prokop et al., 2000; Zhou et al., 2002).

The ETV6/RUNX1 fusion gene, found in 25% of pediatric B-ALL cases, is one of the most prevalent genetic mutations in ALL (Mullighan et al., 2007; Papaemmanuil et al., 2014). As ETV6 functions as a transcription factor, it is no surprise that this fusion gene product acts by targeting the promoters and enhancers of genes that normally regulate lymphocyte differentiation, leading to leukemia (Papaemmanuil et al., 2014). A t(9;22) translocation occurs in 2 - 10% of childhood acute lymphoblastic leukemia patients (Chissoe et al., 1995; Clark et al., 1987). It is more commonly known as the Philadelphia chromosome that creates the BCR/ABL fusion gene (Chissoe et al., 1995; Clark et al., 1987). The gene product encodes a constitutively active tyrosine kinase that is important in JAK/STAT signaling, leading to uncontrolled cell proliferation (Kurzrock et al., 1987). Similarly, somatic mutations in *BAX* are also drivers of pediatric ALL (Findley et al., 1997; Meijerink et al., 1998; Prokop et al., 2000). The BAX/Bcl-2 heterodimer functions as an apoptotic activator (Findley et al., 1997), thus mutations in *BAX* enhance the ability of the tumor cells to resist cell death (Findley et al., 1997).

The tumor microenvironment is a major contributing factor that fosters multiple hallmarks of cancer (Hanahan and Weinberg, 2011). The tumor microenvironment is a collective

of cancer cells and ostensibly normal cells such as parenchymal, stromal and recruited immune cells found within the tumor and its vicinity (Hanahan and Weinberg, 2011). These seemingly normal cells provide sustained proliferative signaling, anti-apoptotic signaling, angiogenesis, and tumor-promoting inflammation. It is thus important to understand the interaction between the tumor microenvironment and cancer cells in order to provide more effective treatments to combat cancer (Hanahan and Weinberg, 2011).

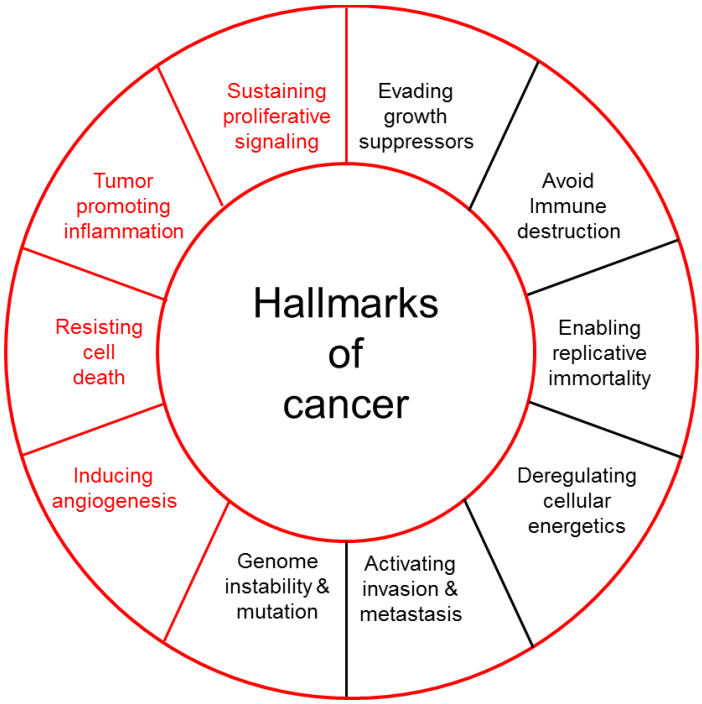

Figure 1.1. Hallmarks of cancer
The ten hallmarks of cancer as adapted from Hanahan, D., and R.A. Weinberg. 2011. Hallmarks of cancer: the next generation. *Cell*. 144:646-674. Hallmarks that are marked in red figure prominently as contributions of the tumor microenvironment that encompass sustained proliferative signaling, resisting cell death, inducing angiogenesis and tumor-promoting inflammation.

1.3 Cell Adhesion Mediated Drug Resistance

The tumor microenvironment plays a crucial role in the development and treatment of malignancies (Hazlehurst and Dalton, 2001; Kessenbrock et al., 2010; Meads et al., 2009; Sethi et al., 1999; Shain et al., 2009; Trédan et al., 2007). One of the features of metastatic malignant cells is the loss of anoikis, where cells that are normally anchorage-dependent fail to undergo programmed cell death upon detachment (Douma et al., 2004; Simpson et al., 2008). Loss of anoikis facilitates tumor cell survival and their dissemination to new niches, whereupon their adhesion to the extracellular matrix or surrounding neighboring cells continues to provide strong cell proliferative and survival signals (Eke and Cordes, 2015; Restrepo et al., 2012). Similarly, in hematological malignancies, cell adhesion to the bone marrow stroma and the extracellular matrix provides important survival signals to malignant cells giving them enhanced drug resistance (Abdi et al., 2014; Hazlehurst and Dalton, 2001; Hazlehurst et al., 2000b; Hideshima et al., 2007; Meads et al., 2008; Shain et al., 2009). This phenomenon is referred to as cell adhesion mediated drug resistance (CAMDR) and is a contributing cause of minimal residual disease following the intense treatment given to patients with ALL (Li and Dalton, 2006; Meads et al., 2009).

CAMDR is primarily mediated via integrins, a family of heterodimeric cell adhesion receptor proteins expressed in all metazoans. Experimental evidence shows that the anti-apoptotic pathways initiated by cell adhesion via integrins promote enhanced resistance to various chemotherapeutics (Hazlehurst and Dalton, 2001). For example, cell adhesion via integrins $\alpha4\beta1$ and $\alpha5\beta1$ upregulates Bcl2 expression and provides resistance to the cytotoxic agents, doxorubicin and melphalan, in multiple myeloma cells (Damiano and Dalton, 2000). In small cell lung cancer cell lines, cell adhesion via integrins containing the $\beta1$ subunit also

provides resistance to doxorubicin, cyclophosphamide and etoposide, in a process linked to protein tyrosine kinase activation (Sethi et al., 1999). Similarly, in acute myelogenous leukemia (AML), adhesion via α4β1-integrin promotes enhanced resistance to cytosine arabinoside through Akt activation and Bcl2 upregulation (Matsunaga et al., 2003). Furthermore, adhesion via α2β1-integrin has been shown to induce CAMDR in T-ALL cell lines (Gendron et al., 2005). In addition, cell adhesion to proteins found in the extracellular matrix leads to a block in cell cycle progression thus minimizing the damage sustained by treatment with chemotherapeutics (Hodkinson et al., 2006). All of the above examples point to integrins as the main cell adhesion receptors implicated in CAMDR.

1.3.1 Integrin Expression as a Prognostic Indicator of Malignancies

A number of published studies have highlighted the correlation between integrin expression and prognosis of patient outcomes. For example: increased expression of several integrins is indicative of poor prognosis and metastasis in prostate cancer (Fornaro et al., 2001); β1-integrin expression is a prognostic indicator in small cell lung cancer (Oshita et al., 2004); αv-integrin expression is a marker of poor prognosis in advanced-stage ovarian carcinoma (Davidson et al., 2003; Goldberg et al., 2001); integrin α3β1 is associated with tumor progression, metastasis, and poor prognosis in breast cancer (Felding-Habermann et al., 2001; Morini et al., 2000); integrin α4β1 enhances the metastatic potential of neuroblastoma and is associated with poor prognosis (Wu et al., 2008; Young et al., 2015); and integrin αvβ6 is highly expressed and associated with poor prognosis and high invasiveness in rectal cancer (Ahn et al., 2014). Taken together, integrin expression and activation contribute to CAMDR and indicate poor prognosis in cancer patients. In addition to the malignancies noted above, integrin α4β1

appears to also indicate a poorer prognosis in both AML and ALL (Becker et al., 2009; Matsunaga et al., 2003; Shalapour et al., 2011; Young et al., 2015). Interestingly, integrin α4β1 function has been found to be associated with MRD which is itself a risk factor of relapse in leukemia (Matsunaga et al., 2003).

1.4 Integrin Structure and Signaling

Integrins are heterodimeric transmembrane receptors that mediate the linkage between extracellular matrix proteins or *trans*-cell surface molecules to the intracellular signaling proteins and the cytoskeleton (Arcangeli and Becchetti, 2010; Barczyk et al., 2010; Campbell and Humphries, 2011; Humphries, 2000; Hynes, 2002; Srichai and Zent, 2010). As an important cell adhesion molecule, all multicellular animals express integrins (Barczyk et al., 2010; Humphries, 2000). There are 18 α- and 8 β-integrin subunits in humans; each pairing with one or more of its counterparts to form 24 known αβ heterodimers observed at the protein level (Arcangeli and Becchetti, 2010; Barczyk et al., 2010; Campbell and Humphries, 2011; Humphries, 2000; Srichai and Zent, 2010). Both α- and β-subunits contain a large extendable extracellular domain, a short one-pass transmembrane domain and a cytoplasmic tail domain that is variable in length (Figure 1.2) (Arcangeli and Becchetti, 2010; Barczyk et al., 2010; Campbell and Humphries, 2011; Humphries, 2000; Srichai and Zent, 2010). As integrins do not have kinase, phosphatase or other enzymatic activities, the heterodimers mediate their signal through complex formation with other receptors or effector proteins either at the plasma membrane through lipid rafts and clustering, or in the cytosol through cytoplasmic tail domain interactions (Barczyk et al., 2010; Baron et al., 2003; Giancotti and Ruoslahti, 1999; Leitinger and Hogg, 2002; Levental et al., 2009; Palazzo et al., 2004; Shattil et al., 1998).

Integrin signaling is closely associated with the concept of "integrin activation" where rapid, reversible changes occur in the conformation of the extracellular domains and the relative positioning of the transmembrane and cytoplasmic domains of the integrin heterodimer (Shattil et al., 2010; Su et al., 2016; Tadokoro et al., 2003). These conformational changes increase the ligand binding affinity of the integrin and initiate integrin signaling (Shattil et al., 2010).

Integrin signaling has been categorized into two forms, termed "inside-out signaling" and "outside-in signaling" (Shattil, 1999; Shen et al., 2012; Takagi et al., 2002). During inside-out signaling, activator proteins such as talins and kindlins bind to the β-integrin cytoplasmic tail, leading to a conformation shift in the integrin dimer that results in higher ligand binding affinity (Figure 1.2) (Shattil, 1999; Shen et al., 2012; Takagi et al., 2002). Functionally, inside-out signaling can control the adhesion strength and modify cell migration behavior.

During outside-in signaling, increased extracellular ligand concentration enhances the binding of integrins to these ligands and changes the conformation of the integrins (Figure 1.2) (Shattil, 1999; Shen et al., 2012; Takagi et al., 2002). Since integrin ligands are often multivalent, this facilitates multiple integrin binding and clustering, in effect enhancing the signal from the extracellular environment. While conceptually considered as two events, inside-out and outside-in signaling are often closely associated together and act to strengthen the overall signaling effectiveness: talin binding changes the integrin conformation to enable ligand binding, while more ligand binding clusters the integrins together and facilitates stronger outside-in signals (Shattil, 1999; Shattil et al., 2010; Shen et al., 2012; Takagi et al., 2002).

Cell adhesion mediated via integrins has been shown to be important for cell survival, proliferation, differentiation, and trafficking (Arroyo et al., 1999; Barringhaus et al., 2004; Miyamoto et al., 1995; Srichai and Zent, 2010; Vacca et al., 2001). Several signaling pathways

including PI3K/Akt, Wnt and mitogen-activated protein kinase kinase/mitogen-activated protein kinase (MEK/ERK) can be initiated through integrin adhesion and activation (Baril et al., 2007; Campos et al., 2004; Chekenya et al., 2008; Jadlowiec et al., 2004; Larue and Bellacosa, 2005; Liu et al., 2009; Rallis et al., 2010; Wang et al., 2011; Zhang et al., 2010). Adhesion through integrins also regulates a number of hematological functions, including the activation of platelets via αIIbβ3-integrin and lymphocyte migration and homing through α4β1- and αLβ2-integrins (Andrews and Berndt, 2004; Barringhaus et al., 2004; Shattil, 1999; Shattil et al., 1998; Watanabe et al., 2008; Xu et al., 2003). Gene deletion experiments also demonstrated the critical role that integrins play in development and survival of the organism, since the deletion of several integrin subunits, including integrins α4, α5 and β1 is embryonic lethal in mice (Bouvard et al., 2001; Scott et al., 2003; Stephens et al., 1995; Yang et al., 1993; Yang et al., 1995). Furthermore, deletion of integrins α3, α6, α7, α8, α9, αv, β4 and β8 is perinatal lethal in mice (Anton et al., 1999; Bader et al., 1998; DiPersio et al., 1997; Dowling et al., 1996; Evans and Müller, 2000; Georges-Labouesse et al., 1998; Huang et al., 2000; Kreidberg et al., 1996; Mayer et al., 1997; Müller et al., 1997; Van Der Neut et al., 1996; Zhu et al., 2002).

In sum, both the adhesion and signaling function mediated by integrins are important for the regulation of the cell cycle, shape, motility, proliferation, survival, and differentiation.

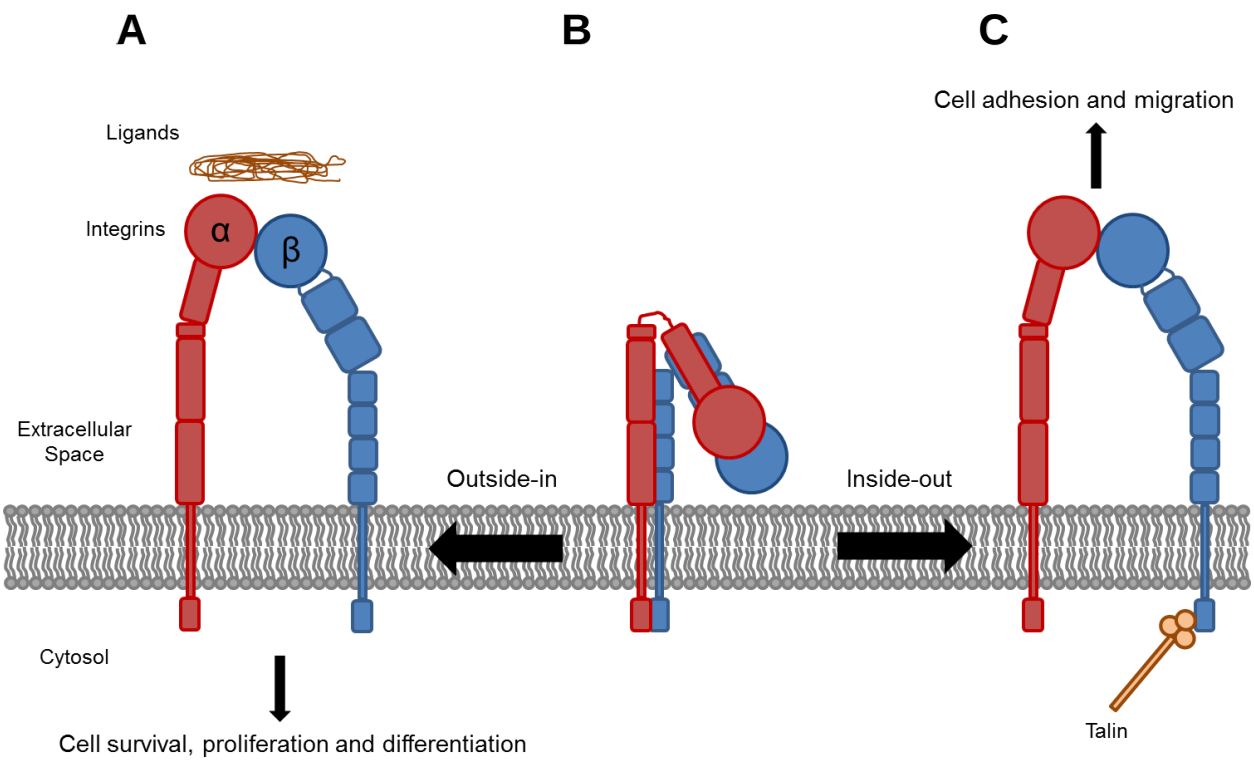

Figure 1.2. Model of integrin outside-in and inside-out signaling
Inactive integrins (B) are in the bent-closed conformation. Integrins can be activated to take on the high-affinity ligand binding state by both outside-in (A) and inside-out (C) signaling of integrins. During outside-in signaling, increased extracellular ligand concentration enhances the binding of integrins to these ligands and changes the conformation of the integrins. The changes in the conformation facilitate integrin binding to signaling proteins leading to cell survival, proliferation and differentiation. During inside-out signaling, activator proteins such as talin bind to the β-integrin cytoplasmic tail domain leading to conformation shifts in the integrin dimer that result in higher ligand binding affinity which promotes cell adhesion and migration. Activated integrins depicted in this model are in the extended-open conformation, highlighting the physical separation of both the transmembrane and cytoplasmic domains.

1.4.1 Extracellular Domains of Integrins

Much of what is currently understood about the conformation of integrins in various states of activation came through efforts over the past decades to produce high-resolution integrin structures via physical methods including crystallography, electron microscopy and NMR (Arnaout et al., 2005; Campbell and Humphries, 2011). For purposes of x-ray

crystallography, it is typically difficult to purify transmembrane proteins while maintaining their tertiary and quaternary structures intact. The difficulty is compounded further for integrins due to the large, highly glycosylated and complex dimeric structure (Carpenter et al., 2008). For years, researchers have had to work with low-resolution electron microscopy images of detergent extracted integrins, complemented with the fragmented single domains produced by high-resolution x-ray crystallography, to estimate the structure of full-length integrin dimers (Arnaout et al., 2005; Campbell and Humphries, 2011). Herein, I summarize key elements of the globular integrin extracellular domains as revealed by these structure studies.

The extracellular segment of α-integrin can be broken down into the headpiece and the lower leg piece (Figure 1.3). The headpiece includes the β-propeller and the thigh, while the lower leg piece includes the genu, calf-1 and calf-2 domains (Figure 1.3) (Campbell and Humphries, 2011; Humphries, 2000; Srichai and Zent, 2010; Su et al., 2016). The extracellular segment of β-integrin has a headpiece that includes the PSI, hybrid, βI and I-EGF-1 domains (Figure 1.3) (Campbell and Humphries, 2011; Humphries, 2000; Srichai and Zent, 2010; Su et al., 2016). The lower leg piece of β-integrin includes the I-EGF-2, I-EGF-3, I-EGF-4 and the β-tail domains (Figure 1.3) (Campbell and Humphries, 2011; Humphries, 2000; Srichai and Zent, 2010; Su et al., 2016). Both the β-propeller and the βI domain have ligand binding pockets that form a trimeric structure between α-integrin, β-integrin and the integrin ligand (Figure 1.3) (Humphries, 2000).

Based on electron microscopy and cell surface ligand affinity measurements, integrins can adopt one of three conformational states: the bent-closed, extended-closed and extended-open (Figure 1.2) (Chigaev et al., 2015; Su et al., 2016). Normally, both the bent-closed and extended-closed have a low affinity for ligands while the extended-open conformation has a high

affinity for ligand. (Chen et al., 2010; Chigaev et al., 2015; Su et al., 2016). Besides the requirement for conformation shift, integrin ligand binding is universally divalent-cation-dependent, requiring the binding of Mg^{2+} or Mn^{2+} to the β-propeller and the βI domain, while Ca^{2+} inhibits integrin ligand binding (Dransfield et al., 1992; Humphries, 2000; López-Ceballos et al., 2016; Smith et al., 1994).

In 2001, the most complete high-resolution integrin structure to date was produced through high-resolution x-ray crystallography by Xiong *et al.* (Xiong et al., 2001). In this publication, Xiong *et al.* described the extracellular structure of integrin αvβ3 in its bent-closed conformation where the integrin extracellular domain exists in an inverted V shape with N-terminal headpieces bent downwards toward the plasma membrane (Figure 1.2) (Xiong et al., 2001). Based on recent publications using electron microscopy to image the ligand binding efficiency of integrins, this conformation is said to have low affinity for extracellular ligands since the ligand binding site on the headpieces of the integrin dimer are bent toward the plasma membrane, effectively hidden by the rest of the integrin extracellular domain (Figure 1.3) (Chen et al., 2010; Chigaev et al., 2015; Eng et al., 2011; Su et al., 2016; Ye et al., 2010). Even though researchers have a good approximation of the overall integrin structure in the extended conformations through the combination of the low-resolution images of whole integrins with the high-resolution images of isolated individual domains, the high-resolution structure of integrins in the extended conformations remains to be solved.

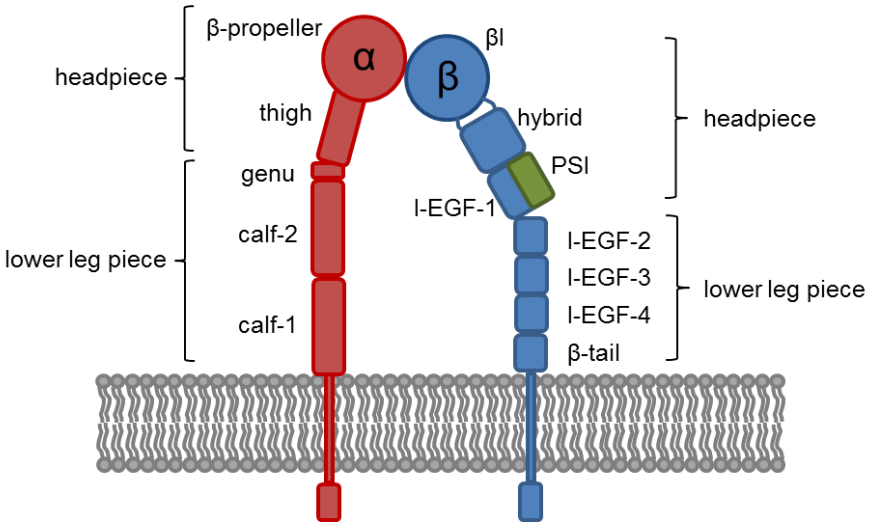

Figure 1.3. Structure of the integrin extracellular domains
The model depicted is the structure of integrin heterodimer in the extended-open conformation with emphasis on the extracellular domains. The α-integrin headpiece includes the β-propeller domain and the thigh domain while the lower leg piece includes the genu, calf-1, and calf-2 domains. The β-integrin headpiece includes the PSI, hybrid, βI and the I-EGF-1 domains while the lower leg piece includes the I-EGF-2, I-EGF-3, I-EGF-4 and the β-tail domains. α-integrin is drawn in red while β-integrin is drawn in blue and green.

1.4.2 Transmembrane Domains of Integrins

Each α and β subunit is a typical one-span type I transmembrane protein (Campbell and Humphries, 2011; Humphries, 2000; Shattil et al., 2010; Srichai and Zent, 2010). Therefore the transmembrane domain is essential in relaying information across either side of the membrane in both inside-out and outside-in integrin signaling.

High-resolution NMR spectroscopy studies using individual α- and β-integrin subunit transmembrane domains embedded in phospholipid bicelles mimicking the plasma membrane environment have been instrumental in revealing the transmembrane domain structures of integrin dimers (Lau et al., 2008a; Lau et al., 2008b; Lau et al., 2009). The β-integrin transmembrane domain consists of a longer helix, whereas the α-integrin structure is a shorter

helix with a backbone reversal at the C-terminal end that forms a small hook using the very last phenylalanine-phenylalanine residues of the transmembrane domain (Figure 1.4) (Lau et al., 2008a; Lau et al., 2008b). This α-integrin transmembrane domain hook and the accompanying β-integrin transmembrane domain form a structure called the inner membrane clasp that is important for both the activation and stable presentation of integrin dimers on the cell surface (Figure 1.4) (Kim et al., 2012; Kim et al., 2011; Shattil et al., 2010). Importantly, these high-resolution studies using phospholipid bicelles or nano-discs also determined the extent of α- and β-integrin embedment within the phospholipid bilayer. When integrins are in the bent-closed or inactive conformation, the KxGFFKR (or simply GFFKR) conserved motif of the α-integrin transmembrane/cytoplasmic domain is partially embedded in the plasma membrane with Glycine-Phenylalanine-Phenylalanine (GFF) residues being inside the phospholipid bilayer (Figure 1.4) (Lau et al., 2008a; Lau et al., 2008b; Lau et al., 2009). As the integrin dimer shifts to an extended or active conformation, the entire α-integrin transmembrane domain kicks out or goes through a piston-like action that moves the entire GFFKR motif into the cytosol (Figure 1.4) (Ginsberg, 2014; Li et al., 2014; Shattil et al., 2010; Thinn and Zhu, 2015). This conformation shift also separates the α- and β-integrin transmembrane domains and by extension, the inner membrane clasp (Figure 1.4).

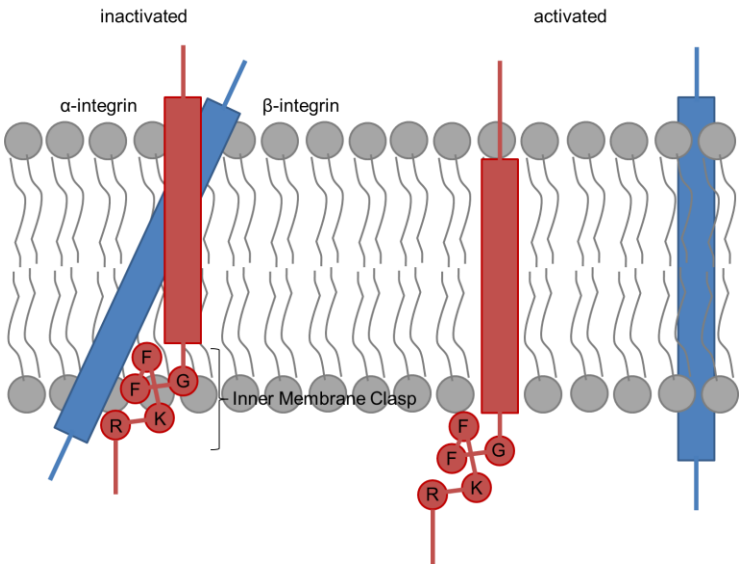

Figure 1.4. Structure of the integrin transmembrane domains
The model depicts the structure of integrin heterodimer transmembrane domains in the inactivated and activated conformations. 'Snorkeling' of the α-integrin transmembrane domain upon integrin activation shifts the GFFKR motif into the cytosolic space from its partially membrane-embedded inactivated form. α-integrin is drawn in red while β-integrin is drawn in blue.

1.4.3 Intracellular Domains of Integrins

During integrin activation, the change in the interaction of the heterodimeric integrin cytoplasmic tail domains with cytoplasmic proteins such as talin and kindlins leads to the activation of the integrin (Du et al., 1993; Ginsberg, 2014; Kim et al., 2011; O'toole et al., 1994; Shattil et al., 2010; Tadokoro et al., 2003; Ye et al., 2010). The association status between α- and β-integrin transmembrane and cytoplasmic tail domains is a key event in regulating integrin signaling (Hughes et al., 1996; Li et al., 2005b; Luo et al., 2005; Luo et al., 2004; Partridge et al., 2005). The artificial clasping of the α- and β-integrin transmembrane domains or cytoplasmic tails with each other using coiled coils inhibited integrin activation (Lu et al., 2001; Zhu et al., 2008). Similarly, artificially linking the α- and β-integrin transmembrane domains together with

introduced disulfide bonds led to the integrin being inactivated (Luo et al., 2004). There are numerous studies of integrin extracellular and transmembrane domain interactions, yet due to the large variability in length and complexity of integrin cytoplasmic interactions, and the difficulty of isolating plasma membrane-embedded proteins, efforts to identify interactions of isolated α- and β-integrin tails using NMR spectroscopy were largely unsuccessful (Metcalf et al., 2010; Ulmer et al., 2001; Vinogradova et al., 2002; Weljie et al., 2002).

Of the three major integrin structural components, the integrin cytoplasmic domain is the most variable and least conserved between different integrins. They are generally short, with 30-50 amino acids in length (Figure 1.5). With the exception of β4-integrin, the tail sequences are partially conserved among the β-integrins, while the tail sequences among the α-integrins are highly divergent (Figure 1.5) (Campbell and Humphries, 2011; Humphries, 2000; Sastry and Horwitz, 1993; Srichai and Zent, 2010). Due to the important roles of integrins in mediating cell adhesion, migration, signal transduction, and gene expression, there have been extensive studies to identify and characterize the functional consequences of integrin cytoplasmic domain interaction with other proteins (Liu et al., 2000). For example, the β-integrin cytoplasmic domain interacts with cytoskeletal proteins such as talin and filamin to regulate cell structure, shape, and motility (Liu et al., 2000). Other interacting proteins such as focal adhesion kinase (FAK), integrin-linked kinase (ILK) and the proto-oncogene tyrosine-protein kinase Src provide cell proliferative and survival signaling through cell adhesion (Abram and Lowell, 2009; Giancotti and Ruoslahti, 1999; Liu et al., 2000; Xia and Smith, 2012). Studies have also shown that integrin signaling is largely dependent on the cytoplasmic interacting proteins regardless of the extracellular ligand it is bound to. As a demonstration of this phenomenon, Kassner *et al.* exchanged the cytoplasmic domain of α5-integrin with that of α4-integrin (producing a hybrid

integrin with α5 outside and transmembrane and α4 inside) and the ensuing cell adhesion phenotype was consistent with that of α4-integrin and not α5-integrin (Kassner et al., 1995).

Taken together, integrin cytoplasmic tail domains not only initiate inside-out signaling by binding to integrin activating proteins such as talin and kindlins, but can also relay outside-in signaling originating from extracellular ligand-integrin interactions by binding to signaling proteins such as FAK, ILK, and Src.

Figure 1.5. Sequence comparison of the α- and β-integrin cytoplasmic domains
(A) The cytoplasmic domain amino acid sequences of all 18 human α-integrins. Highlighted in red is the conserved KxGFFKR motif of α-integrins. (*B)* The cytoplasmic domain amino acid sequences of all 8 human β-integrins. ECD is the extracellular domain while TMD is the transmembrane domain.

1.4.4 Integrin Antibodies as Tools for Detecting and Modulating Integrin Functions

Besides the physical methods used to assess the structure and activation status of integrins, biochemical-based methods also exist to probe and infer these physical properties. One benefit of biochemical methods is that they can be employed to assess the native state of integrins as full-length heterodimers that are physiologically expressed in the cell of choice.

Since active integrins exist in the extended conformation, as opposed to the bent-closed conformation of inactive integrins, antibodies that bind specifically to these conformations can be used to determine the status of integrin activation (Su et al., 2016). Furthermore, certain antibodies that enable the conformation shift of integrins to either the extended or bent forms can be employed to act as integrin activators or inhibitors (Su et al., 2016).

In total, there are 24 known integrin heterodimeric combinations in humans. Of these 24, 12 are made up of various α-subunits paired with β1-integrin, making β1-integrin heterodimers the largest of the integrin subfamilies (Campbell and Humphries, 2011; Humphries, 2000; Srichai and Zent, 2010; Su et al., 2016). As such, numerous β1-integrin activating or inhibitory antibodies are available and generally rather well-characterized. For example, negative-staining electron microscopy studies show that the activating antibodies 9EG7, 8E3 and N29, all stabilize the extended conformation of β1-integrin (Su et al., 2016). Other β1-integrin activating antibodies such as 12G10 and HUTS-4 stabilize the headpiece in an open conformation for ligand binding (Su et al., 2016). Even though HUTS-21 is a frequently used β1-integrin activating antibody, relatively little is known regarding the β1-integrin conformation induced by HUTS-21 binding (Luque et al., 1996; MUÑOZ et al., 1997). For the most part, TS2/16 is useful as a non-activating or non-inhibiting antibody, as its binding to β1-integrin does not result in any visible conformation change (Su et al., 2016). As for β1-integrin inhibiting antibodies, both SG/19 and mAb13 stabilize the closed headpiece conformation that maintains the integrin dimer in a low ligand-affinity state (Su et al., 2016).

1.5 α4-integrins

The α4-integrin subunit, also known as CD49d, can heterodimerize with either the β1- or β7-subunits. When heterodimerized with β1, α4β1-integrin (also known as very late antigen 4, VLA-4) binds to ligands that include fibronectin (Fn) and vascular cell adhesion molecule 1 (VCAM-1) (Humphries et al., 2006). Thrombospondin, ADAM metallopeptidase domain 28 (ADAM28) and osteopontin have also been characterized as ligands for α4β1-integrin (Bridges et al., 2002; González-Amaro et al., 2005; Humphries et al., 2006; Hynes, 2002; Yabkowitz et al., 1993). When heterodimerized with β7, α4β7-integrin (also known as Lymphocyte Peyer patch adhesion molecule, LPAM-1) binds mucosal vascular addressin cell adhesion molecule 1 (MAdCAM-1) (Humphries et al., 2006).

Lymphocytes express several β1-integrin heterodimers that mediate their adhesion to several extracellular matrix proteins (Pribila et al., 2004). Of these, α1β1- and α2β1-integrins are collagen receptors, α4β1- and α5β1-integrins can bind fibronectin, while α3β1 and α6β1 are receptors for laminins (Hynes, 2002). At the beginning of my thesis project, a number of β1-integrin heterodimers were identified as CAMDR contributors in T-lymphoblasts including α1β1- and α2β1-integrins (Xia and Smith, 2012). α4β1-integrin has been implicated in CAMDR of B-ALL, but not of T-ALL (de la Fuente et al., 2002; Xia and Smith, 2012). As such, the investigation into the possible contribution of α4β1-integrin to T-ALL CAMDR may shed new light on integrin involvement in drug resistance. Since α4-integrins play essential and major roles in lymphocyte adhesion, homing, recruitment, co-stimulation, and activation, the function of α4-integrins is reviewed in greater detail in the following subsections.

1.5.1 Function of α4-integrin Ligand Binding

Perhaps the most important and best understood role of α4-mediated adhesion is in the trafficking and recruitment of leukocytes to sites of inflammation. This multistep process involves sequential interactions between leukocytes and the vascular endothelial cells that include tethering/rolling, firm adhesion, spreading, and diapedesis (Springer, 1994). The initial rolling type interaction is mediated via low-affinity interactions involving the selectins (Bevilacqua, 1993; Campbell et al., 1998; Campbell et al., 1996). To achieve firm arrest, integrins expressed on the leukocytes must become activated to take on high-affinity ligand binding states. These are primarily mediated via integrins α4 (as α4β1-VCAM-1 and α4β7-MAdCAM-1 interactions) and αLβ2 (also known as lymphocyte function-associated antigen 1 (LFA-1) which binds to intercellular adhesion protein 1 (ICAM-1)). Collectively, these are commonly referred to as the lymphocyte homing receptors.

In addition to leukocyte recruitment to inflammatory sites, binding of α4β1-integrin to VCAM-1 is also important for the homing and retention of leukocytes in the bone marrow stroma (Craddock et al., 1997). Blockade of α4β1-integrin binding to VCAM-1 interferes quantitatively with the interaction between hematopoietic stem/progenitor cells and the bone marrow stroma (Craddock et al., 1997). α4β1-integrin also participates in T-cell activation as a co-stimulatory signal (Nojima et al., 1990; Shimizu et al., 1990). The binding of Fn to α4β1-integrin together with anti-CD3 antibody treatment mediates CD3-dependent $CD4^+$ T-cell activation and proliferation (Nojima et al., 1990; Shimizu et al., 1990). Similarly, binding of α4β1-integrin to thrombospondin induces co-stimulatory signals that lead to T-cell proliferation and the production of cytokines (Li et al., 2002).

ADAM28 is a type of metalloprotease that cleaves proteins such as cytokines, chemokines, and adhesion molecules (Howard et al., 2000; Howard et al., 2001). ADAM28 is expressed on the surface of lymphocytes, and its interaction with α4-integrin on adjacent cells at inflammatory sites regulates its metalloprotease activity (Bridges et al., 2002).

The expression of the α4 ligand, osteopontin is up-regulated in a number of inflammatory settings, where it is a major secreted product of macrophages (Bayless and Davis, 2001). It functions as both a matrix and as a molecule with cytokine-like properties to support cell adhesion, migration, and recruitment of lymphocytes (Bayless et al., 1998; Denhardt et al., 2001; Gassler et al., 2002; O'Regan et al., 2000).

Interestingly, α4β7-integrin has a crucial role in lymphocyte recruitment to Peyer's patches and the intestinal mucosa, thus its alternative name, lymphocyte Peyer's patch HEV adhesion molecule 1 (Postigo et al., 1993). The interaction between MAdCAM-1 and α4β7-integrin is responsible for regulating lymphocyte homing to mucosal sites (Strauch et al., 1994). In addition, MAdCAM-1 co-stimulates T-cell proliferation through α4β7-integrin (Lehnert et al., 1998).

1.5.2 α4-integrin in Chronic Inflammatory and Autoimmune Diseases

The trafficking of leukocytes mediated by α4-integrin function has been implicated in several autoimmune inflammatory diseases. Indeed, the potential utility of α4-integrin as a therapeutic target has been demonstrated in multiple animal models of chronic inflammation and autoimmunity such as adjuvant arthritis, allergic airway responses, autoimmune thyroiditis, contact hypersensitivity, autoimmune encephalomyelitis and autoimmune diabetes (Mcmurray et al., 1996; Rabb et al., 1994; Seiffge, 1996; Yang et al., 1994; Yednock et al., 1992).

Furthermore, α4-integrin has been implicated in atherogenesis and increased monocyte infiltration to organs, both of which are significant concerns in systemic lupus erythematosus (Rahimi et al., 2013).

Function blocking antibodies that target the extracellular epitope of α4-integrins have been developed and approved for clinical use in the treatment of several autoimmune disorders. Natalizumab is a humanized monoclonal antibody that functionally blocks the ligand binding ability of both α4β1- and α4β7-integrins, thus reducing the ability of T cells to attach and pass through endothelial cells lining the blood-brain barrier, synovial tissue and the intestine (Hutchinson, 2007). While approved for the treatment of Crohn's disease and multiple sclerosis, the widespread utility of Natalizumab has been limited by concerns that complete α4-integrin blockade and resulting immune suppression can lead to potentially fatal side effects of treatment (Bloomgren et al., 2012). Indeed, one of the adverse effects of Natalizumab treatment is the development of progressive multifocal leukoencephalopathy, which arises from an opportunistic infection caused by the JC virus that occurs in immuno-compromised patients (Bloomgren et al., 2012). More recently, Vedolizumab is a humanized monoclonal antibody that specifically blocks α4β7-integrin function thus reducing the recruitment of T cells to MadCAM-1 expressing endothelium in the intestines (Jovani and Danese, 2013). The recruitment of immune cells to Peyer's patches plays an important role in inflammatory bowel diseases such as ulcerative colitis and Crohn's disease (Dave et al., 2014). Vedolizumab is currently approved for the treatment of ulcerative colitis and Crohn's disease, and its use appears to have little of the adverse effects associated with Natalizumab.

1.5.3 α4-integrin in CAMDR

As the bone marrow is the site of ALL expansion and most frequent site for ALL relapse (Gaynon et al., 1998), the bone marrow tumor microenvironment has been considered a protective niche for leukemia cells (Bradstock and Gottlieb, 1995). Previous studies have shown that α4-integrin mediates ALL cell adhesion (Filshie et al., 1998). Similarly, AML cell adhesion leading to CAMDR is specifically mediated by β1-integrin adhesion to Fn, which includes α4β1-integrin (Hazlehurst et al., 2007). *In vitro* co-culture experiments have shown that ALL cells allowed to make direct contact with stromal cells continued to proliferate even in the presence of chemotherapeutic agents (Mudry et al., 2000). This pro-survival effect was shown to be mediated through VCAM-1 binding, a ligand of α4β1-integrin.

As a function of outside-in signaling, α4β1-integrin ligand binding leads to the formation of focal adhesion complexes, to which FAK and ILK are subsequently recruited and then activated (Hannigan et al., 1996; Kornberg et al., 1991). FAK and ILK activation leads to downstream activation of oncogenic pathways that include PI3K/Akt, MEK/ERK and nuclear factor kappa-light-chain-enhancer of activated B cells (NF-κB), all of which mediate important cell survival and proliferative signals (Guan et al., 1999; Guo and Giancotti, 2004; Legate et al., 2006; McDonald et al., 2008).

The PI3K/Akt pathway has been implicated in stromal-cell-mediated chemoresistance and survival of leukemia cells (Wang et al., 2004). Conversely, the inhibition of PI3K-mediated signaling results in the death of leukemia cells (Bertrand et al., 2005). Similarly, inhibition of the MEK/ERK pathway leads to the rapid apoptosis of ALL cells (Bertrand et al., 2005). More recently, α4β1-integrin binding to VCAM-1 was shown to mediate chemoresistance through NF-κB activation (Jacamo et al., 2014).

MRD contributes to relapse after chemotherapy in patients with AML or ALL. Interestingly, high α4β1-integrin expression is correlated with poor overall survival in AML patients (Matsunaga et al., 2003). Similarly, in another study, gene expression analyses from 207 children with ALL MRD showed that α4-integrin is highly associated with poor outcome (Hsieh et al., 2013).

In summary, α4-integrins play crucial roles in chronic inflammatory autoimmune diseases and also in hematological malignancies. Treatments targeted toward α4-integrin may block lymphocyte homing, adhesion and their accumulation in target niches, and may therefore be a means to enhance overall chemotherapeutic efficacy in an effort to reduce MRD and relapse, and increase overall survival.

1.5.4 Binding Partners of the α4-integrin Cytoplasmic Tail

As an immunologically important integrin, the intracellular interactions of α4-integrin are the best studied amongst the α-integrins. The α4-cytoplasmic domain (referred to simply as the α4-tail) has been shown to bind paxillin, which is an important adaptor/scaffold protein that links α4-integrin to protein tyrosine kinases such as Src and FAK, to adaptor proteins such as Crk, and to structural proteins such as vinculin and regulators of the actin cytoskeleton (Turner, 2000a; Turner, 2000b; Webb et al., 2004). Integrin α4 also binds to the scaffold protein, 14-3-3 zeta which is implicated in cell motility, division, signaling and apoptosis (Deakin et al., 2009; Lim et al., 2007; van Hemert et al., 2001). Furthermore, α4-tail also binds to type-I PKA, and the association between α4-integrin and type-I PKA is implicated in directional cell migration (Lim et al., 2007). Non-muscle myosin IIA is another protein that can associate with the α4-tail to regulate cell migration (Rivera Rosado et al., 2011).

Importantly, the interactions mentioned above involve sequences that are unique to the α4-integrin cytoplasmic tail, when considered in relation to the other α-integrins. As shown in Figure 1.5, the membrane proximal GFFKR motif is highly conserved in all of the α-integrins, and in the next section, protein interactions involving the GFFKR motif are described that may be universally applicable to all integrin functions.

1.6 α-integrin GFFKR Motif Binding Proteins

The transmembrane and cytoplasmic domains of integrins play pivotal roles in integrin activation and integrin-mediated cellular functions (Liu et al., 2000; O'toole et al., 1994; Sastry and Horwitz, 1993). While both α- and β-integrin transmembrane domains are largely conserved, and the β-integrin cytoplasmic tails are partially conserved, the α-integrin cytoplasmic tails are greatly variable in both sequence and binding partners (Arcangeli and Becchetti, 2010; Campbell and Humphries, 2011; Humphries, 2000; Lau et al., 2008a; Lau et al., 2008b; Lau et al., 2009; Srichai and Zent, 2010; Weljie et al., 2002). The one exception to the largely variable α-integrin tail is the membrane proximal GFFKR motif that is highly conserved in all of the 18 human α-subunits (Figure 1.5). This motif is partially embedded within the plasma membrane when the integrin is inactive, and fully exposed within the cytosol when the integrin is active (Figure 1.4) (Lau et al., 2008a; Lau et al., 2008b; Lau et al., 2009). Besides serving as the inner membrane clasp on the α-integrin, the GFFKR motif is also a binding motif for several proteins relevant in modulating integrin activation, matrix protein remodeling, calcium binding, apoptosis, and the immune response.

Characterized examples of α-integrin GFFKR motif-binding proteins include Sharpin, MDGI, Mss4, CIB, and calreticulin. Binding of Sharpin to GFFKR serves as an inactivator of

integrins that results in the detachment of migrating lymphocytes (Bouvard et al., 2013; Pouwels et al., 2013; Rantala et al., 2011). Binding of mammary-derived growth inhibitor (MDGI) to GFFKR inhibits integrin activation and is implicated in decreasing cancer cell migration and metastasis (Bouvard et al., 2013; Nevo et al., 2010). The binding of GFFKR to the guanine nucleotide exchange factor, Mss4, regulates matrix metalloproteinase activation and Fn remodeling (Knoblauch et al., 2007). Binding of calcium and integrin-binding protein (CIB) to GFFKR leads to increases in integrin-mediated cell adhesion and spreading (Haataja et al., 2002). The earliest characterized GFFKR binding protein is calreticulin (CRT) (Dedhar, 1994). Since CRT-integrin interaction is a major focus of my thesis research, the following provides specific background and introduction to this intriguing multifunctional protein. Briefly, CRT is functionally implicated in cellular activities that include acting as a regulator of calcium homeostasis, as a protein-folding chaperone, as a receptor for phagocytosis of dying cells, and as a regulator of integrin adhesive functions (Gold et al., 2010; Johnson et al., 2001; Krause and Michalak, 1997).

1.7 The Pleiotropic Functions of Calreticulin

Originally, CRT was identified as a Ca^{2+}-buffering protein that is localized within the endoplasmic reticulum (ER) lumen (Michalak et al., 1992). Calreticulin has also been isolated from diverse sources including mammals, plants, insects and parasites, suggesting that it is a highly conserved and ubiquitous protein serving an important function in cell biology (Joshi et al., 1996; Lenartowska et al., 2009; Michalak et al., 1992; Nash et al., 1994). The phylogenetically diverse CRT proteins have three conserved structural domains: the globular N-terminal domain, the proline-rich P domain and an acidic C-terminal domain (Figure 1.6)

(Lenartowska et al., 2009). At the N-terminus, CRT has a signal sequence that targets its synthesis into the ER lumen. Once inside the lumen, this signal sequence is cleaved, thus leaving the bulk of CRT as a protein that is highly enriched within the ER (Gelebart et al., 2005; Smith and Koch, 1989). The globular N-terminal domain has no net charge and is involved in protein-protein interactions, metal binding, RNA binding, and autoantibody binding (Cheng et al., 1996; Dedhar, 1994; Nakamura et al., 2001; Nakhasi et al., 1998). The proline-rich and charged P domain contains the high-affinity Ca^{2+} binding sites while the negatively charged C domain contains the low-affinity (K_d ~ 2 mM), high capacity (~20 mole calcium/mole CRT) Ca^{2+} binding activity (Giraldo et al., 2010; Michalak et al., 1992; Shen et al., 1998). At the C-terminus, CRT has a KDEL ER retention sequence which enables its binding to KDEL receptors in the Golgi apparatus that act to recycle CRT back into the ER compartment (Opas et al., 1991; Wiersma et al., 2015).

Although CRT was first identified as an ER-resident protein, further investigations have demonstrated that CRT is present in a wide range of cellular compartments (Dedhar, 1994; Gold et al., 2010; Michalak et al., 1992; Nash et al., 1994; Wiersma et al., 2015). CRT has been localized to the cytotoxic granules of T cells, and to the cytosol and cell surface of various animal cells. Furthermore, CRT has been found in soluble form in blood serum, in the cell-free extracellular cavities of specialized tissues such as the synovium, and in tick saliva (Dupuis et al., 1993; Gray et al., 1995; Jaworski et al., 1995; Karska et al., 1995; Molica et al., 2016; Opas et al., 1991; Rojiani et al., 1991).

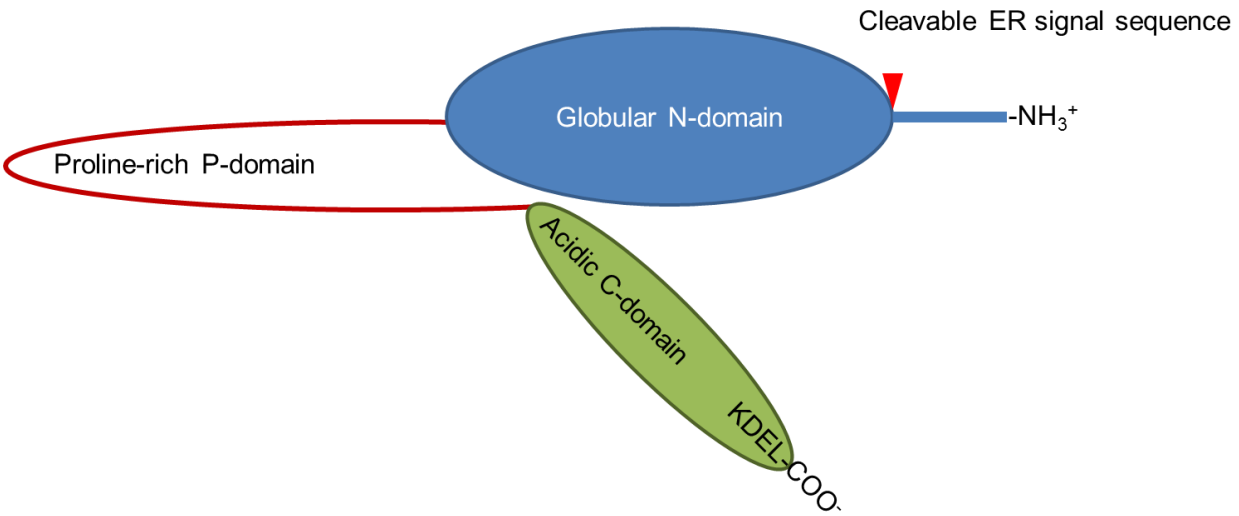

Figure 1.6. Calreticulin structure
The model depicts the structure of calreticulin; including the globular N-terminal domain, the proline-rich P domain, and the acidic C-terminal domain. The P-domain binds one Ca^{2+} with high-affinity, whereas the acidic C-domain has high Ca^{2+}-binding capacity (~20 mole calcium/mole CRT) with low-affinity (K_d ~ 2 mM). The N-terminal ER signal sequence is responsible for targeting the synthesis of calreticulin to the ER. It is cleaved upon insertion of calreticulin into the ER lumen during calreticulin synthesis. The KDEL motif at the C-terminus of calreticulin is responsible for retaining calreticulin in the ER.

1.7.1 ER Functions of Calreticulin

Ca^{2+} is a second messenger important in a number of cellular processes, including muscle contraction, gene expression, protein synthesis and stress signaling (Berridge et al., 2003; Roderick and Cook, 2008; Sanderson et al., 1994). The ER is the largest Ca^{2+} reservoir for maintaining Ca^{2+} homeostasis (Mattson et al., 2000; Sanderson et al., 1994). The release of Ca^{2+} from the ER to the cytosol is controlled by the inositol triphosphate receptor and the ryanodine receptor, while sarcoplasmic/endoplasmic reticulum calcium ATPase 2 (SERCA2) is responsible for Ca^{2+} uptake to the ER (Boitano et al., 1992; Michalak et al., 2009; Misquitta et al., 1999; Watras and Ehrlich, 1991).

The highly conserved function of CRT to bind Ca^{2+} with both high-affinity/low-capacity and low-affinity/high-capacity makes CRT the central Ca^{2+} buffering protein that regulates Ca^{2+} storage and release within the ER (Michalak et al., 1998). The function of CRT in the regulation of Ca^{2+} was demonstrated by altering CRT levels in the cell (Bastianutto et al., 1995; Nakamura et al., 2001). CRT knockouts produced highly defective phenotypes, exemplified by the disruption of Ca^{2+} homeostasis demonstrated in mouse embryonic fibroblasts (MEFs) *in vitro,* while homozygous null mice proved to be embryonic lethal with defective cardiac development (Khalife et al., 1994; Mesaeli et al., 1999; Szabo et al., 2007; Zhu and Wang, 1999).

In addition to its role in regulating Ca^{2+} homeostasis, the other major function for CRT within the ER is to act as a protein chaperone in concert, and as a complex, with calnexin and ER protein of 57-kDa (ERp57) (Schrag et al., 2001; Zapun et al., 1998). The CRT/calnexin cycle ensures the proper folding of newly synthesized glycoproteins before the glycoproteins are secreted to their target locations. These lectin-like chaperones interact with glycoproteins that possess monoglucosylated N-linked oligosaccharides that are generated both by the trimming of outer glucose residues by glucosidases and the reglycosylation of non-glycosylated unfolded proteins (Peterson et al., 1995; Spiro et al., 1996). Overall, CRT deficiency impairs protein quality control, causing the accumulation and export of misfolded proteins (Gelebart et al., 2005; Michalak et al., 2009; Michalak et al., 1998; Schrag et al., 2001).

1.7.2 Cytosolic and Nuclear Functions of Calreticulin

Outside the ER, CRT can localize to a multitude of locations, one of which is the cytosol. In a series of studies conducted by the Dedhar laboratory, cytosolic CRT was shown to bind the GFFKR motif within the cytoplasmic tail of α-integrins in a manner dependent on cell adhesion,

while CRT-deficient cells exhibited defects in cell adhesion and Ca^{2+} regulation (Coppolino et al., 1995; Coppolino and Dedhar, 1999; Coppolino et al., 1997; Dedhar, 1994). The interaction of CRT with the cytoplasmic tail of integrins appears to regulate extracellular Ca^{2+} flux into the cell in a manner independent of the ER Ca^{2+} levels (Kwon et al., 2000). Furthermore, cell adhesion to extracellular matrix (ECM) proteins increases the level of CRT that co-immunoprecipitated with integrins, and CRT has been localized to focal adhesion complexes with low-density lipoprotein receptor related protein 1 (LRP1) (Coppolino et al., 1995; Tran et al., 2002). The CRT-LRP1 complex appears to stabilize integrin-ligand binding and facilitates the activation of FAK and Src (Coppolino et al., 1995; Coppolino et al., 1997; Papp et al., 2007). Several publications from the Opas laboratory suggested a competing mechanism of action to account for CRT's role in regulating cell adhesion that was not directly coupled to its interaction with integrins, but to reduced expression of the cytoskeletal protein vinculin and reduced Src activity (Opas et al., 1996; Papp et al., 2007).

Besides the cytosol and the ER, CRT can also be found in the nucleus and functions as a nuclear export protein for both protein kinase inhibitor (PKI) and glucocorticoid receptor (GR) (Holaska et al., 2001; Holaska et al., 2002; Walther et al., 2003). The CRT-dependent export of PKI requires a functional nuclear export signal (NES) within PKI and involves the formation of an export complex that contains RanGTP (Holaska et al., 2001; Holaska et al., 2002). On the other hand, the CRT-dependent nuclear export of GR does not require an NES but is facilitated by the DNA-binding domain of GR, which is shown to function as an NES (Holaska et al., 2001; Walther et al., 2003).

1.7.3 Cell Surface Functions of Calreticulin

CRT can also be expressed on the extracellular cell surface (herein referred to as surface CRT). Also commonly referred to as ecto-CRT, surface CRT is an important 'eat me' molecule that facilitates the phagocytic uptake of dying cells (Gardai et al., 2005; Obeid et al., 2007). This is another function of non-ER localized CRT that utilizes LRP1 in the clearance of apoptotic cells, a process referred to as efferocytosis (Gardai et al., 2005; Obeid et al., 2007). Phosphatidylserine (PS) associated cell surface CRT has been shown to provide the recognition signal for the removal of apoptotic cells by both professional and nonprofessional phagocytes (Gardai et al., 2005; Obeid et al., 2007). During efferocytosis, CRT and LRP1 are in a *trans*-state where CRT is exposed on the surface of the apoptotic cell to be engulfed by the phagocyte expressing LRP1 (Nilsson et al., 2012). In addition, this process requires reduced expression or antibody-mediated neutralization of CD47 on the target cell. This decreases the ability of CD47 to engage cell surface tyrosine-protein phosphatase non-receptor type substrate 1 (SIRP-α) on the phagocyte which acts as a signal of 'self', and prevents phagocytosis from proceeding (Chao et al., 2010).

CRT and LRP1 can also interact in a *cis* configuration in the same cell within focal adhesion complexes (Pallero et al., 2008). The N-terminal domain of matricellular protein thrombospondin 1 (TSP1) binds to the CRT-LRP1 complex to signal down-regulation of cell adhesion, and increases cell motility through focal adhesion disassembly (Pallero et al., 2008). TSP1 signaling through CRT-LRP1 activates cell survival signals such as PI3K leading to resistance to apoptosis during anoikis (Pallero et al., 2008).

1.7.4 Extracellular Functions of Calreticulin

There is an emerging body of work supporting the presence of extracellular CRT as a physiologically relevant phenomenon (Gold et al., 2006; Johnson et al., 2001; Tesniere et al., 2008; Wang et al., 2012). There is a low level of CRT present in normal human serum; the source is presumably the release from dying, apoptotic cells (Ni et al., 2013). In certain pathological conditions, cells exposed to high levels of stress may undergo cell death that triggers the release of intracellular proteins including chaperones. When proteins that are normally intracellular become exposed to the immune system, an autoantibody response is likely to occur. Indeed, in patients with inflammatory autoimmune diseases such as systemic lupus erythematosus, rheumatoid arthritis or celiac disease, there not only is a heightened level of serum CRT, but autoantibodies against CRT can be found as well (Den Berg and Van, 1998; Garcia et al., 1994; Karska et al., 1995; Ni et al., 2013; Sanchez et al., 2000; Tarr et al., 2010a).

Besides a role in autoimmune diseases, one of the extracellular functions of CRT is facilitating wound healing (Nanney et al., 2008). The administration of soluble CRT to exposed wounds significantly increased the rate of cutaneous wound healing in multiple animal models including pigs, rats, and mice (Greives et al., 2012; Ignacio Arias et al., 2015; Nanney et al., 2008). The administration of CRT to wounds was shown to increase the expression of transforming growth factor β3, an important wound healing factor, and also to increase cellular proliferation and migration of keratinocytes and fibroblasts (Nanney et al., 2008).

1.7.5 Translocation of Calreticulin from ER to Cell Surface

In order for CRT to be present and function in the cytosol, cell surface or the extracellular environment, it must first translocate from the ER to these target locations. The ER is the main

organelle of protein synthesis and modification in the cell. To avoid a waste of resources, ER resident proteins such as chaperones must be distinguished from secretory proteins in order to prevent their release via the secretory pathway. Indeed, researchers have identified a carboxy terminal sequence of Lysine-Aspartic Acid-Glutamic Acid-Leucine (KDEL), termed the ER retention sequence, on ER resident proteins such as CRT, protein disulfide-isomerase (PDI) and binding immunoglobulin protein (BiP) (Munro and Pelham, 1987; Smith and Koch, 1989). ER resident proteins with a KDEL sequence can traffic proteins destined for secretion in vesicles between the ER and Golgi apparatus. The Golgi apparatus expresses KDEL receptors that can recapture KDEL containing proteins and return them to the ER. Much like the multiple localization examples for CRT, other chaperones or ER resident proteins containing the KDEL sequence such as gp96, calnexin and heat shock protein 47 can also be detected in non-ER locations (Altmeyer et al., 1996; Robert et al., 1999; Sauk et al., 1998; Wiest et al., 1997), suggesting that the KDEL motif does not sentence a protein to an exclusive life within the ER.

To date, multiple CRT translocation mechanisms have been proposed with varying degrees of evidence to support each of the hypotheses. Firstly, as observed in immature hematopoietic cells, it was speculated that the lack of ER retention of KDEL-containing proteins was likely due to nascent ER proteins that adopt a folded state which masks the KDEL sequence, and that is later corrected in mature hematopoietic cells (Wiest et al., 1997). Similarly, the presence of a high-stress environment, which can trigger cellular apoptosis, can influence the pH or oxidative status of the ER of the dying cell. Such an influence stems from the high concentration of reactive oxygen species (ROS) produced in response to the stress. These changes in the ER environment may impact the folding conformation of ER chaperones such as CRT, leading to masking of the KDEL sequence and eventual release of CRT through the ER-

Golgi pathway (Corbett et al., 2000). Similarly, changes in pH can lead to decreased binding efficiency and capacity of the KDEL receptors, and this also results in presentation of heat shock proteins or chaperones on the cell surface (Sauk et al., 1998; Wilson et al., 1993).

CRT is typically retained within the ER through the KDEL receptor-mediated retrograde retention pathway. The presence of CRT on the cell surface or the extracellular environment could be explained if CRT can be demonstrated to pass through the anterograde type secretory pathways. Indeed, a glycosylated form of CRT was shown to traffic to the cell surface via the Golgi complex/actin-mediated exocytic vesicle anterograde pathway in the murine colon cancer cell line, CT26, and a myeloid tumor cell line, HL60 (Denning et al., 1997; Panaretakis et al., 2009).

There is also evidence to suggest that CRT can leave the ER via a retrotranslocation pathway (Tarr et al., 2010b). Misfolded proteins are typically ubiquitinated and marked for retrotranslocation into the cytosol for proteasome degradation (Tsai et al., 2002). Using digitonin to specifically permeabilize only the plasma membrane of mammalian cells while leaving the membranes of intracellular organelles such as the ER intact, Afshar *et al.* estimated that 14% of total CRT is non-ER localized (Afshar et al., 2005). This non-ER CRT was not ubiquitinated, indicating that the CRT retrotranslocation pathway is independent of ubiquitin. Other evidence indicates that the CRT retrotranslocation pathway occurs via the nucleus, where CRT acts as a nuclear export protein and reaches the cytosol through nuclear export complexes (Holaska et al., 2001).

Besides glycosylation, other post-translational modifications such as arginylation and citrullination of CRT that occur in the cytosol seem to play a role in CRT presentation on the cell surface (Decca et al., 2007; Sambrooks et al., 2012). As discussed above, CRT may leave the ER

through retrotranslocation, or by overwhelming the KDEL receptor during cellular stress. Once in the cytosol, citrullinated CRT may be presented on the cell surface through binding with ERp57 and lipid raft flipping (Kepp et al., 2010). Other evidence also suggests that citrullinated CRT has a high affinity for PS and they may cluster with ERp57 on the lipid raft (Païdassi et al., 2011). Less is known about arginylated CRT, but it is interesting to note that in cell types lacking arginyl-tRNA protein transferase (ATE1), a protein responsible for arginylation, CRT cannot be detected on the cell surface (Decca et al., 2007; Sambrooks et al., 2012).

In summary, while CRT is predominantly an ER-enriched protein, it can also be found in multiple intra- and extra-cellular locales. As such, many possible mechanisms have been proposed to suggest the transit mode of CRT to the non-ER cellular compartments. Owing to the diversity of functions regulated by CRT, the mechanism of CRT trafficking remains a subject of keen interest.

1.8 Immunogenic Cell Death

At any given time in a healthy human body, millions of cells undergoing apoptosis are removed without invoking an inflammatory response. This type of apoptosis, known as tolerogenic or non-immunogenic, promotes tolerance to self and does not impact the immune system in any significant way (Galluzzi et al., 2012b; Green et al., 2009). Naturally, the counterpart to non-immunogenic cell death is immunogenic cell death (ICD), where the antigens originating from the dead or dying cell are able to stimulate an immune response. This past decade has seen research into the phenomenon of ICD gaining traction, in particular when it is studied in the context of the cancer cell (Green et al., 2009).

ICD involves changes in the cell surface presentation of specific proteins as well as the release of soluble mediators, both of which usually occur in a defined temporal sequence (Galluzzi et al., 2012b; Green et al., 2009; Kepp et al., 2009; Obeid et al., 2007). Such signals are collectively termed damage-associated molecular patterns (DAMPs). They engage a series of receptors such as Toll-like receptor (TLR) 2 and 4, CD91, CD40 and LRP1, that are expressed by phagocytes to stimulate the presentation of tumor antigens to T cells (Garg et al., 2012; Spisek and Dhodapkar, 2007). Important DAMPs that collaborate to elicit an immune response include CRT, HMGB1, ATP and a number of heat shock proteins such as HSP27, HSP70 and HSP90 (Graner, 2016; Krysko, 2013; Ren et al., 2016; Roy et al., 2014).

Most of the ICD-inducing agents have a profound effect on ER homeostasis, leading to ER stress and generation of ROS (Garg et al., 2012; Kroemer et al., 2013; Krysko et al., 2012). Both ER stress and accumulation of ROS play an important role in the signaling pathways leading to ICD and the secretion of DAMPs (Garg et al., 2012; Kroemer et al., 2013; Krysko et al., 2012). CRT that normally resides in the ER is translocated to the cell surface during ICD, where it functions as an “eat me” signal for phagocytes (Garg et al., 2012; Obeid et al., 2007). HMGB1 is an important nuclear chromatin protein that is released into the extracellular space during the last stages of immunogenic apoptosis. Released HMGB1 binds to TLR2 and TLR4, a process that is required for the optimal presentation of tumor antigens to phagocytes (Apetoh et al., 2007a; Apetoh et al., 2007b; Kazama et al., 2008). ATP is the last of the important DAMPs released by cells undergoing ICD. Released or secreted ATP functions as a “find-me” signal that guides professional phagocytes to the site where cellular apoptosis is occurring (Garg et al., 2012).

1.8.1 Treatments that Induce Immunogenic Cell Death

Immunogenic cell death or immunogenic apoptosis can be induced by chemotherapeutic agents such as the anthracyclines (doxorubicin, daunorubicin, and mitoxantrone, to name a few), oxaliplatin and bortezomib, or by radiotherapy and photodynamic therapy (PDT) (Casares et al., 2005; Garg et al., 2012; Garg et al., 2010; Obeid et al., 2007; Spisek et al., 2007). It has been shown that tumor cell lines treated *ex vivo* with the aforementioned therapies and then transplanted into immunocompetent mice, effectively function as a cancer vaccine in the absence of any adjuvants or immunostimulatory substances (Kroemer et al., 2013). Furthermore, these mice are protected against the same tumor cell lines when re-challenged with them.

To date, many more treatments have been found to elicit an immune response against malignant tumors. The mAb 7A7 induces CRT, HSP70, and HSP90 cell surface presentation in D122 lung carcinoma cells, subsequently leading to protective immune responses in vaccination experiments (Garrido et al., 2011). BK channel agonists such as phloretin and pimaric acid induce the overexpression of HSP60, HSP70, and HSP90 as well as the release of HMGB1 in rat glioma cells leading to protective immune responses *in vivo* (Hoa et al., 2009). Mafosfamide, which is a type of cyclophosphamide, promotes surface CRT presentation and HMGB1 release from EG7 lymphoma cells that then stimulated a protective immune response in vaccination experiments (Schiavoni et al., 2011).

Besides single agent treatments that can stimulate the presentation of the three major DAMPs (CRT, HMGB1, and ATP), combinations of agents may also achieve the same effect (Kroemer et al., 2013). For example, cardiac glycosides are ineffective in killing cancer cells, but can effectively induce CRT exposure, ATP release, and HMGB1 release. When used in conjunction with non-ICD inducing chemotherapeutics such as cisplatin or mitomycin C, cardiac

glycosides can stimulate ICD in vaccination experiments (Menger et al., 2012). Another example of combination chemotherapy capable of inducing ICD is thapsigargin and cisplatin. Thapsigargin is an ER stressor that stimulates cell surface presentation of CRT but fails to induce the release of ATP and HMGB1. Cisplatin, on the other hand, is a non-ICD inducing chemotherapeutic that causes the release of ATP and HMGB1 but does not stimulate CRT cell surface presentation. The combination of thapsigargin and cisplatin induces the release of these three DAMPs and ICD in vaccination experiments (Galluzzi et al., 2012a; Martins et al., 2011). Although not technically a treatment, certain viral infections, such as measles, can also induce ICD (Donnelly et al., 2013).

In summary, therapeutic regimes that facilitate the induction of ICD in tumor cells can exert strong anti-cancer effects beyond simply killing the target cells (Martins et al., 2011; Menger et al., 2012). Therefore, suboptimal chemotherapeutic regimens which fail to induce ICD, changes in cancer cells that prevent the secretion of DAMPs, or defects in the immune system that prevent recognition of the malignant cells, can all play a role in treatment failure.

1.9 Somatic Calreticulin Mutations Associated with Myeloproliferative Neoplasms

Myeloproliferative neoplasms (MPNs) are a rare and heterogeneous group of hematological neoplasms with similar biology (Vardiman et al., 2009). In MPNs, mutations originating within the hematopoietic stem cell lead to clonal amplification of certain myeloid progenitors, which ultimately result in excess production of mature and immature cells in either a single or multiple myeloid lineages. The classic MPNs include polycythemia vera, essential thrombocythemia, and primary myelofibrosis. The combined annual incidence rates for polycythemia vera, essential thrombocythemia, and primary myelofibrosis, calculated from

electronic database reports to August 2012, were 0.84, 1.03, and 0.47 per 100,000, respectively (Titmarsh et al., 2014). Even though MPNs start out as benign tumors, they can spontaneously transform and evolve into either myelodysplastic syndrome or acute myeloid leukemia that are associated with a much worse prognosis (Abdel-Wahab et al., 2010; Björkholm et al., 2011; Finazzi et al., 2005).

To date, multiple genetic markers have been found to be associated with MPNs and this has enabled their better diagnosis and treatment. Approximately 95% of polycythemia vera patients and approximately 50% of essential thrombocythemia and 65% of primary myelofibrosis patients have the *JAK2V617F* gain-of-function mutation (Tefferi, 2010). In addition, 5 to 10% of patients with essential thrombocythemia or primary myelofibrosis with nonmutated *JAK2* carry activating mutations in the thrombopoietin receptor gene, *MPL* (Pikman et al., 2006; Rumi et al., 2013). Taken together, nearly all polycythemia vera patients have the *JAK2* mutation while approximately 2/3 of essential thrombocythemia and primary myelofibrosis patients carry either *JAK2* or *MPL* mutations. This leaves 1/3 of essential thrombocythemia and primary myelofibrosis patients with an as yet uncharacterized mutation or genotype associated with the disease. In 2013, somatic mutations in *CALR*, which encodes for CRT, were identified in 70-84% of patients who are both *JAK2* and *MPL* negative, making mutated *CALR* the second most frequently occurring genetic marker for MPNs right after mutated *JAK2* (Klampfl et al., 2013; Nangalia et al., 2013).

All *CALR* mutations associated with MPN happen at exon 9; they are either insertions or deletions that cause a frameshift to an alternative reading frame which creates a new C-terminal domain for the mutated CRT protein (Klampfl et al., 2013; Nangalia et al., 2013). The two most frequently occurring *CALR* variants are termed type I and type II, where type 1 (L367fs*46)

results from a 52 base pair deletion and type 2 (K385fs*47) results from a 5 base pair insertion (Klampfl et al., 2013). Both the type I and II mutations encode a predicted CRT protein with a significantly altered C-terminal region in which most of the acidic sequences and the KDEL ER retention sequence are lost. Taking its place is an alternate translation reading frame derived from the genomic DNA sequences which flank the mutated *CALR* loci corresponding to exon 9. Importantly, the type I mutant CRT retains 92%, while the type II mutant CRT retains 97%, of the wildtype CRT protein. However, as of the writing of this thesis, whether or not the MPN-associated activities of the novel C-terminus might be attributed to the loss of the KDEL ER retention sequence remains unknown.

1.10 Calreticulin Facilitation of JAK/STAT Signaling

The occurrence of the MPN-associated somatic mutations in *CALR* (Klampfl et al., 2013; Nangalia et al., 2013) and the *JAK2* gain-of-function mutation is mutually exclusive, suggesting a possible overlap in functionality between the *CALR* and *JAK2* mutations. The valine-to-phenylalanine (V617F) alteration constitutively activates JAK2, resulting in increased phosphorylation of downstream STAT proteins, increased cytokine responsiveness and cytokine-independent proliferation of myeloid cells (James et al., 2005; Kralovics et al., 2005). Indeed, expression of type I mutant CRT in the BaF3 reporter pro-B cell line increased the level of STAT5 phosphorylation compared to cells expressing non-mutated wildtype CRT (Klampfl et al., 2013).

Further investigations have provided mechanistic insights into the manner by which mutated CRT induces the proliferation of myeloid cells leading to MPN. CRT appears to be a key mediator that facilitates the activation of the JAK/STAT signaling pathway downstream of

myeloproliferative leukemia protein (MPL), which is the thrombopoietin cytokine receptor (Araki et al., 2016; Chachoua et al., 2016). The C-domain of type I mutated CRT interrupts the N-P domain interaction to expose the CRT N-domain (see Figure 1.6 for CRT domains), which is then able to interact directly with the JAK2-MPL protein complex (Araki et al., 2016). This triplex of mutant CRT, JAK2 and MPL facilitates the thrombopoietin-independent activation of JAK2, and subsequent JAK-mediated phosphorylation of STAT proteins (Araki et al., 2016). Interestingly, this activation, although constitutive, appears to be much weaker than thrombopoietin-induced activation of JAK2, or mutant JAK2V617F mutation, thus providing a possible explanation as to why MPNs with mutated *CALR* have a better prognosis than those of JAK2V617F (Araki et al., 2016; Chachoua et al., 2016). Interestingly, perhaps occurring through a similar or different mechanism/s, overexpression of wildtype CRT facilitates JAK/STAT signaling in multiple tumor cell types including in both solid and hematopoietic malignancies (Abraham et al., 2010; Du et al., 2009; Li et al., 2005a). Therefore, based on the current state of knowledge, it is conceivable that wildtype CRT facilitates JAK/STAT signaling, while the somatically mutated CRT variant found in MPNs disrupts the normal conformation of CRT and results in constitutive activation of STAT proteins.

1.11 Hypotheses

As discussed, CAMDR is a contributor to MRD, chemotherapeutic failure and relapse in ALL as well as other hematologic malignancies (Damiano et al., 2001; Matsunaga et al., 2003; Meads et al., 2009; Naci et al., 2012). Integrins are the major mediators of CAMDR. Most integrin-mediated activities, including in CAMDR, have been attributed to β-integrins. Much less is known regarding the contribution of α-integrins. The general hypothesis investigated in

this work is that *the α-integrin cytoplasmic domain contributes to adhesion-mediated survival and drug resistance in leukemia*. More specific hypotheses are addressed in the following chapters as follows.

The work described in Chapter 3 evaluated the hypothesis that *interactions mediated by the cytoplasmic tail of α4-integrin regulate T-ALL cell survival and chemoresistance*. I found that resistance to drug-induced apoptosis was mediated by a conserved motif found in α-integrins, requiring only the GFFKR membrane-proximal sequence.

When CRT is on the cell surface, it acts as an "eat me" signal for phagocytes to engulf the cell (Coppolino et al., 1995; Liu et al., 2013; Obeid et al., 2007). However, because the interaction of CRT with the GFFKR motif in α-integrins promotes cytosolic localization of CRT, it is possible that this influences whether or not CRT is present on the cell surface. This leads to the work described in Chapter 4 that determined whether the CRT-integrin interactions that occur in the cytosol can reduce the immunogenicity of tumor cells treated with ICD-inducers. I evaluated the hypothesis that *α-integrin expression and function can modulate the presentation of cell surface CRT*. I found that α-integrin activation and GFFKR motif expression decrease cell surface CRT presentation.

MPN type I CRT mutation constitutively activates STAT proteins whereas wildtype CRT facilitates JAK/STAT signaling (Abraham et al., 2010; Du et al., 2009; Klampfl et al., 2013; Li et al., 2005a). Therefore, the work described in Chapter 5 explored further the hypothesis that *the association between the α-integrin GFFKR motif and CRT is involved in JAK/STAT signaling and chemoresistance*. I aimed to demonstrate the requirement for CRT in CAMDR and in GFFKR motif-mediated chemoresistance. Furthermore, I evaluated whether CRT facilitates JAK/STAT signaling in T-lymphoblasts. I found that CRT is partially required for GFFKR

motif-mediated chemoresistance and CAMDR. In addition, I found evidence implicating CRT function in the control of cytokine-induced STAT protein phosphorylation.

Chapter 2: Materials and Methods

2.1 Materials

2.1.1 Cells and Cell Culture

The human T-ALL cell line, Jurkat clone E6-1, was obtained from American Type Culture Collection (ATCC). JB4 is a Jurkat derivative lacking α4-integrin expression (Rose et al., 2003). The Jurkat derivative $\beta1^{-/-}$ cells (Jurkat 6A-A1, subsequently referred to as $\beta1^{-/-}$ cells in this thesis) were provided by Dr. Shimizu (Romzek et al., 1998). Dr. Andrew Weng (BCCRC) provided the T-ALL cell lines THP-6, SUP-T1, and DND-41.

All cells were cultured at 37°C, 5% CO_2 in complete RPMI (RPMI 1640 [R8758; Sigma-Aldrich] supplemented with 10% fetal bovine serum [FBS], penicillin-streptomycin and nonessential amino acids [Gibco, ThermoFisher Scientific]). In some experiments, cells were gradually adapted for growth in media supplemented with Cell-Ess® (Essential Pharmaceuticals) in place of FBS, as per the manufacturer's instructions.

The primary human T-ALL cells, BD-53 and BD-67, were obtained from the BC Children's Hospital Biobank with ethics approval from the BC Women's and Children's Hospital institutional review board (H12-03216). The relapsed bone marrow aspirate was thawed and 10^6 cells injected via tail vein into NOD-SCID/IL-2Rγ null **(**NSG) mice (Jackson Laboratory). Recipient mice were monitored for human leukemia cell engraftment and expansion by flow cytometric analysis of peripheral blood. Mice with high leukemia burden were euthanized, and their spleens (80% human $CD45^+$ lymphoblasts) immediately used as the source for primary T-ALL cells.

2.1.2 CRISPR-Cas9 Generation of CRT$^{-/-}$ cells

CRT$^{-/-}$ cells was generated by CRISPR-Cas9 methodology (Cong et al., 2013).The guide RNA sequence targeting the first coding exon for *CALR* (5' CGAGCCTGCCGTCTACTTCA 3') was ligated into the Bbs1 site of pX330. Jurkat cells were nucleoporated and clonally sorted into 96-well dishes. CRT$^{-/-}$ clones were initially identified by immunofluorescence staining with the α-CRT antibody (PA3-900), and later confirmed by sequencing of the targeted genomic loci. Multiple clones were isolated and further screened to ensure comparable integrin expression relative to the parental clone. Clone hCRT1-3 was used to generate the data shown here, with the major phenotypes reproduced in at least 2 other clonal CRT$^{-/-}$ isolates. CRT$^{-/-}$ clones in the other Jurkat derivative, Tacδ, were generated in identical fashion to this description. Clone hCRT1-6 was used for Tacδ/CRT$^{-/-}$ experiments.

2.1.3 Plasmids

The truncated α4δ integrin corresponding to human α4 amino acids 1-1007 was amplified by polymerase chain reaction (PCR) using primers, adding a stop codon following the KAGFFKR sequence of α4, and subcloned into pcDNA3.1 (Invitrogen). Tacδ was cloned as a fusion of Tac (human CD25 amino acids 1-263) to KLGFFKR encoded with double stranded oligonucleotides. To facilitate convenient swapping of the cytosolic tail, KLGFFKR was used instead of KAGFFKR since it incorporates the HindIII restriction site. As a control for Tacδ, Tac was fused to KLRFGFK to produce Tacδ^{scr}, which encodes the scrambled version of GFFKR as the cytosolic tail. Expression plasmids for full-length α4-integrin and Tac epitope were gifts from Dr. Mark Ginsberg (UCSD). The expression plasmids for IL6Rα and IL7Rα were obtained from the DNASU Plasmid Repository (Arizona State University).

GFP-CRT is an N-terminal Green Fluorescent Protein (GFP) fusion to human CRT (amino acids 18-417), provided by Dr. Eggleton (Tarr et al., 2010b). To reconstitute ER-targeting function, the signal sequence (ss) of CRT (amino acids 1-17) was fused N-terminal to GFP-CRT, producing ssGFP-CRT. The KDEL ER retention sequence deleted, GFP-tagged CRT with ER-targeting signal sequence (ssGFP-CRT-KDELdel) was made from PCR amplifying ssGFP-CRT using primers that artificially inserted restriction enzyme cut site and subcloned back into EGFP-C3. The inserted restriction enzyme cut sites were used to replace the C-terminal KDEL sequence with a stop codon. The GFP-tagged myeloproliferative neoplasm CRT mutant type I with ER-targeting signal sequence (ssGFP-CRT-mutant type I) was made from PCR amplifying ssGFP-CRT using primers that artificially inserted restriction enzyme cut site and subcloned back into EGFP-C3. The inserted restriction enzyme cut sites were used to replace the wildtype C-terminal sequence with mutant sequence. IRES-GFP-CRT was made from replacing the cytomegalovirus (CMV) promoter with the internal ribosome entry site (IRES) for GFP-CRT.

2.1.4 Recombinant Proteins and Fibronectin

Glutathione *S*-transferase (GST)-tagged proteins were purified from BL21 *Escherichia coli* lysates by affinity chromatography through glutathione sepharose (GE Healthcare) according to the manufacturer's instructions. GST-CS1 and GST-Fn9.11 are GST fusions to fibronectin CS1 region and repeats 9-11, respectively (Jongewaard et al., 1996; Ramos and DeSimone, 1996). Expression vectors for GST-KLGFFKR and GST-KLRFGFK proteins were made as double-stranded oligonucleotides encoding for the peptides fused C-terminal to GST encoded by pGEX-4T (GE Healthcare). Fibronectin (Fn) from human plasma was purified in-

house by affinity chromatography through gelatin sepharose (GE Healthcare). FITC-Fn was prepared by labeling Fn with fluorescein isothiocyanate according to the manufacturer's instruction (Sigma-Aldrich).

2.1.5 Antibodies

The following antibodies were used for flow cytometric labeling of cell surface proteins: α4-integrin (9F10), α5-integrin (NKI-SAM-I), Tac (BC96), F4/80 (BM8) and IL6Rα (UV4) from BioLegend; β1-integrin (sc-53711) from Santa Cruz Biotechnology; CRT (ab2907) and IFNARα (ab90498) from Abcam; and GFP (GF28R) from ThermoFisher Scientific. Antibodies used for intracellular labeling and immunofluorescence microscopy were: CRT (ab2907) and PDI (ab2792) from Abcam. Antibodies used for immunoblotting are: Akt (40D4), α4-integrin (#4600), phospho-Akt substrate (23C8D2), phospho-Tyr705 STAT3 (D3A7), phospho-Tyr694 STAT5 (D47E7), STAT3 (124H6) and STAT5 (#9363) from Cell Signaling Technology; α4-integrin (sc-365209) and Tac (sc-665) from Santa Cruz Biotechnology; GAPDH (FF26A/F9) from BioLegend; calreticulin (PA3-900) from Thermo Scientific; phospho-Thr308 Akt (EP2107Y) and phospho-Ser473 Akt (EP2109Y) from Epitomics. Antibodies used for immunoprecipitation were: α4-integrin (sc-365209) from Santa Cruz Biotechnology or α4-integrin (HP2/1) from Becton-Coulter and Tac (BC96) from BioLegend. Antibodies used for integrin activation and phagocytosis assays were: β1-integrin (9EG7) from ThermoFisher Scientific; β1-integrin (TS2/16) from BioLegend and CD47 (B6H12) from BD Pharmingen.

2.1.6 Services

Flow cytometry work was conducted at the Child and Family Research Institute (CFRI) Flow Core Facility. Analytical work was conducted on FACSCalibur, FACSCanto, and LSRFortessa, while fluorescence activated cell sorting was conducted on a FACSAria (BD Biosciences). Some analytical work mentioned in Chapter 4 and 5 was conducted on a BDAccuri located in the Michael Cuccione Laboratories. Post-acquisition analysis was done using FlowJo (Tree Star).

2.2 Methods

2.2.1 Cell Transfection

Cell transfections with α4, α4δ, Tacδ and Tacδ^{scr} constructs were performed using Amaxa Nucleofection Kit V (Lonza) by nucleofection using the program X-001 on the Amaxa Nucleofector (Lonza) and selected accordingly for hygromycin or G418 (Invitrogen) resistance. Cell transfections of CRISPR-Cas9 plasmids, IL6Rα, IL7Rα and all CRT related mutant constructs were performed using Opti-MEM (Gibco) by nucleofection using the program X-001 on the Amaxa Nucleofector. Routinely, transfection used 2 x 10^6 cells in 100 μL of either Nucleofection Kit V solution or Opti-MEM with 2500 ng of plasmids. Cells stably expressing the desired receptor levels were sorted to homogeneity following surface immunolabeling with antibodies. Cells with CRT knockout by CRISPR-Cas9 were blindly cloned in single cell suspension and identified through immunofluorescence imaging for the lack of intracellular CRT.

2.2.2 Preparation of Adhesion Substrates

Routinely, tissue culture dishes (Corning Costar) were incubated with 40 μg/mL of GST-CS1, GST-Fn9.11, GST, Fibronectin (Fn) and bovine serum albumin (BSA) in phosphate buffered saline (PBS, 137 mM NaCl, 2.7 mM KCl, 1.5 mM KH_2PO_4, 8 mM Na_2HPO_4, pH 7.4 (Sigma)) overnight at 4^oC. Following 2 washes with PBS, the coated dishes were ready for seeding with cells.

2.2.3 Cell Apoptosis

12-well substrate-coated plates were seeded with cells at 2 x 10^5 cells/well in 1 mL Complete-RPMI for 4 hours before addition of doxorubicin to the desired concentration. The half maximal effective concentrations (EC_{50}) of doxorubicin for Jurkat and JB4 cells were determined to be 0.05 and 0.03 μg/mL, respectively. After 48 hours of incubation, cells were resuspended and incubated with Annexin V-Cy5 (BD Biosciences) according to the manufacturer's instructions prior to flow cytometry analysis. In some experiments, cells were treated with: (i) Akt Inhibitor IV (Millipore) at the indicated concentrations; (ii) with 0.6 mM EGTA (Sigma) or 60 μM verapamil (Enzo), either alone or with doxorubicin for 48 hours before determination of apoptosis.

2.2.4 Cell Adhesion Assay

Cells were seeded on substrate-coated 6-well dishes for 30 minutes before imaging. For each condition, 12 different fields-of-view (FOV) were acquired before physical agitation of the dishes, followed by re-acquisition of the same FOVs. Alignment markers imprinted on the dish were used for registration of images. Imaging was with an Olympus IX81 microscope equipped

with 20X Phase objective, CoolSnap HQ2 camera (Photometrics), H-117 linear-encoded stage (Prior Scientific) and control by MetaMorph® (Molecular Devices). Post-acquisition image processing was with ImageJ (http://rsb.info.nih.gov/ij/) as follows: Before and after images were pseudocolored, aligned and overlaid. Non-translocated cells were scored as adhered and those displaced as non-adhered. % cell adhesion was calculated for each FOV (# adhered/total cells) with Mean and standard deviation computed for 12 FOVs. On average, each FOV had ~150 cells, with ~1800 cells scored per cell-substrate combination.

Some adhesion assays were done with cells pre-labeled with CellTracker™ Green CMFDA (Invitrogen) according to manufacturer's instructions, seeded at 2 x 10^5 cells/well in substrate-coated 96 well plates, and incubated at 37°C for 45 minutes. Fluorescence readings were acquired with an Enspire spectrofluorometer (485 nm excitation, 515 nm emission) before, and after 3 washes with PBS. Background fluorescence from the incubation medium was subtracted from each reading and the percent adhesion was calculated as follows: 100 • (Fluorescence after washes/Initial fluorescence).

2.2.5 Affinity Chromatography, Immunoprecipitations, and Western Blot Analysis

Cell lysates were routinely prepared in PN-buffer (5 mM PIPES, 25 mM NaCl, 75 mM sucrose, 25 mM NaF, 20 mM $Na_4P_2O_710H_2O$, 1 mM $CaCl_2$, 1 mM $MgCl_2$, 1% Triton X-100, complete protease inhibitors (Roche)). For phospho-Akt and Akt phospho-substrate analysis, cells were serum-starved in 0.5% FBS/RPMI for 48 hours before plating on 100 mm substrate-coated dishes for up to 60 minutes. For immunoprecipitations, 1 mg cell lysate was incubated with 2 μg antibodies for 14 hours. Then, 10 μL bed-volume protein A/G sepharose (Pierce) was added and incubated for a further 2 hours before washes and elution in SDS-PAGE sample

buffer. Where applicable, cells were pre-treated with combinations of 4 μg/mL doxorubicin and 1 μg/mL 9EG7 for 4 hours prior to lysis. For phospho-STAT3 analysis, cells were resuspended in fresh serum-free RPMI and stimulated with 2.5 ng/mL IFNα 2b (GenScript) or 25 ng/mL IL6 (GenScript) for 15 minutes. For phospho-STAT5 analysis, cells were resuspended in fresh serum-free RPMI and stimulated with 10 ng/mL IFNα 2b for 15 minutes. For recombinant GST-protein pull down of CRT, 1 mg Jurkat lysate was incubated with 12 μg GST-KLGFFKR or GST-KLRFGFK immobilized on GSH-sepharose for 14 hours. The loading of GST-proteins was done by Coomassie Blue staining of an excised portion of the SDS-PAGE gel. For Western blot analyses, SDS-PAGE separated proteins transferred onto nitrocellulose membranes (BioRad) were incubated with primary and IR-dye conjugated secondary antibodies (Pierce and Rockland). Blots were imaged on an Odyssey Imaging System (LI-COR). The Akt activation index (relative units) was calculated as the fluorescence intensity of Akt phospho-substrates divided by GAPDH as a loading reference.

2.2.6 Intracellular Calcium Measurements

Cells re-suspended in Ca^{2+}-free PBS were incubated with 1 μM Fluo-4-AM, 0.02% w/v Pluronic F-127 (Invitrogen), 0.1% dimethyl sulfoxide (Sigma-Aldrich) for 30 minutes at 22^{o}C. Following washes, cells were re-suspended in PBS, 1 mM $CaCl_2$/PBS, or 1 mM $CaCl_2$/5 mM EGTA/PBS for 10 minutes at 22^{o}C, and then kept chilled on ice prior to flow cytometry measurements. The median fluorescent intensity (MFI) values were used to compare intracellular Ca^{2+} levels within one experiment. Intracellular calcium levels were identical for cells incubated with PBS alone or with 1 mM $CaCl_2$/5 mM EGTA/PBS, indicating that Ca^{2+} efflux was not a significant factor in the assay. Ca^{2+} influx was calculated as intracellular Fluo-4-AM

fluorescence levels in 1 mM $CaCl_2$/PBS subtracted by measurements in PBS alone. To monitor adhesion mediated changes in intracellular Ca^{2+}, aliquots containing $1x10^5$ Fluo-4-AM-labeled cells resuspended in Complete RPMI or Complete RPMI/0.6 mM EGTA were seeded onto BSA, CS1 or fibronectin coated wells at 37°C, and microplate fluorescence readings taken at intervals following cell plating (Enspire, Perkin-Elmer).

2.2.7 Calcein-AM Efflux Assay

Harvested cells were re-suspended in pre-warmed (37°C) Complete RPMI, and seeded as 100 μL aliquots containing 2 x 10^5 cells per well in 96-well plates. Plates were incubated for 15 minutes at 37°C, 5% CO_2 prior to addition of equal volume calcein-AM (Invitrogen) dissolved in pre-warmed Complete RPMI at a final concentration of 250 nM. Cellular esterases convert the non-fluorescent calcein-AM to fluorescent calcein that is retained in the cell. Calcein fluorescence measurements (Ex: 485 nm, Em: 520 nm) were collected immediately (t=0) and thereafter at the indicated time points at room temperature. Between t=15 and t=30 minutes, the cells were re-incubated at 37°C, 5% CO_2. The data plotted are the fluorescence values after subtraction of the fluorescence values for cell-free wells, which were taken as blank measurements.

2.2.8 Doxorubicin Efflux Assay

Harvested cells were re-suspended in complete RPMI and incubated with 2 μg/mL doxorubicin for 2 hours at 37°C. Cells were then washed free of extracellular doxorubicin, and resuspended in PBS or 1 mM $CaCl_2$/PBS at $6x10^6$ cells/mL and incubated at 37°C, 5% CO_2. At the indicated time points, aliquots of cell suspensions were removed, centrifuged to pellet cells,

and 150 μL of the supernatant recovered to assay for effluxed doxorubicin in a microplate format (Ex: 488 nm, Em: 578 nm). The data plotted are the fluorescence values minus the fluorescence values for solution only blank measurements.

2.2.9 Stimulation of Cell Surface Calreticulin

Routinely, 1 x 10^6 cells/mL in complete RPMI were treated with or without 4 μg/mL doxorubicin (Sigma-Aldrich) for 4 hours or 300 μM oxaliplatin (Tocris Bioscience) for 2 hours, at 37^{o}C. In some assays, cells were serum-starved in serum-free RPMI for 24 hours prior to drug treatments. Where indicated, cells were transiently transfected by nucleoporation 24 hours prior to drug treatments. For assays involving cell adhesion, cells were seeded on substrate-coated wells 1 hour prior to drug treatments. To assess the effect of integrin-binding antibodies, the antibody was added to cells 15 minutes prior to drug treatments. Cell surface CRT or GFP-CRT levels were measured by flow cytometry analysis of α-CRT or α-GFP antibody-labeled cells using 633 nm excitation. Only the non-apoptotic population, defined as Annexin V (BD) negative cells, was gated for analysis using Geometric Mean calculation.

2.2.10 Fluorescence Microscopy

Cells were seeded on fibronectin-coated coverslips to allow adhesion and fixed in 3.7% formaldehyde/PBS for 15 minutes, permeabilized in 0.1% Triton X-100/PBS for 5 minutes and immunostained for CRT and the ER marker, PDI, with the corresponding antibodies. Images were acquired on an Olympus IX81 microscope equipped with a 60x NA1.35 oil immersion objective. Post-acquisition processing of images was conducted using ImageJ. Where applicable, 3.7% formaldehyde/PBS fixed cells were partially permeabilized in 25μg/mL digitonin/PBS

(Acros) for 5 minutes. The digitonin concentration was optimized based on the ability to maintain ER integrity that precluded staining for PDI, an ER-marker (Afshar et al., 2005).

2.2.11 Partial Permeabilization and Immunostaining for CRT

Cells were treated with combinations of 300 μM of oxaliplatin for 2 hours and 1 μg/mL of 9EG7 for 4 hours, followed by fixation in suspension with 3.7% formaldehyde/PBS for 15 minutes. Fixed cells were then divided into 2 groups each treated with 0.1% Triton X-100/PBS or 25 μg/mL digitonin/PBS (Acros), for 5 minutes. Following 3 washes with PBS, cells were immuno-stained for CRT and PDI and analyzed by flow cytometry. The digitonin concentration was optimized based on the ability to maintain ER integrity that precluded staining for PDI, an ER-marker (Afshar et al., 2005).

2.2.12 Antibody-Induced Integrin Activation

WT and $\beta1^{-/-}$ cells were treated with 0.015625 (1/64 dilution) μg/mL to 1 μg/mL of 9EG7 (β1-activating) antibody for 4 hours. Flow cytometry was used to measure activated β1-integrin labeled with the 9EG7 antibody.

2.2.13 Soluble Ligand Binding

Cells were pre-treated with 1 μg/mL 9EG7 or 1 μg/mL TS2/16 for 4 hours or 1 mM Mn^{2+} or 3 mM EGTA for 30 minutes prior to rinsing with PBS twice. Pre-treated cells were then incubated with 0.2 mg/mL of FITC-Fn for 30 minutes and rinsed with PBS afterward. Flow cytometry was used to measure the FITC-Fn binding to treated cells.

2.2.14 Phagocytosis Assay

To prepare macrophages, bone marrow aspirates were flushed from the femur and tibiae of 8-week-old C57BL/6 mice into complete IMDM (IMDM, 10% FBS, pen/strep). Aspirates were seeded at a density of 5 x 10^5 nucleated cells/mL for 4 hours. Non-adherent cells were pelleted at 300g for 5 minutes and re-suspended in complete IMDM with 10 ng/mL recombinant murine MCSF (StemCell Technologies) for 10 days with complete media changes at 4 and 7 days. Adherent cells (macrophages) from 10-day cultures were >95% Mac-1^+ and F4/80^+ as determined by flow cytometry. Macrophages were lifted using Cell Dissociation Buffer (enzyme free) as per manufacturer's instructions (Gibco, Thermo-Scientific) and re-suspended in complete IMDM at 5 x 10^5 cells/mL. Macrophages were spun down and re-suspended in blank IMDM for 1 hour prior to co-incubating with target cells in phagocytosis assays.

To prepare target cells, Jurkat cells were labeled with CellTracker™ Green (Invitrogen) according to the manufacturer's instructions. Labeled cells were then incubated with or without 1 μg/mL 9EG7 (β1-integrin activating antibody) for 4 hours at 37^{o}C. As applicable, cells were also co-incubated for the final 2 hours with or without 7 μg/mL α-CD47 (B6H12) and/or 300 μM oxaliplatin. Treated cells were washed twice with PBS and re-suspended in serum-free IMDM. Phagocytosis assays were initiated by mixing 2.4 x 10^5 macrophages with 1.2 x 10^6 Jurkat cells per well in 24-well plates for 2 hours in serum-free IMDM at 37^{o}C. Murine macrophages were subsequently stained with F4/80 antibodies, and total cells recovered using Cell Dissociation Buffer for analysis by flow cytometry. Phagocytosis was calculated as follows: % Phagocytosis = 100 • (CellTracker$^+$, F4/80^+ macrophages/total macrophages). In some experiments,

macrophages were re-plated on coverslips for imaging by fluorescence microscopy to confirm successful internalization of target cells.

2.2.15 Statistical Analysis

The unpaired 2 tail Student's t-test was used to calculate p-values. Error bars shown are the standard deviation values obtained from at least 3 treatment replicates conducted within an experiment. Each experiment is representative of similar results obtained in at least 2 independently conducted experiments.

Chapter 3: Integrin Cell Adhesion Mediated Drug Resistance in T-ALL

3.1 Overview and Rationale

Work published by other groups has demonstrated the phenomenon of CAMDR occurring in hematological cancers such as acute myelogenous leukemia and multiple myeloma (Hazlehurst et al., 2000a; Matsunaga et al., 2008; Matsunaga et al., 2003; Mori et al., 2004). Naci and colleagues used the Jurkat T-ALL cell line to demonstrate that CAMDR can be effected via integrin α2-mediated adhesion (Naci et al., 2012). However, the possible involvement of the immunologically important integrin α4 in T-ALL CAMDR has not been shown. High integrin α4 expression correlates with MRD in ALL (DiGiuseppe et al., 2009), and MRD is a good predictor of treatment failure and tumor relapse (Borowitz et al., 2008). Indeed, high integrin α4 mRNA expression was identified as an adverse risk factor in childhood ALL at first relapse (Shalapour et al., 2011). Integrin α4 is also an important integrin for retention and homing of hematopoietic cells to the bone marrow stroma (Hidalgo et al., 2001; Miyake et al., 1991; Möhle et al., 1995; Petty et al., 2009). In addition, a number of important protein interactions involving α4 integrin cytoplasmic interactions have been characterized, including interactions that promote pro-survival signaling occurring via PI3K/Akt signaling (Chekenya et al., 2008; Lim et al., 2001; Song et al., 2005; Xia et al., 2004). This formed the original basis of my investigation into the role of integrin α4 in CAMDR of T-ALL. I found that the phenomenon of CAMDR can be induced by cell adhesion mediated by a number of T cell integrins. In particular, the minimal integrin cytoplasmic motif required to effect drug resistance was found to be the conserved GFFKR motif that is present in all α-integrins.

3.2 Integrin Adhesion Promotes Chemoresistance in Jurkat T-ALL

Jurkat is a T-lymphoblastic cell line established from the peripheral blood of a 14-year-old male with T-ALL (Schneider et al., 1977). In addition to being a tissue culture model for T-ALL, Jurkat cells have seen widespread use as a powerful genetic model to study various T cell functions. In addition, our laboratory has a collection of Jurkat derivative cell lines that are deficient in specific integrin expression, including integrin α4 and β1. Thus, the work reported in this thesis primarily utilize Jurkat lymphoblasts as a genetic and biochemical signaling model for the functional study of integrins and their signaling partners in T-ALL subjected to chemotherapy *in vitro*.

To determine if Jurkat T-ALL cells gain drug resistance upon α4-integrin-mediated cell adhesion, I seeded Jurkat cells (the wildtype parental strain is referred to as WT from here on) on tissue culture plates that were pre-coated with the following glutathione S-transferase (GST) recombinant proteins: GST, GST-CS1, and GST-Fn9.11. GST is used as a control substrate that will not engage integrins, while CS1 and Fn9.11 are polypeptide fragments derived from fibronectin that specifically engage integrins α4β1 and α5β1, respectively (Jongewaard et al., 1996; Ramos and DeSimone, 1996). The seeded cells were then treated with doxorubicin and assayed for apoptosis by flow cytometry using Annexin V binding to cell surface phosphatidylserine (PS). In the absence of drug treatment, the fraction of apoptotic WT cells seeded on GST-CS1, GST-Fn9.11 or GST was not significantly different (Figure 3.1A). In contrast, there was a higher percentage of cells undergoing apoptosis in doxorubicin-treated WT cells seeded on a control non-adherent substrate compared to cells seeded on GST-CS1 or GST-Fn9.11.

Previously, α2β1-integrin has been shown to mediate CAMDR in T-ALL (Naci et al., 2012). Here, my results show that ligation via α4β1-integrin or α5β1-integrin could also mediate CAMDR in Jurkat T cells. Since α2, α4 and α5 are all expressed as heterodimers with β1-integrins in Jurkat cells, CAMDR appears to be a phenomenon that is applicable to multiple β1-integrins. It was also reported that adhesion via αLβ2-integrin (also known as LFA-1) can also promote CAMDR in multiple myeloma (Schmidmaier and Baumann, 2008; Winter et al., 2001). To address the possibility that Jurkat cell adhesion via αLβ2 can also promote CAMDR, WT cells were seeded on the αLβ2-integrin substrate, ICAM-1. As expected, the fraction of apoptotic WT cells seeded on ICAM-1 and treated with doxorubicin was lower than those seeded on the control substrate, BSA (Figure 3.1B). I noted that WT cells seeded on both ICAM-1 and GST-CS1 showed similar resistance to apoptosis with doxorubicin treatment, indicating that CAMDR in Jurkat T cells can be mediated by multiple integrins including α4β1-, α5β1- or αLβ2-integrins.

To confirm the contribution of α4-integrin to CAMDR, I made use of the JB4 Jurkat-derivative cell line (Rose et al., 2003) which lacks α4-expression (referred to as $\alpha4^{-/-}$ from here on), and $\alpha4^{wt}$ cells, which are JB4 cells stably reconstituted with α4-expression. These cells were seeded on GST-CS1 and treated with doxorubicin, resulting in a higher percentage of apoptosis in $\alpha4^{-/-}$ cells compared to $\alpha4^{wt}$ cells (Figure 3.2). The chemoresistance exhibited by $\alpha4^{wt}$ cells is directly attributed to α4-integrin function since $\alpha4^{-/-}$ cells lack α4-integrin expression and thus cannot adhere to the α4-specific ligand, GST-CS1.

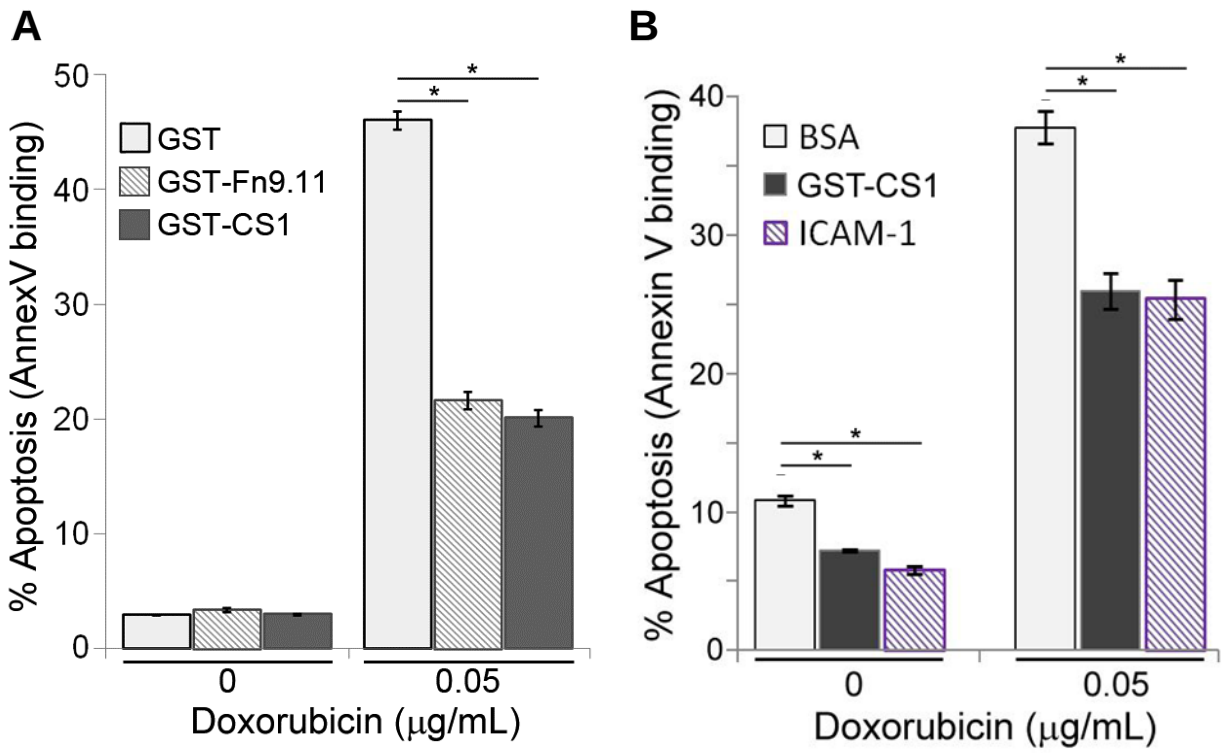

Figure 3.1. Adhesion on integrin substrates confers enhanced resistance to doxorubicin in Jurkat T cells

Wildtype Jurkat cells were seeded on (*A)* dishes coated with GST-CS1, GST-Fn9.11 or GST or (*B)* dishes coated with GST-CS1, ICAM-1 or BSA for 4 hours, followed by treatment with the indicated concentration of doxorubicin for 48 hours. Flow cytometry was used to assess the percentage of total cells undergoing apoptosis as labeled by Annexin V binding. The bars show the mean ± S.D.; n=3 replicates; *p<0.01.

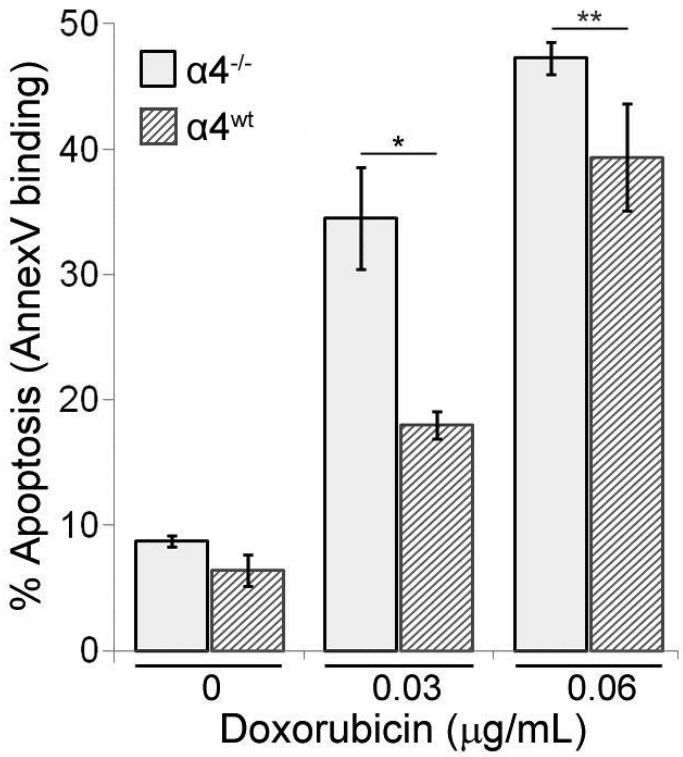

Figure 3.2. Adhesion mediated via α4-integrin confers enhanced resistance to doxorubicin $\alpha4^{wt}$ and $\alpha4^{-/-}$ cells were seeded on dishes coated with GST-CS1 for 4 hours, followed by treatment with the indicated concentration of doxorubicin for 48 hours. Flow cytometry was used to assess the percentage of total cells undergoing apoptosis as labeled by Annexin V binding. The bars show the mean ± S.D.; n=3 replicates; *p<0.02; **p<0.05.

3.3 α4-integrin with a Truncated Cytoplasmic Domain Exhibits Adhesion-Independent Chemoresistance

The adhesion phenotypes for specific integrins are dependent on the individual cytoplasmic tail sequences and their interacting proteins. In instances when integrin heterodimers share a common subunit, such as α4β1 and α5β1, then the adhesion phenotype is determined by the α-integrin cytoplasmic domain (Kassner and Hemler, 1993). One of the best studied α-integrin cytoplasmic domain interactions is that of α4-integrin. In this regard, the α4-tail interacts with proteins including paxillin, Type I PKA, and non-muscle Myosin IIA to control cell

adhesion and migration (Lim et al., 2007; Liu et al., 1999; Rivera Rosado et al., 2011). The α4-integrin cytoplasmic tail is also required for α4β1-mediated adhesion to extracellular ligands (Kassner et al., 1994).

To determine the requirement of the α4-integrin cytoplasmic tail in supporting α4-mediated CAMDR, the tail-truncated variant α4δ was constructed (Figure 3.3A). α4δ retained the complete extracellular and transmembrane domain of α4 and the minimal α4-tail encoding only the juxtamembrane KAGFFKR sequence. This motif is essential for heterodimerization with β1-integrin and for maintaining surface α4-expression; thus it cannot be deleted, further truncated, or altered (Kassner et al., 1994). $\alpha4^{-/-}$ cells were transfected and selected to stably express $\alpha4^{wt}$ or α4δ, and further sorted by flow cytometry to obtain cells with a comparable surface expression between $\alpha4^{wt}$ and α4δ (Figure 3.3B). Compared to the parental $\alpha4^{-/-}$ cells, $\alpha4^{wt}$ and α4δ cells have a higher β1-integrin expression (Figure 3.3B), which indicates that the expressed α4 or α4δ formed heterodimers with β1-integrin. Neither $\alpha4^{wt}$ nor α4δ cells were compared directly to WT cells in subsequent experiments, which trivialized the lower α4-integrin and β1-integrin expression levels obtained on $\alpha4^{wt}$ and α4δ cells. Periodic measurements conducted throughout experimentation with these cells revealed no significant differences in the expression levels of integrins α4, α4δ, and β1, indicating their expression was stable. I also observed no significant differences in the general morphology for Jurkat, $\alpha4^{-/-}$, $\alpha4^{wt}$ and α4δ cell lines cultured under standard conditions (Figure 3.4).

To determine the ligand binding properties of $\alpha4^{-/-}$, $\alpha4^{wt}$, and α4δ cells, I performed a cell adhesion assay using the substrates GST-CS1, GST-Fn9.11 and GST (Figure 3.5). $\alpha4^{-/-}$, $\alpha4^{wt}$ and α4δ cells adhered to GST-Fn9.11 and not to the control GST substrate. Unlike $\alpha4^{wt}$ cells, $\alpha4^{-/-}$ and α4δ did not adhere to the α4β1-specific substrate GST-CS1. This result is in agreement with

similar tail-truncation work done by others which also showed that the deleted portion of α4-tail is required to support adhesion (Kassner et al., 1994).

Since CAMDR requires adhesion mediated via integrins, and α4δ expression failed to support adhesion to GST-CS1, I evaluated the impact of α4δ expression on drug resistance in the presence and absence of cell adhesion. Cells were seeded on the various substrates, treated with doxorubicin and the % of apoptotic cells determined. Consistent with their adhesion properties, cells showed significantly reduced apoptosis when seeded on substrates that they can adhere to, in this case, $\alpha4^{-/-}$ cells seeded on GST-Fn9.11, and $\alpha4^{wt}$ cells seeded on GST-CS1 or GST-Fn9.11 (Figure 3.6). Interestingly, $\alpha4^{wt}$ cells seeded on GST exhibited slightly less doxorubicin-induced apoptosis compared to $\alpha4^{-/-}$, suggesting that $\alpha4^{wt}$-expression alone can mediate a weaker drug resistance without adhesion. More importantly, α4δ cells seeded on GST-CS1 or GST, which does not support their adhesion, showed low levels of apoptosis comparable to cells that were adhered through integrins (Figure 3.6). Thus, α4δ cells exhibited a form of chemoresistance that is independent of integrin-mediated adhesion.

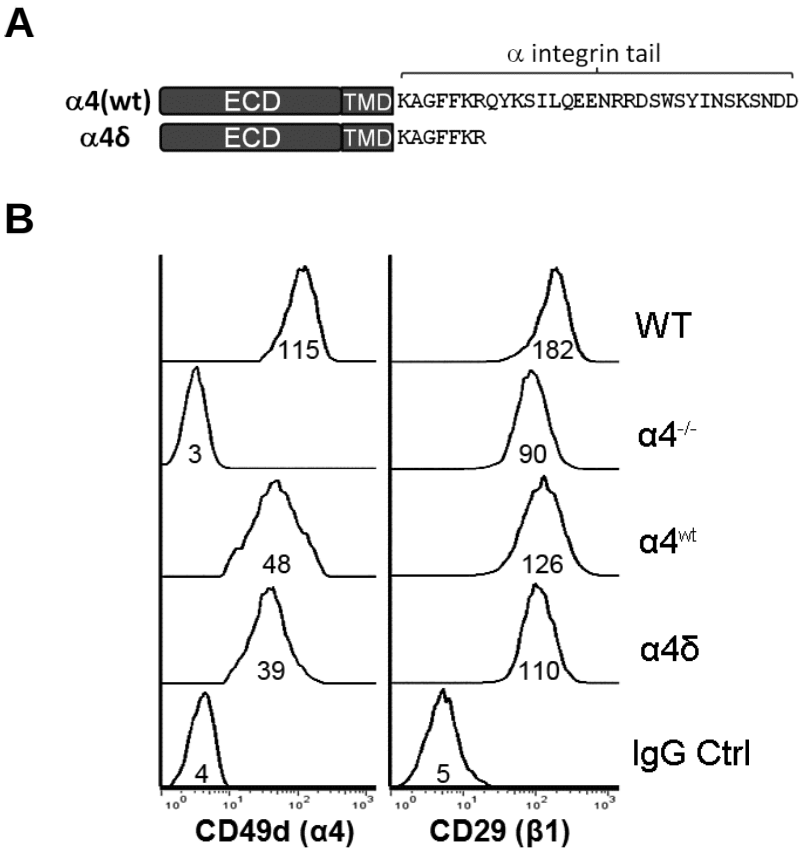

Figure 3.3. Schematic and expression of the α4-tail truncated variant, α4δ

(A) Schematic of α4-integrin and truncated α4-integrin (α4δ) used depicting the cytoplasmic domain sequences. α4δ is truncated as indicated and retains the KAGFFKR portion of the cytoplasmic tail. ECD denotes the extracellular domain and TMD denotes the transmembrane domain. (*B)* Flow cytometry determination of cell surface integrin α4 and β1 expression in WT, $\alpha4^{-/-}$, $\alpha4^{wt}$, and α4δ cells. Numbers under the histograms show the median fluorescence intensity. To ensure the stable expression of α4-integrin and β1-integrin, routine measurements were conducted that found no significant differences in expression.

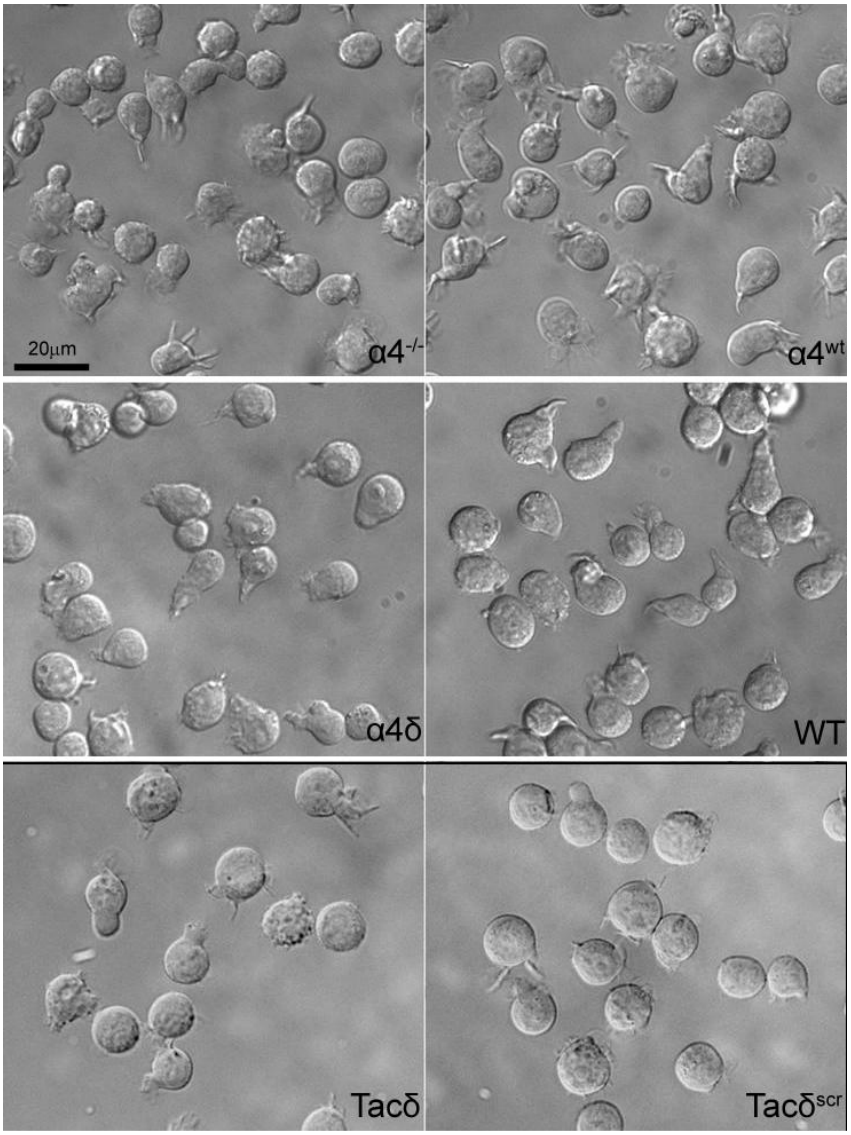

Figure 3.4. Cell morphology

Representative differential interference contrast images of WT, $\alpha4^{-/-}$, $\alpha4^{wt}$, α4δ, Tacδ and $Tac\delta^{scr}$ cell lines. Tacδ is a fusion of Tac (human CD25 amino acids 1-263) to the α4-integrin motif, KLGFFKR. As a control for Tacδ, $Tac\delta^{scr}$ is a fusion of Tac to the scrambled version of α4-integrin motif, which is KLRFGFK. The cultured cells were grown in suspension and imaged live in the absence of an adhesion substrate (non-adherent conditions). Bar: 20 μm.

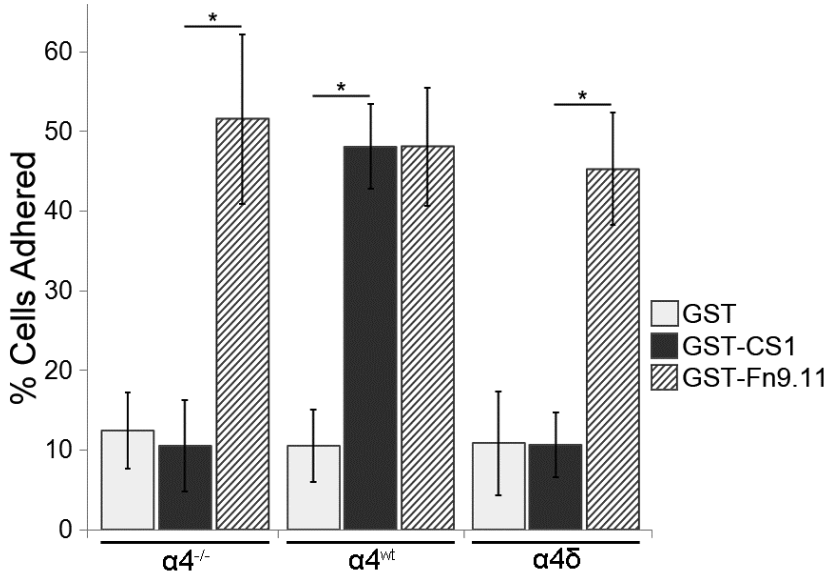

Figure 3.5. Adhesion assay for $\alpha4^{wt}$, α4δ, and $\alpha4^{-/-}$ cells plated on GST-CS1, GST-Fn9.11 and GST substrates

$\alpha4^{wt}$, α4δ, and $\alpha4^{-/-}$ cells were seeded for 30 minutes on dishes pre-coated with GST-CS1, GST-Fn9.11 or GST and then scored for adhesion as described in Methods. Briefly, images of cells were taken before and after physical agitation, and cells not displaced were scored as adherent. The percentage of total cells adhered were computed as an average from 12 fields of view (FOV) per cell type and treatment condition for one experiment. The bars show the mean ± S.D.; n=3; *p<0.0001.

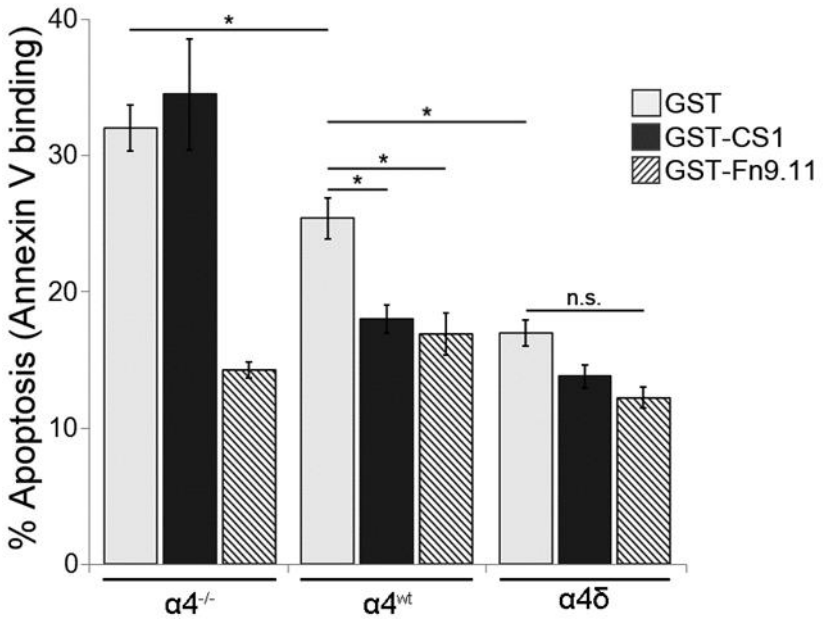

Figure 3.6. Drug resistance assay for $\alpha4^{wt}$, α4δ, and $\alpha4^{-/-}$ cells plated on GST-CS1, GST-Fn9.11 and GST substrates

$\alpha4^{wt}$, α4δ, and $\alpha4^{-/-}$ cells were seeded on dishes pre-coated with GST-CS1, GST-Fn9.11 or GST for 4 hours, followed by treatment with 0.03 μg/mL of doxorubicin for 48 hours. Flow cytometry was used to assess the percentage of total cells undergoing apoptosis as labeled by Annexin V binding. The bars show the mean ± S.D.; n=3; *p<0.02; ns, p not significant.

3.4 The Membrane-Proximal GFFKR Motif is Sufficient for Chemoresistance

Since the truncated cytoplasmic tail encoded by α4δ-integrin still allowed heterodimerization with β1-integrin as α4δβ1 (Figure 3.3B)(Kassner et al., 1994), the adhesion-independent chemoresistance observed with α4δ cells could be attributed either to the β1-integrin-mediated signals or to the α4δ-tail that carries the juxtamembrane GFFKR motif. To evaluate the observed chemoresistance in the absence of β1-integrin, I constructed chimeric receptor proteins termed Tacδ and $Tac\delta^{scr}$ (Figure 3.7A). Tac is the extracellular and transmembrane domains of CD25 with no cytoplasmic domain (Bodeau et al., 2001). Tacδ is a fusion of Tac to the C-terminal KLGFFKR peptide, while $Tac\delta^{scr}$ carries the scrambled

KLRFGFK version of the peptide. Notably, Tacδ is a monomer that does not heterodimerize with β1-integrin thus allowing the assessment of GFFKR-mediated effects that excludes the signal contributed by β1-integrin. $\alpha4^{-/-}$ cells were transfected and sorted to obtain cell lines that express comparable levels of Tacδ and $Tac\delta^{scr}$ (Figure 3.7B). Routine expression monitoring for the Tac epitope indicated the expression was stable and did not change over time. In terms of general morphology, Tacδ and $Tac\delta^{scr}$ cells were comparable and indistinguishable to the WT Jurkat and other cell lines described earlier (Figure 3.4). In apoptosis assays conducted in the absence of cell adhesion substrates, Tacδ, but not $Tac\delta^{scr}$ cells, exhibited low levels of doxorubicin-induced apoptosis comparable to α4δ cells (Figure 3.8), indicating that the membrane-proximal GFFKR motif is sufficient to promote an adhesion-independent form of chemoresistance.

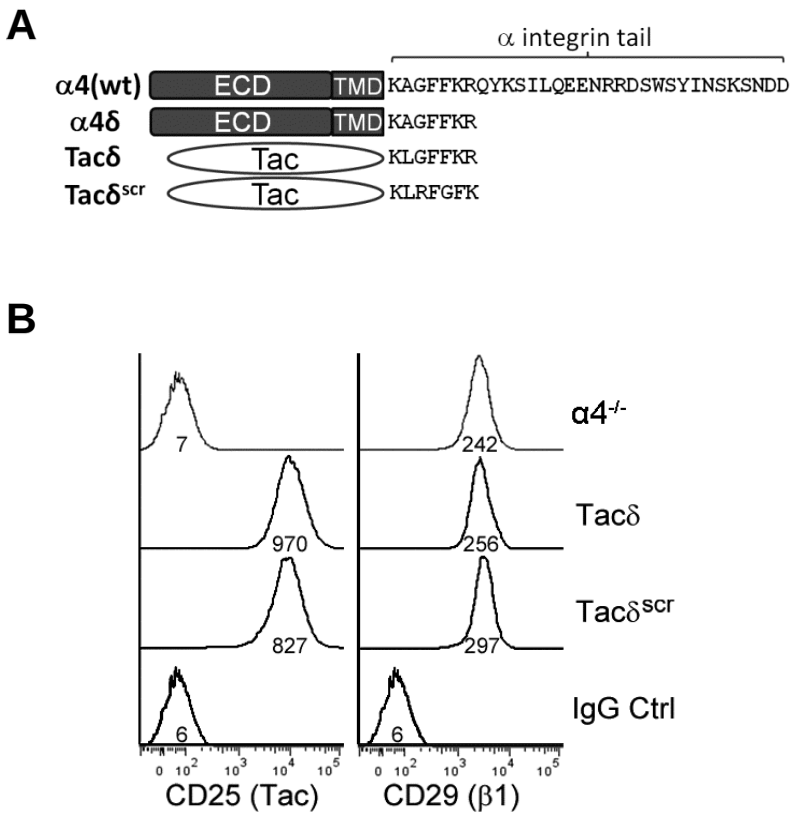

Figure 3.7. Schematic and expression of Tac and integrin receptors

(A) Schematic of fusion proteins containing the extracellular and transmembrane domains of the carrier epitope, Tac, in comparison with $\alpha4^{wt}$ and α4δ. Tacδ and $Tac\delta^{scr}$ are fusions of Tac with the cytoplasmic peptide, KLGFFKR, and the scrambled version, KLRFGFK, respectively. ECD is the extracellular domain while TMD is the transmembrane domain. (*B)* Flow cytometry determination of cell surface Tac and integrin β1 expression in Tacδ, $Tac\delta^{scr}$, and $\alpha4^{-/-}$ cells. Numbers under the histograms show the median fluorescence intensity. No significant difference was found during measurements that were conducted routinely to ensure the stable expression of Tacδ and $Tac\delta^{scr}$.

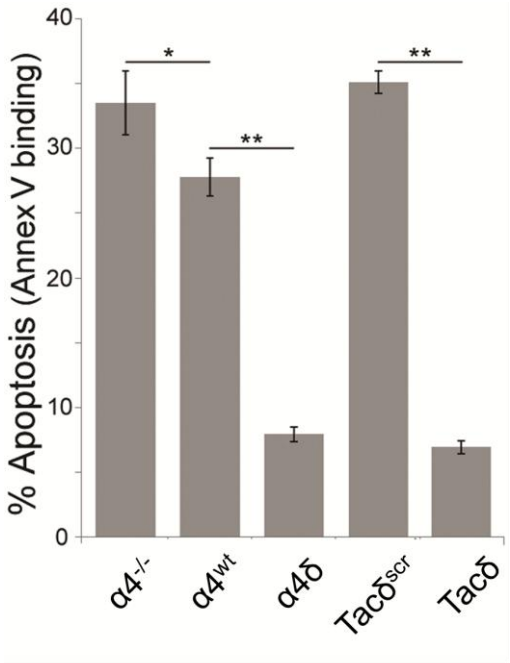

Figure 3.8. Expression of the membrane-proximal GFFKR motif confers enhanced chemoresistance in an adhesion-independent manner

$\alpha4^{wt}$, α4δ, $\alpha4^{-/-}$, Tacδ, and $Tac\delta^{scr}$ cells were seeded on GST-coated dishes for 4 hours, followed by treatment with 0.03 μg/mL of doxorubicin for 48 hours. Flow cytometry was used to assess the percentage of total cells undergoing apoptosis as labeled by Annexin V binding. The bars show the mean ± S.D.; n=3; *p<0.03; **p<0.01.

3.5 Expression of the GFFKR Motif as α4δ and Tacδ Activates Akt

Integrin-mediated cell adhesion leads to the activation of Akt (King et al., 1997). This phenomenon is implicated in promoting cell survival and increased cell proliferation (Song et al., 2005). To determine if Akt is involved in T-ALL CAMDR, I seeded cells on integrin substrates and performed Western blot analysis to detect phosphorylated Akt as an indicator of Akt activation. $\alpha4^{wt}$ cells seeded on GST-CS1 to engage α4-integrin showed increased levels of phospho(T308)-Akt at 40 and 60 minutes post-stimulation (Figure 3.9). In contrast, phospho(T308)-Akt levels were not changed for $\alpha4^{wt}$ cells seeded on the control GST substrate,

or for $\alpha4^{-/-}$ cells seeded on GST-CS1, indicating the requirement for integrin-substrate engagement to stimulate Akt phosphorylation.

To determine whether the adhesion-independent chemoresistance demonstrated by α4δ and Tacδ cells correlates with Akt phosphorylation, I compared phospho(T308)-Akt levels for the cell lines seeded on GST-CS1, GST-Fn9.11 or BSA. Consistent with the results obtained for doxorubicin-induced apoptosis, cells adhered on ligands that bind to the corresponding expressed integrins have increased phospho(T308)-Akt levels; in this case $\alpha4^{-/-}$ and $Tac\delta^{scr}$ on GST-Fn9.11, and $\alpha4^{wt}$ on GST-CS1 or GST-Fn9.11 (Figure 3.10). Furthermore, α4δ and Tacδ cells showed elevated levels of phospho(T308)-Akt independent of the substrate that they were seeded on (Figure 3.10).

Phosphorylation of Akt at both T308 and S473 sites is required for full activation of Akt kinase activity (Liu et al., 2014; West et al., 2003). To determine if GFFKR expression regulates Akt phosphorylation at both of these sites, I compared the lysates of non-adherent and adherent Tacδ or $Tac\delta^{scr}$ cells by Western blot analyses (Figure 3.11). As before, Tacδ cells showed constitutively high phospho(T308)-Akt levels in an adhesion-independent manner. In contrast, cell adhesion was required to upregulate phospho(S473)-Akt for both Tacδ and $Tac\delta^{scr}$ cells. Taken together, these results indicated that expression of the monomeric form of the membrane-proximal GFFKR motif leads to constitutive phosphorylation of Akt at T308, while phosphorylation of S473 remains adhesion-dependent.

Since the extent of the adhesion-independent phosphorylation of Akt in Tacδ cells is limited to the T308 site, I proceeded to determine if this was sufficient to promote the activity of Akt in Tacδ cells. Akt specifically recognizes the consensus sequence, RXRXXS*/T* as its phosphorylation target (Cardone et al., 1998). Lysates of Tacδ and $Tac\delta^{scr}$ cells were probed with

an antibody that recognizes phosphorylated Akt substrates (RXRXXS*/T*) as an indirect readout for Akt kinase activity. Under non-adherent conditions, Tacδ cells exhibited higher levels of Akt phospho-substrates compared to Tacδ^{scr} cells (Figure 3.12). Similarly, this enhanced level of Akt activation was also observed in WT cells that adhered to fibronectin when compared to non-adherent conditions (Figure 3.13).

Finally, to assess if the enhanced Akt activity mediates resistance to apoptosis, cells were treated with Akt inhibitor IV, which blocks Akt activation. I found that a higher concentration of Akt inhibitor IV was required to induce a comparable level of apoptosis in Tacδ cells when compared to Tacδ^{scr} cells (Figure 3.14). A higher concentration of Akt inhibitor IV was also required to reduce the Akt activity observed in lysates of Tacδ cells relative to Tacδ^{scr} cells (Figure 3.15). Taken together, the results indicated that integrin-mediated adhesion increases Akt phosphorylation and activation, and enhances resistance to apoptosis, while cells expressing the membrane-proximal GFFKR cytoplasmic tail bypass the adhesion requirement.

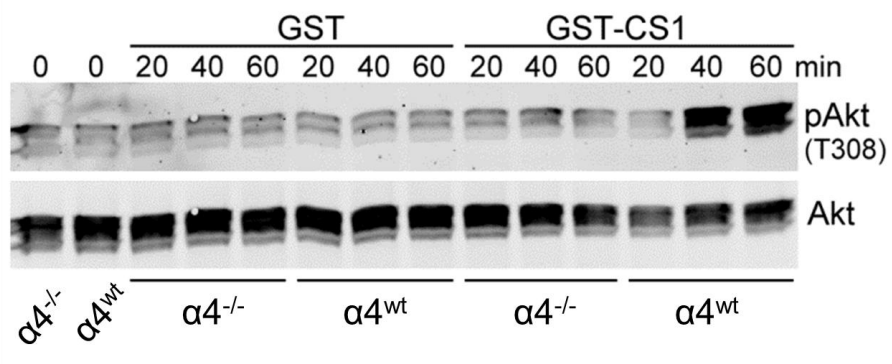

Figure 3.9. Adhesion through α4 integrin mediates Akt phosphorylation
α4^{wt} and α4$^{-/-}$ cells were seeded on dishes coated with GST or GST-CS1 for the indicated times, and cell lysates were immunoblotted to detect phospho(T308)-Akt and total Akt levels. The results shown are representative of more than 3 experiments.

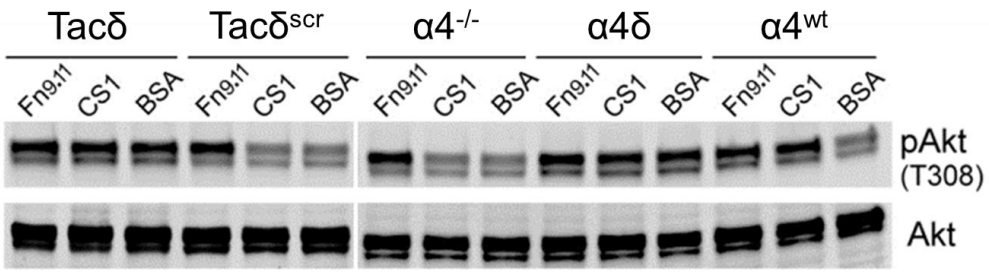

Figure 3.10. α4δ and Tacδ expression circumvent the requirement for cell adhesion mediated stimulation of Akt phosphorylation

Tacδ, Tacδ^{scr}, α4$^{-/-}$, α4^{wt} and α4δ cells were seeded on dishes coated with GST-CS1, GST-Fn9.11, or BSA for 45 minutes, and cell lysates were immunoblotted to detect phospho(T308)-Akt and total Akt levels. The results shown are representative of more than 3 experiments.

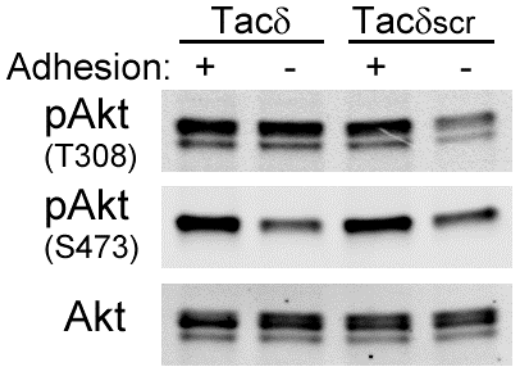

Figure 3.11. Tacδ expression mediates constitutive Akt phosphorylation at T308

Tacδ and Tacδ^{scr} cells were seeded on dishes coated with GST-Fn9.11 (adhesion +ve) or GST (adhesion -ve) for 45 minutes, and cell lysates were immunoblotted to detect phospho(T308)-Akt, phospho(S473)-Akt, and total Akt levels. The results shown are representative of more than 3 experiments.

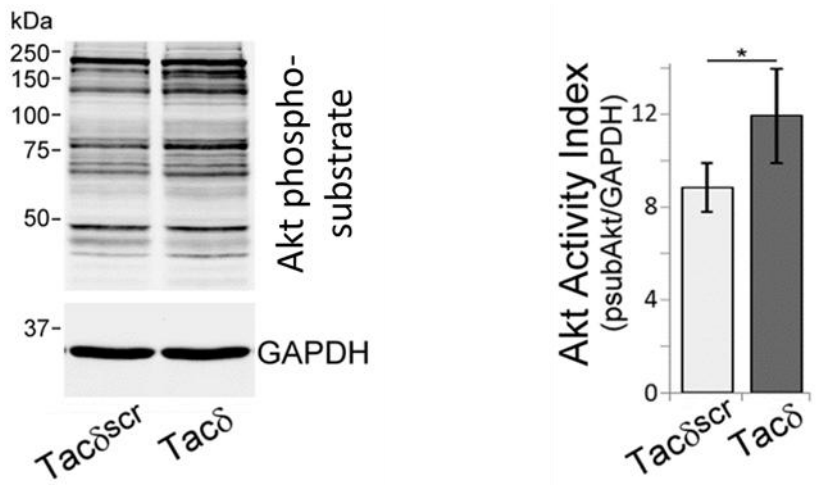

Figure 3.12. Tacδ expression promotes Akt activation

Lysates of Tacδ and Tacδ^{scr} cells were immunoblotted to detect Akt phospho-substrates and GAPDH. The Akt activation index was calculated as the total signal of Akt phospho-substrates divided by the signal of GAPDH. The bars show the mean ± S.D.; n=3 independent experiments; **p*<0.05.

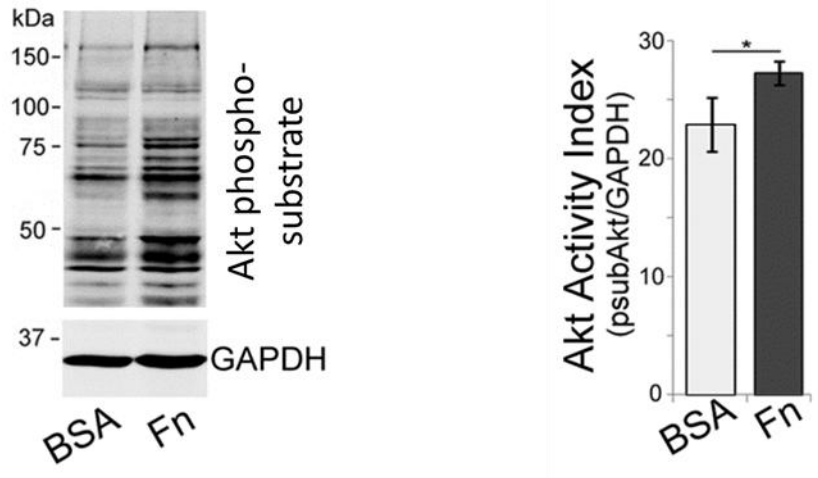

Figure 3.13. Cell adhesion to an integrin substrate promotes Akt activation

WT cells were seeded on dishes coated with BSA or fibronectin (Fn) for 30 minutes, and cell lysates were immunoblotted to detect Akt phospho-substrates and GAPDH. The Akt activation index was calculated as the total signal of Akt phospho-substrates divided by the signal of GAPDH. The bars show the mean ± S.D.; n=3 independent experiments; **p*<0.03.

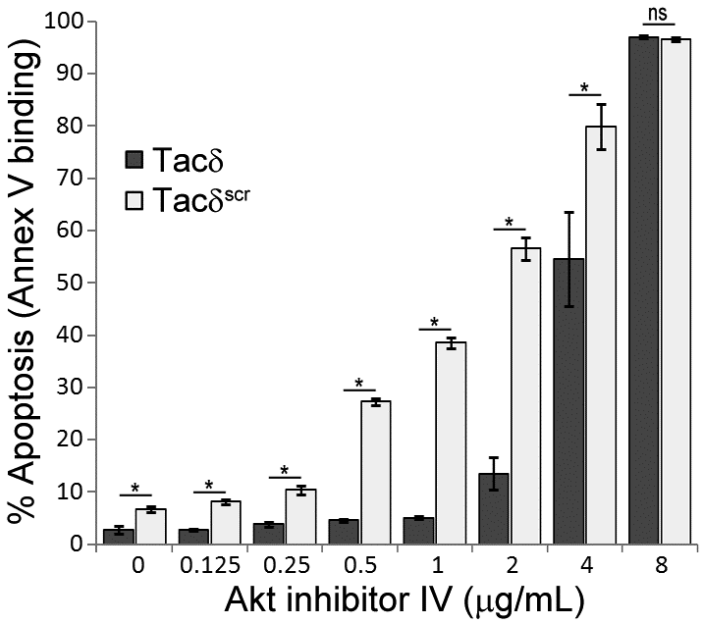

Figure 3.14. Induction of apoptosis in Tacδ cells requires a higher level of Akt inhibitor
Tacδ and Tacδ^{scr} cells were treated with Akt inhibitor IV at the indicated concentrations for 48 hours. Flow cytometry was used to assess the percentage of total cells undergoing apoptosis as labeled by Annexin V binding. The bars show the mean ± S.D.; n=3; *p<0.02; ns, p not significant.

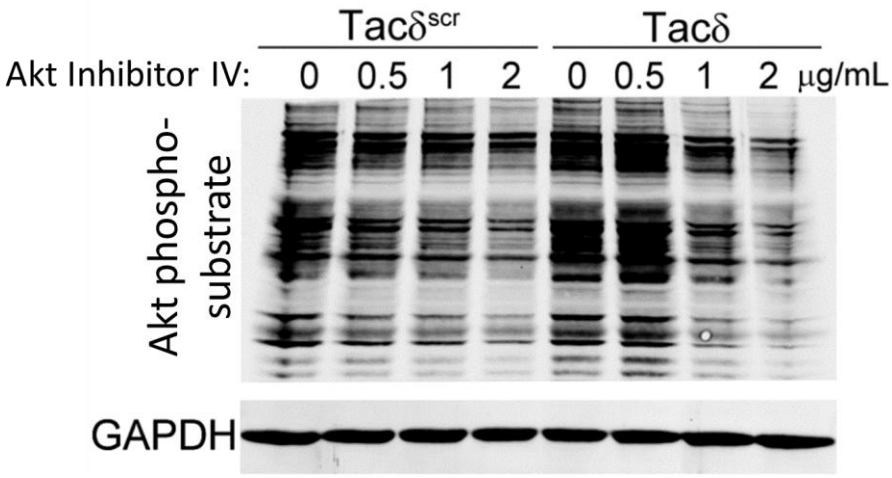

Figure 3.15. Inhibition of Akt activity in Tacδ cells requires a higher level of Akt inhibitor
Tacδ and Tacδ^{scr} cells were treated with Akt inhibitor IV at the indicated concentrations for 24 hours, and cell lysates were immunoblotted to detect Akt phospho-substrates and GAPDH. The results shown are representative of more than 3 experiments.

3.6 Integrin GFFKR Motif-Mediated Chemoresistance is Coupled with Calcium Influx

To interrogate the underlying mechanism responsible for the GFFKR motif-mediated drug resistance, I analyzed the literature for possible pathways. It has been shown that T-cell adhesion promotes the elevation of intracellular Ca^{2+} and that Ca^{2+} channel blocking agents can restore chemosensitivity of otherwise chemoresistant cells (Weismann et al., 1997; Xia and Smith, 2012). I then proceeded to explore the link between integrin-mediated chemoresistance and Ca^{2+} flux in CAMDR.

To measure intracellular Ca^{2+} levels, a cell permeant fluorescent Ca^{2+} indicator, Fluo-4-AM, was added to Tacδ, Tacδ^{scr}, α4$^{-/-}$, α4^{wt} and α4δ cells and assayed under non-adherent conditions. Aliquots of the Fluo-4-AM labeled cells were then incubated in media containing Ca^{2+}, or in Ca^{2+}-free media. The difference in cellular Fluo-4-AM fluorescence between the two conditions provided a measure of Ca^{2+} influx. I found that α4δ and Tacδ cells exhibited the highest levels of Ca^{2+} influx, α4^{wt} cells had intermediate Ca^{2+} influx, while α4$^{-/-}$ and Tacδ^{scr} cells had the lowest levels of Ca^{2+} influx (Figure 3.16). Thus, cells exhibiting adhesion-independent chemoresistance (Figure 3.8) also exhibited increased Ca^{2+} influx (Figure 3.16).

Next, I sought to determine the association between GFFKR-mediated chemoresistance and Ca^{2+} influx by blocking Ca^{2+} influx into Tacδ cells. I assessed the apoptotic index of cells treated with combinations of doxorubicin and EGTA (Figure 3.17). For this purpose, EGTA was used at a concentration sufficient to chelate all extracellular Ca^{2+}. I showed that blocking Ca^{2+} influx with EGTA increased the apoptotic index of doxorubicin-treated Tacδ^{scr} cells by 2-fold over that of doxorubicin treatment alone. In contrast, EGTA treatment increased the apoptotic index of the chemoresistant Tacδ cells by 9-fold over that of doxorubicin treatment alone.

As an alternative to chelating the extracellular Ca^{2+}, the L-type Ca^{2+} channel inhibitor, verapamil, was used to determine if the chemoresistance-coupled Ca^{2+} influx in T-ALL is mediated via L-type Ca^{2+} channels (Figure 3.18). At a concentration that blocked ~70% of extracellular Ca^{2+} influx, verapamil enhanced the chemosensitivity of Tacδ cells to doxorubicin by 21-fold over that of doxorubicin alone, while that of the already chemosensitive $Tac\delta^{scr}$ cells only increased by 1.5-fold. These results suggest that blocking extracellular Ca^{2+} influx via L-type channel increased the chemosensitivity of T-ALL cells that are otherwise chemoresistant.

It has been reported that integrin-mediated cell adhesion can promote the elevation of intracellular Ca^{2+} (Sjaastad and Nelson, 1997; Weismann et al., 1997). Along this line of thought, I determined if integrin engagement is sufficient to stimulate increases in intracellular Ca^{2+} in WT Jurkat cells. WT cells pre-labeled with Fluo-4-AM were seeded onto substrate-coated dishes, and fluorescence was monitored over time (Figure 3.19). As expected, the cells exhibited comparable fluorescence at t=0 in all conditions, reflecting the comparable quantity of cells seeded and before significant adhesion had occurred. Over the next 35 minutes, cells seeded on GST-CS1 or fibronectin had significantly higher intracellular Ca^{2+} levels compared to cells seeded on BSA. No changes in intracellular Ca^{2+} were observed when EGTA was added to chelate extracellular Ca^{2+}, indicating that integrin-mediated adhesion promoted the influx of extracellular Ca^{2+} into cells.

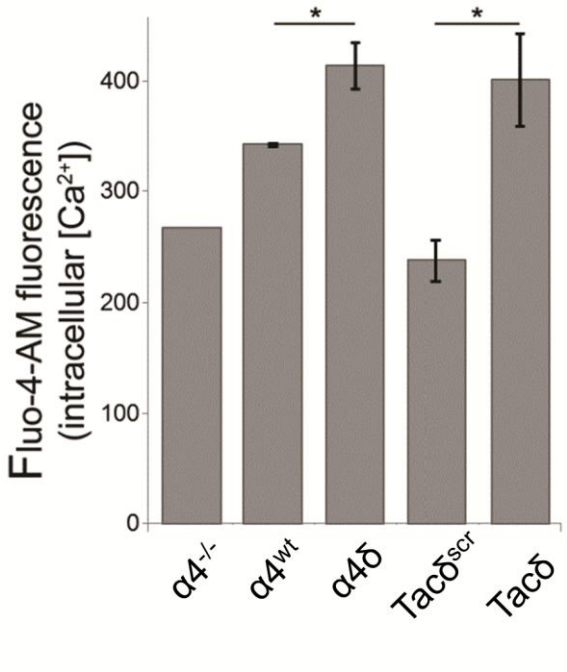

Figure 3.16. Intracellular Ca^{2+} measurements of cells by flow cytometry

Tacδ, Tacδ^{scr}, α4$^{-/-}$, α4^{wt} and α4δ cells were labeled with Fluo-4-AM as described in Methods and incubated in PBS with or without 1 mM $CaCl_2$ at 22^{o}C for 10 minutes prior to measurements. Flow cytometry was used to assess the concentration of intracellular Ca^{2+} as indicated by Fluo-4-AM fluorescence. Plotted are the intracellular calcium measurements obtained from cells in 1 mM $CaCl_2$/PBS after subtracting measurements obtained from cells in PBS alone (mean ± S.D.; n=4; *p<0.01).

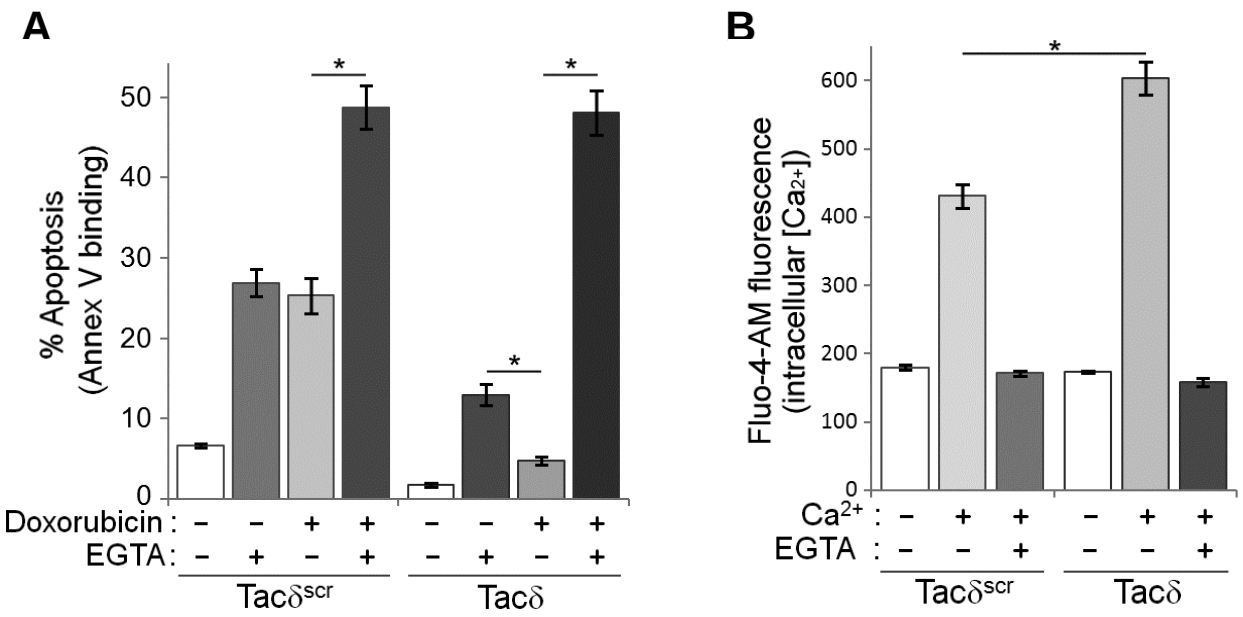

Figure 3.17. Sequestration of extracellular Ca^{2+} attenuates chemoresistance to doxorubicin
(A) Tacδ and Tacδ^{scr} cells were treated with combinations of 0.04 µg/ml doxorubicin and 0.6 mM EGTA for 48 hours. Flow cytometry was used to assess the percentage of total cells undergoing apoptosis as labeled by Annexin V binding. As plotted is the mean ± S.D.; n=4; **p*<0.001. (*B)* Tacδ and Tacδ^{scr} cells were labeled with Fluo-4-AM and incubated with combinations of 1 mM Ca^{2+} and 0.6 mM EGTA at 22^{o}C for 10 minutes. Flow cytometry was used to assess the concentration of intracellular Ca^{2+} as indicated by Fluo-4-AM fluorescence. The bars show the mean ± S.D.; n=3; **p*<0.03.

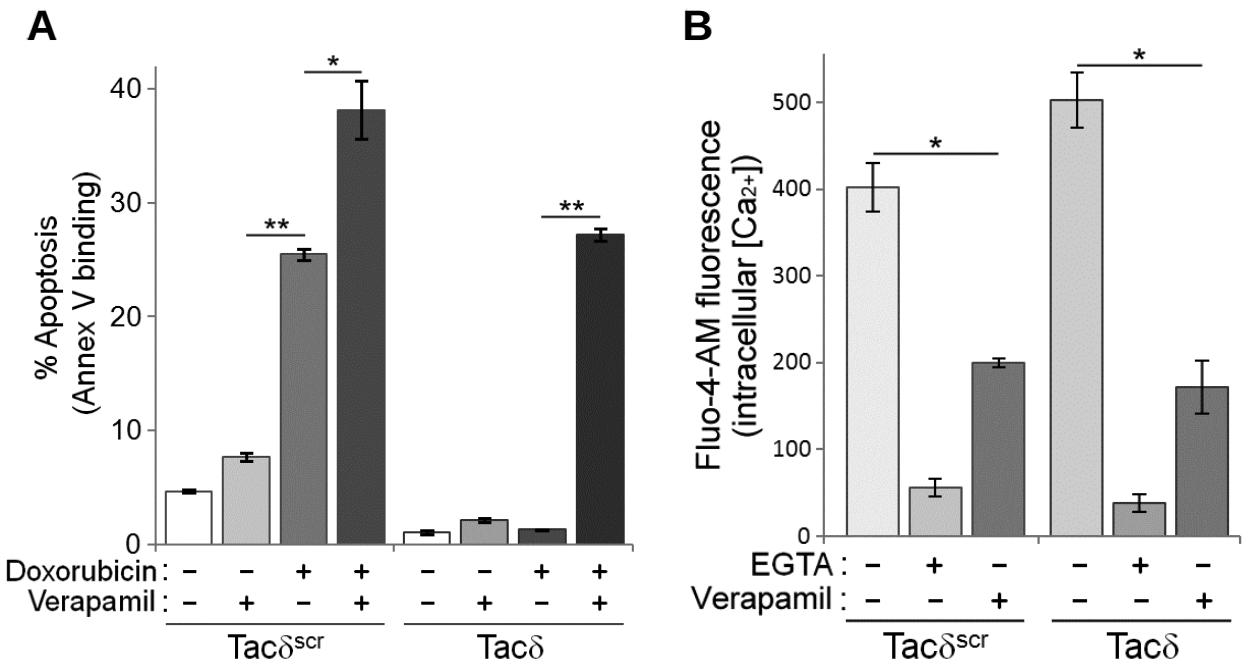

Figure 3.18. Blockade of L-type calcium channels with verapamil attenuates chemoresistance to doxorubicin

(A) Tacδ and Tacδ^{scr} cells were treated with combinations of 0.03 μg/mL doxorubicin and 60 μM verapamil for 48 hours. Flow cytometry was used to assess the percentage of total cells undergoing apoptosis as labeled by Annexin V binding. As plotted is the mean ± S.D.; n=3; **p*<0.002, ***p*<0.0001. *(B)* Tacδ and Tacδ^{scr} cells were labeled with Fluo-4-AM and incubated with 1 mM Ca^{2+} and either 0.6 mM EGTA or 60 μM verapamil at 22^{o}C for 10 minutes. Flow cytometry was used to assess the concentration of intracellular Ca^{2+} as indicated by Fluo-4-AM fluorescence. The bars show the mean ± S.D.; n=3; **p*<0.001.

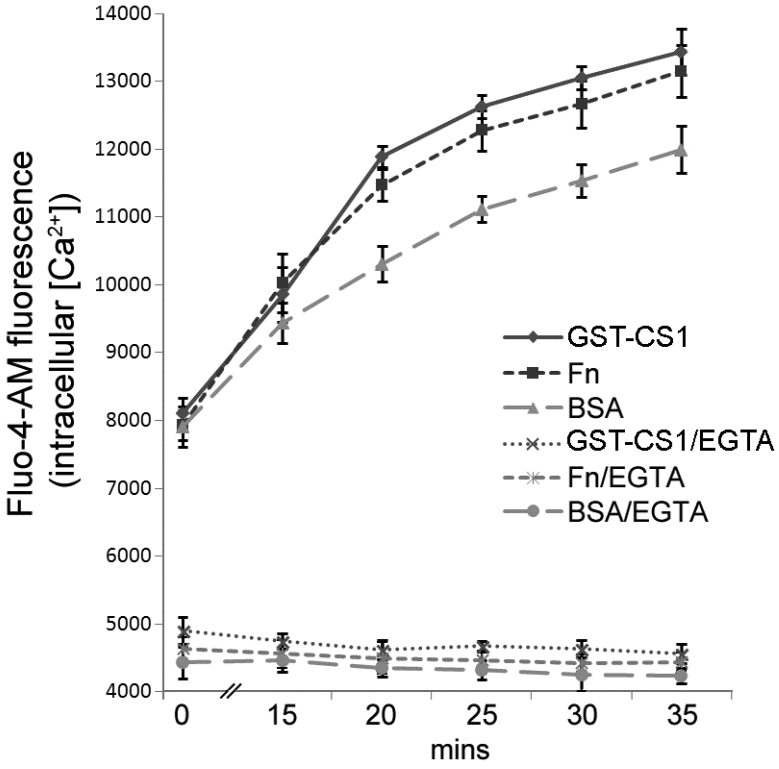

Figure 3.19. Cell adhesion promotes increases in intracellular Ca^{2+}
Fluo-4-AM labeled WT cells were seeded on dishes coated with GST-CS1, fibronectin (Fn) or BSA with and without EGTA added to the extracellular media. Fluo-4-AM fluorescence was measured at the indicated times following cell seeding. The data points show the mean ± S.D.; n=5; $p<0.01$ for t=20-35 minutes for Fn versus BSA; *p* not significant for t=0-15 minutes for Fn versus BSA; *p* not significant for EGTA treated conditions.

3.7 GFFKR Motif-Mediated Chemoresistance is Coupled with Drug Efflux

One of the mechanisms contributing to chemoresistance is the enhanced expression and activity of drug efflux transporters. A recent study reported that β1-integrin-mediated Jurkat cell adhesion increased the expression of the p-glycoprotein transporter, MRP1, and decreased the intracellular accumulation of doxorubicin (El Azreq et al., 2012).

To determine if the GFFKR motif-mediated adhesion-independent chemoresistance observed in Tacδ cells can be attributed to changes in drug efflux activity, Tacδ and $Tac\delta^{scr}$ cells

were incubated with calcein-AM, an indicator substrate used to assess the activity of certain p-glycoprotein-based transporters, including MRP1. I found that Tacδ cells accumulate fluorescent calcein at a significantly lower rate than Tacδ^{scr} cells, indicating that Tacδ expression led to enhanced efflux of calcein-AM (Figure 3.20).

Since doxorubicin has an inherently high level of fluorescence, I measured the fluorescence of doxorubicin present in the media as an indicator of drug efflux over time. Cells were incubated with, and then washed free of, extracellular doxorubicin before being incubated in fresh buffer supplement with or without Ca^{2+}. The release of cellular doxorubicin back to the buffer was assayed by measuring the fluorescence of the cell-free supernatant. When incubated in the Ca^{2+}-supplemented buffer, the supernatants of Tacδ cells accumulated a significantly higher level of doxorubicin when compared to those of Tacδ^{scr} cells (Figure 3.21). In contrast, incubation of Tacδ cells in a Ca^{2+}-free buffer led to lower rates of doxorubicin efflux compared to Tacδ cells in Ca^{2+}-supplemented buffer (Figure 3.21), indicating that available extracellular Ca^{2+} is an important modulator of doxorubicin efflux. Taken together, these findings showed that GFFKR expression leads to chemoresistance to doxorubicin in a manner that is correlated with enhanced Ca^{2+} influx and drug efflux.

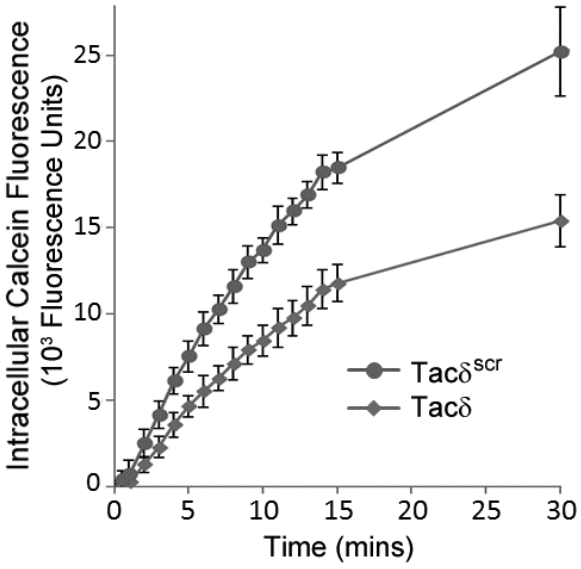

Figure 3.20. Effect of GFFKR expression on calcein efflux

Tacδ and Tacδ^{scr} cells were incubated with the cell permeant calcein-AM substrate, and fluorescence readings were taken at the indicated times. Non-fluorescent calcein-AM is hydrolyzed to the highly fluorescent calcein by intracellular esterases; thus the rate of calcein accumulation is an indirect and inverse measure of the cellular efflux rates of calcein-AM. The data points the show mean ± S.D.; n=4; p not significant for t<2 minutes; p<0.05 for 2<t<5 minutes; p<0.002 for t>5 minutes.

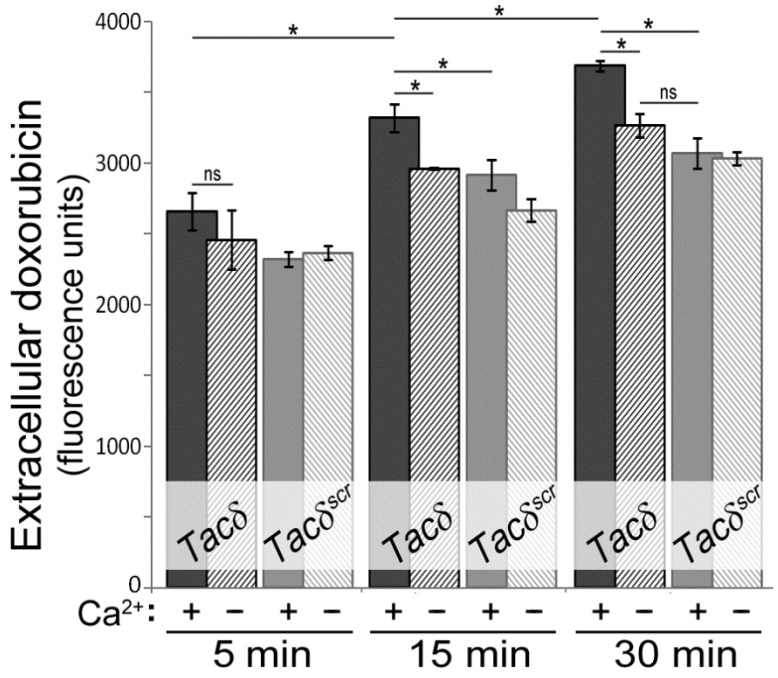

Figure 3.21. Effect of GFFKR expression on doxorubicin efflux
Tacδ and Tacδ^{scr} cells were incubated with 2 μg/mL doxorubicin for 2 hours at 37^{o}C prior to rinse and re-suspension in PBS with or without 1 mM Ca^{2+}. At the indicated times, cell-free supernatants were assessed for fluorescence as an indication of doxorubicin efflux from cells. The bars show the mean ± S.D.; n=3; *p<0.009; ns, p not significant.

3.8 Discussion

CAMDR contributes to minimal residual disease and relapse in hematological malignancies (Bradstock and Gottlieb, 1995; Matsunaga et al., 2003; Meads et al., 2009), and integrin function is a major contributor to CAMDR (Damiano et al., 1999; Hazlehurst et al., 2000a; Hazlehurst and Dalton, 2001; Hazlehurst et al., 2000b). My study describes the contribution of the juxtamembrane GFFKR cytoplasmic motif of α-integrins to chemoresistance in a T lymphoblast model. Using α4$^{-/-}$ cells reconstituted with wildtype α4-integrin, I confirmed that T cell CAMDR requires α4β1-mediated engagement with its substrate. CAMDR in T cells may be supported by other integrins as well, as T cells adhered through α4β1-, α5β1- or αLβ2-

integrin exhibited chemoresistance when plated to adhere on the corresponding substrates. $\alpha4^{-/-}$ cells expressing the mutant α4δ, where the cytoplasmic domain is truncated to the minimal GFFKR motif, revealed a form of chemoresistance that is adhesion-independent. Expression of the Tacδ non-integrin transmembrane fusion protein bearing GFFKR as the cytoplasmic domain also conferred an adhesion-independent chemoresistant phenotype. Thus, the GFFKR sequence conserved in α-integrins constitutes a common pro-survival regulatory motif.

As a major integrin expressed by hematopoietic cells, α4-integrin has been implicated in CAMDR of various hematologic malignancies (Damiano et al., 1999; de la Fuente et al., 2002; Gattei et al., 2008; Matsunaga et al., 2008; Matsunaga et al., 2003). However, the chemoresistance that is exhibited by cells adhering to substrates engaging other integrins including α5, α6, and α2, hints at the generality of this phenomenon (Damiano et al., 2001; De Toni-Costes et al., 2010; Naci et al., 2012; Yamakawa et al., 2012). A common denominator for these α-integrins is their pairing with β1, without which the adhesion receptor is incomplete. Another commonality is the conserved GFFKR motif found in nearly all of the human α-integrins; of which the α-tail sequences C-terminal to GFFKR are largely divergent (Abram and Lowell, 2009). Interactions involving the α4-tail have been characterized with reported effects on cell adhesion and migration (Lim et al., 2007; Liu et al., 1999; Rivera Rosado et al., 2011). I had anticipated abrogating CAMDR upon reconstituted expression of the tail-truncated α4δ. Although cell adhesion to the α4β1-specific substrate was predictably disrupted (Kassner et al., 1994), α4δ-expressing cells exhibited chemoresistance in the absence of integrin-mediated adhesion. The contribution of β1 (as α4δβ1) in adhesion-independent chemoresistance was negated upon expression of the monomeric fusion Tacδ construct, indicating that the GFFKR

motif is sufficient to promote chemoresistance normally stimulated by integrin-mediated adhesion.

Cells expressing the Tacδ construct provided an opportunity to assess the role of a conserved motif found in α-integrins in regulatory roles and survival signaling typically stimulated by adhesion. I found that T308-Akt is constitutively highly phosphorylated in the GFFKR-expressing cells exhibiting high levels of Ca^{2+} influx, while levels of phospho(S473)-Akt remains adhesion regulated. Importantly, higher phospho(T308)-Akt levels correlated with higher levels of Akt activity detected in lysates of non-adherent Tacδ cells, suggesting phospho(T308)-Akt as an important pro-survival event that is regulated downstream of the α-integrin GFFKR motif. My results are also consistent with the hypothesis postulated by other groups that the phosphorylation status of T308-Akt may be a more reliable indicator of Akt activity (Vincent et al., 2011), and may serve as a better prognosticator for certain tumor outcomes that include acute leukemias (Gallay et al., 2009).

The increased Ca^{2+} influx may also explain the adhesion-independent high levels of phospho(T308)-Akt and Akt activity that I observed in α4δ- and Tacδ-expressing cells, as well as in adhered cells expressing wildtype α4. As reported previously, the Ca^{2+}/calmodulin-dependent protein kinase kinase (CAMKK) can directly phosphorylate T308-Akt in a Ca^{2+}-dependent manner (Yano et al., 1998). This raises the interesting possibility that high levels of intracellular Ca^{2+} may sustain Akt activation following its initial activation via the classical PI3K-dependent processes (Vanhaesebroeck and Alessi, 2000). An interesting follow up study can include the inhibition or knockout of CAMKK to determine whether GFFKR motif mediated phosphorylation of Akt at T308 indeed involves CAMKK as the mediator.

Increases in intracellular Ca^{2+} levels stimulated by integrin-mediated adhesion have been reported in cell types that include myocytes and T-lymphocytes (Weismann et al., 1997; Wu et al., 2001). The Ca^{2+} increases appear to involve extracellular Ca^{2+} influx via L-type channels in the plasma membrane, as well as Ca^{2+} release from intracellular stores (Kwon et al., 2000). In my assays using Fluo-4-AM to measure free cytosolic Ca^{2+}, I observed that the availability of extracellular Ca^{2+} is an important determinant to obtaining the intracellular Ca^{2+} increases mediated by integrin signaling. Since extracellular Ca^{2+} is required to support integrin-mediated adhesion, I cannot conclude that adhesion-stimulated increases in intracellular Ca^{2+} can occur without extracellular Ca^{2+} influx. However, cells expressing α4δ or Tacδ did not require adhesion to promote the measured increases in intracellular Ca^{2+}, so long as extracellular Ca^{2+} is available. Verapamil was able to blockade Ca^{2+} influx associated with Tacδ expression, thus my findings are consistent with the involvement of L-type channels in α-integrin GFFKR motif-mediated Ca^{2+} transport.

Ca^{2+} influx has been associated with the drug efflux function mediated by p-glycoprotein transporters, and is thus a possible modulator of chemoresistance (Sulova et al., 2009). This relationship is complex, as the use of various Ca^{2+} indicators as well as Ca^{2+} channel inhibitors, such as verapamil, have revealed interactions with the p-glycoprotein transporters themselves. These interactions may become possible sources of complication. I attempted to control for these effects in my assays, as follows. Drug efflux was assessed using both the calcein-AM assay, as well as release of doxorubicin from cells. In both cases, enhanced efflux was obtained for cells expressing Tacδ. Fluo-4-AM, which is used to assess intracellular Ca^{2+}, may itself be a substrate for efflux by p-glycoproteins. However, my assay conditions revealed higher intracellular Fluo-4-AM fluorescence (and hence Ca^{2+}) for α4δ and Tacδ cells, thus any loss due to Fluo-4-AM

efflux is minimal. I assessed the contribution of Ca^{2+} influx to chemoresistance either by chelating extracellular Ca^{2+} with EGTA or by inhibiting L-type Ca^{2+} channels with verapamil. At concentrations that appreciably reduced Ca^{2+} influx, I was able to synergize the apoptotic inducing effects of doxorubicin. Thus, my results support a correlation between intracellular Ca^{2+} levels, drug efflux, and apoptosis.

It is now established from extensive structure-function based studies that activated integrins undergo conformational changes that include the physical separation of the cytoplasmic domains of α- and β-integrins (Abram and Lowell, 2009; Kim et al., 2011). Such conformational changes allow the binding of signaling and structural proteins to the otherwise inaccessible cytoplasmic domains of α- and β-integrins. Extrapolating from the available evidence, I postulate that for cells expressing the minimal GFFKR motif (α4δ and Tacδ), GFFKR is potentially accessible for binding to a pro-survival factor in the absence of adhesion. For cells expressing full-length α4-, α5-, or αL-integrins, structural changes within the integrin dimer accompanying integrin-mediated adhesion may facilitate the increased association. Ca^{2+} influx may be mediated via L-type channel activation, triggering Akt-mediated pro-survival signaling and in the case for chemoresistance, increased drug efflux. Thus, cell adhesion via integrins forms a switch for activation of pro-survival signaling and chemoresistance.

Chapter 4: Integrin Modification of Tumor Immunogenicity

4.1 Overview and Rationale

To carry out the work described in Chapter 3, I had constructed several cell lines based on Jurkat T-lymphoblasts that express $\alpha4^{wt}$ or the mutant form, α4δ, in which the cytoplasmic tail was truncated to retain only the α-integrin membrane-proximal GFFKR motif. Expression of GFFKR as α4δ and as Tacδ promoted chemoresistance to doxorubicin, activation of Akt and influx of Ca^{2+} in a manner independent of cell adhesion. I also showed that these events are normally triggered in cells expressing non-mutated integrins when presented with integrin adhesion substrates. These findings suggest the importance of the α-integrin GFFKR motif in transmitting cell adhesion-mediated pro-survival signaling.

To infer the possible mechanisms responsible for the GFFKR-mediated chemoresistance, I evaluated the literature for α-integrin GFFKR-interacting proteins. Calreticulin (CRT), a ubiquitous multi-functional Ca^{2+} binding protein, was identified as a favored candidate since CRT is implicated in the regulation of apoptosis, integrin-mediated adhesion, focal adhesion assembly, adhesion-mediated Ca^{2+} influx, and associates with several α-integrins (Bastianutto et al., 1995; Coppolino et al., 1995; Coppolino and Dedhar, 1999; Coppolino et al., 1997; Dedhar, 1994; Du et al., 2009; Dupuis et al., 1993; Fadel et al., 1999; Fadel et al., 2001; Gelebart et al., 2005; Goicoechea et al., 2000; Gold et al., 2010). Although originally discovered as an ER resident protein, the presence of CRT on the cell surface during immunogenic cell death (ICD) is a widely accepted phenomenon (Green et al., 2009; Kepp et al., 2009; Kroemer et al., 2013; Obeid et al., 2007; Tesniere et al., 2008). Certain cancer treatments and chemotherapeutics induce the translocation of CRT from the ER lumen to the cell surface where it marks the CRT-

presenting cell for engulfment by macrophages (Green et al., 2009; Kepp et al., 2009; Kroemer et al., 2013; Obeid et al., 2007; Tesniere et al., 2008). Studies have shown that CRT may flip between the inner plasma membrane leaflet and outer plasma membrane leaflet in association with phosphatidylserine (PS) (Kepp et al., 2010; Païdassi et al., 2011). Thus, as the α-integrin GFFKR motif was postulated to interact with CRT, it is plausible that this interaction occurring at the inner plasma membrane may impact the cell surface presentation of CRT at the outer plasma membrane. The work described in this chapter was carried out to assess the role of integrin-regulated cell surface localization of CRT in controlling the immunogenicity of tumor cells that are undergoing ICD.

4.2 α-integrin Associates with Calreticulin through the GFFKR Motif

I first determined if the expression of various constructs affected total CRT levels, since cell sensitivity to chemotherapeutics can be modulated by changes in total CRT (Nakamura et al., 2000). By Western blot analyses, I found comparable total CRT levels in the cell lines used in my experiments (Figure 4.1), suggesting that the phenotypes observed thus far were not due to gross changes in total CRT. To determine if CRT interacts with GFFKR, Jurkat WT cell lysates were incubated with matrix-immobilized GST-KLGFFKR or GST-KLRFGFK fusion proteins. CRT was detected at higher levels in a complex with GST-KLGFFKR, indicating the specificity of the interaction (Figure 4.2). To determine if CRT interacts with α4-integrin, I performed co-immunoprecipitation assays using lysates derived from cells under non-adherent conditions. I detected much higher levels of CRT co-immunoprecipitating with α4δ than with α4 (Figure 4.3.A). In a similar fashion, higher levels of CRT co-immunoprecipitated with Tacδ compared to Tacδ^{scr} (Figure 4.3.B). Since cells expressing wildtype α4 exhibited enhanced Akt signaling and

chemoresistance only in the adherent state, I determined if plating cells on an adhesion substrate may result in an increased association of CRT with α4. Plating of WT cells either on GST-CS1 or on fibronectin promoted an increased interaction of CRT with immunoprecipitated α4 (Figure 4.4). Thus, CRT associates with the truncated α4δ in a manner requiring the GFFKR peptide motif, and cell adhesion acts as a stimulus to enhance the interaction of CRT with wildtype α4.

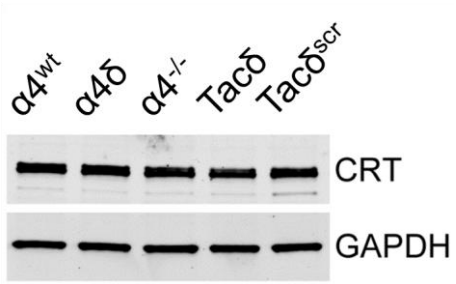

Figure 4.1. Total CRT expression in various Jurkat-based cell lines
Comparison of total CRT expression in lysates of $\alpha4^{wt}$, α4δ, $\alpha4^{-/-}$, Tacδ and $Tac\delta^{scr}$ cells by Western blotting. Equal protein loading was assessed by immunoblotting for GAPDH. The results shown are representative of more than 3 experiments.

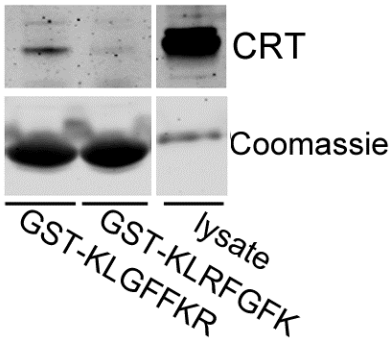

Figure 4.2. Pulldown of calreticulin with matrix-immobilized GFFKR protein
Affinity chromatography using matrix immobilized GST-KLGFFKR or GST-KLRFGFK (scrambled) recombinant proteins incubated with Jurkat cell lysates. Binding of CRT was assessed by Western blotting. Loading of the GST recombinant proteins was visualized by Coomassie Blue staining. The results shown are representative of more than 3 experiments.

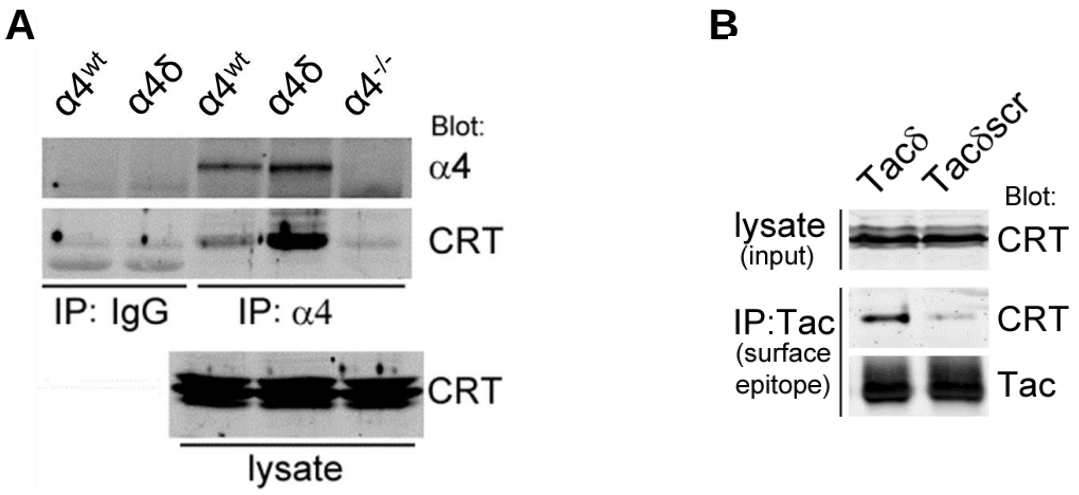

Figure 4.3. Detection of calreticulin in immunoprecipitates of α4-integrin and Tacδ
(A) Lysates of $\alpha4^{wt}$, α4δ, and $\alpha4^{-/-}$ cells were incubated with an α4-surface epitope antibody or IgG control, and the co-immunoprecipitated proteins detected with antibodies against CRT and α4 by Western blotting. *(B)* Tacδ and $Tac\delta^{scr}$ cell lysates were immunoprecipitated with a Tac-surface epitope antibody, and associated proteins detected with antibodies against CRT and Tac. The results shown are representative of more than 3 experiments.

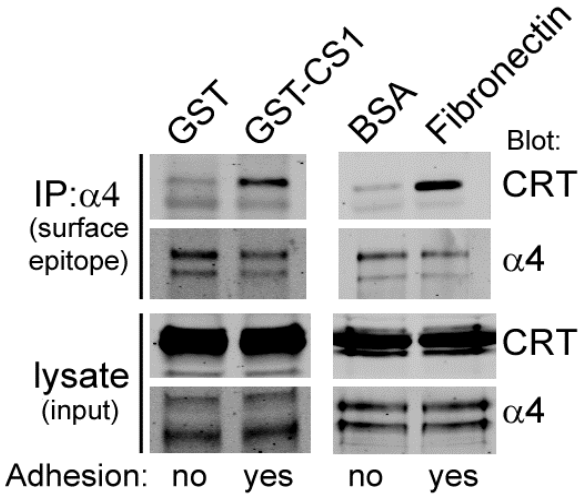

Figure 4.4. Effect of cell adhesion on α4-integrin and calreticulin interaction
WT cells were seeded on dishes coated with GST-CS1 (adhesion), GST (no adhesion), fibronectin (adhesion), or BSA (no adhesion). The adhesion status was assessed visually. After 45 minutes, cell lysates were prepared, incubated with an α4-surface epitope antibody and the co-immunoprecipitated proteins detected with antibodies against CRT and α4 by Western blotting. The results shown are representative of more than 3 experiments.

4.3 Doxorubicin Induces Cell Surface Calreticulin Presentation in Jurkat T-lymphoblasts

To study the possible contribution of CRT in chemoresistance and ICD in T-lymphoblasts, I constructed a Jurkat (WT) derivative CRT knockout cell line ($CRT^{-/-}$) using the CRISPR-Cas9 gene editing system (Cong et al., 2013). Western blot analysis and sequencing of the genomic *CALR* loci showed a complete loss of CRT expression due to a targeted frameshift insertion resulting in a predicted early translation termination (Figure 4.5). I will address the contribution of CRT to chemoresistance in Chapter 5 of this thesis. In this chapter, I will focus on elucidating the role of integrin function on cell surface CRT expression in ICD.

To assess the effects of anthracyclines on cell surface CRT expression, WT and $CRT^{-/-}$ cells were subjected to treatment with and without doxorubicin, and the level of surface CRT in live cells was assayed by flow cytometry using an α-CRT antibody. As shown in Figure 4.6, doxorubicin-treated WT cells exhibited an approximately 2-fold increase in surface CRT, whereas no change in surface CRT was evident for $CRT^{-/-}$ cells. Despite lacking CRT expression, I noted that $CRT^{-/-}$ cells exhibited an apparent and significant level of surface CRT staining when compared to the IgG control (Figure 4.6A). One possible source for the α-CRT reactive signal may have been the fetal bovine serum (FBS) in the culture media since a low level of CRT may be found in serum (Ni et al., 2013; Ren et al., 2016). Therefore, I repeated the assay and used cells that were serum-starved for 24 hours prior to treatment with doxorubicin (Figure 4.6.B). WT cells that were either serum-starved (0% FBS) or normally cultured in 10% FBS supplemented media exhibited an ~2-fold increase in surface CRT upon doxorubicin-treatment. As before, surface CRT levels remain unchanged following doxorubicin-treatment of $CRT^{-/-}$ cells. When compared to non-starved $CRT^{-/-}$ cells, I found that serum-starvation did result in a reduction of surface CRT signals detected with the α-CRT antibody (Figure 4.6.B).

Presumably, the residual signal detected on serum-starved CRT$^{-/-}$ cells was due to the serum coating of cells that persisted during the starvation (Figure 4.6.B). This reduction can also be observed in WT cells, albeit at levels that were not statistically significant. Importantly, these results indicated that anthracycline-treatment of a Jurkat T-leukemic cell line stimulates increased presentation of surface CRT and that this phenomenon is abrogated in cells lacking CRT expression.

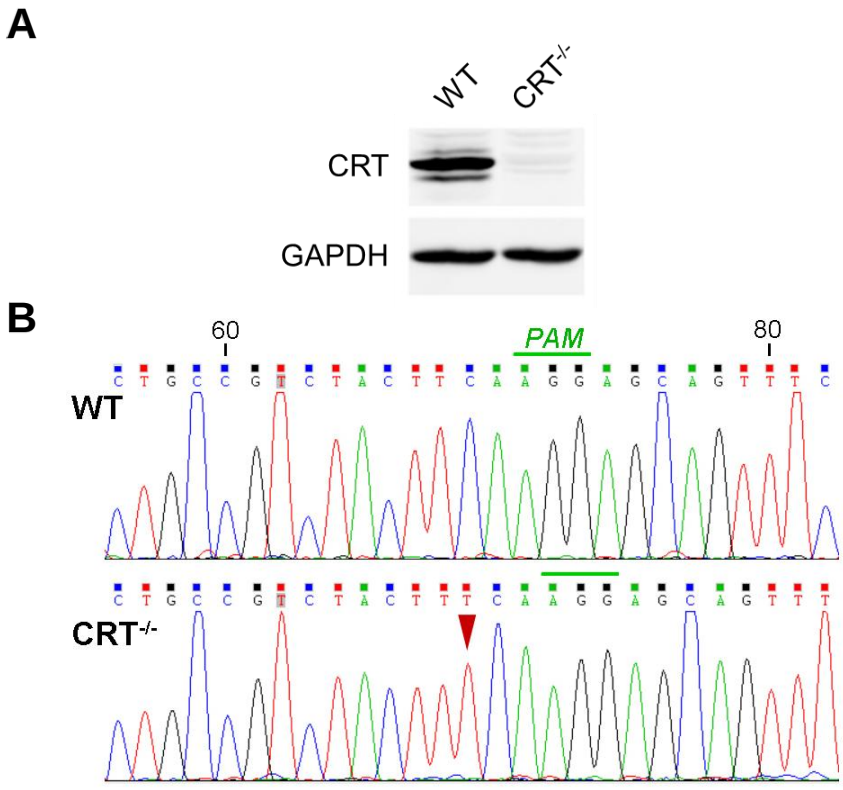

Figure 4.5. Generation of a CRT$^{-/-}$ cell line by CRISPR-Cas9 mediated gene editing
WT Jurkat cells were transfected with a CRISPR-Cas9 construct targeting *CALR*, and clones were screened for CRT expression as detailed in Methods. *(A)* Confirmation of loss of CRT expression in a representative CRT$^{-/-}$ clone by Western blotting using antibodies against CRT. Equal protein loading was assessed by immunoblotting for GAPDH. *(B)* Sequencing of the *CALR* genomic loci showing single nucleotide insertion (red triangle) occurring at 68 bp from the predicted start codon and -3 bp from the PAM recognition motif (green bar). The frame shift mutated variant encodes for a predicted 58 amino acid protein product due to a premature termination codon.

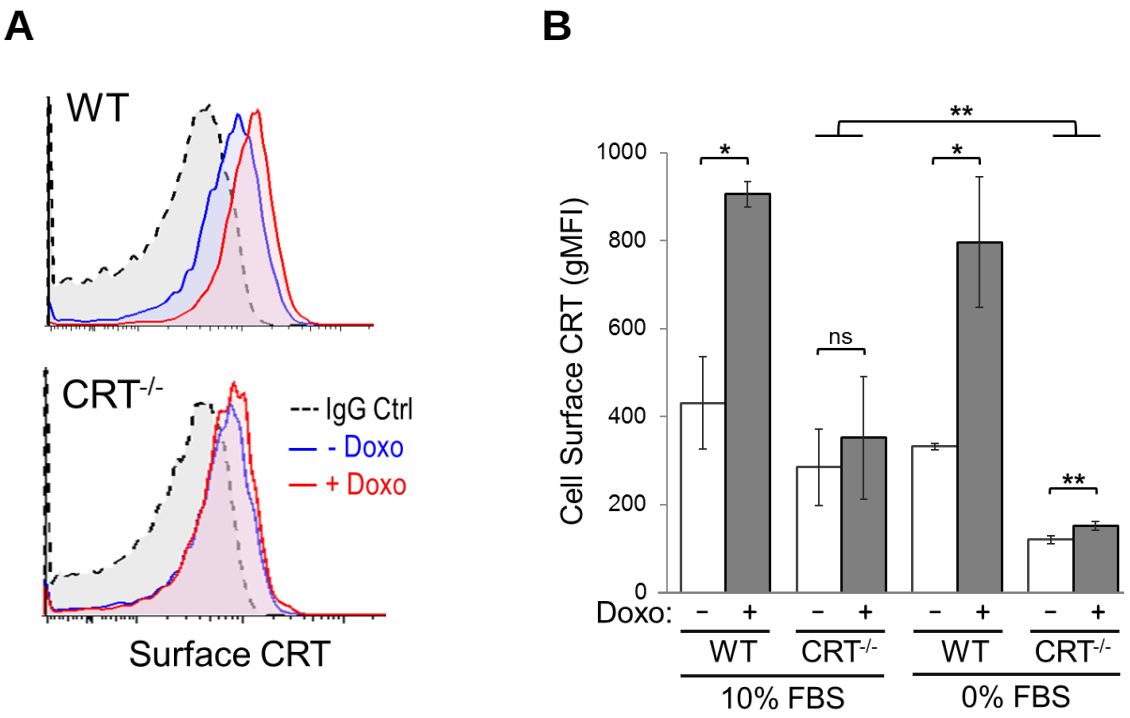

Figure 4.6. Doxorubicin-treatment induces cell surface CRT expression in Jurkat T cells
(A) Jurkat wildtype (WT) and CRT$^{-/-}$ cells were cultured in 10% FBS supplemented media for 24 hours, followed by treatment with or without 4 μg/mL of doxorubicin (Doxo) for 4 hours. Flow cytometry was used to measure surface CRT labeled with an α-CRT antibody. The histograms show the surface CRT expression under different treatment conditions. Cells treated with doxorubicin are marked in red while non-treated cells are marked in blue. Cells labeled with an IgG control antibody are denoted with a dashed black line. The results shown are representative of more than 3 experiments. *(B)* WT and CRT$^{-/-}$ cells were cultured in either 10% FBS supplemented media or serum-starved (0% FBS) for 24 hours, followed by treatment with or without 4 μg/mL of doxorubicin for 4 hours. Flow cytometry was used to measure the geometric mean fluorescence intensity (gMFI) of surface CRT labeled with the α-CRT antibody. The bars show the mean ± S.D.; n=3; *p<0.01; **p<0.05; ns, p not significant.

4.4 FBS Supplemented Culture Media Contributes to Cell Surface Calreticulin

The results thus far suggested that the detection of surface CRT can be complicated by α-CRT reactive signals present in serum-containing media. To determine the contribution of FBS to surface CRT signals, I subjected serum-starved cells to brief re-exposure to media containing various amounts of FBS. I found that a 2-hour re-incubation with serum is sufficient to restore the level of surface CRT in serum-starved WT and $CRT^{-/-}$ cells to the level detected for the corresponding non-starved, serum-cultured cells (Figure 4.7A). Interestingly, the impact of serum appears to be dose-dependent and is similar in WT and $CRT^{-/-}$ cells. A Western blot analysis of cell-free FBS together with WT and $CRT^{-/-}$ cell lysates revealed an α-CRT reactive band that is present in FBS (Figure 4.7.B). This FBS band has an apparent molecular weight that is higher than human CRT. Bovine and human CRT are both 417 amino acids in length (400 when the signal peptide is cleaved) and 93% identical, thus it remains unclear if the α-CRT reactive signal found in FBS is due to non-specific binding to impurities or to bona fide bovine CRT.

To further demonstrate the effect of serum, I used a serum-free synthetic replacement media (Cell-Ess®) to adapt and culture WT and $CRT^{-/-}$ cells. The cells fared poorly in the complete absence of serum, but I did achieve a final culture state that consisted of 0.3% FBS and 9.7% Cell-Ess®. Under these conditions, I observed that $CRT^{-/-}$ cells exhibited no significant staining for surface CRT when compared to cells maintained in 10% FBS-supplemented media (Figure 4.8). Doxorubicin-mediated stimulation of surface CRT in WT cells was still equally robust (~2-fold increase) in 10% and 0.3% FBS-cultured conditions. This indicated that most, if not all, of the surface CRT that was stimulated by anthracycline and detected with the α-CRT antibody is endogenous to the cell.

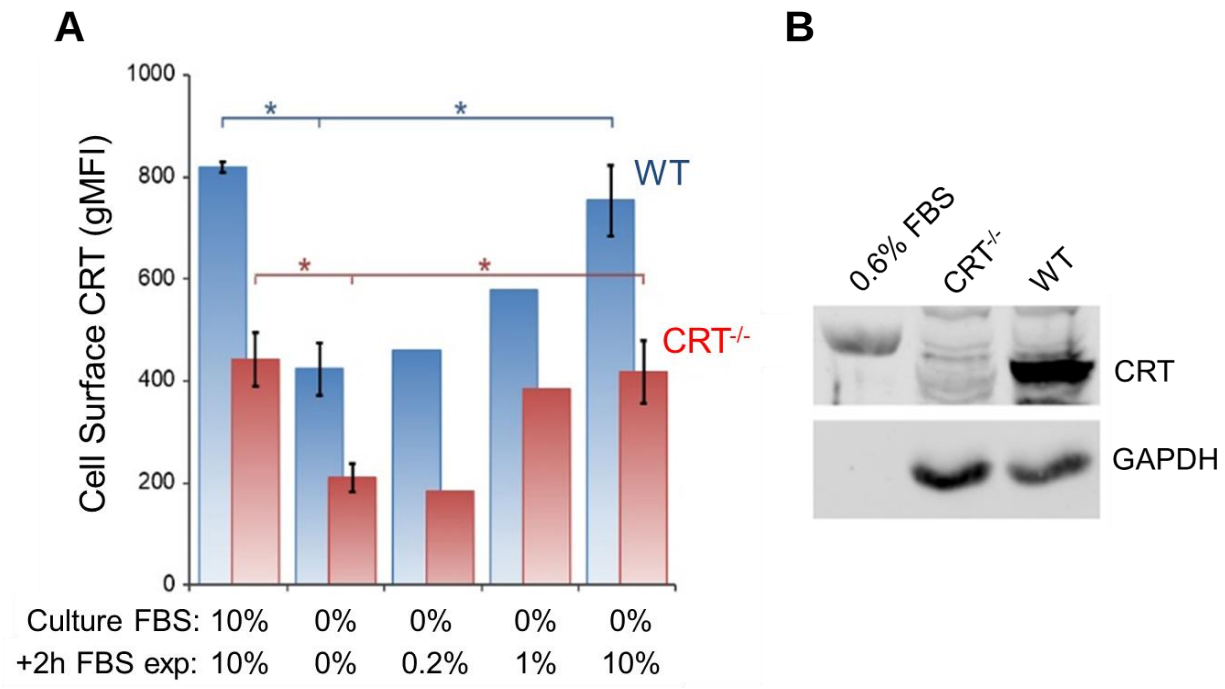

Figure 4.7. FBS contributes significantly to surface CRT signals detected with an antibody (*A)* Flow cytometry gMFI plots of surface CRT on WT (blue) and CRT$^{-/-}$ (red) cells cultured in 10% FBS supplemented media or serum-starved (0% FBS) for 24 hours as indicated (Culture FBS). Following the 24-hour pre-treatment with or without FBS, the cells were re-incubated for 2 hours in FBS-supplemented media at the indicated levels prior to cell surface labeling with the α-CRT antibody. The bars show the mean ± S.D.; n=3; *p<0.01. The absence of error bars indicates samples conducted without replicates. (*B)* Detection of α-CRT reactive signals comparing cell-free 0.6% FBS media alone, and lysates of WT or CRT$^{-/-}$ cells. GAPDH is included for normalization of cell lysates. The results shown are representative of more than 3 experiments.

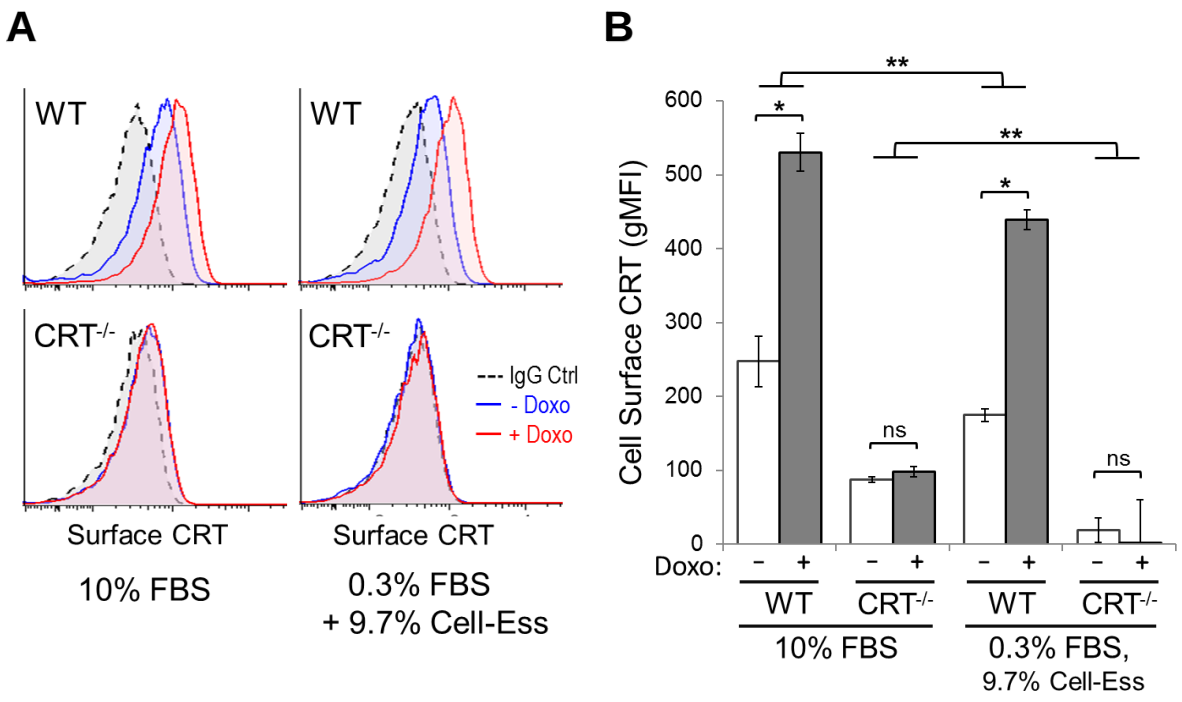

Figure 4.8. Antibody-mediated detection of surface CRT is abolished when cells are cultured in low serum media

(A) WT and CRT$^{-/-}$ cells were cultured in 10% FBS supplemented media or 0.3% FBS/9.7% Cell-Ess® supplemented media, followed by treatment with or without 4 μg/mL of doxorubicin (Doxo) for 4 hours. Flow cytometry was used to measure surface CRT labeled with the α-CRT antibody. The histograms show surface CRT expression of WT and CRT$^{-/-}$ cells under different treatment conditions. Cells treated with doxorubicin are marked in red while non-treated cells are marked in blue. Cells labeled with an IgG control antibody are denoted with a dashed black line. The results shown are representative of more than 3 experiments. *(B)* The flow cytometry gMFI plots of surface CRT as described in *(A)*. The bars show the mean ± S.D.; n=3; **p*<0.001; ***p*<0.05; ns, *p* not significant.

4.5 Doxorubicin-induced increase in cell surface CRT requires the ER-resident form

Under normal cell physiological conditions, CRT is a protein that is highly enriched within the lumen of the ER. As such, the mechanisms by which a cell undergoing ICD is able to present CRT on the cell surface to act as an ‘eat me’ phagocytic signal remains a subject of keen

interest for tumor cell biologists. The construction of the CRT null T-lymphoblast line now enables our investigation into mechanisms of CRT trafficking to the cell surface during ICD.

To identify the source of surface CRT, I created multiple CRT constructs tagged with green fluorescent protein (GFP) for visualization and labeling (Figure 4.9). Dr. Paul Eggleton (University of Exeter) provided the base construct GFP-CRT, which is an N-terminal GFP-tagged CRT without the ER-targeting signal sequence. Thus, GFP-CRT is expected to be expressed within the extra-ER cytosolic compartment (Tarr et al., 2010b; Walter and Johnson, 1994). The construct ssGFP-CRT reproduces the 17-amino acid ER-targeting signal sequence at the N-terminus that directs the synthesis of ssGFP-CRT into the ER lumen (Walter and Johnson, 1994). To confirm the expected subcellular expressed localization, I performed immunofluorescence imaging of CRT in conjunction with the ER marker PDI in WT, $CRT^{-/-}$, or $CRT^{-/-}$ cells transfected to express ssGFP-CRT or GFP-CRT. As expected, endogenously expressed CRT co-localized with PDI within the ER compartment of WT cells, while $CRT^{-/-}$ cells showed no CRT staining (Figure 4.10). In similar fashion, ssGFP-CRT expressed in $CRT^{-/-}$ cells colocalized with PDI, indicating proper targeting of ssGFP-CRT to the ER (Figure 4.10). When expressed in $CRT^{-/-}$ cells, GFP-CRT exhibited a diffuse localization staining that did not co-localize with PDI, confirming that GFP-CRT was expressed in the extra-ER cytosol (Figure 4.10).

In addition to GFP-CRT and ssGFP-CRT, I also made the following constructs that have a mutated or variant CRT C-terminal domain. ssGFP-CRT-KDELdel is similar to ssGFP-CRT except that the C-terminal KDEL motif is deleted (Figure 4.9). In principal, this protein cannot engage KDEL receptors that retrieve KDEL-containing proteins from the Golgi apparatus back to the ER, thus promoting its exit from the ER (Wilson et al., 1993). ssGFP-CRT-mutant type I

reproduces the alternate C-terminal reading frame identified as the causative somatic mutation in patients with myeloproliferative neoplasms (MPN) (Figure 4.9) (Klampfl et al., 2013; Nangalia et al., 2013). Importantly, CRT-mutant type I's alternate C-terminus also lacks the KDEL ER retention motif (Klampfl et al., 2013; Nangalia et al., 2013).

I transfected $CRT^{-/-}$ cells with the various GFP-tagged CRT constructs and used flow cytometry to determine their relative expression levels on the basis of the GFP signal intensities (Figure 4.11). Notably, while ssGFP-CRT and GFP-CRT showed comparable GFP expression, the expression of ssGFP-CRT-KDELdel and ssGFP-CRT-mutant type I was much lower (Figure 4.11). The transiently transfected cells were then subjected to treatment with or without doxorubicin and labeled with anti-CRT antibody for flow cytometry analysis of surface CRT. Figure 4.12 shows an example of my gating scheme, where GFP-positive signals were used to gate for transfected cells (CRT-positive) for subsequent analysis. Consistent with my previous experiments, WT cells exhibit a ~2-fold increase in surface CRT upon treatment with doxorubicin, while no increase was seen in $CRT^{-/-}$ cells (Figure 4.13A). $CRT^{-/-}$ cells transfected with the ER-targeted ssGFP-CRT also exhibited the ~2-fold increase in surface CRT upon treatment with doxorubicin, comparable to WT cells (Figure 4.13A). In contrast, $CRT^{-/-}$ cells transfected with the cytosol-targeted GFP-CRT exhibited high levels of surface CRT with or without doxorubicin treatment (Figure 4.13A). These levels were comparable to or higher than the doxorubicin-treated cells that expressed ssGFP-CRT (Figure 4.13A).

Notably, expression of ssGFP-CRT-KDELdel and ssGFP-CRT-mutant type I in $CRT^{-/-}$ cells produced a phenotype that more closely resembles that of cells expressing the ER-targeted ssGFP-CRT, in that doxorubicin treatment was able to stimulate a significant increase in surface CRT (Figure 4.13A). I noted too that cells transfected to express ssGFP-CRT, ssGFP-CRT-

KDELdel and ssGFP-CRT-mutant type I exhibited somewhat higher levels of surface CRT without doxorubicin treatment when compared to WT cells. This result may be due to overexpression of the transfected proteins relative to endogenous levels of CRT, or it may be due to the GFP-tagged form.

To confirm the functionality of the GFP-tagged CRT constructs, I repeated the surface CRT assay using an α-GFP antibody in place of the α-CRT antibody to detect the fusion GFP-CRT when presented on the surface of live cells (Figure 4.13B). Non-transfected WT or $CRT^{-/-}$ cells showed only background signals indicating minimal non-specific binding of α-GFP antibodies to the cell surface (Figure 4.13B). The results obtained for surface staining with the α-GFP antibody for cells expressing the various GFP-CRT constructs were similar to those seen with the α-CRT antibody (Figure 4.13A), indicating that the fusion proteins were translocated to the cell surface and behave in a manner comparable to endogenous CRT. As an additional control, I showed that in $CRT^{-/-}$ cells transfected to express GFP alone, GFP remains cytosolic and was not present on the cell surface (Figure 4.13B, inset).

Importantly, these results demonstrated that doxorubicin-mediated stimulation of surface CRT requires the ER-resident form. The ssGFP-CRT and both of the KDEL-null constructs retain the N-terminal signal sequence which mediates its synthesis and insertion into the ER lumen. As shown by Klampfl *et al.*, overexpressed CRT Type I mutant remains enriched within the ER (Klampfl et al., 2013). My results with either Type I or the KDEL deleted form of CRT suggests that deletion of the KDEL ER retention sequence does not drastically modify the ability to present surface CRT upon treatment with doxorubicin.

To evaluate the possibility that the high GFP-CRT observed on the cell surface may be a result of overexpression, I made an additional construct, IRES-GFP-CRT. With this construct,

GFP-CRT expression is under the control of the less efficient IRES (internal ribosome entry site) promoter (Mizuguchi et al., 2000). Compared with the CRT expression driven by the CMV (cytomegalovirus) promoter, the IRES-driven expression of GFP-CRT in cells was ~10 fold lower (Figure 4.14A). Indeed, cells expressing IRES-GFP-CRT showed lower surface CRT levels compared to cells expressing CMV-GFP-CRT (Figure 4.14B). Similar to results obtained with CMV-GFP-CRT (Figure 4.13), doxorubicin treatment of cells expressing IRES-GFP-CRT did not result in an observable increase of surface GFP-CRT levels (Figure 4.14B). This result is consistent with the high cell surface expression of GFP-CRT not being merely due to overexpression (Figure 4.14B). Moreover, since the cytosol-targeted GFP-CRT showed a high level of surface CRT that was comparable to the other ER-targeted constructs when stimulated with doxorubicin, I hypothesized that cytosolic CRT is readily presented on the cell surface in a manner not requiring induction of ER-stress. Collectively, my results suggest a mechanism of action whereby drug-mediated induction of ER stress leads to CRT release from the ER into the cytosol, whereupon its increased concentration enables its presentation on the cell surface. This mechanism likely bypasses or overwhelms alternate mechanisms that involve the Golgi apparatus where KDEL receptors reside.

Figure 4.9. Schematic of variant CRT constructs compared with the wildtype
Wildtype CRT is depicted with the N-terminal 17 amino acid signal sequence (ss) and the C-terminal KDEL ER-retention motif. GFP-CRT lacks the signal sequence and is targeted to the cytosol. ssGFP-CRT, ssGFP-CRT-KDELdel and ssGFP-CRT-mutant type I are ER-targeted due to the signal sequence. ssGFP-CRT-KDELdel and ssGFP-CRT-mutant type I do not contain the ER-retention motif. The red box depicts the alternate C-terminal reading frame for CRT associated with myeloproliferative neoplasms (type I mutant). GFP: green fluorescent protein.

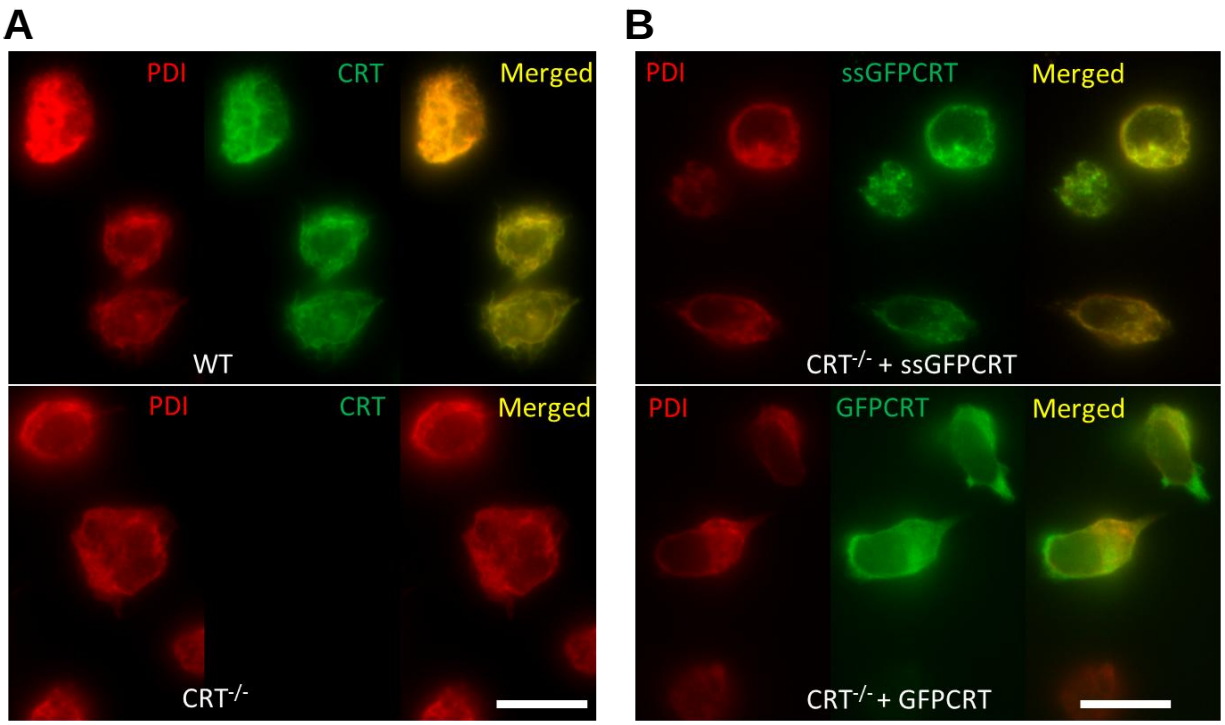

Figure 4.10. Immunofluorescence staining for CRT and PDI
(A) Immunofluorescence images of endogenous CRT (green) and an ER marker, PDI (red) in WT and $CRT^{-/-}$ cells. *(B)* $CRT^{-/-}$ cells were transfected to express ssGFP-CRT (green) or GFP-CRT (green), and co-stained for PDI (red). Scale bars=10 µm.

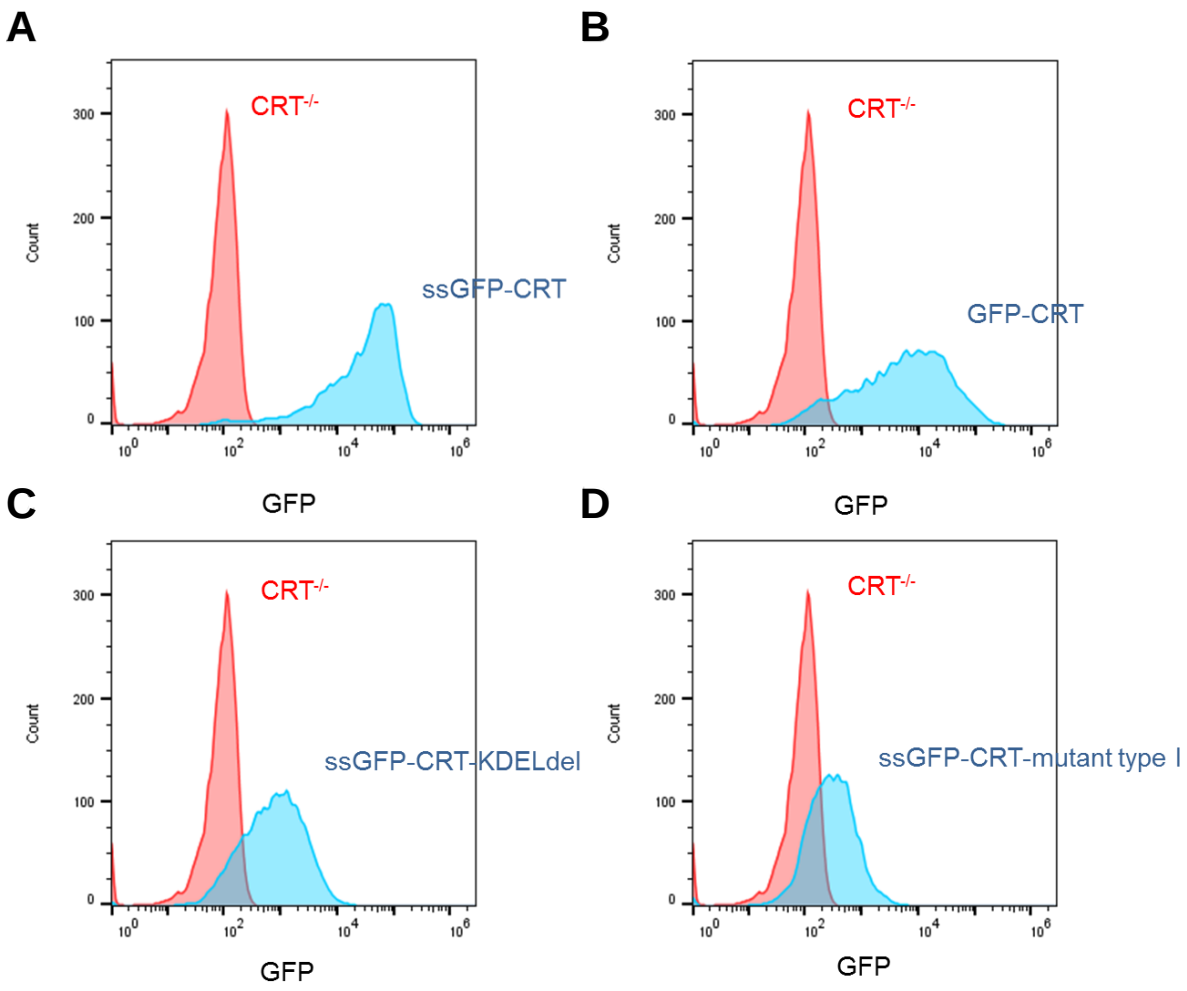

Figure 4.11. Comparison of expression for the various GFP-CRT constructs
Flow cytometry was used to determine the expression level of CRT$^{-/-}$ cells transiently transfected to express the following constructs: *(A)* ssGFP-CRT, *(B)* GFP-CRT, *(C)* ssGFP-CRT-KDELdel, and *(D)* ssGFP-CRT-mutant type I. The histograms show GFP signals for the indicated GFP-CRT construct (blue) overlaid upon those of non-transfected CRT$^{-/-}$ cells (red).

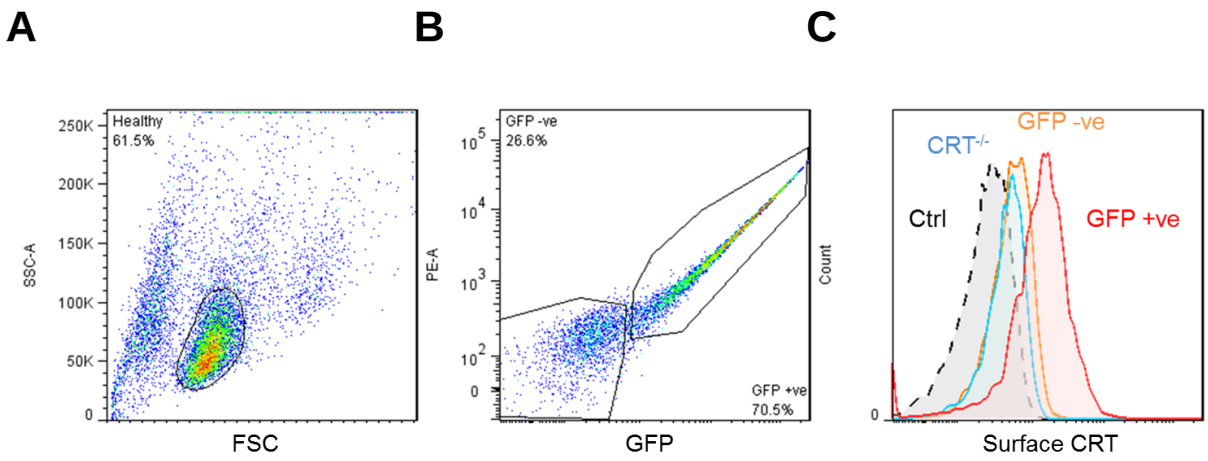

Figure 4.12. Example of flow cytometry gating scheme for analysis of GFP+ cells
$CRT^{-/-}$ cells were transiently transfected to express a GFP-tagged CRT construct. (*A)* The healthy population is gated (as indicated) on the basis of the forward and side scatter properties. This population was previously validated to be non-apoptotic as Annexin V and PI negative (data not shown). (*B)* The gated population from A is analyzed for GFP fluorescence to distinguish between transfected (GFP^+) and non-transfected (GFP^-) cells. (*C)* Then GFP^+ (red) and GFP^- (orange) populations are separately analyzed for cell surface CRT levels by α-CRT labeling. In addition to GFP^+ and GFP^- cells, the data includes overlays with unlabeled Ctrl cells (black) and labeled $CRT^{-/-}$ cells (blue).

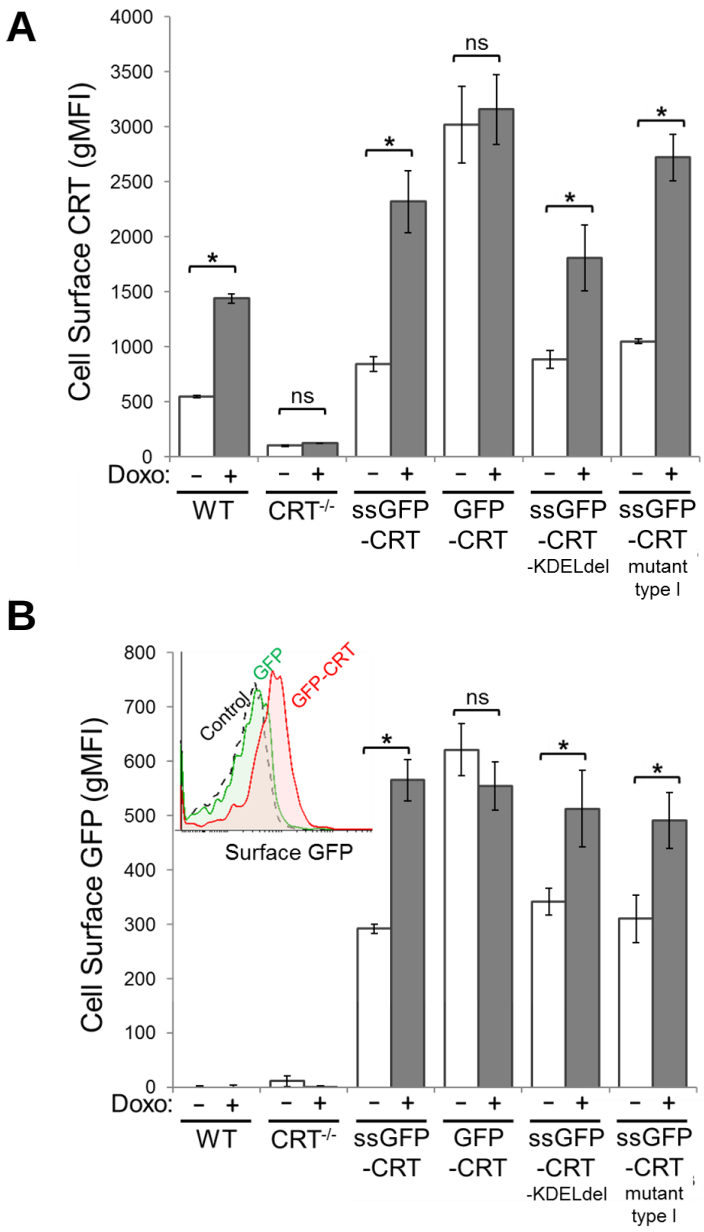

Figure 4.13. Doxorubicin-mediated increase in surface CRT requires the ER-resident form of CRT

(A) WT, CRT$^{-/-}$, and CRT$^{-/-}$ cells transfected to express ssGFP-CRT, GFP-CRT, ssGFP-CRT-KDELdel or ssGFP-CRT-mutant type I were treated with or without 4 μg/mL of doxorubicin (Doxo) for 4 hours. Flow cytometry was used to measure the gMFI of surface CRT labeled with the α-CRT antibody. (*B)* Same as *(A)*, except the cells were labeled with α-GFP antibody instead. Inset is a representative histogram overlay of surface GFP expression of non-transfected CRT$^{-/-}$ cells (Control) and CRT$^{-/-}$ cells transfected to express GFP-CRT (red) or GFP alone (green). The bars show the mean ± S.D.; n=3; *p<0.01; ns, p not significant.

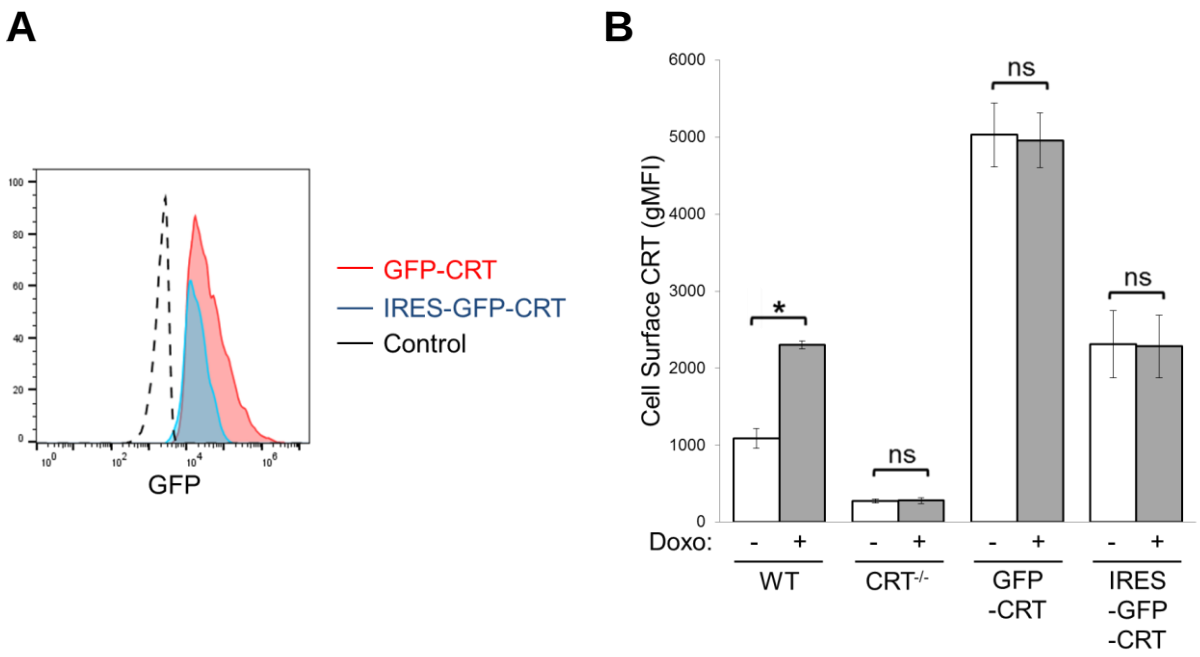

Figure 4.14. Differential expression of GFP-CRT and its effects on surface CRT
(A) The representative histogram overlay of CMV-GFP-CRT expression (red) versus IRES-GFP-CRT expression (blue). Black is the non-transfected GFP -ve control. *(B)* WT, $CRT^{-/-}$, GFP-CRT and IRES-GFP-CRT cells were treated with or without 4 μg/mL of doxorubicin (Doxo) for 4 hours. Flow cytometry was used to measure the gMFI of surface CRT labeled with the α-CRT antibody. The bars show the mean ± S.D.; n=3; *p<0.01; ns, p not significant.

4.6 Expression and Function of α-integrins Reduce Cell Surface Calreticulin

As I showed in Figure 4.4, cells that engage integrin substrates exhibit increased interaction of CRT with the immunoprecipitated α-integrins. This phenomenon has also been reported by Dr. Shoukat Dedhar's group (Coppolino et al., 1995; Coppolino and Dedhar, 1999). This interaction is dependent upon the GFFKR peptide motif found at the juxtamembrane cytosolic tail of α-integrins, leading to our speculation that α-integrin function may modulate surface CRT presentation. To address this, I assessed the contribution of cell adhesion to surface CRT levels for cells treated with doxorubicin. As described in Chapter 3, I used the Jurkat

derivative cell line lacking α4-integrin expression ($\alpha4^{-/-}$), and $\alpha4^{-/-}$ cells stably reconstituted with full-length α4 ($\alpha4^{wt}$) or with a C-terminal truncated variant termed α4δ that terminates with the GFFKR cytosolic motif (Figure 3.3). The results described in Chapter 3 demonstrated that cells expressing α4δ do not adhere to an α4β1-specific substrate (Figure 3.5), yet exhibit increased α4δ binding to CRT in a manner that bypasses the requirement for cell adhesion (Figure 4.3).

To assess the impact of integrin engagement on surface CRT, cells were seeded on the substrates GST-CS1 (α4β1-ligand), GST-Fn9.11 (α5β1-ligand) or GST (non-integrin engaging) and treated with or without doxorubicin at concentrations that induce robust levels of surface CRT. When seeded on GST, doxorubicin-treated α4δ cells showed significantly lower surface CRT compared to $\alpha4^{-/-}$ and $\alpha4^{wt}$ cells (Figure 4.15). When seeded on GST-CS1, doxorubicin-treated $\alpha4^{wt}$ cells had lower surface CRT compared to $\alpha4^{-/-}$ cells. When seeded on GST-Fn9.11, a substrate that can engage multiple integrins including α5β1-integrin that is expressed in all 3 cell lines, doxorubicin-treated $\alpha4^{-/-}$ and $\alpha4^{wt}$ cells had lower surface CRT compared to the same cells seeded on GST. Importantly, α4δ cells exhibited low surface CRT in both adherent and non-adherent conditions, and this low level was comparable to $\alpha4^{-/-}$ and $\alpha4^{wt}$ cells under adherent conditions (Figure 4.15).

Since α4δ binds CRT in a constitutive manner, I postulated that the juxtamembrane GFFKR motif might act to sequester CRT within the cytosol and reduce its translocation to the cell surface. Consequently, I predicted that cells with higher α4δ expression would have lower surface CRT levels. To investigate this idea, I used flow cytometry to gate cells expressing high, medium, and low α4δ expression, and showed that surface CRT levels were inversely correlated with α4δ levels, both with and without doxorubicin treatment (Figure 4.16).

To determine if the juxtamembrane CRT-binding motif, GFFKR, is sufficient to inhibit surface CRT, I also assessed cells expressing the Tac carrier epitope fused to KLGFFKR (Tacδ) or a scrambled version KLRFGFK (Tacδ^{scr}) as the cytosolic tails (Figure 3.7). Similar to α4δ cells, doxorubicin-treated Tacδ cells had significantly reduced surface CRT when compared with control or Tacδ^{scr} cells (Figure 4.17).

These results demonstrated that anthracycline-mediated surface CRT presentation is reduced for cells engaging integrin substrates. In contrast, cells expressing the juxtamembrane GFFKR motif (as α4δ or Tacδ) exhibited constitutively low levels of surface CRT in a manner that bypasses the requirement for cell adhesion.

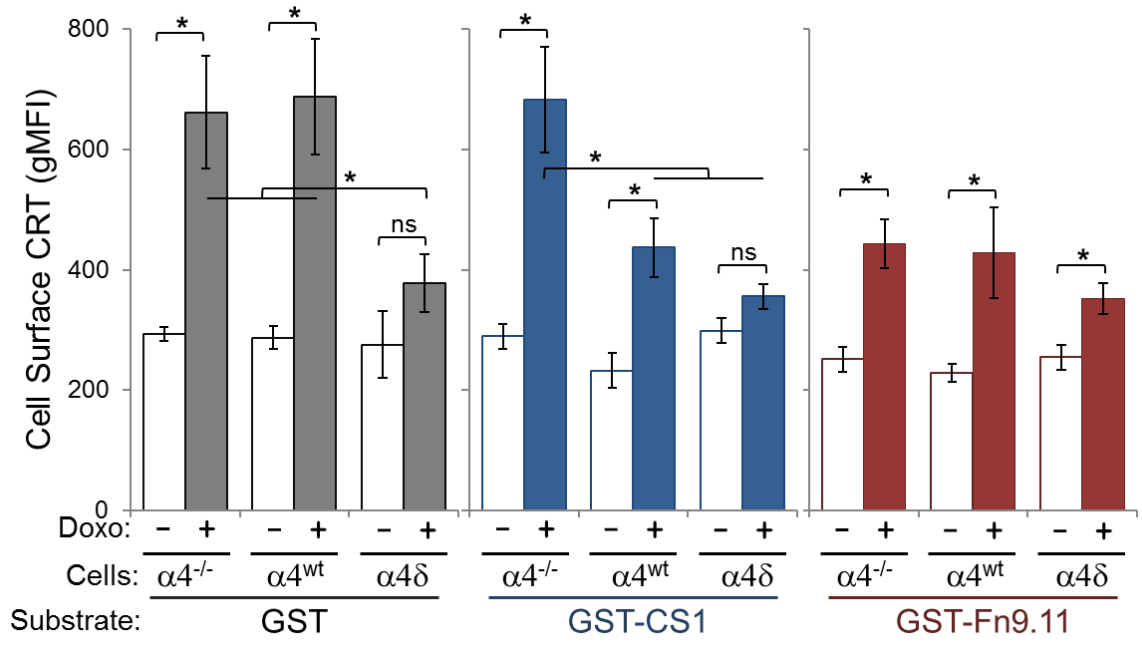

Figure 4.15. Expression and function of α-integrin reduce presentation of surface calreticulin

α4$^{-/-}$, α4^{wt} (α4$^{-/-}$ reconstituted with α4^{wt}), or α4δ cells (α4$^{-/-}$ reconstituted with α4δ) were seeded on dishes coated with GST-CS1 (α4β1-ligand), GST-Fn9.11 (α5β1-ligand) or GST for 1 hour, followed by treatment with or without 4 μg/mL of doxorubicin (Doxo) for 4 hours. Flow cytometry was used to measure the gMFI of surface CRT labeled with the α-CRT antibody. The bars show the mean ± S.D.; n=3; *p<0.05; ns, p not significant.

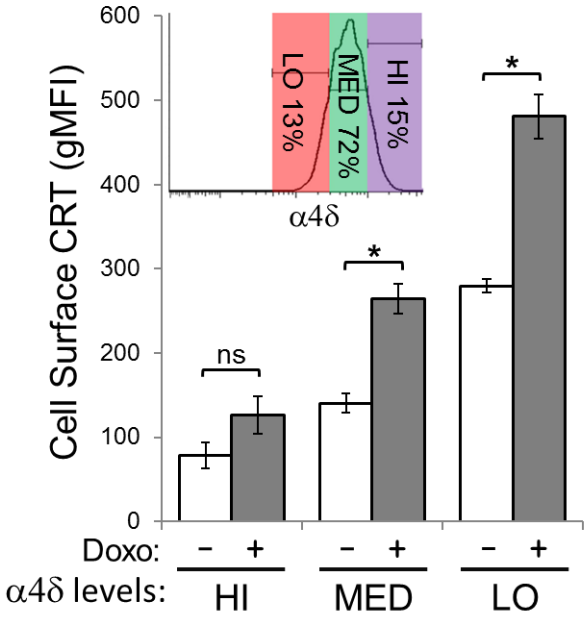

Figure 4.16. α4δ-integrin expression reduces presentation of surface calreticulin
α4δ cells were serum-starved for 24 hours, followed by treatment with or without 4 μg/mL of doxorubicin (Doxo) for 4 hours. α4δ cells were co-stained for surface α4 and surface CRT and gated for low, medium and high levels of α4δ expression as indicated. The bar graph shows the gMFI of surface CRT of each α4δ expression group (mean ± S.D.; n=3; *p<0.01; ns, p not significant).

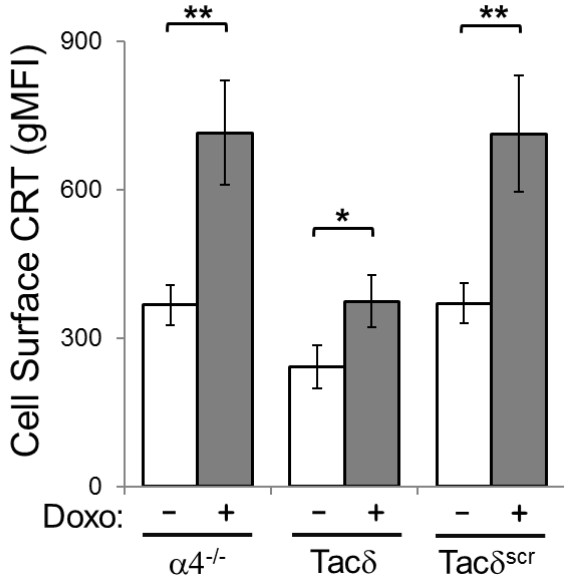

Figure 4.17. Expression of the GFFKR motif as Tacδ reduces presentation of surface calreticulin

$\alpha4^{-/-}$, $\alpha4^{-/-}$ cells expressing Tacδ and $\alpha4^{-/-}$ cells expressing $Tac\delta^{scr}$ were serum-starved for 24 hours, followed by treatment with or without 4 μg/mL of doxorubicin (Doxo) for 4 hours. Flow cytometry was used to measure the gMFI of surface CRT labeled with the α-CRT antibody. The bars show the mean ± S.D.; n=3; $^{**}p<0.01$, $^{*}p<0.05$.

4.7 Cell Adhesion Mediated Activation of β1-integrins Decreases Surface Calreticulin Presentation

Integrins are stably expressed as heterodimeric cell surface receptors. Since β1-integrin pairs with multiple α-integrins, loss of the β1-subunit yields corresponding decreases in the expression of multiple integrins. Indeed, I found dramatically decreased expression of α3-, α4-, and α5-integrins (all known to pair with β1) in a β1-deficient Jurkat-derivative cell line compared to wildtype cells (Figure 4.18). Other than β1, α4 can also pair with the β7-subunit. However, wildtype Jurkat cells do not express any detectable level of β7-integrins (data not shown), thus it was surprising to find that the β1-deficient cell line still expressed significant

levels of α4. When assayed for β7 expression, I found that $\beta1^{-/-}$ cells expressed a significant level of β7-integrin (data not shown), suggesting that formation of α4β7 heterodimer had compensated for loss of α4β1. We confirmed that the ability of cells to adhere to the α4β1-specific substrate GST-CS1 was completely lost by $\beta1^{-/-}$ cells (Figure 4.19). To test the requirement of β1-integrin in surface CRT presentation, I seeded $\beta1^{-/-}$ and WT cells on GST-CS1 or the control substrate GST, prior to treatment with doxorubicin. Both $\beta1^{-/-}$ and WT cells responded to doxorubicin treatment as manifested by comparable increases in surface CRT when seeded on GST (Figure 4.20). When seeded on GST-CS1 to engage α4β1-integrin, the β1-expressing WT cells exhibited a marked decrease in surface CRT, while the $\beta1^{-/-}$ cells exhibited no reduction in surface CRT compared with non-adherent conditions (Figure 4.20). Taken together, the evidence indicated a modulatory role for adhesion-mediated activation of integrins in decreasing surface CRT presentation for cells treated with doxorubicin.

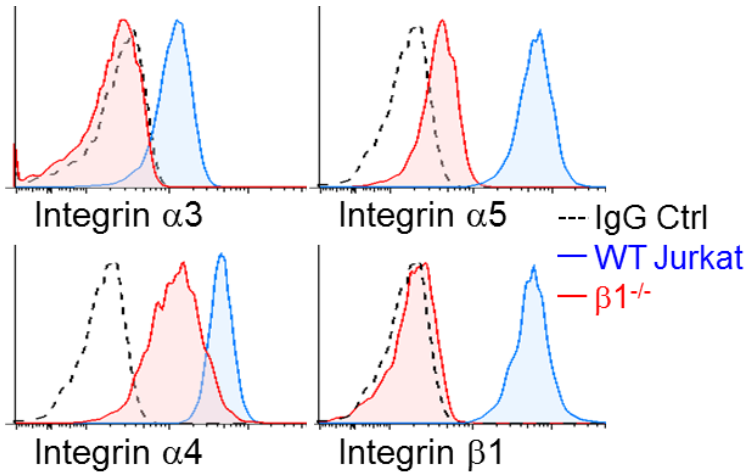

Figure 4.18. Loss of β1-integrin decreases paired α-integrin expression
Histogram overlays of WT (blue) and $\beta1^{-/-}$ (red) Jurkat cells showing relative surface expression of integrins α3, α4, α5, and β1. Black dotted line denotes IgG control. Flow cytometry was used to measure surface integrin expression labeled with the respective antibodies. The results shown are representative of more than 3 experiments.

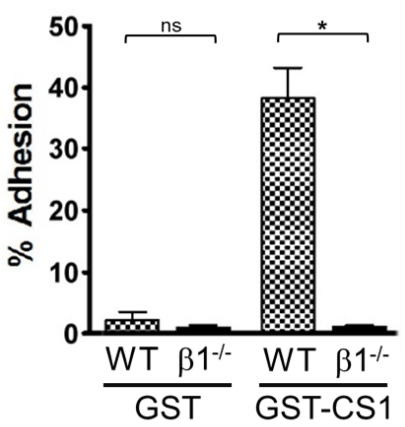

Figure 4.19. Loss of β1-integrin abolishes β1-integrin mediated cell adhesion
WT and $\beta1^{-/-}$ cells were labeled with CellTracker™ Green, followed by seeding on dishes coated with GST or GST-CS1 for 45 minutes. Fluorescence readings were acquired with an Enspire spectrofluorometer (485 nm excitation, 515 nm emission) before and after 3 washes with PBS. Background fluorescence from the incubation medium was subtracted from each reading, and the percentage of total cells that was adhered was calculated as follows: 100*(Fluorescence after washes/initial fluorescence). The bars show the mean ± S.D.; n=3; *p<0.01; ns, p not significant.

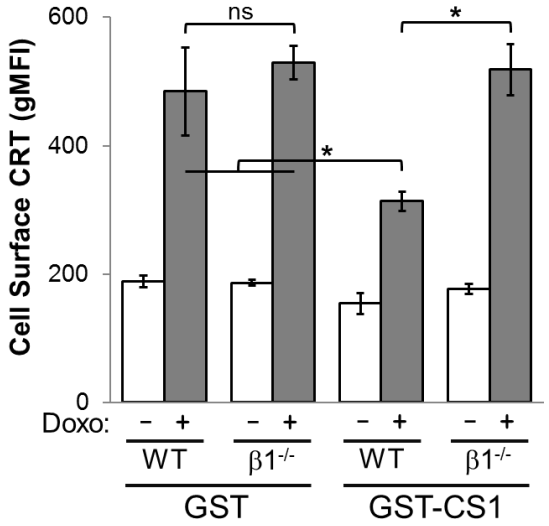

Figure 4.20. Loss of β1-integrin abolishes cell adhesion-mediated reduction in surface CRT
WT and $\beta1^{-/-}$ cells were seeded on dishes coated with GST or GST-CS1 for 1 hour, followed by treatment with or without 4 μg/mL of doxorubicin (Doxo) for 4 hours. Flow cytometry was used to measure the gMFI of surface CRT labeled with the α-CRT antibody. The bars show the mean ± S.D.; n=3; *p<0.01; ns, p not significant.

4.8 Antibody Activation of β1-integrins Reduces Surface Calreticulin Presentation

For cells to adhere to an integrin substrate, the integrins must be activated to take on the high-affinity ligand binding state. The results presented thus far suggest that the reduced surface CRT level is observed for native integrins that were activated by engaging their ligands. 9EG7 is a monoclonal antibody widely used as a reporter for the activated state of β1-integrin heterodimers (Bazzoni et al., 1995). Unique to 9EG7, however, is its reported ability to promote ligand binding by maintaining β1-integrin in the activated conformation (Su et al., 2016). I wondered if 9EG7-mediated activation of β1-integrin in the absence of cell adhesion could also down-regulate surface CRT presentation.

First, I tested if 9EG7 promotes integrin activation in WT cells. Increasing concentrations of 9EG7 incubated with cells in suspension resulted in its increased binding as an indicator of increased integrin activation (Figure 4.21A). I then tested if 9EG7 binding can promote integrin ligand binding as a confirmation of increased β1-integrin activation. I found that both 9EG7 and a known integrin activator, Mn^{2+}, significantly increased the binding of fibronectin as a ligand to WT cells, when compared to untreated control cells or cells treated with TS2/16, a β1-specific but non-activating antibody (Figure 4.21B). Notably, EGTA-treatment abolished β1-integrin ligand binding completely, an observation consistent with the requirement for Ca^{2+} to support integrin activation (Figure 4.21B).

Next, I treated WT, $CRT^{-/-}$ and $\beta1^{-/-}$ cells with various concentrations of 9EG7 and with doxorubicin to induce surface CRT. I found that increasing concentrations of 9EG7 reduced surface CRT on WT cells to the low levels observed on $CRT^{-/-}$ cells (Figure 4.22). Importantly, incubation of 9EG7 with $\beta1^{-/-}$ cells had no inhibitory consequence on doxorubicin-induced surface CRT levels. In similar fashion, treatment of WT cells with TS2/16 had no inhibitory

consequence on doxorubicin-induced surface CRT levels. Notably, the 9EG7-mediated decrease of surface CRT in WT cells was observed for both doxorubicin-treated and non-treated conditions (Figure 4.22), suggesting the generality of an integrin activation-mediated effect that does not require anthracycline induction of ER-stress.

To gain insight on how integrin function can prevent surface presentation of CRT upon treatment with ICD inducers, I conducted integrin immunoprecipitation assays for cells treated with or without doxorubicin, and with or without 9EG7, as before. Doxorubicin effectively promoted an increased level of CRT that immunoprecipitated with α4-integrin, and this association was increased further for 9EG7-treated cells (Figure 4.23). Furthermore, $CRT^{-/-}$ cells expressing either the ER-targeted ssGFP-CRT or the cytosol-targeted GFP-CRT that were treated with 9EG7 but not doxorubicin both exhibited significantly reduced levels of surface CRT and GFP (Figure 4.24). This confirmed that 9EG7-mediated integrin activation can inhibit surface translocation of CRT from a predominantly cytosolic localization.

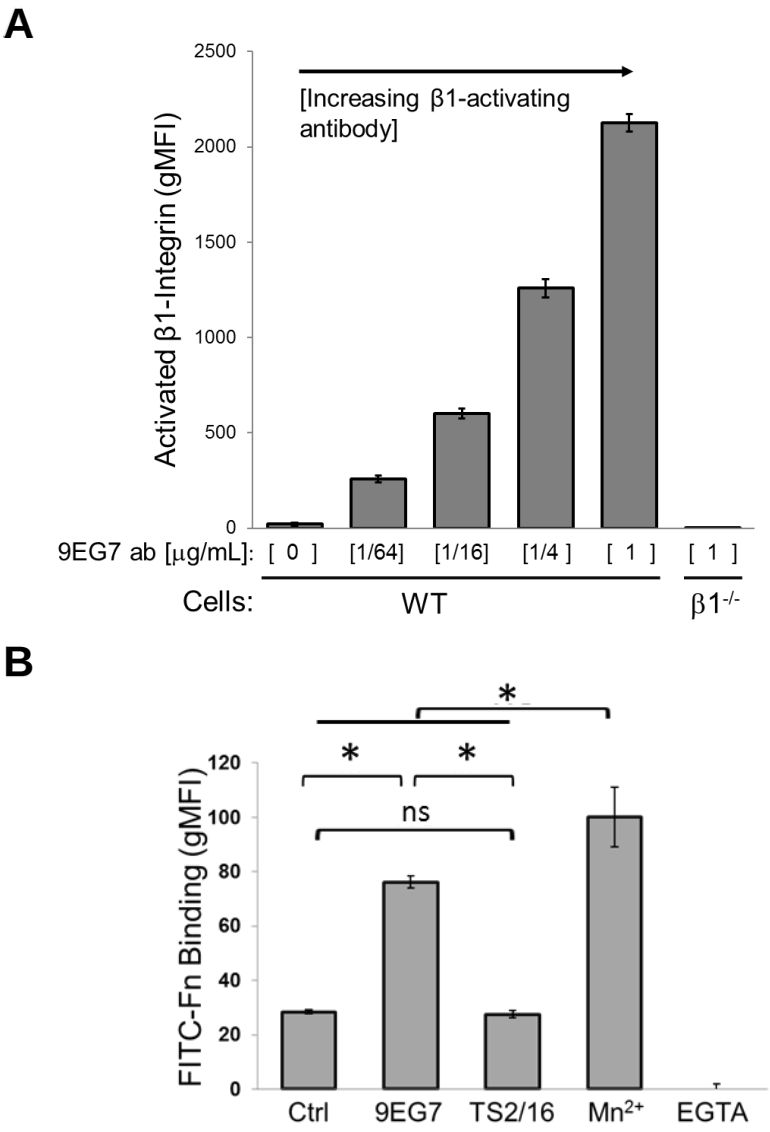

Figure 4.21. Incubation of cells with 9EG7 antibody promotes β1-integrin activation
(A) WT and $\beta1^{-/-}$ cells were treated with the indicated concentrations of 9EG7 (β1-activating) antibody for 4 hours. Flow cytometry was used to measure the gMFI of activated β1-integrin labeled with the 9EG7 antibody. The bars show the mean ± S.D.; n=3; *p<0.01. *(B)* WT cells were not treated (Ctrl), or treated with 1 μg/mL of 9EG7 (β1-activating) or TS2/16 (β1-binding, non-activating) antibodies for 4 hours, 1 mM of Mn^{2+} for 30 minutes, or 3 mM of EGTA for 30 minutes, followed by incubation with 0.2 mg/mL of FITC-Fn for 30 minutes. Flow cytometry was used to measure the gMFI of FITC-Fn binding. The bars show the mean ± S.D.; n=3; *p<0.01; ns, p not significant.

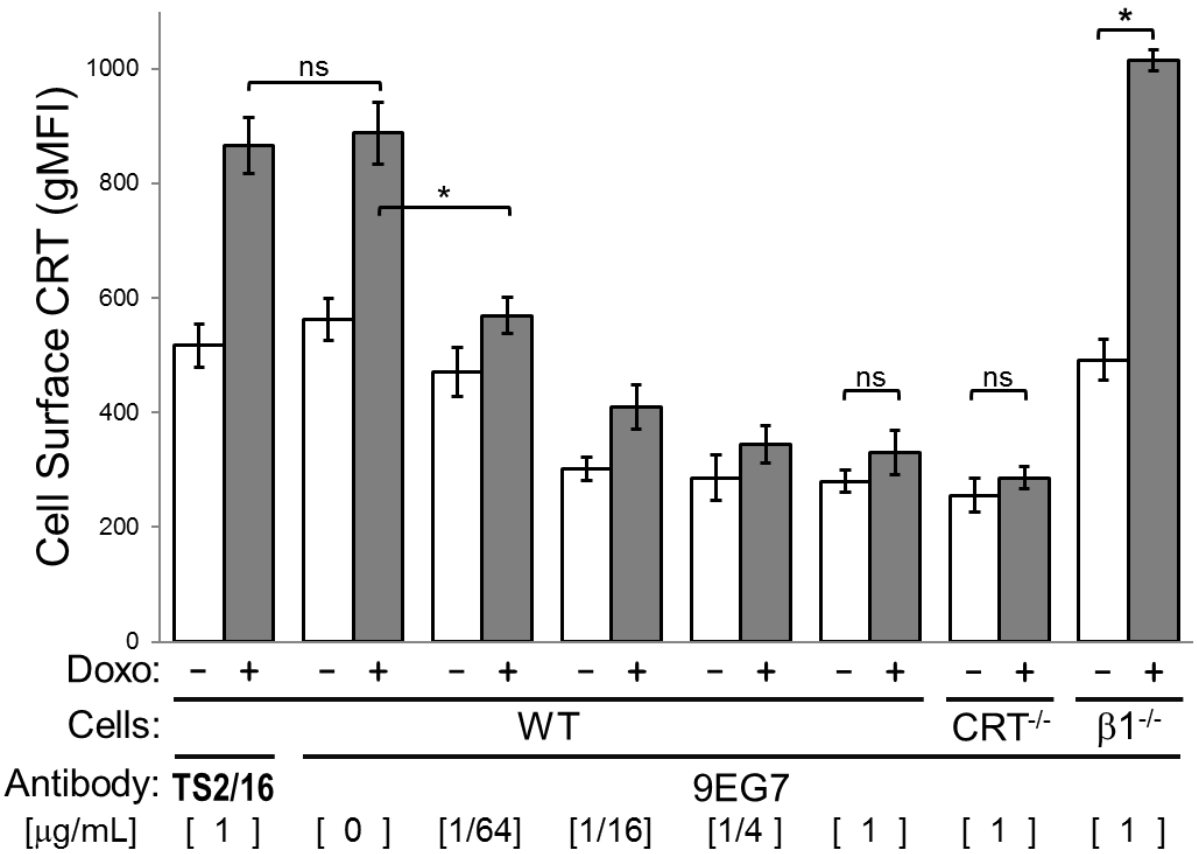

Figure 4.22. Activation of integrins with 9EG7 antibody reduces surface CRT levels
WT, CRT$^{-/-}$ and β1$^{-/-}$ cells were treated with the indicated concentrations of 9EG7 (β1-activating) or TS2/16 (β1 non-activating) antibodies for 15 minutes, followed by treatment with or without 4 μg/mL of doxorubicin (Doxo) for 4 hours. Flow cytometry was used to measure the gMFI of surface CRT labeled with the α-CRT antibody. The bars show the mean ± S.D.; n=3; *p<0.01; ns, p not significant.

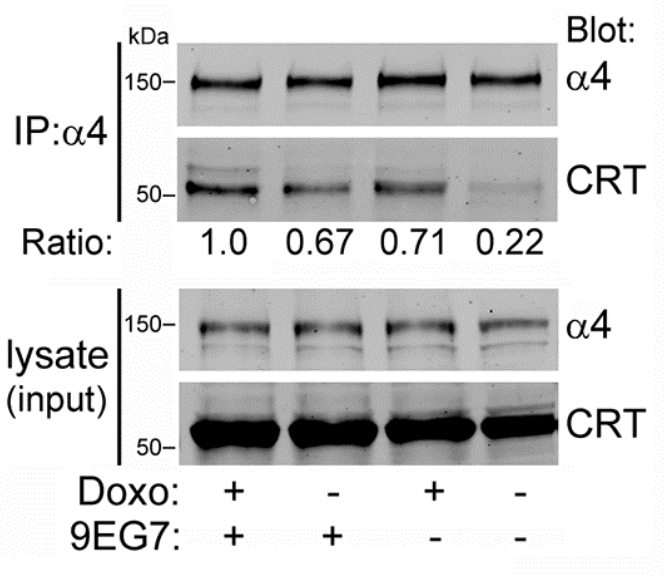

Figure 4.23. Doxorubicin and 9EG7 treatment increase CRT binding to α4-integrin
α4-integrin was immunoprecipitated (IP) from lysates of WT cells that was treated in suspension with combinations of 4 μg/mL of doxorubicin (Doxo) and 1 μg/mL of 9EG7 for 4 hours, as indicated, and analyzed by immunoblotting for CRT and α4. Densitometry analysis was performed to determine the CRT-α4 signal intensity ratio in the immunoprecipitates. The results shown are representative of more than 3 experiments.

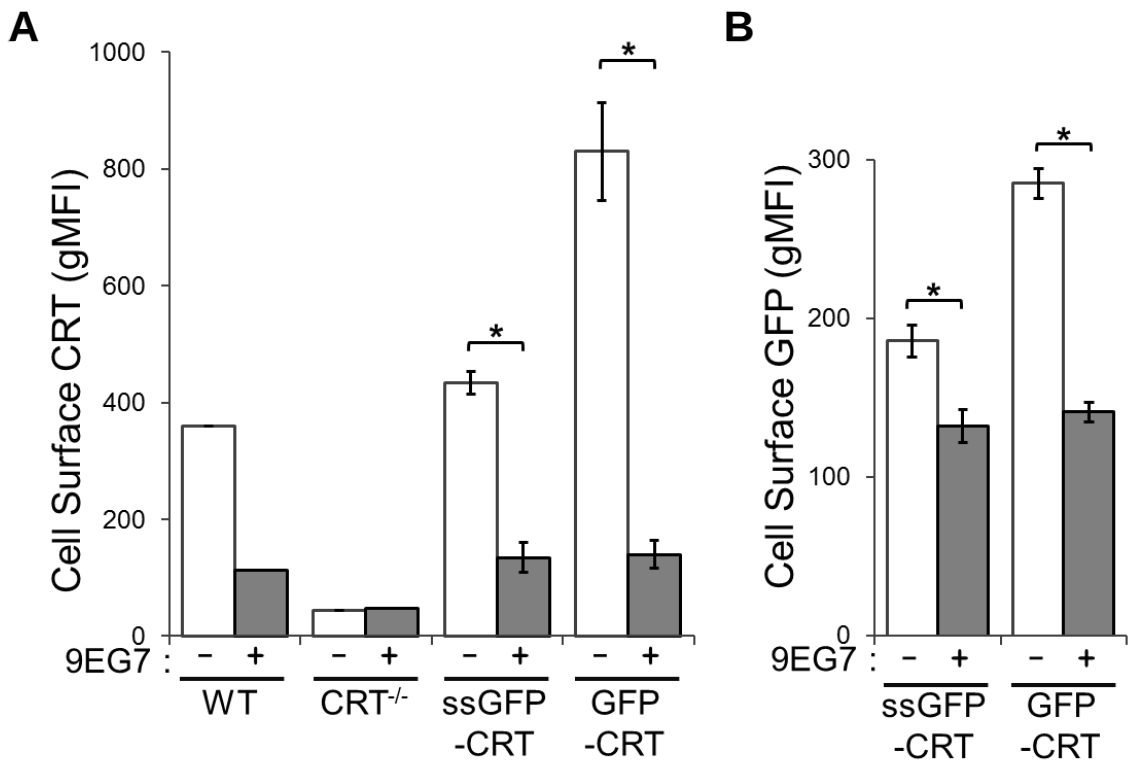

Figure 4.24. Activation of integrins with 9EG7 antibody reduces surface ssGFP-CRT and GFP-CRT levels

WT, CRT$^{-/-}$, and CRT$^{-/-}$ cells expressing ssGFP-CRT or GFP-CRT were treated with or without 1 µg/mL of 9EG7 antibody for 4 hours. Flow cytometry was used to measure the gMFI of *(A)* surface CRT or *(B)* surface GFP labeled with α-CRT or α-GFP antibodies respectively. The bars show the mean ± S.D.; n=3; *p<0.01. The absence of error bars indicates samples conducted without replicates.

4.9 Integrin Activation Reduces Surface CRT Presentation in T-cell Leukemias

Thus far, I have shown that integrin function either stimulated by cell adhesion or induced by an activating antibody can suppress surface CRT expression in Jurkat cells. To determine if the phenomenon can be observed in other T-ALL lymphoblasts, I repeated key assays using the human T-ALL cell lines THP-6, SUP-T1, and DND-41, as well as two primary human T-ALL patient samples, BD-67 and BD-53, which had been expanded by engraftment in

NSG mice. As before, cells were treated with or without doxorubicin to stimulate surface CRT. To assess the effects of adhesion, I seeded cells on dishes coated with BSA or fibronectin. To assess the effects of integrin activation, cells were treated in suspension with 9EG7 activating antibodies, or with TSP2/16, as a non-activating β1-integrin binding control. As shown in Figure 4.25, doxorubicin-induced surface CRT was significantly reduced for cells adhered to fibronectin and for cells treated with 9EG7, compared to their respective controls, in agreement with my observations using Jurkat T-lymphoblasts.

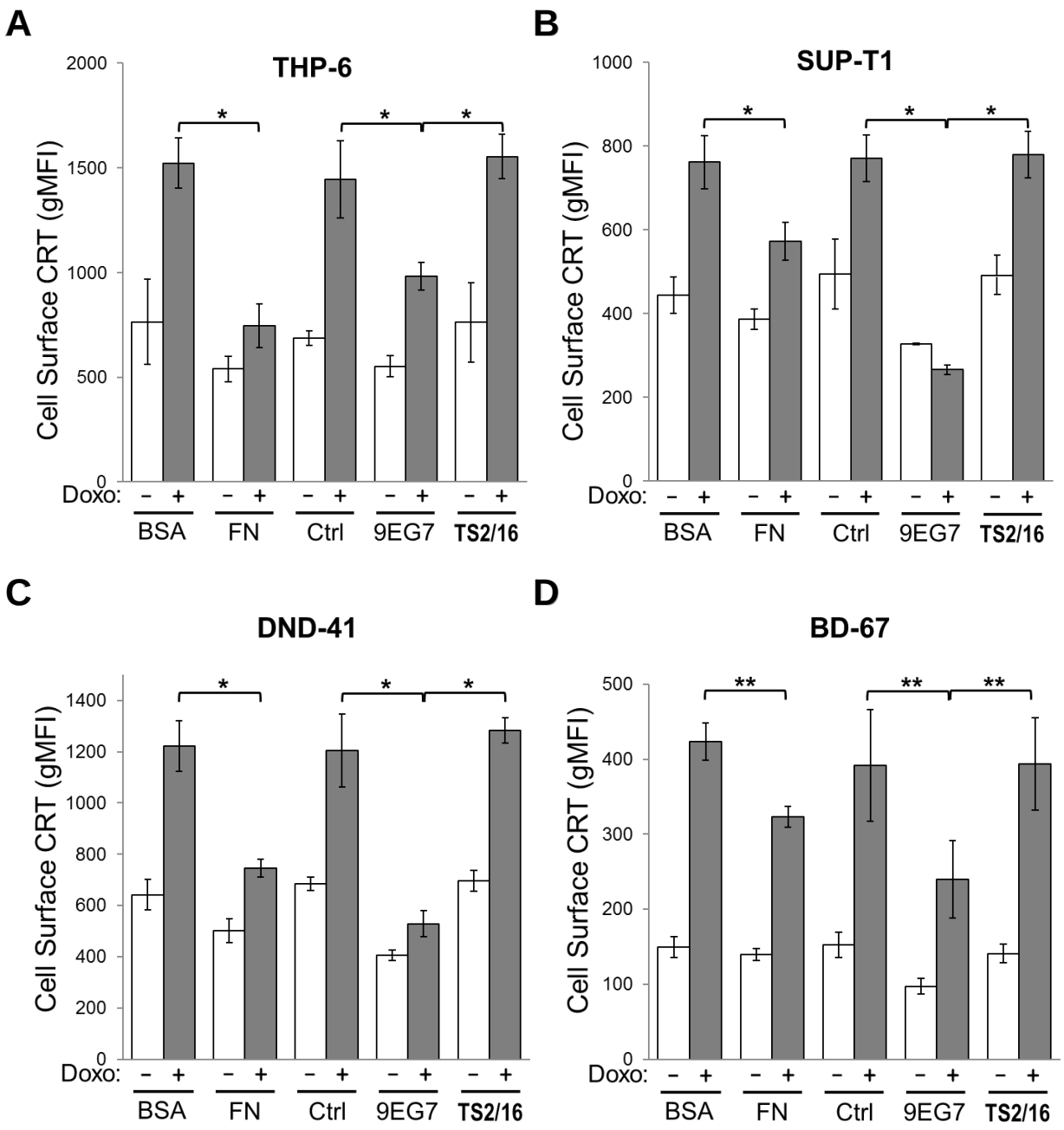
A
THP-6
Cell Surface CRT (gMFI)
2000
1500
1000
500
0
Doxo: − + − + − + − + − +
BSA FN Ctrl 9EG7 TS2/16
B
SUP-T1
Cell Surface CRT (gMFI)
1000
800
600
400
200
0
Doxo: − + − + − + − + − +
BSA FN Ctrl 9EG7 TS2/16
C
DND-41
Cell Surface CRT (gMFI)
1400
1200
1000
800
600
400
200
0
Doxo: − + − + − + − + − +
BSA FN Ctrl 9EG7 TS2/16
D
BD-67
Cell Surface CRT (gMFI)
500
400
300
200
100
0
Doxo: − + − + − + − + − +
BSA FN Ctrl 9EG7 TS2/16

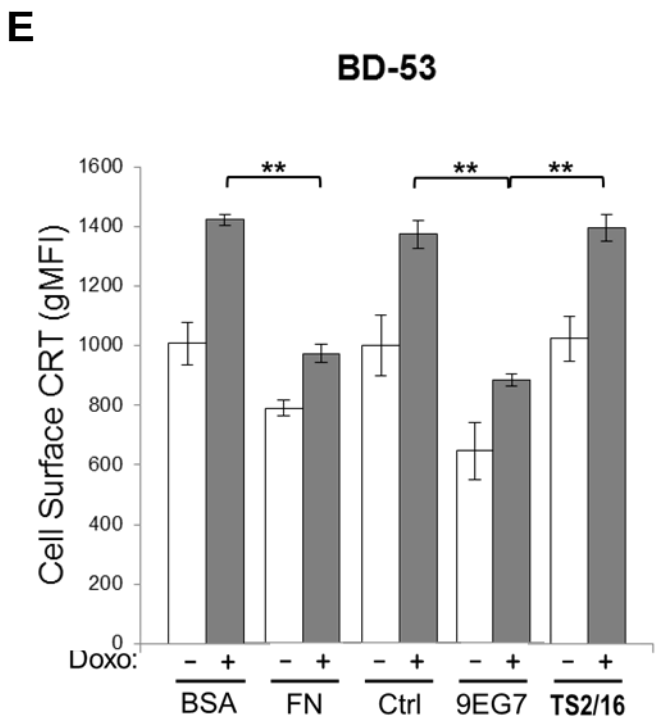

Figure 4.25. Cell adhesion or 9EG7 antibody treatment reduces surface CRT presentation in various T-ALL leukemias

Flow cytometry gMFI plots of surface CRT on various cells subjected to the following treatments, as indicated. Cells were seeded on BSA or fibronectin (FN) for 1 hour, incubated with 1 μg/mL of 9EG7 or TS2/16 antibodies for 15 minutes, or no antibody treatment (Ctrl), prior to incubation with or without 4 μg/mL of doxorubicin (Doxo) for 4 hours. The bars show the mean ± S.D.; n=3; *p<0.01; **p<0.05. As indicated, the cells are: (A) THP-6; (B) SUPT-1; (C) DND41; murine expanded primary human leukemia (D) BD-67 and (E) BD-53.

4.10 CRT Released upon Drug Treatment is Bound by Activated Integrins within the Cytosol

As 9EG7 co-treatment with doxorubicin inhibited surface CRT and increased CRT–integrin interaction (Figure 4.22 and Figure 4.23), I postulated that drug treatment promoted the release of ER-resident CRT into the cytosol where it is able to interact with the integrin cytosolic domain. Doxorubicin is fluorescent and incompatible with multicolor immunofluorescence

imaging; thus I used oxaliplatin, a non-fluorescent and well-characterized ICD-inducing agent (Tesniere et al., 2010). First, I confirmed that surface CRT expression is induced in oxaliplatin-treated Jurkat cells and that 9EG7 similarly inhibited surface CRT exposure (Figure 4.26). To enable differential immunostaining of cytosolic- and ER resident CRT, I used partial permeabilization of cells with digitonin, versus full permeabilization using Triton X-100 (Afshar et al., 2005). WT cells showed robust staining for PDI and CRT when fully permeabilized with TX-100, but not when treated with a digitonin concentration that enables permeabilization of the plasma membrane but not the ER (Figure 4.27). I observed a low but significant level of CRT in oxaliplatin-treated WT cells that were digitonin-permeabilized, suggesting staining of CRT other than the CRT in the ER pool.

To quantify the results, I repeated the assay by flow cytometry, as this allows assessment of total fluorescence that is not limited by optical sectioning (Figure 4.28). Cells were treated with oxaliplatin, 9EG7, or both, prior to fixation with formaldehyde and permeabilization with either TX-100 or digitonin. Regardless of the treatment conditions, TX-100-permeabilized WT cells exhibited comparable staining for CRT at levels significantly greater than that observed for $CRT^{-/-}$ cells, indicating that total CRT levels were unaltered by the various treatments. In contrast, digitonin-permeabilized WT cells treated with oxaliplatin exhibited significantly elevated CRT staining when compared to no drug treatment. The oxaliplatin-induced elevated CRT staining occurred both in the absence and presence of 9EG7 co-treatment with comparable levels (Figure 4.28), suggesting that 9EG7-mediated inhibition of surface CRT does not impact the release of CRT from the ER. In a similar manner, cells expressing Tacδ exhibited no increase in surface CRT upon oxaliplatin treatment, even though cytosolic CRT was significantly increased (Figure 4.29).

Taken together, my results showed that cells treated with the integrin activator 9EG7, or expressing the minimal α-integrin GFFKR, have markedly reduced surface CRT when challenged with an ICD inducer, even though CRT was elevated in the extra-ER, cytosolic compartment. This cytosolic pool of CRT is also detected as an increased interaction with α4-integrin. As α-integrins interact with CRT via the cytosolic GFFKR motif, my results support a model where activated integrins can bind to cytosolic CRT and prevent its translocation to the cell surface.

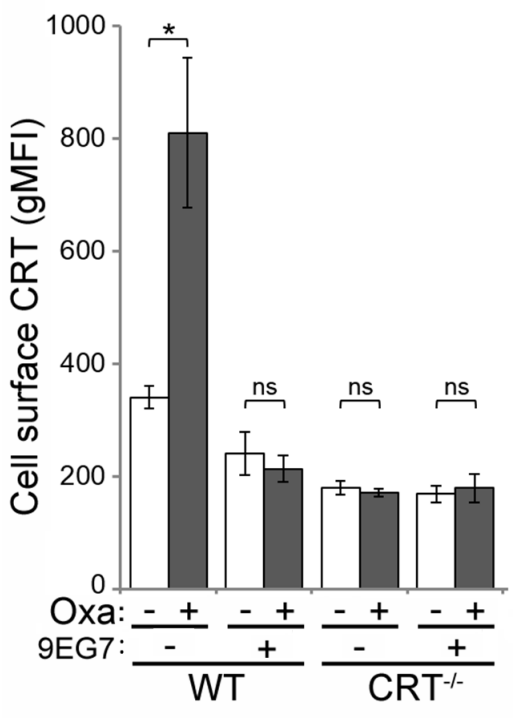

Figure 4.26. Oxaliplatin-induced elevation of surface CRT is inhibited by 9EG7
WT and CRT$^{-/-}$ cells were treated with combinations of 1 μg/ml of 9EG7 antibody for 4 hours and 300 μM of oxaliplatin (Oxa) for 2 hours. Flow cytometry was used to measure the gMFI of surface CRT labeled with the α-CRT antibody. The bars show the mean ± S.D.; n=3; *p<0.01; ns, p not significant.

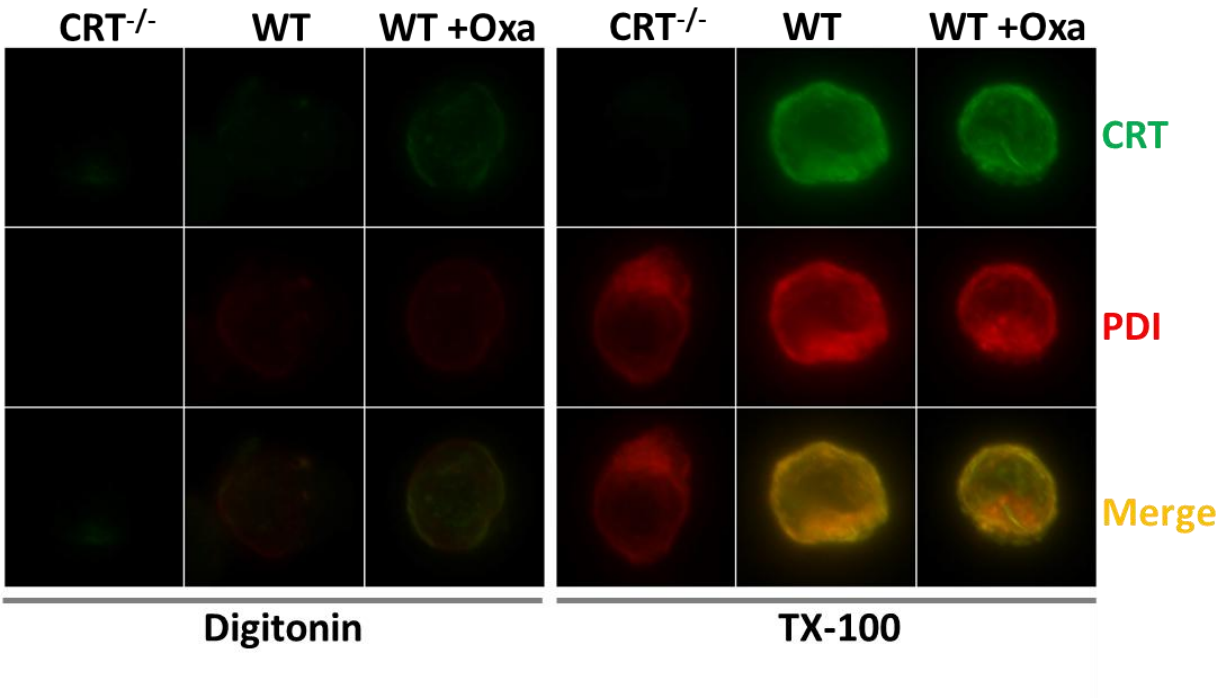

Figure 4.27. Comparative CRT staining using cells permeabilized with Digitonin or TX-100
$CRT^{-/-}$ cells and WT cells were treated with or without 300 μM of oxaliplatin (Oxa) for 2 hours, followed by fixation with formaldehyde and either partial permeabilization with digitonin or full permeabilization with Triton X-100 (TX-100). Cells were then immunostained for CRT (green) and an ER marker, PDI (red). The results shown are representative of more than 3 experiments.

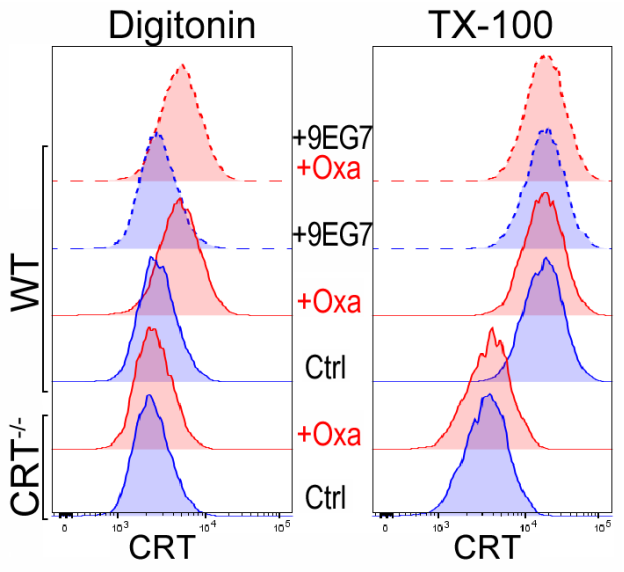

Figure 4.28. Flow cytometry comparison of CRT staining using cells permeabilized with Digitonin or TX-100

WT and CRT$^{-/-}$ cells were treated with combinations of 300 μM of oxaliplatin (Oxa) for 2 hours and 1 μg/mL of 9EG7 for 4 hours, followed by fixation in suspension with formaldehyde and either partial permeabilization with digitonin or full permeabilization with TX-100. Flow cytometry was used to measure CRT labeled with the α-CRT antibody. The histograms show the CRT signals detected under different treatment conditions; n=3.

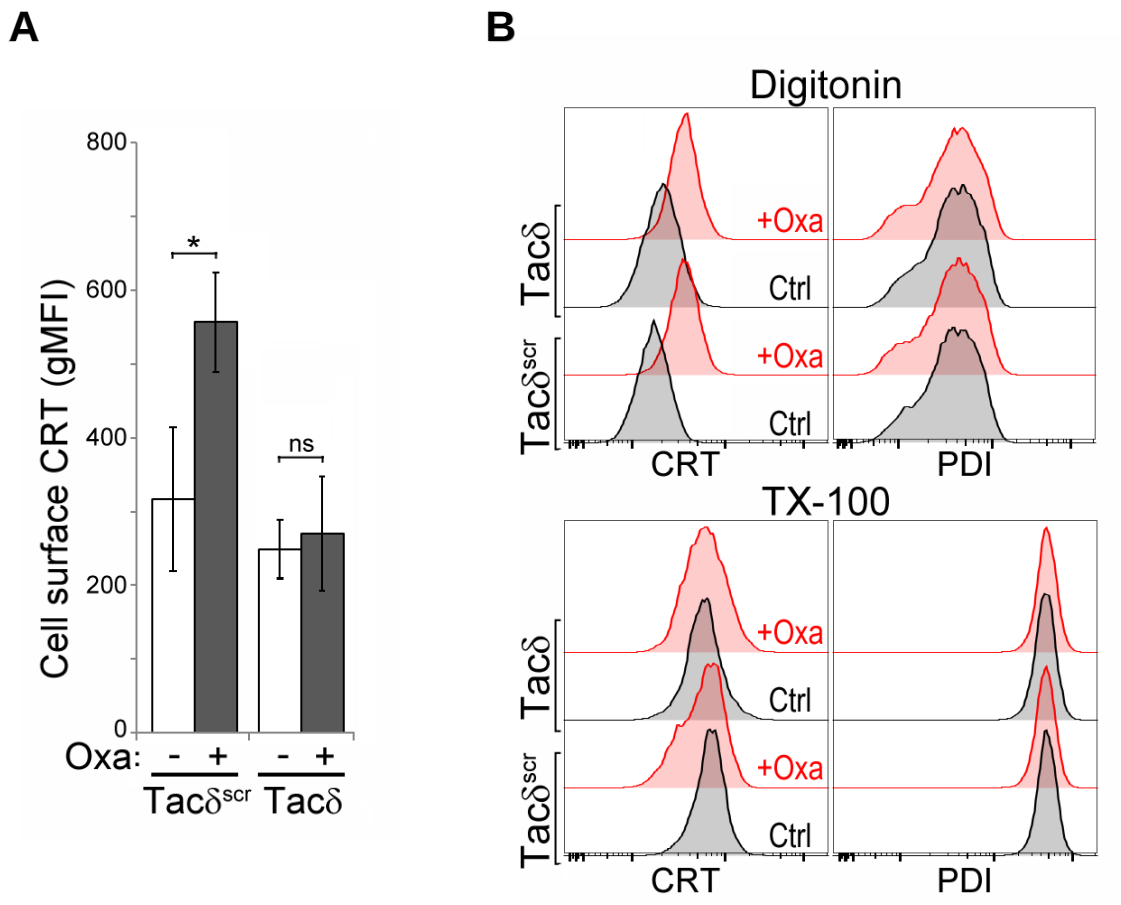

Figure 4.29. Oxaliplatin-treatment increases extra-ER cytosolic CRT that is not presented on the surface of cells expressing Tacδ

A) Tacδ and Tacδ^{scr} cells were treated with or without 300 μM oxaliplatin (Oxa) for 2 hours. Flow cytometry was used to measure the gMFI of surface CRT labeled with the α-CRT antibody. The bars show the mean ± S.D.; n=3; *p<0.01; ns, p not significant. *B)* The flow cytometry experiment is conducted in a similar manner to that described in Figure 4.29 using Tacδ and Tacδ^{scr} cells. Cells were untreated or treated with oxaliplatin for 2 hours, fixed and permeabilized with Digitonin or TX-100 prior to co-staining for both CRT and PDI. The histograms show the CRT and PDI signals detected under different treatment conditions; n=3.

4.11 Integrin-Mediated Decrease in Cell Surface CRT Reduces Phagocytosis by Macrophages

To determine if the integrin-mediated inhibition of surface CRT mediated by ICD inducers has a measurable outcome on target cell engulfment by professional phagocytes, I performed a phagocytosis assay using macrophages. WT target cells were treated with oxaliplatin, 9EG7, and combinations thereof. To counter WT cells' high levels of cluster of differentiation 47 (CD47) expression, a known inhibitory receptor for macrophage-mediated phagocytosis, cells were co-incubated with the CD47-neutralizing antibody, B6H12 (Chao et al., 2010; Jaiswal et al., 2009; Leclair and Lim, 2014). The treated WT cells were incubated with macrophages, and the labeled cell mixture was analyzed by flow cytometry to delineate and quantitate single-positive (WT cells or macrophages) and double-positive (WT cells engulfed by macrophages) populations (Figure 4.30A). The data for all conditions are plotted as a phagocytosis index (Figure 4.30B).

In agreement with similar assays conducted by others (Tseng et al., 2013; Willingham et al., 2012), I found that CD47 neutralization with B6H12 antibody was necessary to reveal a three- to four-fold higher rate of phagocytosis (Figure 4.30B). Under these conditions, macrophage-mediated phagocytosis was significantly increased for oxaliplatin-treated cells compared with untreated WT cells. Importantly, co-treatment with 9EG7 antibody resulted in reduced phagocytosis of cells treated with or without oxaliplatin. Taken together, my results showed that the integrin activating 9EG7 antibody can suppress surface presentation of CRT in T-lymphoblasts to levels that reduce cell engulfment by macrophages.

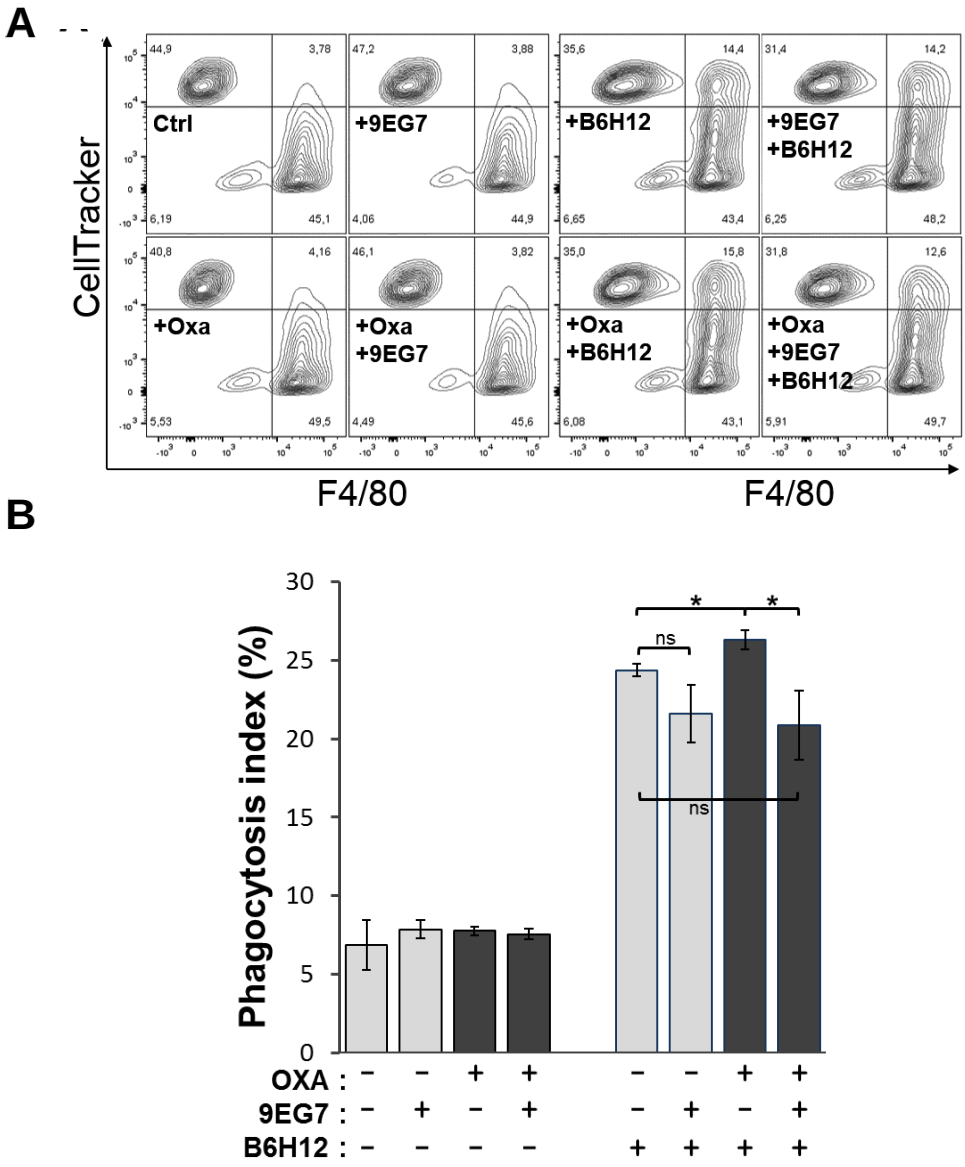

Figure 4.30. Cells treated with 9EG7 antibody exhibit reduced phagocytosis

(A) CellTracker™ labeled WT cells were treated with combinations of 1 μg/mL of 9EG7 (β1-activating) for 4 hours, 7 μg/mL of B6H12 (α-CD47) antibodies for 2 hours, and/or 300 μM of oxaliplatin (Oxa) for 2 hours, followed by co-incubation with F4/80 labeled primary mouse macrophages for 2 hours. Flow cytometry was used to determine phagocytosis (CellTracker$^+$ and F4/80$^+$ macrophages). The scatter plots show the CellTracker™ and F4/80 signals under different treatment conditions. The results shown are representative of more than 3 experiments. *(B)* The calculated phagocytosis index depicted as bar graphs for the data obtained in *(A)*. Phagocytosis index (%) is calculated as 100 • (CellTracker$^+$, F4/80$^+$ macrophages/ total macrophages). The bars show the mean ± S.D.; n=3; *p<0.02; ns, p not significant.

4.12 Discussion

One of the three important hallmarks of ICD is the presentation of CRT on the extracellular cell surface that acts as a pro-phagocytic signal for macrophages (Krysko et al., 2013). Since cell adhesion is a physiologically relevant stimulus previously shown to increase CRT interaction with α-integrins via the juxtamembrane, cytosolic GFFKR motif (Coppolino et al., 1995; Coppolino and Dedhar, 1999; Liu et al., 2013), the work described in this chapter sought to further our understanding of the relationship between the α-integrin-CRT interaction that occurs within the cytosol and the extracellular surface-presented CRT that occurs during ICD. This work is the first to demonstrate a regulatory role for α-integrin function in modulating cell surface CRT presentation.

The many functions mediated by CRT, combined with evidence for its multiple subcellular and extracellular localization, has proven to be a challenge to our ability to dissect the specific roles of this pleiotropic protein. By first generating $CRT^{-/-}$ T-lymphoblasts, and then reconstituting expression with GFP-tagged CRT that was either expressed in the cytosol or enriched within the ER lumen, I was able to investigate the subcellular source of surface CRT resulting from an ICD inducer. The increased surface CRT presentation following doxorubicin treatment of cells expressing the ER-targeted ssGFP-CRT is consistent with earlier reports, suggesting that the path to the cell surface requires induction of ER stress and CRT release from its highly enriched localization within the ER lumen (Garg et al., 2010; Korbelik et al., 2011; Obeid et al., 2007). This increase was detectable with either CRT or GFP antibodies, indicating that the translocation involved the intact fusion protein. When expressed within the cytosol without transiting the ER, GFP-CRT was presented at high levels on the cell surface in a manner that could not be stimulated further with doxorubicin, thus effectively bypassing the requirement

for ER stress. Both ssGFP-CRT_KDELdel and ssGFP-CRT mutant type I contain the ER-targeting signal sequence and lack the KDEL ER retention sequence, thus enabling targeted synthesis of both mutant proteins into the ER while allowing for possible exit through the ER-Golgi secretory pathway. Indeed, the doxorubicin-inducible surface CRT presentation in cells expressing either one of the mutant proteins is consistent with the idea that both proteins remained primarily expressed within the ER. Similarly, both ssGFP-CRT_KDELdel and ssGFP-CRT mutant type I had much lower expression compared to ssGFP-CRT or GFP-CRT, hinting that a large portion of ssGFP-CRT_KDELdel and ssGFP-CRT mutant type I proteins may have been secreted from the cell through the ER-Golgi pathway. Notably, I was not able to obtain satisfactory immunofluorescence images of ssGFP-CRT-KDELdel and ssGFP-CRT-mutant type I transfected $CRT^{-/-}$ cells. Immunofluorescence images of ssGFP-CRT-KDELdel and ssGFP-CRT-mutant type I expressed in Chinese hamster ovary (CHO) cells confirmed their ER localization (data not shown). Several hypotheses have proposed the pathway for which CRT transit from the ER to the cell surface (Holaska et al., 2001; Panaretakis et al., 2008; Panaretakis et al., 2009; Raghavan et al., 2013; Wiersma et al., 2015). My findings suggested that CRT is released from the stressed ER to the cytosol during ICD-inducer treatment, followed by translocation of cytosolic CRT to the cell surface.

At the plasma membrane, α-integrins appear to regulate surface CRT presentation. The C-terminal cytosolic tail encoded by all α-integrins has a conserved GFFKR peptide motif required for heterodimer stabilization with β-integrin (de Melker et al., 1997; Kassner et al., 1994). Structural studies have revealed that the α- and β-integrin tails become physically separated upon integrin activation, facilitating binding of proteins to the tails (Kim et al., 2003). This work, as well as work described by the Dedhar group (Coppolino et al., 1995; Coppolino

and Dedhar, 1999; Liu et al., 2013), demonstrated the phenomenon that cell adhesion promoted the increased interaction of CRT with α-integrins. I adopted several strategies to test the assumption that increased integrin activation leads to increased intracellular CRT-integrin interaction, thus reducing the amount of 'free' cytosolic CRT able to translocate to the extracellular surface. As a physiologically relevant stimulus, I showed that T-lymphoblast adhesion to an integrin substrate significantly reduced surface CRT in cells treated with ICD inducers. Similarly, suspension cells treated with the β1-integrin-activating antibody, 9EG7, elicited a greater suppressive effect on surface CRT when compared with adhesion, in most cases reducing surface CRT on WT cells to the levels observed for $CRT^{-/-}$ cells. Combined with the observations that 9EG7 treatment, or expression of the juxtamembrane-anchored cytosolic GFFKR motif, suppressed the appearance of surface CRT for $CRT^{-/-}$ cells expressing the cytosol-targeted GFP-CRT, I suggest that a cytosolic pool of CRT exists in T-lymphoblasts and that activated integrins interact primarily with this pool of cytosolic CRT.

I also showed that expression of a transmembrane-anchored α-integrin tail consisting of only the GFFKR motif (as α4δ or Tacδ) resulted in increased interaction with CRT in an adhesion-independent manner and in a manner requiring the GFFKR sequence. α4δ and Tacδ cells also exhibit constitutively lower levels of surface CRT, again in an adhesion-independent manner. Furthermore, higher α4δ expression correlated with lower levels of surface CRT, suggesting that the truncation may enable binding of CRT to the now more accessible juxtamembrane GFFKR motif. More CRT associated with α4-integrin when cells were treated with an ICD inducer, likely resulting from a marked increase in cytosolic CRT released from the ER, now able to interact with α-integrin tails. This suggested that the increased CRT-integrin or

CRT-GFFKR interaction effectively sequestered CRT within the cytosol and prevented its translocation to the extracellular surface.

The work presented in this chapter showed that cell surface CRT presentation is decreased when T-ALL cell lines are seeded on several integrin-engaging substrates or when treated with a β1-integrin activating antibody such as 9EG7. Beyond the GFFKR-conserved motif, α-integrin tails share little sequence homology (Abram and Lowell, 2009); thus, an interesting question for future studies would be to compare surface CRT levels of cells specifically engaging various α-integrins. In addition to α4β1, lymphocytes also express high levels of αLβ2-integrins, considered to be an equally important homing receptor. Thus, it would be of great interest to test if cell adhesion on ICAM-1, a substrate for αLβ2-integrins, may also be inhibitory to surface CRT presentation in cells treated with ICD-inducing agents.

Another interesting possibility to consider is if the α-integrin interaction with CRT is absolutely dependent on the conserved GFFKR sequence. As shown in Figure 1.5, the α-integrins represented by α8, α9, α10, and α11 exhibit small variations to this otherwise highly conserved motif, as GFFxR or GFFxx (where x is a deviation from the consensus motif). Thus, cell adhesion via these specific integrins may or may not result in increased CRT-α-integrin interaction nor in decreased surface CRT upon treatment of cells with ICD-inducing agents.

As a DAMP expressed on the surface of cells undergoing ICD, surface CRT is crucial for the clearance of tumor cells by the host immune system, mediated by professional phagocytes (Chao et al., 2010; Spisek et al., 2007; Spisek and Dhodapkar, 2007). Therefore, cell physiological events contributing to reduced surface CRT expression may lead to reduced antitumor responses resulting from ICD-based chemotherapy. The tumor microenvironment such as the bone marrow stroma may provide these protective stimuli in the form of adhesion

substrates and stimulatory chemokines that promote integrin activation (Meads et al., 2009; Meads et al., 2008). Thus, effective chemotherapy using ICD inducers may benefit from co-administration with integrin function-blocking therapeutic antibodies.

Chapter 5: Role of Calreticulin in Chemoresistance and as a Mediator of JAK/STAT Signaling in T-Lymphoblasts

5.1 Overview and Rationale

JAK/STAT signaling pathways transmit extracellular signals through the plasma membrane into the cell nucleus, leading to expression of proteins involved in the regulation of cell proliferation, differentiation, and apoptosis (Darnell Jr et al., 1994; Rawlings et al., 2004). As multiple JAK/STAT pathways are involved in lymphocyte proliferation and differentiation, they are often mutated or overexpressed in hematological malignancies, for example, mutations in STAT3 and STAT5 pathways are often found in leukemias (Koskela et al., 2012; Shuai et al., 1996). As a multifunctional protein, CRT has been shown to facilitate the phosphorylation of STAT3 (Abraham et al., 2010; Du et al., 2009; Li et al., 2005a). More recently, multiple genome-based studies have shown that somatic mutations in *CALR* (which encodes for CRT) form the second largest group of markers after the JAKV617F gain of function mutation in myeloproliferative neoplasms (MPN) (Klampfl et al., 2013; Nangalia et al., 2013). Interestingly, the same groups found that the somatic CRT or JAK mutations in MPNs were, for the most part, mutually exclusive (Klampfl et al., 2013; Nangalia et al., 2013), leading to the tantalizing postulate that CRT and JAK function within the same signaling pathway. Indeed, expression of mutated CRT was found to sustain a low level of constitutive STAT3 phosphorylation (Klampfl et al., 2013).

JAK/STAT signaling has been studied extensively regarding its involvement in tumor proliferation, development, and chemoresistance. For example, STAT3 and STAT5 have been

shown to mediate the proliferation and survival of multiple types of leukemia, multiple myeloma and numerous solid tumor cell types such as breast cancer and ovarian cancer (Bhardwaj et al., 2007; Bharti et al., 2004; Jinawath et al., 2010; Nakajima et al., 1996; Real et al., 2002; Sexl et al., 2000; Van der Plas et al., 1996; Weisberg et al., 2012). Combined with my previous findings that CRT binds to α-integrin via the GFFKR membrane-proximal cytoplasmic motif, and that the GFFKR motif is associated with enhanced chemoresistance in T-ALL cells, I sought to determine if CRT is associated with drug resistance in T-ALL cells in a manner involving JAK/STAT signaling.

5.2 Calreticulin is Associated with α-integrin GFFKR Motif-Mediated Drug Resistance

To investigate if CRT is associated with GFFKR motif-mediated drug resistance, I used CRISPR-Cas9 (Cong et al., 2013) to silence CRT expression in the chemoresistant Tacδ cells previously described in Chapter 3 (Tacδ/CRT$^{-/-}$). Western blot analysis and sequencing of the genomic *CALR* loci showed a complete loss of CRT expression due to a targeted frameshift deletion resulting in a predicted early translation termination (Figure 5.1). Similar to the apoptosis assays described in Chapter 3, I also used cells expressing Tacδ^{scr} with the scrambled GFFKR motif as the control for Tacδ cells. Cells were treated with doxorubicin for 48 hours, and apoptosis was determined by Annexin V binding using flow cytometry. In agreement with previous assays described in Chapter 3 (Figure 3.8), I found that doxorubicin-induced apoptosis was lowest in Tacδ cells and highest in Tacδ^{scr} cells (Figure 5.2A). In contrast with Tacδ cells, Tacδ/CRT$^{-/-}$ cells exhibited partial loss of chemoresistance to doxorubicin (Figure 5.2A); thus implicating CRT as a positive mediator of GFFKR-mediated drug resistance. Stable re-

expression of CRT in the form of ssGFP-CRT in Tacδ/CRT$^{-/-}$ cells (Figure 5.2B) successfully restored chemoresistance to levels comparable to Tacδ cells (Figure 5.2A).

The work described in Chapter 3 showed that GFFKR motif-mediated chemoresistance requires the influx of extracellular Ca^{2+} (Figure 3.17 and Figure 3.18). Since CRT has been described as an L-type Ca^{2+} channel and a Ca^{2+} reservoir regulatory protein (Kwon et al., 2000), it is plausible that CRT's role in drug resistance may be coupled to its role in regulating Ca^{2+} flux. To investigate this, I measured intracellular Ca^{2+} levels for Tacδ, Tacδ/CRT$^{-/-}$ and Tacδ^{scr} cells using the cell permeant Ca^{2+} indicator, Fluo-4-AM. As before, cells were incubated in media with and without extracellular Ca^{2+} and under non-adherent conditions. In this manner, the difference in cellular Fluo-4-AM fluorescence between the two conditions provides a measure of Ca^{2+} influx. Similar to previous results (Figure 3.16), I found that Tacδ cells exhibited the highest levels of Ca^{2+} influx (Figure 5.3). Surprisingly, Tacδ^{scr} had intermediate Ca^{2+} influx, while Tacδ/CRT$^{-/-}$ cells had the lowest Ca^{2+} influx, suggesting that CRT is a more important factor in regulating Ca^{2+} influx than the GFFKR motif (Figure 5.3).

Previously, I showed that drug efflux contributes to GFFKR motif-mediated adhesion-independent chemoresistance (Figure 3.20 and Figure 3.21). Drug efflux is coupled with Ca^{2+} influx to achieve the export of drugs out of cells (Schinkel and Jonker, 2003). Since CRT impacts cellular Ca^{2+} influx in a significant manner, I sought to determine if CRT contributes to drug efflux activity observed in Tacδ cells. Tacδ, Tacδ/CRT$^{-/-}$ and Tacδ^{scr} cells were incubated with calcein-AM, an indicator substrate used to assess the activity of certain p-glycoprotein based transporters (Legrand et al., 1998). I found that Tacδ cells retained fluorescent calcein at a significantly lower rate compared to Tacδ^{scr} cells while Tacδ/CRT$^{-/-}$ cells had the highest

fluorescent calcein retention rate (Figure 5.4). This indicated that CRT expression was a more important factor in the efflux of calcein-AM than GFFKR motif expression.

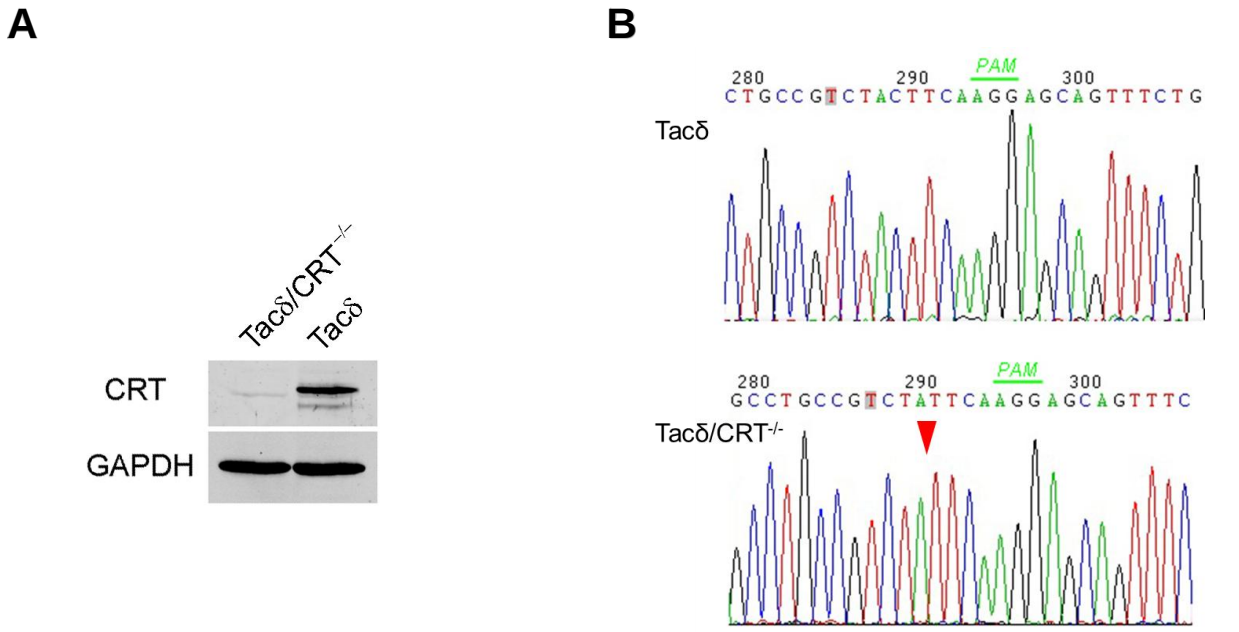

Figure 5.1. Generation of a Tacδ/CRT$^{-/-}$ cell line using CRISPR-Cas9
Tacδ cells were transfected with a CRISPR-Cas9 construct targeting *CALR*, and clones were screened for CRT expression as detailed in Methods. *(A)* Confirmation of loss of CRT expression in a representative Tacδ/CRT$^{-/-}$ clone by Western blotting using antibodies against CRT. Equal protein loading was assessed by immunoblotting for GAPDH. (*B)* Sequencing of CALR genomic loci showing single nucleotide deletion (red triangle) occurring at 67 bp from the predicted start codon and -4 bp from the PAM recognition motif (green bar). The frame shift mutated variant encodes a predicted 96 amino acid protein product due to a premature termination codon.

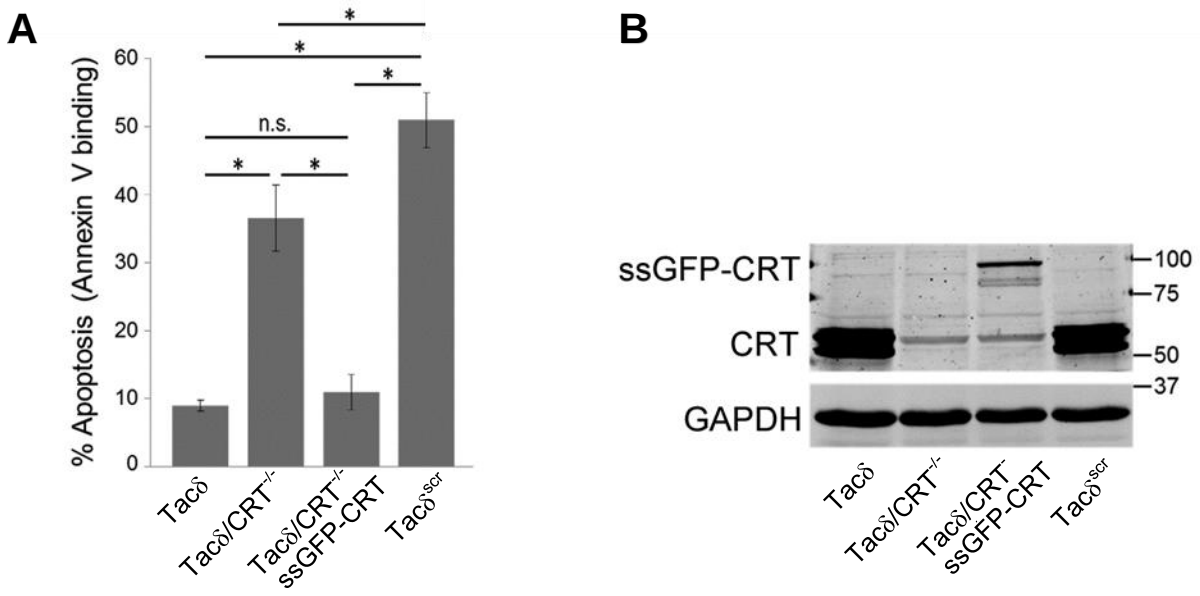

Figure 5.2. Involvement of CRT in GFFKR motif-mediated drug resistance

(A) The indicated cells were treated with 0.06 μg/mL of doxorubicin for 48 hours and flow cytometry was used to assess the percentage of total cells undergoing apoptosis as labeled by Annexin V binding. The bars show the mean ± S.D.; n=3; **p*<0.01. *(B)* Western immunoblot to detect CRT and GAPDH (loading control) in lysates of the same cells.

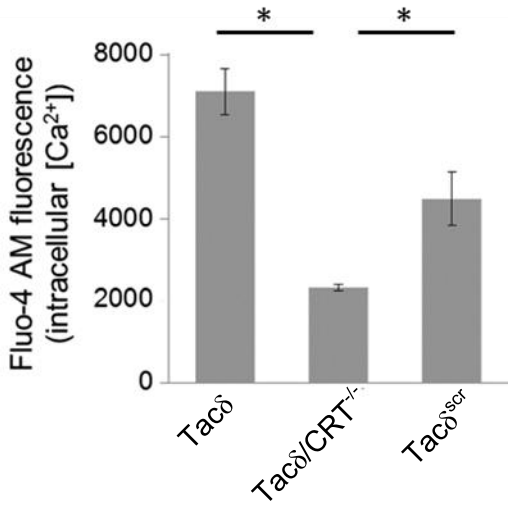

Figure 5.3. Involvement of CRT in regulation of intracellular Ca^{2+} levels

The indicated cells were labeled with Fluo-4-AM as described in Methods and incubated in PBS with or without 1 mM $CaCl_2$ at 22°C for 10 minutes prior to measurements. Flow cytometry was used to assess the concentration of intracellular Ca^{2+} as indicated by Fluo-4-AM fluorescence. Plotted are the intracellular calcium measurements obtained from cells in 1 mM $CaCl_2$/PBS after subtracting measurements obtained from cells in PBS alone (mean ± S.D.; n=4; **p*<0.01).

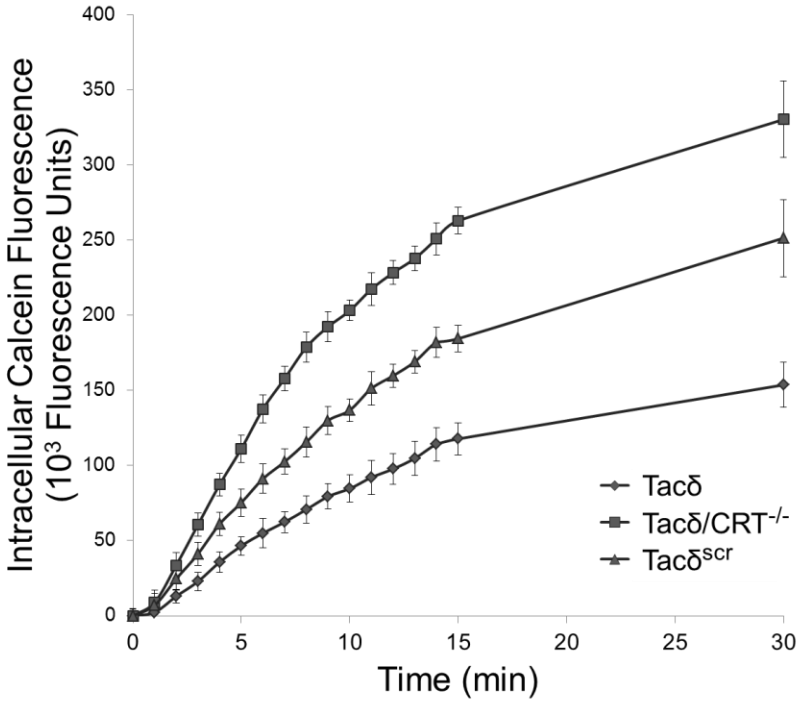

Figure 5.4. Involvement of CRT in calcein-simulated drug efflux
The indicated cells were incubated with the cell permeant calcein-AM substrate and fluorescence readings were taken at the indicated times. The rate of fluorescent calcein accumulation is an indirect and inverse measure of the cellular efflux rates of calcein-AM. The data points show the mean ± S.D.; n=3; *p* not significant for t<2 minutes; $p<0.05$ for 2<t<4 minutes; $p<0.002$ for t>4 minutes.

5.3 Calreticulin is Involved in CAMDR Signaling

Previously, I showed that cells expressing the truncated GFFKR motif as α4δ and Tacδ exhibited constitutive binding to CRT in a manner independent of cell adhesion, while cell adhesion via integrins enhanced the interaction between α-integrin and CRT (Figure 4.3 and Figure 4.4). To determine if CRT also plays a significant role in drug resistance upon α-integrin-mediated adhesion, I seeded WT, $CRT^{-/-}$ and $CRT^{-/-}$ cells stably expressing ssGFP-CRT on the integrin substrate fibronectin (Fn) or on BSA as a non-adherent control, prior to treatment with doxorubicin (Figure 5.5). Consistent with my previous results, the fraction of apoptotic cells was

reduced for all three cell lines when plated on Fn when compared with BSA as a substrate (Figure 5.5A). However, the adhesion-dependent reduction in apoptosis was not as large for $CRT^{-/-}$ cells when compared to WT cells, or to $CRT^{-/-}$ cells rescued with ssGFP-CRT expression (Figure 5.5A and B). This indicated that CRT plays a role in adhesion-dependent integrin-mediated chemoresistance (CAMDR). Notably, the fraction of apoptotic cells after treatment with doxorubicin and seeding on BSA was comparable among the three cell lines, indicating that loss of CRT did not adversely affect cell survival under adhesion-independent conditions.

The work described in Chapter 3 showed that integrin-mediated cell adhesion in WT cells promoted Ca^{2+} influx (Figure 3.19) and that drug resistance was coupled with Ca^{2+}-dependent drug efflux. To determine if CRT is involved in this process, WT and $CRT^{-/-}$ cells were labeled with Fluo-4-AM and fluorescence monitored over time following seeding of the cells onto Fn- or BSA-coated dishes (Figure 5.6). The cells exhibited comparable fluorescence at t=0 under all conditions tested, indicating comparable labeling and quantity of cells. Over the next 35 minutes, WT cells seeded on Fn exhibited significantly higher intracellular Ca^{2+} levels compared to WT cells seeded on BSA. Even though plating of $CRT^{-/-}$ cells on Fn elicited a small increase in intracellular Ca^{2+} levels compared to $CRT^{-/-}$ cells on BSA, overall, the Ca^{2+} influx for $CRT^{-/-}$ cells was significantly less than that of WT cells plated on a non-adherent substrate (Figure 5.6).

To determine if CRT is involved in cell adhesion-dependent promotion of drug efflux, WT and $CRT^{-/-}$ cells were incubated with the cell-permeant calcein-AM substrate and then seeded onto Fn- or BSA-coated dishes. The rate of fluorescence accumulation inversely correlates with the efflux rate of calcein-AM, and as shown in

Figure 5.7, I found that the efflux rates of WT and $CRT^{-/-}$ cells plated on Fn or BSA correlated precisely with their rates of Ca^{2+} influx (Figure 5.6). Taken together, these results

implicate a role for CRT in cell adhesion-mediated drug resistance, and indicate that the effects are mediated in part by CRT's critical role in regulating Ca^{2+} flux.

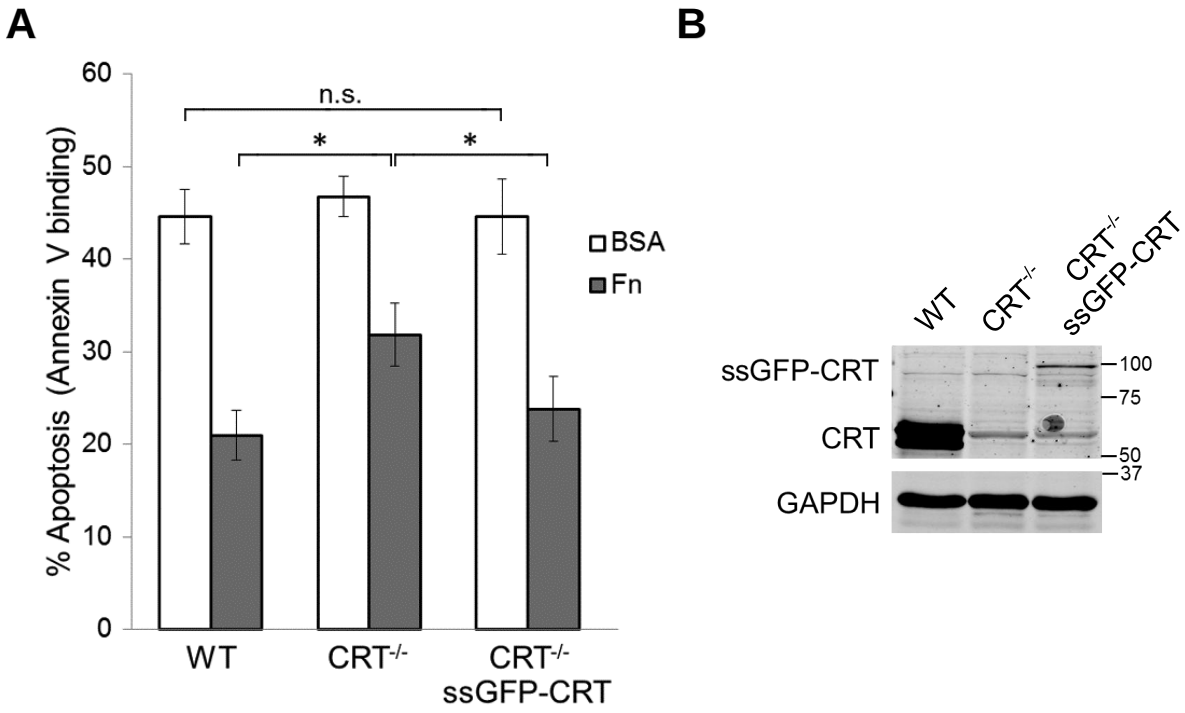

Figure 5.5. Involvement of CRT in CAMDR

(A) WT, $CRT^{-/-}$ and $CRT^{-/-}$ cells stably expressing ssGFP-CRT were seeded on dishes coated with Fn or BSA for 4 hours, followed by treatment with 0.05 μg/mL of doxorubicin for 48 hours. Flow cytometry was used to assess the percentage of total cells undergoing apoptosis as labeled by Annexin V binding. The bars show the mean ± S.D.; n=3; **p*<0.05; ns, *p* not significant. *(B)* Western immunoblot to detect CRT and GAPDH (loading control) in lysates of the cells as indicated.

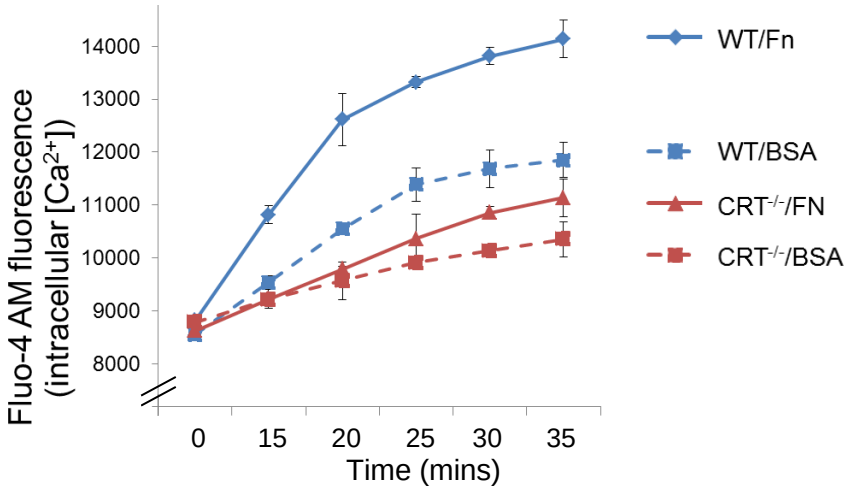

Figure 5.6. Involvement of CRT in adhesion-dependent Ca^{2+} flux
WT and $CRT^{-/-}$ cells were labeled with Fluo-4-AM and seeded on dishes coated with fibronectin (Fn) or BSA and fluorescence readings were taken at the indicated times following cell seeding. The data points show the mean ± S.D.; n=3; $p<0.05$ for t=30-35 minutes for all comparisons, and not significant for t=0 minutes for all comparisons.

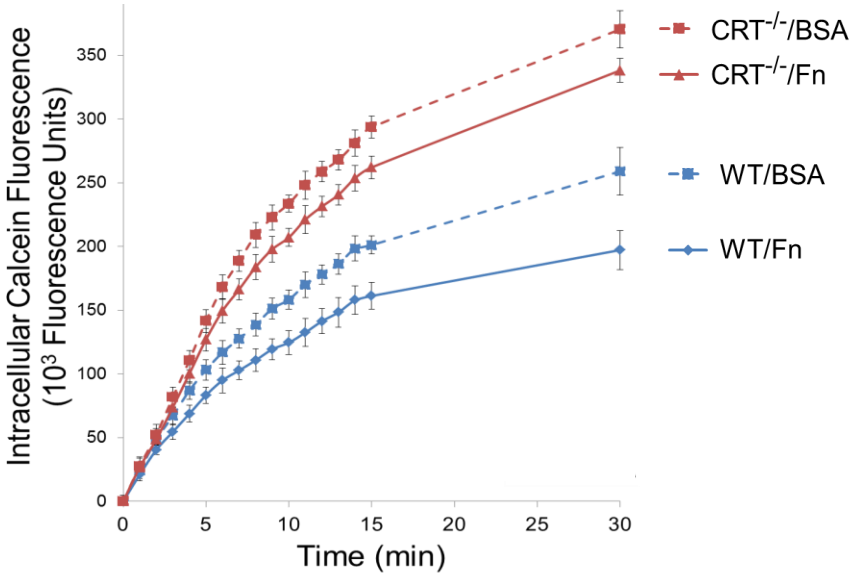

Figure 5.7. Involvement of CRT in adhesion-dependent calcein simulated drug efflux
WT and $CRT^{-/-}$ cells were incubated with the cell permeant calcein-AM substrate and seeded on dishes coated with Fn or BSA. Fluorescence readings were measured at the indicated times. The rate of calcein accumulation is an indirect and inverse measure of the cellular efflux rates of calcein-AM. The data points show the mean ± S.D.; n=3; *p* not significant for t=0-2 minutes for all comparisons; $p<0.01$ for t>7 minutes for all comparisons.

5.4 Involvement of Calreticulin in STAT Protein Phosphorylation in T-ALL

As mentioned in the introductory chapter (Section 1.9 and 1.10), mutant forms of CRT have been associated with myeloproliferative neoplasms (MPNs), occurring at a frequency that is second only to gain-of-function JAK2 mutation (Klampfl et al., 2013; Nangalia et al., 2013). Klampfl *et al* found that expression of mutated CRT led to sustained phosphorylation of STAT5 in a manner no longer requiring cytokine stimulation (Klampfl et al., 2013; Nangalia et al., 2013). Both STAT3 and STAT5 have been shown to be important players in the development and prognosis of leukemia, and also in contributing to chemoresistance in refractory tumors (Bhardwaj et al., 2007; Bharti et al., 2004; Nakajima et al., 1996; Sexl et al., 2000; Van der Plas et al., 1996; Weisberg et al., 2012). The MPN-associated somatic mutations result in a CRT protein without the C-terminal KDEL ER retention sequence, and this is hypothesized to promote increased accumulation of CRT in the cytosol. Of particular interest, there is now evidence to suggest that the MPN-associated mutant CRT acts at the receptor level by interacting with the thrombopoietin receptor, myeloproliferative leukemia protein (MPL) in essential thrombocytopenia, that produces sustained JAK/STAT signaling (Araki et al., 2016; Chachoua et al., 2016). While this has not been shown in MPNs, work by another group has indicated that CRT is naturally present in the cytosol, albeit at very low levels compared to the ER and in the absence of cell treatment with ICD-inducers (Afshar et al., 2005). Along with my finding that CRT is involved in GFFKR motif-mediated drug resistance, and that both STAT3 and STAT5 signaling are potential oncogenic drivers in leukemia (Koskela et al., 2012; Shuai et al., 1996), I investigated if CRT is involved in regulation of STAT3 and STAT5 phosphorylation occurring downstream of cytokine receptor signaling in T-ALL lymphoblasts.

To determine if CRT is involved in STAT3 and STAT5 activation in Jurkat T lymphoblasts, I performed Western blot analysis to detect phospho(Y705)-STAT3 and phospho(Y694)-STAT5 in cells stimulated with cytokines. Initially, cells were stimulated with IFNα 2b, a cytokine that binds to interferon-α/β receptor (IFNAR) and known to non-specifically activate a number of STAT proteins, to assess possible CRT involvement in STAT signaling (Platanias, 2005). Flow cytometry analysis for surface IFNAR indicated comparable expression levels in WT, $CRT^{-/-}$, and $CRT^{-/-}$ cells stably expressing ssGFP-CRT (Figure 5.8), suggesting little consequence on receptor expression due to CRT disruption. From initial optimization studies, I found that a higher concentration of IFNα 2b was required to induce tyrosine phosphorylation of STAT5 compared to that of STAT3 (not shown). Subsequently, WT, $CRT^{-/-}$, and $CRT^{-/-}$/ssGFP-CRT cells were stimulated with 10 ng/mL and 2.5 ng/mL of IFNα 2b for analysis of phospho(Y694)-STAT5 and phospho(Y705)-STAT3, respectively. Compared to non-stimulated controls, IFNα 2b-stimulated WT cells showed increased phosphorylation levels of both STAT5 and STAT3 (Figure 5.9). In contrast, IFNα 2b-stimulated $CRT^{-/-}$ cells exhibited significantly reduced phosphorylation levels of both STAT5 and STAT3, even though total expression of the proteins was comparable between WT and $CRT^{-/-}$ cells (Figure 5.9). To confirm the requirement of CRT in IFNα 2b-stimulated phosphorylation of STAT proteins, the assay was conducted with $CRT^{-/-}$cells stably reconstituted with ssGFP-CRT expression. I found that ssGFP-CRT expression fully reconstituted the IFNα 2b-stimulated increase of phospho(Y694)-STAT5, but not of phospho(Y705)-STAT3 (Figure 5.9). In summary, my results indicated that CRT is required for efficient IFNα 2b-stimulated phosphorylation of STAT5 and STAT3, and that ssGFP-CRT expression was able to restore IFNα 2b stimulation of phospho(Y694)-STAT5 in $CRT^{-/-}$ cells.

Since IFNα 2b binding to its receptors lead to phosphorylation of multiple STAT proteins, including STAT1, 2, 3 and 5, I sought to gain greater cytokine specificity by using interleukin-6 (IL6) and interleukin-7 (IL7), which preferentially stimulate the phosphorylation of STAT3 and STAT5, respectively (Goetz et al., 2004; Hodge et al., 2005; Nakajima et al., 1996; Platanias, 2005; Wofford et al., 2008). Initial attempts revealed no evidence of STAT phosphorylation when the WT Jurkat cells were stimulated with IL6 or IL7. The fault with this approach was traced to the fact that Jurkat cells do not express a detectable level of the corresponding receptors, IL6R and IL7R (data not shown). To circumvent this limitation, I transfected and flow sorted the WT and $CRT^{-/-}$ cells to obtain comparable stable expression of IL6Rα (WT/IL6Rα and $CRT^{-/-}$/IL6Rα, Figure 5.10). Unfortunately, similar attempts to generate cells stably expressing IL7Rα were unsuccessful. As shown in Figure 5.11, WT/IL6Rα cells stimulated with IL6 showed increased levels of phospho(Y705)-STAT3 compared to the non-stimulated control. In contrast, IL6 stimulated $CRT^{-/-}$/IL6Rα cells showed a smaller increase in STAT3 phosphorylation when compared to WT/IL6Rα cells. This result is similar to that obtained for cells stimulated with IFNα 2b and suggests that CRT is involved in STAT signaling downstream of IL6Rα or IFNAR stimulation (Figure 5.9 and Figure 5.11).

Taken together, these results indicate that CRT deficiency resulted in decreased cytokine-stimulated STAT3 and STAT5 phosphorylation in Jurkat T-lymphoblasts. However, reconstitution of the $CRT^{-/-}$ cells with ssGFP-CRT rescued STAT5 but not STAT3 phosphorylation. It is notable that the ssGFP-CRT levels obtained in the stable expressers were lower than that detected for the endogenous protein in WT cells, and this may account for the lack of rescue with regards to STAT3 phosphorylation.

To better understand the role of CRT in JAK/STAT signaling in T cells, I analyzed additional T-ALL cell lines to identify phenotypes that might be amenable for further characterization. Three T-ALL cells lines, THP-6, SUP-T1 and DND41 were either not stimulated or stimulated with IL6 or IFNα 2b, and the STAT3 and STAT5 phosphorylation levels determined by immunoblotting (Figure 5.12). No stimulation was observed with IL6, while IFNα 2b stimulated the phosphorylation of STAT3 and STAT5 in THP-6 and SUP-T1 cells. DND41 cells were found to have constitutive STAT5 phosphorylation. In follow-up studies, it will be of interest to knockout CRT expression in DND41 cells to further delineate the point along the cytokine receptor/JAK/STAT signaling pathway at which CRT acts.

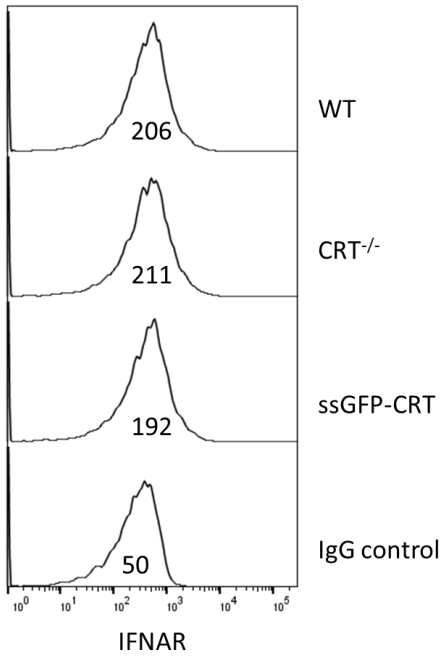

Figure 5.8. IFNAR expression
Flow cytometry determination of cell surface interferon-α/β receptor (IFNAR) expression in WT, $CRT^{-/-}$, and $CRT^{-/-}$ cells stably expressing ssGFP-CRT (ssGFP-CRT). Numbers under the histograms show the geometric mean fluorescence intensity.

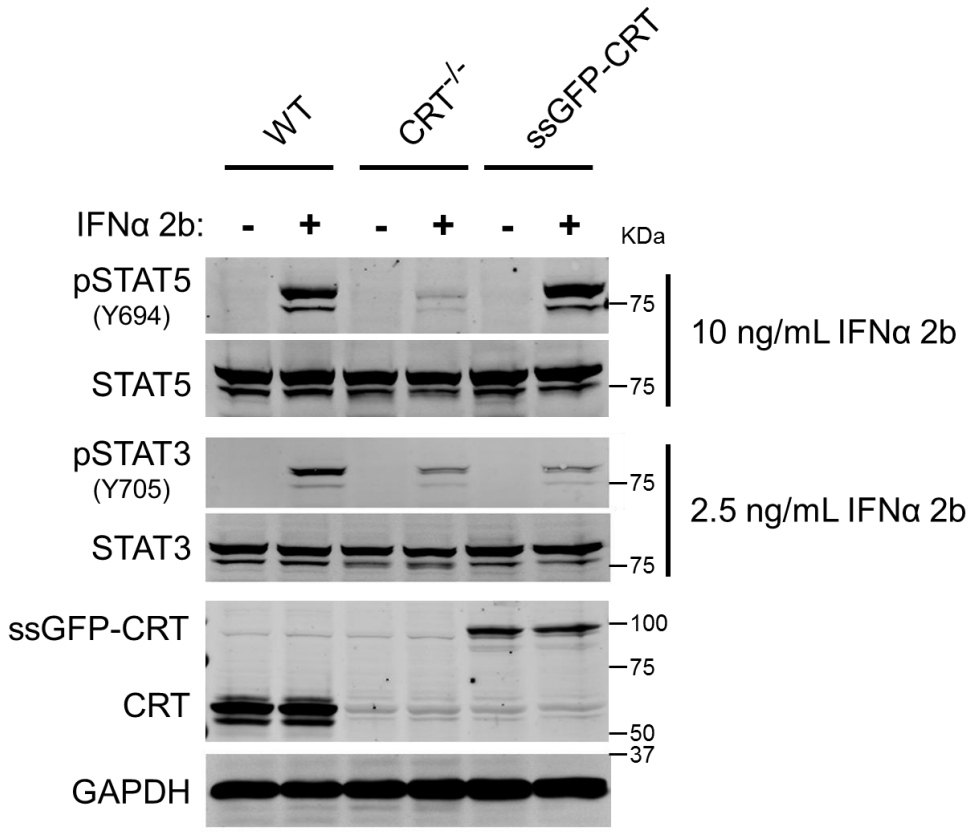

Figure 5.9. IFNα 2b stimulated STAT3 and STAT5 phosphorylation
WT, CRT$^{-/-}$ and ssGFP-CRT were treated with 10 ng/mL or 2.5 ng/mL IFNα 2b for 15 minutes as indicated and cell lysates immunoblotted to detect phospho(Y694)-STAT5, total STAT5, phospho(Y705)-STAT3, total STAT3, and CRT levels. Equal protein loading was assessed by immunoblotting for GAPDH. The results shown are representative of more than 3 experiments.

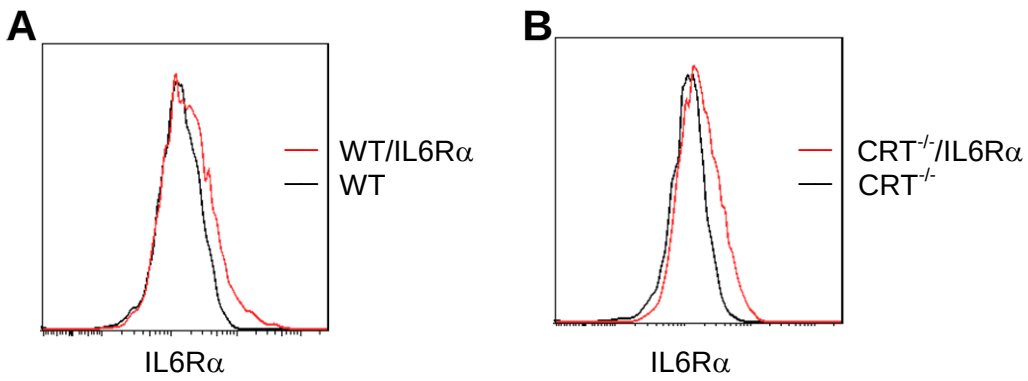

Figure 5.10. Stable IL6Rα expression in Jurkat cells
WT and CRT$^{-/-}$ cells were transfected to express IL6Rα and flow cytometry used to sort for IL6Rα-expressing cells. The histograms show cells exhibiting stabilized IL6Rα expression in comparison to the parental strain. *(A)* WT/IL6Rα versus WT cells. *(B)* CRT$^{-/-}$/IL6Rα versus CRT$^{-/-}$ cells. Flow cytometry was used to measure IL6Rα labeled with the α-IL6Rα antibody.

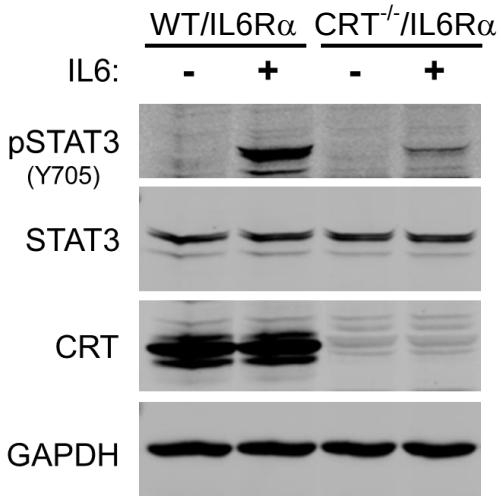

Figure 5.11. IL6 stimulation of STAT3 phosphorylation
WT/IL6Rα and CRT$^{-/-}$/IL6Rα cells were treated with or without IL6 for 15 minutes and cell lysates immunoblotted to detect phospho(Y705)-STAT3, total STAT3, and CRT levels. Equal protein loading was assessed by immunoblotting for GAPDH. The results shown are representative of more than 3 experiments.

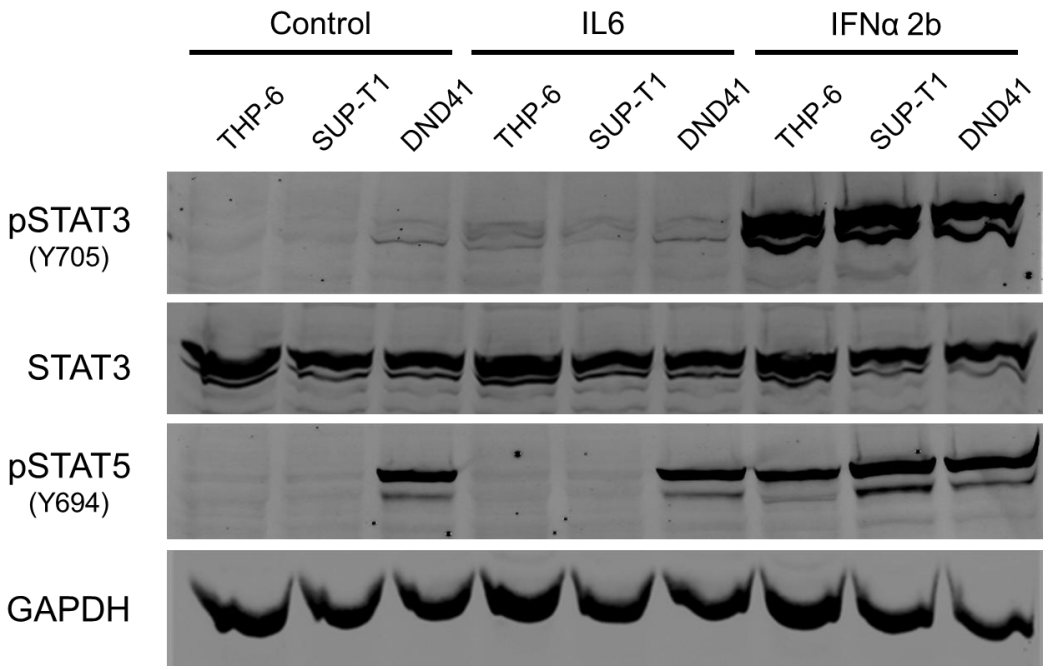

Figure 5.12. DND41 has constitutive STAT5 phosphorylation
THP-6, SUP-T1 and DND41 cells were treated with IL6 or IFNα 2b for 15 minutes and cell lysates immunoblotted to detect phospho(Y705)-STAT3, total STAT3, and phospho(Y694)-STAT5. Control indicates untreated cells. Equal protein loading was assessed by immunoblotting for GAPDH. The results shown are representative of more than 3 experiments.

5.5 Discussion

STAT3 and STAT5 signaling are known to regulate the transcription of genes involved in proliferation and survival, and not surprisingly, abnormal STAT3 and STAT5 activation commonly occur in multiple cancer types (Bharti et al., 2004; Du et al., 2009; Hodge et al., 2005; Jinawath et al., 2010; Sexl et al., 2000; Shain et al., 2009; Walker et al., 2014). In MPNs, somatic *CALR* mutations occur at a rate that is second only to that of *JAK2V617F*, which encodes for a constitutively active JAK2 (Klampfl et al., 2013; Nangalia et al., 2013). In MPNs, the somatically mutated CRT causes constitutive STAT phosphorylation through CRT association with MPL (Araki et al., 2016; Chachoua et al., 2016). This line of evidence is suggestive of co-

involvement of CRT and JAK in cytokine-mediated STAT activation and signaling. Expression of wildtype CRT was also found to facilitate JAK/STAT signaling in multiple cell types (Abraham et al., 2010; Du et al., 2009; Li et al., 2005a). Therefore, the work described in Chapter 5 investigated whether CRT may be involved in integrin-mediated drug resistance and in cytokine-mediated signaling involving STATs. This line of reasoning presumes that CRT's role in facilitating drug resistance and JAK/STAT signaling is highly conserved in multiple cellular systems and that misregulation of CRT's function may reveal its oncogenic potential.

From the results described in Chapters 3 and 4, I provided evidence that cell adhesion via integrins increased the chemoresistance properties of WT Jurkat cells and that cells expressing Tacδ (with the cytosolic GFFKR motif) exhibited chemoresistance in a manner not requiring cell adhesion. I also showed that cell adhesion promoted the enhanced interaction of CRT with α-integrins, while CRT constitutively interacts with Tacδ in a manner not requiring cell adhesion. This led to the idea that integrin-mediated chemoresistance may involve CRT-GFFKR interaction occurring in the cytosol. With the ability to easily generate CRT null cells using the CRISPR-Cas9 system, I was able to confirm that CRT is at least partially involved in both adhesion-dependent chemoresistance observed in WT cells, and in adhesion-independent chemoresistance observed in Tacδ cells.

It is not yet clear why the loss of CRT expression only partly attenuated the observed chemoresistance. For example, the chemosensitivity of Tacδ/CRT$^{-/-}$ cells was not restored to the levels observed for the control Tacδ^{scr} cells. However, the effects are specific to CRT expression, since re-expression of CRT (as ssGFP-CRT) was sufficient to restore the chemoresistance properties of the CRT$^{-/-}$ cell lines back to the levels observed in the parental cells with

endogenous CRT expression. Thus, the gain in chemoresistance resulting from GFFKR expression as Tacδ can be categorized as dominant over the requirement for CRT.

It is clear that one of CRT's critical roles is in the modulation of cellular Ca^{2+} flux. I found that CRT-deficient T-lymphoblasts exhibit dramatic reductions in both Ca^{2+} influx and drug efflux. However, the decrease in drug efflux could not account for the partial restoration of chemosensitivity, thus other mechanisms contributed by the GFFKR motif expression or by cell adhesion remain plausible. Obvious possibilities include GFFKR-interacting proteins not evaluated in this study, a list that includes Sharpin, MDGI, and Mss4. The binding of Sharpin or MDGI to GFFKR inhibits β1-integrin activation (Nevo et al., 2010; Rantala et al., 2011), thus the functional consequence of the binding of either of these two proteins would be predicted to inhibit, and not promote, CAMDR. It is not immediately apparent how Mss4 activity would regulate CAMDR. Mss4 is known to regulate matrix metalloproteinases and matrix remodeling (Knoblauch et al., 2007; Nevo et al., 2010; Rantala et al., 2011), thus alterations to the ECM regulated by Mss4 may impact integrin-mediated drug resistance signaling. To begin to investigate these other GFFKR-binding proteins as regulators of GFFKR-mediated drug resistance, one could begin by assessing the levels of Sharpin, MDGI or Mss4 that are immunoprecipitated with α4δ or Tacδ in my model system, and confirm if the interaction with native α4-integrins is increased in a manner dependent on cell adhesion.

The other emerging possibility is the role of CRT in facilitating JAK/STAT signaling important in cell proliferation, survival and chemoresistance signaling. I showed that cytokine-stimulated $CRT^{-/-}$ cells exhibited reduced phosphorylation of both STAT3 and STAT5 compared to WT cells. Notably, reconstitution with ssGFP-CRT restored the phosphorylation of STAT5 but did not restore the phosphorylation of STAT3. This is a possible indication that the GFP-

tagged CRT may not function in a manner that fully reproduces the activity mediated by the endogenous wildtype version. The CRT N-domain was found to interact directly with the JAK2-MPL protein complex, and this interaction mediates the phosphorylation of STAT proteins (Araki et al., 2016). It is possible that placement of the globular GFP tag at the N-terminus of CRT (as ssGFP-CRT) may interfere with the CRT N-domain interaction with cytokine receptors for STAT phosphorylation. This issue could be addressed by rescue experiments with wildtype CRT instead of the GFP-tagged version. Another possibility that cannot be ruled out is that the level of ssGFP-CRT expression in the stable cell lines was significantly less than the levels detected for endogenously expressed CRT. In this regard, cytokine receptor-mediated STAT3 signaling may require higher levels of CRT to efficiently couple the process when compared to STAT5. The MPL cytokine receptor that was implicated in MPNs was shown to interact with mutated CRT in a complex that also includes JAK2 (Araki et al., 2016; Chachoua et al., 2016). It remains to be shown if CRT can interact with other cytokine receptors and with other JAKs, the elucidation of which will be important for our mechanistic understanding of the role of CRT in proliferative STAT signaling.

Ideally, one of the specific aims set out in this study was to evaluate the functional contribution of cytosolic CRT in cell chemoresistance as well as in JAK/STAT signaling. Having created cell lines deficient in CRT expression, I was able to reconstitute expression with various mutant forms of CRT, which include the cytosol-targeted GFP-CRT, as well as the KDEL deleted versions described in the preceding chapter. However, multiple attempts to establish cell lines that stably express GFP-CRT, ssGFP-CRT-KDELdel, and ssGFP-CRT-mutant type I met with no success. It is not clear why this is, but I am led to conclude that expression of these proteins was either cytotoxic or led to a diminished proliferative potential. The effects appear to

be cell line or cell type dependent, as parallel efforts by our lab to establish CHO cells stably expressing the above mutant CRT constructs have been successful. Characterization of these cells is underway, but it is not clear if we will be able to model key signaling pathways that have been the focus of my studies. In addition, there will be renewed efforts to create Jurkat-based WT and $CRT^{-/-}$ cells with stable IL7R expression as it is becoming apparent that the IL7-IL7R-JAK-STAT5 signaling pathway is likely implicated in CRT function.

Since JAK/STAT signaling is an important pathway involved in cell proliferation and survival (Bhardwaj et al., 2007), I speculate that CRT functions to promote chemoresistance partly through facilitating STAT phosphorylation and signaling. I have shown in my studies that CRT binds to the α-integrin GFFKR motif during integrin activation events (Liu et al., 2016; Liu et al., 2013). Integrin activation typically accompanies the clustering of integrins and cytokine receptors (Shattil et al., 2010) and indeed, interleukin receptors are clustered at focal adhesions in substrate attached cells or enriched in lipid rafts alongside integrins (Streuli and Akhtar, 2009; Yanagisawa et al., 2004). As such, I speculate that CRT may act as a bridge to link integrins with JAK-associated cytokine receptor signaling in focal adhesions or lipid rafts.

Taken together, the work described in Chapter 5 demonstrates that CRT is an important contributor to GFFKR motif-mediated drug resistance. This contribution may originate from CRT's function in regulating Ca^{2+} influx, drug efflux, and JAK/STAT signaling.

Chapter 6: General Discussion and Perspectives

6.1 The α-integrin GFFKR Motif and CRT Regulate Chemoresistance

The α-integrin GFFKR motif interacts with several proteins described to regulate integrin function including Sharpin, MDGI, Mss4, CIB and CRT (Barry et al., 2002; Coppolino et al., 1995; Coppolino et al., 1997; Knoblauch et al., 2007; Nevo et al., 2010; Rantala et al., 2011). I analyzed published data to identify the candidate effector that best fitted my finding that expression of the cytosolic GFFKR motif as a plasma membrane-anchored protein was sufficient to promote drug resistance in an adhesion-independent manner. Both Sharpin and MDGI act as inhibitors of integrin activation and cell adhesion (Nevo et al., 2010; Rantala et al., 2011). If α4δ or Tacδ expression resulted in Sharpin or MDGI binding to the exposed GFFKR, then the adhesion and chemoresistance observed via other integrins such as α5β1-ligation to GST-Fn9.11 would be expected to increase in α4δ or Tacδ expressing cells; a phenomenon I did not observe. Mss4 is implicated in the secretion of matrix metalloproteinases and fibronectin remodeling, neither of which applies to my assay system (Knoblauch et al., 2007). CIB is a calcium and integrin-binding protein, however, detailed interaction studies indicate specificity for αIIb-integrin sequences N-terminal to and in addition to GFFKR, sequences not found in α4δ or Tacδ (Barry et al., 2002).

This leaves CRT, a ubiquitous calcium-binding and chaperone protein found predominantly within the lumen of the endoplasmic reticulum (ER) (Michalak et al., 2009), and whose reported interactions with integrins α2 and α7 are associated with transient Ca^{2+} fluxes upon integrin-substrate ligation (Coppolino et al., 1997; Kwon et al., 2000). Furthermore, CRT is reported in several studies to upregulate the JAK/STAT signaling pathway in a cytokine-

independent manner, likely contributing to tumor proliferation and enhanced cell survival. Using immunoprecipitation studies, I showed an increased interaction of CRT with the truncated GFFKR motif of non-adherent cells and with α4-integrin from adhesion-stimulated cells. Thus, this study adds to the list of α-integrins shown to interact with CRT in a manner stimulated by cell adhesion, which now includes α2, α3, α4, α6 and α7 (Coppolino et al., 1995; Coppolino and Dedhar, 1999; Kwon et al., 2000; Tran et al., 2002; Zhu et al., 1997). It remains unclear how an ER resident protein like CRT may bind to the juxtamembrane cytoplasmic tail of α-integrins. An increasing body of work has highlighted the non-ER resident localization and function of CRT that includes cytosolic, cell surface and secreted forms (Gold et al., 2010). Several elegant studies described mechanisms that can account for the minor cytosolic localization of CRT (Afshar et al., 2005; Shaffer et al., 2005). The demonstration that CRT null cells have impaired integrin-mediated adhesion and adhesion-stimulated Ca^{2+} influx suggest a more intimate role for CRT in integrin function (Coppolino et al., 1997). This is supported by the finding that restoring or enhancing the expression of a cytosolic targeted form of CRT was able to rescue the adhesion defect exhibited by CRT-deficient fibroblasts (Afshar et al., 2005).

The stoichiometry of the CRT-α4 integrin interaction that I observed was estimated to be very low. This is not surprising considering the disparate locales of the interacting partners, with most CRT found within the ER lumen (Johnson et al., 2001). However, using the CRT knockout cell lines, $CRT^{-/-}$ and $Tac\delta/CRT^{-/-}$, in conjunction with their respective CRT rescues, I showed that CRT is involved in acquired chemoresistance against doxorubicin. Using the same CRT knockout and rescue model, I showed that CRT facilitates Ca^{2+} influx, drug efflux, and STAT phosphorylation. All of these pathways have been implicated in drug resistance (Chiu et al.,

2010; Real et al., 2002). Thus, CRT-α-integrin interaction potentially affects both Ca^{2+}-mediated and JAK/STAT-mediated chemoresistance.

6.2 Integrin Modulation of Immunogenic Cell Death

As a DAMP expressed on the surface of cells undergoing immunogenic cell death, surface CRT is crucial for the clearance of tumor cells by the host immune system, mediated by professional phagocytes (Garg et al., 2010; Krysko, 2013; Krysko et al., 2012; Krysko et al., 2013). Therefore, physiological events contributing to reduced surface CRT expression may lead to reduced anti-tumor responses resulting from anthracycline-based chemotherapy. I showed that integrin activation reduced cell surface CRT presentation in various T-ALL cells, and resulted in the reduced phagocytosis of Jurkat T-lymphoblasts by macrophages. The tumor microenvironment such as the bone marrow stroma may provide these protective stimuli in the form of adhesion substrates and stimulatory chemokines that promote integrin activation (Meads et al., 2008) and lead to decreased phagocytosis of the cancer cells. I also showed that the integrin-mediated effects on phagocytosis only became evident when the CD47 ‘don’t eat me’ signal was blocked with neutralizing antibodies, a result consistent with published reports (Tseng et al., 2013; Willingham et al., 2012). Thus, effective chemotherapy employing anthracyclines may benefit from co-administration with integrin- and CD47-function blocking therapeutic monoclonal antibodies.

6.3 Translocation of Calreticulin from the ER to the Cell Surface During Immunogenic Cell Death

Several enabling methodologies were necessary to achieve confidence for assessing the transition of CRT through the subcellular compartments, due in large part to the fact that CRT is a multifunctional protein with varied subcellular localizations including the ER, cytosol, or the cell surface. I utilized CRISPR-Cas9 to target *CALR* in Jurkat T-lymphoblasts to derive $CRT^{-/-}$ cells with no detectable expression of CRT protein (Cong et al., 2013). With $CRT^{-/-}$ cells as a blank canvas, I was able to reconstitute expression with GFP-tagged CRT that was either expressed in the cytosol or inserted via a signal sequence into the ER lumen in a manner resembling the native protein. This provided an opportunity to probe the subcellular source for surface CRT resulting from an ICD-inducer. It is widely accepted that the path to the surface requires induction of ER-stress and subsequent release of CRT from its highly enriched localization within the ER-lumen (Garg et al., 2012; Korbelik et al., 2011; Obeid et al., 2007). My results with $CRT^{-/-}$ cells reconstituted with the ER-targeted ssGFP-CRT, ssGFP-CRT-KDELdel and ssGFP-CRT-mutant type I confirm earlier findings, in that doxorubicin-treatment stimulated surface CRT presentation. The fact that this increase is detectable with either α-CRT or α-GFP antibodies indicated that the translocation involved the intact fusion protein. When expressed within the cytosol without transiting the ER, GFP-CRT presented at high levels on the cell surface in a manner that could not be stimulated further with doxorubicin. In effect, this bypassed the requirement for induction of ER-stress.

I utilized partial permeabilization techniques with digitonin to show that CRT is enriched within the extra-ER, cytosolic compartment of the cell following treatment with the ICD-inducer, oxaliplatin. When cells were co-treated with oxaliplatin and 9EG7, an antibody that promotes the

activation of β1-integrins, cell surface CRT levels were not elevated in live, non permeabilized cells, even though digitonin permeabilization revealed an increase in the extra-ER cytosolic pool of CRT. In a similar fashion, cells expressing Tacδ exhibited no increase in surface CRT upon oxaliplatin treatment, even though the extra-ER cytosolic CRT was significantly increased. These findings support a mechanism that involves CRT release from the stressed-ER to the cytosol (Goitea and Hallak, 2015; Sambrooks et al., 2012; Tarr et al., 2010b; Tsai et al., 2002), following which CRT may translocate to the cell surface. Furthermore, enforced activation of integrins, or expression of Tacδ, prevented the translocation of cytosolic CRT to the cell surface. Since the GFFKR motif for binding CRT is found within the cytoplasmic tail of α-integrin, it is plausible that GFFKR may be acting to sequester CRT within the cytosol. This effect is switchable, in that integrin activation facilitated by cell adhesion or by activation-specific agonists inhibited surface CRT presentation. To my knowledge, this is the first known functional role for integrins in the regulation of immunogenic cell death.

6.4 Contribution of Serum CRT to Cell Surface CRT

During experimental methodology optimization, rather surprisingly, I found that the α-CRT antibody used to detect surface CRT revealed a residual signal that was significantly above background on $CRT^{-/-}$ cells. CRT can be detected in serum and is often found at higher levels in patients with inflammatory autoimmune conditions, leading to suggestions that it may be a marker for inflammation (Molica et al., 2016; Ni et al., 2013; Ren et al., 2016). This led us to test the FBS-supplemented media as a source for CRT detected on the cell surface. I conclude that an α-CRT reactive signal is present in FBS and that this signal can be eliminated by culturing cells in serum-reduced or serum-free conditions. Importantly, the typical 2-fold increases in cell

surface CRT observed for doxorubicin-treated cells was found to originate from endogenous cellular pools of the protein, with a negligible contribution from FBS-supplemented media. It is noteworthy that the antibody-based phenomenon is not restricted to this one rabbit polyclonal antibody used in this study as I have detected serum-based CRT background staining using other antibodies sourced from other manufacturers (data not shown). To address issues relating to consistency, we have initiated efforts to identify a monoclonal antibody for detecting surface CRT. While this is not anticipated to eliminate the serum-derived signals, it will at least provide a standardized measure for comparing batches of FBS that will likely have variable levels of serum CRT. In sum, I believe my findings will begin to consolidate the existence of CRT in various sub- and extra-cellular compartments of the cell, and also provide some explanation for anecdotal contradictions within the CRT research community on the validity of antibody-based detection for cell surface CRT.

6.5 Calreticulin Facilitates JAK/STAT Signaling in Leukemia

Recent studies suggested that the MPN-associated CRT lacking the KDEL ER retention sequence may allow passage of the mutant CRT through the Golgi secretory pathway, leading to greater accumulation of non-ER localized intracellular and/or extracellular CRT (Chachoua et al., 2016). Furthermore, the mutation may also lead to changes in the conformation of the CRT protein that facilitate its binding to the MPL/JAK2 complex, leading to a low but sustained constitutive phosphorylation of STAT proteins (Araki et al., 2016; Chachoua et al., 2016). Interestingly, various -1/+2 frameshift mutations introduced within exon 9 of *CALR* leads to expression of mutant CRT with a novel C-terminus predicted to carry a positive electrostatic charge that defines the oncogenic potential of the MPN-associated mutant protein by facilitating

interaction with the MPL receptor (Chachoua et al., 2016; Elf et al., 2016). Mere expression of a KDEL deleted variant was not sufficient to promote JAK/STAT signaling in the BaF3 reporter cell line, while altering the novel C-terminus sequence to retain a positive charge did. These structural insights provided our first clues into the mechanism of action for MPN-associated mutant CRT, in that the positively charged C-terminus is likely to act as a gain of function oncogenic protein to bind the MPL/JAK complex and promote the activation of STAT.

In contrast, expression of wildtype CRT was not found to impact STAT phosphorylation in the same series of experiments conducted using a pre-B reporter cell line (Chachoua et al., 2016). On the other hand, previous studies using other cell lines have reported that wildtype CRT facilitates STAT3 phosphorylation (Abraham et al., 2010; Du et al., 2009; Li et al., 2005a). It is thus conceivable that CRT may impact STAT signaling pathways differently in different cell types, depending upon the combination of cytokine receptor and JAK proteins expressed (Murray, 2007). For example, the cytokine receptor MPL preferentially binds to JAK2, and the MPL/JAK2 complex facilitates the association, phosphorylation and activation of STAT5 (Murray, 2007). In contrast, the IFNα receptor preferentially binds to JAK1 and TYK2, and this combination has been shown to promote activation of STAT1, STAT2, STAT3 and/or STAT5 (Chow and Gale, 2015; Platanias, 2005). As a further example, the phosphorylation and activation of STAT3 is primarily mediated by IL6R binding to JAK1 (Murray, 2007). It is possible that wildtype CRT may facilitate the IL6R/JAK1/STAT3 pathway while having a minimal impact on the MPL/JAK2/STAT5 pathway.

My study describes the involvement of wildtype CRT in facilitating JAK/STAT signaling in a T-lymphoblast cell model. I utilized CRISPR-Cas9 to knockout CRT expression in Jurkat T-lymphoblasts and subsequently performed rescue experiments with ssGFP-CRT. Comparing the

parental wildtype, $CRT^{-/-}$ and ssGFP-CRT rescued cells, I confirmed that CRT plays a significant role in facilitating STAT phosphorylation. $CRT^{-/-}$ cells showed significantly lower STAT3 and STAT5 phosphorylation compared to parental wildtype and rescue cells when treated with IFNα 2b or IL6. Similarly, using both $CRT^{-/-}$ and $Tac\delta/CRT^{-/-}$ and their respective CRT rescues, I showed that CRT is required for chemoresistance against doxorubicin. Since JAK/STAT signaling is involved in cell proliferation and survival (Bhardwaj et al., 2007), I speculate that CRT functions to promote chemoresistance partly through facilitating STAT activity. Furthermore, I showed that ssGFP-CRT expression successfully reconstituted IFNα 2b-stimulated phosphorylation of STAT5 but not STAT3. It is plausible that ssGFP-CRT may have a weaker association with the IFNα receptor/JAK1/STAT3 complex when compared to the IFNα receptor/TYK2/STAT5 complex, and therefore the low ssGFP-CRT expression was insufficient to rescue STAT3 phosphorylation. Interestingly, expression of type I MPN mutated CRT is not sufficient to bypass the requirement for IFNAR stimulation of STAT5 activity, thus it appears that mutated CRT uniquely mediates the cytokine-independent stimulation of MPL (Chachoua et al., 2016). This leaves open the possibility that wildtype CRT may retain the ability to signal via the IFNα receptor/TYK2/STAT5 complex while the type I MPN CRT mutant does not.

Interleukin receptors are clustered at focal adhesions in substrate-attached cells or enriched in lipid rafts alongside integrins during integrin activation (Streuli and Akhtar, 2009; Yanagisawa et al., 2004). Indeed, PKC phosphorylation downstream of integrin activation facilitates STAT1 activation (Ivaska et al., 2003) while JAK2 promotes integrin activation through the hierarchical activation of Rho and Rap (Montresor et al., 2013; Montresor et al., 2015). These crosstalk studies revealed an interwoven relationship between integrin activation and JAK/STAT signaling. Taken together with the demonstration that integrin activation

promotes the binding of CRT to the α-integrin GFFKR motif (Liu et al., 2016; Liu et al., 2013), I speculate that CRT may act as a bridge to link integrin receptor signaling with JAK-associated cytokine receptor signaling within focal adhesions or lipid rafts.

6.6 Closing Perspectives

The findings presented in this thesis indicate that the α-integrin GFFKR motif is sufficient to induce resistance against chemotherapeutics and that Ca^{2+} influx is involved in this process. CRT appears to be one of the key mediators of GFFKR motif-mediated drug resistance and Ca^{2+} influx. Furthermore, the α-integrin GFFKR motif appears to modify immunogenicity of T-ALL cells by regulating cell surface CRT presentation during immunogenic cell death.

CRT is an L-type Ca^{2+} channel regulator and Ca^{2+} reservoir, and CRT associates with multiple α-integrins through their GFFKR motif (Coppolino et al., 1997; Kwon et al., 2000). CRT binding to wildtype α-integrin GFFKR motif requires integrin activation (Coppolino et al., 1997; Kwon et al., 2000; Liu et al., 2016). My findings showed that loss of CRT leads to increased chemosensitivity in otherwise chemoresistant cell lines expressing the GFFKR motif. Similarly, loss of CRT leads to decreased Ca^{2+} influx and decreased Ca^{2+}-dependent drug efflux. Taken together, I present Figure 6.1 as a summative model to depict the possible mechanisms of α-integrin GFFKR motif-mediated drug resistance: (1) the conformation change in integrin heterodimers during integrin activation allows CRT binding, leading to Ca^{2+} influx and subsequent drug efflux mediated by p-glycoproteins (Xia and Smith, 2012); and (2) through yet unknown mechanisms, the α-integrin GFFKR motif mediates phosphorylation and activation of Akt pro-survival signaling pathways.

However, the proposed model also raises additional questions. First, the investigations described in Chapters 3 and 5 did not explain how expression of the juxtamembrane GFFKR motif alone can lead to the specific phosphorylation of Akt at Thr308 in a manner independent of cell adhesion. It has been amply described that cell adhesion-mediated activation of the PI3K/Akt pathway requires integrin activation and formation of focal adhesion complexes; however this mechanism requires the participation of focal adhesion proteins and both the α- and β-integrin cytoplasmic tails (Chekenya et al., 2008; King et al., 1997; Legate et al., 2006; Xia et al., 2004; Zhang et al., 2010). It is also known that integrin-mediated cell adhesion triggers the influx of extracellular Ca^{2+} into cells (Waitkus-Edwards et al., 2002; Wu et al., 2001; Wu et al., 1998). In neuroblastoma cells, the calcium/calmodulin-dependent protein kinase kinase (CAMKK) was found to directly phosphorylate Akt at Thr308 in a manner that bypasses PI3K to effect enhanced survival (Yano et al., 1998). It has also been shown that Ca^{2+} influx triggers Akt signaling in neuroblastoma cells, neurons, and osteoblasts (Danciu et al., 2003; Nicholson-Fish et al., 2016; Yano et al., 1998). As a known Ca^{2+} regulatory protein, it is possible that recruitment of CRT to the GFFKR motif of α-integrins following integrin activation is the key event promoting Ca^{2+} influx, following which rising intracellular Ca^{2+} levels facilitate the activation of Ca^{2+}-dependent signaling that includes the phosphorylation and activation of Akt. Thus, formation of the GFFKR-CRT complex is proposed to be a key mediator of cell adhesion-mediated activation of Akt requiring Ca^{2+} influx. Further elucidation of the exact mechanism by which Ca^{2+} influx triggers the activation of Akt will be necessary to further our understanding of integrin function and the role of cell adhesion in chemoresistance.

The second question arising from my studies is whether endogenous wildtype CRT is involved in the regulation of STAT protein activity and if so, whether there is enough

endogenous wildtype CRT in the cytosolic compartment to couple to JAK/STAT signaling. I demonstrated that cytokine-stimulated CRT-deficient cells exhibit reduced phosphorylation of STAT3 and STAT5 proteins compared to wildtype cells. This supports there being enough endogenous wildtype CRT to couple to JAK/STAT signaling. Furthermore, if indeed endogenous wildtype CRT facilitates the phosphorylation of STAT proteins, how does this relate to the GFFKR motif-mediated chemoresistance pathway involving CRT? Since STATs regulate a plethora of transcriptional events, it is possible that the sustained signaling may lead to upregulation of proteins that more directly account for chemoresistance, such as p-glycoproteins and other apoptotic regulatory proteins. Answering this question may further our understanding of cytosolic CRT as an oncogenic protein in hematological malignancies. Reported studies on the MPN-associated mutant CRT indicated that its ability to activate STAT is mediated specifically by its binding to the extracellular domain of *N*-glycosylated MPL through the glycan binding site in a manner requiring the electrostatic positive charge encoded by the mutated CRT C-domain (Chachoua et al., 2016; Elf et al., 2016). This mutant CRT-specific mechanism likely does not apply to our understanding of how endogenous wildtype CRT couples the phosphorylation and activation of STAT proteins via multiple cytokine receptors.

The proposed mechanism so far has centered on CRT being a positive signaling mediator of drug resistance and cell survival through its interaction with the GFFKR motif of α-integrins. However, the possibility remains that the GFFKR-bearing Tacδ and α4δ cell lines achieved adhesion-independent chemoresistance through its interaction and sequestration of inhibitors of integrin activation such as sharpin and MDGI; this may translate to increased ratio of activated integrins resulting in increased integrin signaling. In support of this possibility, I have found that the CRT-deficient Tacδ cells (Tacδ/CRT$^{-/-}$) did not reduce or modulate the constitutive high

levels of phospho(T308)-Akt observed in Tacδ cells, suggesting that CRT does not mediate GFFKR motif-mediated Akt activation (data not shown). The integrin GFFKR motif-mediated effects on calcium influx may also be interpreted by a similar mechanism. Loss of CRT removes its role as a GFFKR-binding competitive inhibitor of the integrin inactivators such as sharpin and MDGI, thus the loss of CRT may be interpreted as having detrimental outcomes on integrin-mediated cell adhesion and adhesion-mediated calcium influx (Coppolino et al., 1997; Leung-Hagesteijn et al., 1994). Similarly, the increased calcium influx observed in Tacδ cells may be due to the sequestration of integrin inactivators resulting in increased integrin activation and subsequent calcium influx. This alternative proposal may prove interesting as a follow-up project for this thesis.

My findings described in Chapter 4 showed that the α-integrin GFFKR motif and integrin activation play a role in decreasing surface CRT presentation. Figure 6.2 is a summative model depicting the function of α-integrin in modifying immunogenicity: (1) in healthy cells, CRT is primarily enriched within the lumen of the ER; (2) Treatment of the cells with an ICD-inducer promotes the release of CRT from the ER into the cytosolic compartment; in the absence of activated integrins, the increasing cytosolic pool of CRT is readily translocated to the cell surface where it acts as a signal to promote engulfment by professional phagocytes; (3) Cell adhesion promotes the activation of integrins, and the resulting conformational change in the heterodimers exposes the GFFKR juxtamembrane motif on α-integrin and enables its binding to cytosolic CRT. Greater levels of integrin activation lead to greater sequestration of CRT within the cytosolic compartment and decrease the available CRT presented at the outer plasma membrane leaflet or cell surface.

This work did not address the exact mechanism of how CRT translocates to the cell surface. As mentioned before, many hypotheses with supporting evidence have been proposed on how CRT can leave the ER and present on the cell surface (Corbett et al., 2000; Denning et al., 1997; Holaska et al., 2001; Kepp et al., 2010; Païdassi et al., 2011; Panaretakis et al., 2009; Sauk et al., 1998; Tarr et al., 2010b; Wiest et al., 1997; Wilson et al., 1993). However, none of these hypotheses can provide undisputable evidence of the transit mode of CRT. Evidence suggests that CRT co-translocates with another ER resident protein, ERp57, to the cell surface and that the deletion of either protein leads to translocation failure (Obeid, 2008; Panaretakis et al., 2008). However, I found that ERp57 translocation to the cell surface does not require the presence of CRT in human T-ALL cells (Appendix Figure D.1). Such conflicting evidence, along with the possibility that CRT can translocate via different mechanisms in different cell types, adds to the difficulty in discerning the transit mode of CRT. Investigations into CRT's mechanism of translocation may help in finding possible targets for drug action that increase the immunogenicity of the tumor cell.

The discovery that the α-integrin GFFKR motif is sufficient to mediate chemoresistance is a major step forward in our understanding of the pro-tumor effects of cell adhesion and CAMDR. Targeted drug therapies that directly inhibit the interaction between the GFFKR motif and downstream signaling proteins may be a therapeutic avenue to explore in the effort to increase the efficacy of chemotherapy while decreasing unnecessary side effects resulting from cytotoxicity to healthy cells. For example, disrupting the CRT interaction with the GFFKR motif may be the key to reducing chemoresistance and MRD in cancer treatment, since full functional blockade of certain integrins involved in immune regulation (such as α4-integrin) carry inherent dangers such as immune suppression (Berger and Koralnik, 2005; Bloomgren et al., 2012;

Clifford et al., 2010). Notably, the research described in this thesis is the first to identify α4-integrin as a CAMDR contributor in T-ALL and the first to characterize a functional role for integrins in determining the immunogenicity of the tumor cell.

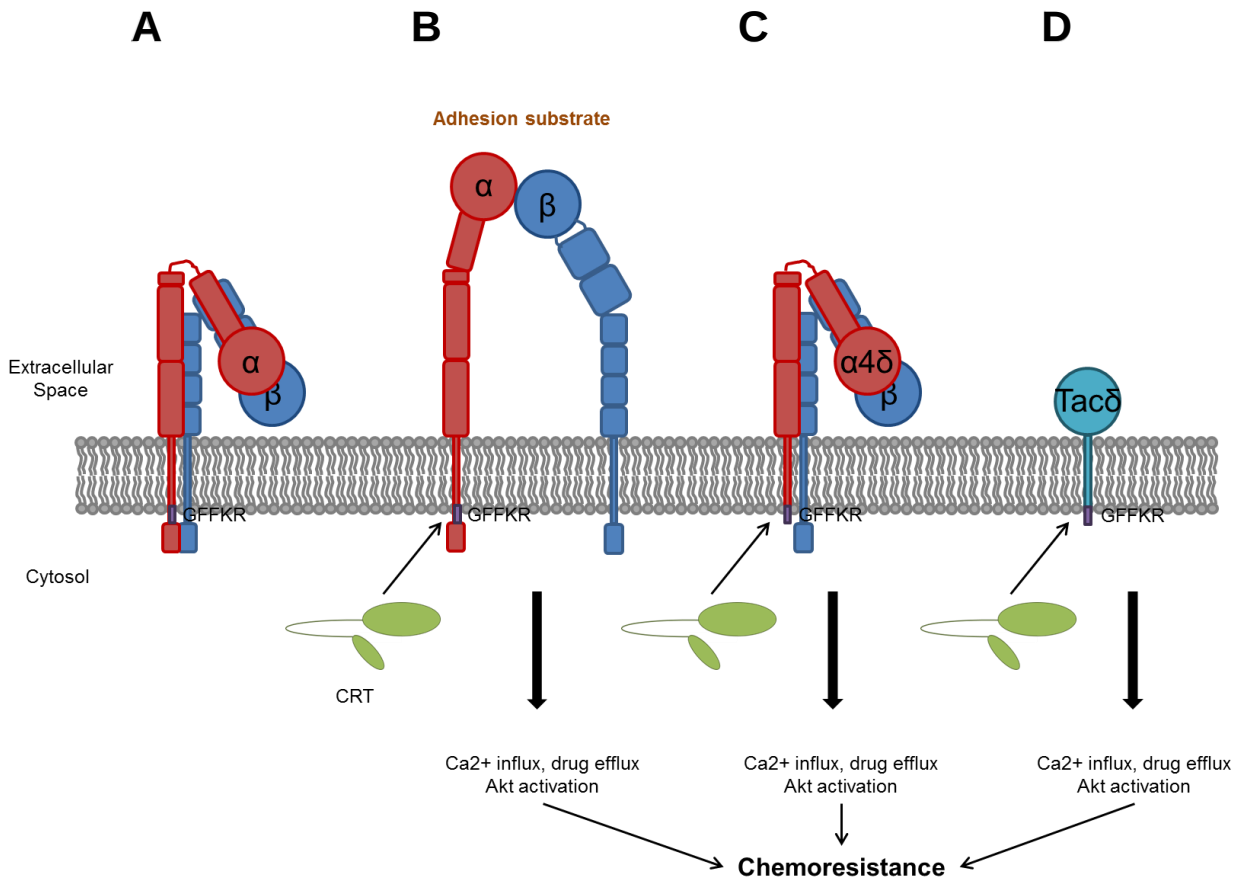

Figure 6.1. Mechanism of α-integrin GFFKR motif-mediated drug resistance
The model depicts possible mechanisms of α-integrin GFFKR motif-mediated drug resistance: *(A)* the inactive integrin heterodimer does not mediate drug resistance while *(B)* the active integrin heterodimer, *(C)* α4δ-integrin heterodimer, and *(D)* Tacδ mediate drug resistance that is associated with CRT binding to the GFFKR motif, Ca^{2+} influx, drug efflux and Akt activation.

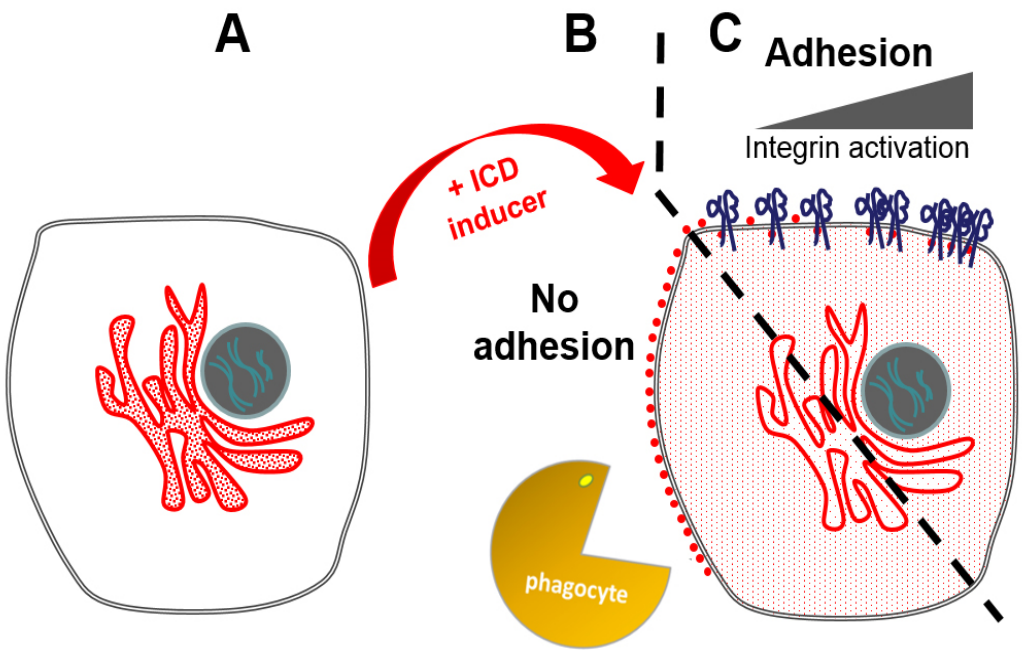

Figure 6.2. The model depicting the function of α-integrin in modifying immunogenicity
(A) In healthy cells, CRT (red dots and shading) is primarily enriched within the lumen of the ER. When cells are treated with an ICD-inducer, the resultant ER-stress promotes the release of ER-resident CRT into the cytosolic compartment. Two scenarios are depicted to represent the involvement of integrin function and the consequence on CRT localization. *(B)* In non-adherent cells without activated integrins, cytosolic CRT readily translocates and is presented on the cell surface. Surface CRT is a potent 'eat me' signal for targeting and engulfment by professional phagocytes. *(C)* In adherent cells with activated integrins, the physical separation of the α-β cytoplasmic domains exposes the GFFKR motif for ready binding to cytosolic CRT. This leads to sequestration of CRT within the cytosolic compartment and reduces the level of surface CRT presented.

References

Abdel-Wahab, O., T. Manshouri, J. Patel, K. Harris, J. Yao, C. Hedvat, A. Heguy, C. Bueso-Ramos, H. Kantarjian, and R.L. Levine. 2010. Genetic analysis of transforming events that convert chronic myeloproliferative neoplasms to leukemias. *Cancer research*. 70:447-452.

Abdi, J., L. Qiu, and H. Chang. 2014. Micro-RNAs, New performers in multiple myeloma bone marrow microenvironment. *Biomarker research*. 2:1.

Abraham, A., E. Turgut-Neary, H. Omar, H. Massaeli, and N. Mesaeli. 2010. Calreticulin mediated control of polycystin-2 expression. *In* Qatar Foundation Annual Research Forum Proceedings. Bloomsbury Qatar Foundation Journals. BMPS6.

Abram, C.L., and C.A. Lowell. 2009. The ins and outs of leukocyte integrin signaling. *Annu Rev Immunol*. 27:339-362.

Afshar, N., B.E. Black, and B.M. Paschal. 2005. Retrotranslocation of the chaperone calreticulin from the endoplasmic reticulum lumen to the cytosol. *Mol Cell Biol*. 25:8844-8853.

Ahn, S.B., A. Mohamedali, C. Chan, J. Fletcher, S.Y. Kwun, C. Clarke, O.F. Dent, P.H. Chapuis, E. Nice, and M.S. Baker. 2014. Correlations between Integrin αvβ6 Expression and Clinico-Pathological Features in Stage B and Stage C Rectal Cancer. *PLoS One*. 9:e97248.

Altmeyer, A., R.G. Maki, A.M. Feldweg, M. Heike, V.P. Protopopov, S.K. Masur, and P.K. Srivastava. 1996. Tumor-specific cell surface expression of the-KDEL containing endoplasmic reticular heat shock protein gp96. *International journal of cancer*. 69:340-349.

Andrews, R.K., and M.C. Berndt. 2004. Platelet physiology and thrombosis. *Thrombosis research*. 114:447-453.

Anton, E.S., J.A. Kreidberg, and P. Rakic. 1999. Distinct functions of α 3 and α v integrin receptors in neuronal migration and laminar organization of the cerebral cortex. *Neuron*. 22:277-289.

Apetoh, L., F. Ghiringhelli, A. Tesniere, A. Criollo, C. Ortiz, R. Lidereau, C. Mariette, N. Chaput, J.P. Mira, and S. Delaloge. 2007a. The interaction between HMGB1 and TLR4 dictates the outcome of anticancer chemotherapy and radiotherapy. *Immunological Reviews*. 220:47-59.

Apetoh, L., F. Ghiringhelli, A. Tesniere, M. Obeid, C. Ortiz, A. Criollo, G. Mignot, M.C. Maiuri, E. Ullrich, and P. Saulnier. 2007b. Toll-like receptor 4–dependent contribution of the immune system to anticancer chemotherapy and radiotherapy. *Nature medicine*. 13:1050-1059.

Araki, M., Y. Yang, N. Masubuchi, Y. Hironaka, H. Takei, S. Morishita, Y. Mizukami, S. Kan, S. Shirane, and Y. Edahiro. 2016. Activation of the thrombopoietin receptor by mutant calreticulin in CALR-mutant myeloproliferative neoplasms. *Blood*. 127:1307-1316.

Arcangeli, A., and A. Becchetti. 2010. Integrin structure and functional relation with ion channels. *In* Integrins and Ion Channels. Springer. 1-7.

Aricò, M., M. Schrappe, S.P. Hunger, W.L. Carroll, V. Conter, S. Galimberti, A. Manabe, V. Saha, A. Baruchel, and K. Vettenranta. 2010. Clinical outcome of children with newly diagnosed philadelphia chromosome–positive acute lymphoblastic leukemia treated between 1995 and 2005. *Journal of clinical oncology*. 28:4755-4761.

Arnaout, M., B. Mahalingam, and J.-P. Xiong. 2005. Integrin structure, allostery, and bidirectional signaling. *Annu. Rev. Cell Dev. Biol.* 21:381-410.

Arroyo, A.G., J.T. Yang, H. Rayburn, and R.O. Hynes. 1999. Alpha4 integrins regulate the proliferation/differentiation balance of multilineage hematopoietic progenitors in vivo. *Immunity*. 11:555-566.

Bader, B.L., H. Rayburn, D. Crowley, and R.O. Hynes. 1998. Extensive vasculogenesis, angiogenesis, and organogenesis precede lethality in mice lacking all αv integrins. *Cell*. 95:507-519.

Barczyk, M., S. Carracedo, and D. Gullberg. 2010. Integrins. *Cell and tissue research*. 339:269-280.

Baril, P., R. Gangeswaran, P. Mahon, K. Caulee, H. Kocher, T. Harada, M. Zhu, H. Kalthoff, T. Crnogorac-Jurcevic, and N. Lemoine. 2007. Periostin promotes invasiveness and resistance of pancreatic cancer cells to hypoxia-induced cell death: role of the β4 integrin and the PI3k pathway. *Oncogene*. 26:2082-2094.

Baron, W., L. Decker, and H. Colognato. 2003. Regulation of integrin growth factor interactions in oligodendrocytes by lipid raft microdomains. *Current Biology*. 13:151-155.

Barringhaus, K.G., J.W. Phillips, J.S. Thatte, J.M. Sanders, A.C. Czarnik, D.K. Bennett, K.F. Ley, and I.J. Sarembock. 2004. α4β1 Integrin (VLA-4) Blockade Attenuates both Early and Late Leukocyte Recruitment and Neointimal Growth following Carotid Injury in Apolipoprotein E (–/–) Mice. *Journal of vascular research*. 41:252-260.

Barry, W.T., C. Boudignon-Proudhon, D.D. Shock, A. McFadden, J.M. Weiss, J. Sondek, and L.V. Parise. 2002. Molecular basis of CIB binding to the integrin alpha IIb cytoplasmic domain. *J Biol Chem*. 277:28877-28883.

Bastianutto, C., E. Clementi, F. Codazzi, P. Podini, F. De Giorgi, R. Rizzuto, J. Meldolesi, and T. Pozzan. 1995. Overexpression of calreticulin increases the Ca2+ capacity of rapidly exchanging Ca2+ stores and reveals aspects of their lumenal microenvironment and function. *The Journal of cell biology*. 130:847-855.

Bayless, K.J., and G.E. Davis. 2001. Identification of dual α4β1 integrin binding sites within a 38 amino acid domain in the N-terminal thrombin fragment of human osteopontin. *Journal of Biological Chemistry*. 276:13483-13489.

Bayless, K.J., G.A. Meininger, J.M. Scholtz, and G.E. Davis. 1998. Osteopontin is a ligand for the alpha4beta1 integrin. *Journal of cell science*. 111:1165-1174.

Bazzoni, G., D.T. Shih, C.A. Buck, and M.E. Hemler. 1995. Monoclonal antibody 9EG7 defines a novel beta 1 integrin epitope induced by soluble ligand and manganese, but inhibited by calcium. *J Biol Chem*. 270:25570-25577.

Becker, P.S., K.J. Kopecky, A.N. Wilks, S. Chien, J.M. Harlan, C.L. Willman, S.H. Petersdorf, D.L. Stirewalt, T. Papayannopoulou, and F.R. Appelbaum. 2009. Very late antigen-4 function of myeloblasts correlates with improved overall survival for patients with acute myeloid leukemia. *Blood*. 113:866-874.

Berger, J.R., and I.J. Koralnik. 2005. Progressive multifocal leukoencephalopathy and natalizumab--unforeseen consequences. *N Engl J Med*. 353:414-416.

Berridge, M.J., M.D. Bootman, and H.L. Roderick. 2003. Calcium signalling: dynamics, homeostasis and remodelling. *Nature Reviews Molecular Cell Biology*. 4:517-529.

Bertrand, F., J. Spengemen, J. Shelton, and J. McCubrey. 2005. Inhibition of PI3K, mTOR and MEK signaling pathways promotes rapid apoptosis in B-lineage ALL in the presence of stromal cell support. *Leukemia*. 19:98-102.

Bevilacqua, M.P. 1993. Endothelial-leukocyte adhesion molecules. *Annual review of immunology*. 11:767-804.
Bhardwaj, A., G. Sethi, S. Vadhan-Raj, C. Bueso-Ramos, Y. Takada, U. Gaur, A.S. Nair, S. Shishodia, and B.B. Aggarwal. 2007. Resveratrol inhibits proliferation, induces apoptosis, and overcomes chemoresistance through down-regulation of STAT3 and nuclear factor-κB–regulated antiapoptotic and cell survival gene products in human multiple myeloma cells. *Blood*. 109:2293-2302.
Bharti, A.C., S. Shishodia, J.M. Reuben, D. Weber, R. Alexanian, S. Raj-Vadhan, Z. Estrov, M. Talpaz, and B.B. Aggarwal. 2004. Nuclear factor–κB and STAT3 are constitutively active in CD138+ cells derived from multiple myeloma patients, and suppression of these transcription factors leads to apoptosis. *Blood*. 103:3175-3184.
Björkholm, M., Å.R. Derolf, M. Hultcrantz, S.Y. Kristinsson, C. Ekstrand, L.R. Goldin, B. Andreasson, G. Birgegård, O. Linder, and C. Malm. 2011. Treatment-related risk factors for transformation to acute myeloid leukemia and myelodysplastic syndromes in myeloproliferative neoplasms. *Journal of clinical oncology*. 29:2410-2415.
Bloomgren, G., S. Richman, C. Hotermans, M. Subramanyam, S. Goelz, A. Natarajan, S. Lee, T. Plavina, J.V. Scanlon, and A. Sandrock. 2012. Risk of natalizumab-associated progressive multifocal leukoencephalopathy. *New England Journal of Medicine*. 366:1870-1880.
Board, P.P.T.E. 2016. Childhood Acute Lymphoblastic Leukemia Treatment (PDQ®).
Bodeau, A.L., A.L. Berrier, A.M. Mastrangelo, R. Martinez, and S.E. LaFlamme. 2001. A functional comparison of mutations in integrin beta cytoplasmic domains: effects on the regulation of tyrosine phosphorylation, cell spreading, cell attachment and beta1 integrin conformation. *J Cell Sci*. 114:2795-2807.
Boitano, S., E.R. Dirksen, and M.J. Sanderson. 1992. Intercellular propagation of calcium waves mediated by inositol trisphosphate. *Science*. 258:292-295.
Borowitz, M.J., M. Devidas, S.P. Hunger, W.P. Bowman, A.J. Carroll, W.L. Carroll, S. Linda, P.L. Martin, D.J. Pullen, and D. Viswanatha. 2008. Clinical significance of minimal residual disease in childhood acute lymphoblastic leukemia and its relationship to other prognostic factors: a Children's Oncology Group study. *Blood*. 111:5477-5485.
Bouvard, D., C. Brakebusch, E. Gustafsson, A. Aszódi, T. Bengtsson, A. Berna, and R. Fässler. 2001. Functional consequences of integrin gene mutations in mice. *Circulation research*. 89:211-223.
Bouvard, D., J. Pouwels, N. De Franceschi, and J. Ivaska. 2013. Integrin inactivators: balancing cellular functions in vitro and in vivo. *Nature Reviews Molecular Cell Biology*. 14:430-442.
Bradstock, K.F., and D.J. Gottlieb. 1995. Interaction of acute leukemia cells with the bone marrow microenvironment: implications for control of minimal residual disease. *Leukemia & lymphoma*. 18:1-16.
Bridges, L.C., P.H. Tani, K.R. Hanson, C.M. Roberts, M.B. Judkins, and R.D. Bowditch. 2002. The lymphocyte metalloprotease MDC-L (ADAM 28) is a ligand for the integrin α4β1. *Journal of Biological Chemistry*. 277:3784-3792.
Broccoli, D., J.W. Young, and T. de Lange. 1995. Telomerase activity in normal and malignant hematopoietic cells. *Proceedings of the National Academy of Sciences*. 92:9082-9086.
Campbell, I.D., and M.J. Humphries. 2011. Integrin structure, activation, and interactions. *Cold Spring Harbor perspectives in biology*. 3:a004994.

Campbell, J.J., J. Hedrick, A. Zlotnik, M.A. Siani, D.A. Thompson, and E.C. Butcher. 1998. Chemokines and the arrest of lymphocytes rolling under flow conditions. *Science*. 279:381-384.

Campbell, J.J., S. Qin, K.B. Bacon, C.R. Mackay, and E.C. Butcher. 1996. Biology of chemokine and classical chemoattractant receptors: differential requirements for adhesion-triggering versus chemotactic responses in lymphoid cells. *The Journal of cell biology*. 134:255-266.

Campos, L.S., D.P. Leone, J.B. Relvas, C. Brakebusch, R. Fässler, and U. Suter. 2004. β1 integrins activate a MAPK signalling pathway in neural stem cells that contributes to their maintenance. *Development*. 131:3433-3444.

Cardone, M.H., N. Roy, H.R. Stennicke, G.S. Salvesen, T.F. Franke, E. Stanbridge, S. Frisch, and J.C. Reed. 1998. Regulation of cell death protease caspase-9 by phosphorylation. *Science*. 282:1318-1321.

Carpenter, E.P., K. Beis, A.D. Cameron, and S. Iwata. 2008. Overcoming the challenges of membrane protein crystallography. *Current opinion in structural biology*. 18:581-586.

Casares, N., M.O. Pequignot, A. Tesniere, F. Ghiringhelli, S. Roux, N. Chaput, E. Schmitt, A. Hamai, S. Hervas-Stubbs, and M. Obeid. 2005. Caspase-dependent immunogenicity of doxorubicin-induced tumor cell death. *The Journal of experimental medicine*. 202:1691-1701.

Chachoua, I., C. Pecquet, M. El-Khoury, H. Nivarthi, R.-I. Albu, C. Marty, V. Gryshkova, J.-P. Defour, G. Vertenoeil, and A. Ngo. 2016. Thrombopoietin receptor activation by myeloproliferative neoplasm associated calreticulin mutants. *Blood*. 127:1325-1335.

Chao, M.P., S. Jaiswal, R. Weissman-Tsukamoto, A.A. Alizadeh, A.J. Gentles, J. Volkmer, K. Weiskopf, S.B. Willingham, T. Raveh, and C.Y. Park. 2010. Calreticulin is the dominant pro-phagocytic signal on multiple human cancers and is counterbalanced by CD47. *Science translational medicine*. 2:63ra94-63ra94.

Chekenya, M., C. Krakstad, A. Svendsen, I. Netland, V. Staalesen, B. Tysnes, F. Selheim, J. Wang, P.Ø. Sakariassen, and T. Sandal. 2008. The progenitor cell marker NG2/MPG promotes chemoresistance by activation of integrin-dependent PI3K/Akt signaling. *Oncogene*. 27:5182-5194.

Chen, X., C. Xie, N. Nishida, Z. Li, T. Walz, and T.A. Springer. 2010. Requirement of open headpiece conformation for activation of leukocyte integrin αXβ2. *Proceedings of the National Academy of Sciences*. 107:14727-14732.

Cheng, S.-T., T.Q. Nguyen, Y.-S. Yang, J.D. Capra, and R.D. Sontheimer. 1996. Calreticulin binds hYRNA and the 52-kDa polypeptide component of the Ro/SS-A ribonucleoprotein autoantigen. *The Journal of Immunology*. 156:4484-4491.

Chessells, J.M. 2001. Pitfalls in the diagnosis of childhood leukaemia. *British journal of haematology*. 114:506-511.

Chigaev, A., Y. Smagley, M.K. Haynes, O. Ursu, C.G. Bologa, L. Halip, T. Oprea, A. Waller, M.B. Carter, and Y. Zhang. 2015. FRET detection of lymphocyte function–associated antigen-1 conformational extension. *Molecular biology of the cell*. 26:43-54.

Chissoe, S.L., A. Bodenteich, Y.-F. Wang, Y.-P. Wang, D. Burian, S.W. Clifton, J. Crabtree, A. Freeman, K. Iyer, and L. Jian. 1995. Sequence and analysis of the human ABL gene, the BCR gene, and regions involved in the Philadelphia chromosomal translocation. *Genomics*. 27:67-82.

Chiu, L.Y., J.L. Ko, Y.J. Lee, T.Y. Yang, Y.T. Tee, and G.T. Sheu. 2010. L-type calcium channel blockers reverse docetaxel and vincristine-induced multidrug resistance independent of ABCB1 expression in human lung cancer cell lines. *Toxicology letters*. 192:408-418.

Chow, K.T., and M. Gale. 2015. SnapShot: Interferon Signaling. *Cell*. 163:1808-1808. e1801.

Clark, S.S., J. McLaughlin, W.M. Crist, R. Champlin, and O.N. Witte. 1987. Unique forms of the abl tyrosine kinase distinguish Ph1-positive CML from Ph1-positive ALL. *Science*. 235:85-88.

Clifford, D.B., A. De Luca, D.M. Simpson, G. Arendt, G. Giovannoni, and A. Nath. 2010. Natalizumab-associated progressive multifocal leukoencephalopathy in patients with multiple sclerosis: lessons from 28 cases. *Lancet neurology*. 9:438-446.

Colangelo, T., G. Polcaro, P. Ziccardi, B. Pucci, L. Muccillo, M. Galgani, A. Fucci, M. Milone, A. Budillon, and M. Santopaolo. 2016. Proteomic screening identifies calreticulin as a miR-27a direct target repressing MHC class I cell surface exposure in colorectal cancer. *Cell death & disease*. 7:e2120.

Cong, L., F.A. Ran, D. Cox, S. Lin, R. Barretto, N. Habib, P.D. Hsu, X. Wu, W. Jiang, and L.A. Marraffini. 2013. Multiplex genome engineering using CRISPR/Cas systems. *Science*. 339:819-823.

Coppolino, M., C. Leung-Hagesteijn, S. Dedhar, and J. Wilkins. 1995. Inducible interaction of integrin alpha 2 beta 1 with calreticulin. Dependence on the activation state of the integrin. *J Biol Chem*. 270:23132-23138.

Coppolino, M.G., and S. Dedhar. 1999. Ligand-specific, transient interaction between integrins and calreticulin during cell adhesion to extracellular matrix proteins is dependent upon phosphorylation/dephosphorylation events. *Biochem J*. 340 (Pt 1):41-50.

Coppolino, M.G., M.J. Woodside, N. Demaurex, S. Grinstein, R. St-Arnaud, and S. Dedhar. 1997. Calreticulin is essential for integrin-mediated calcium signalling and cell adhesion.

Corbett, E.F., K.M. Michalak, K. Oikawa, S. Johnson, I.D. Campbell, P. Eggleton, C. Kay, and M. Michalak. 2000. The conformation of calreticulin is influenced by the endoplasmic reticulum luminal environment. *Journal of Biological Chemistry*. 275:27177-27185.

Corrigan, J., and S. Feig. 2004. Guidelines for pediatric cancer centers. *Pediatrics*. 113:1833-1835.

Craddock, C., B. Nakamoto, M. Elices, and T. Papayannopoulou. 1997. The role of CS1 moiety of fibronectin in VLA4-mediated haemopoietic progenitor trafficking. *British journal of haematology*. 97:15-21.

Damiano, J.S., A.E. Cress, L.A. Hazlehurst, A.A. Shtil, and W.S. Dalton. 1999. Cell adhesion mediated drug resistance (CAM-DR): role of integrins and resistance to apoptosis in human myeloma cell lines. *Blood*. 93:1658-1667.

Damiano, J.S., and W.S. Dalton. 2000. Integrin-mediated drug resistance in multiple myeloma. *Leuk Lymphoma*. 38:71-81.

Damiano, J.S., L.A. Hazlehurst, and W.S. Dalton. 2001. Cell adhesion-mediated drug resistance (CAM-DR) protects the K562 chronic myelogenous leukemia cell line from apoptosis induced by BCR/ABL inhibition, cytotoxic drugs, and gamma-irradiation. *Leukemia*. 15:1232-1239.

Danciu, T.E., R.M. Adam, K. Naruse, M.R. Freeman, and P.V. Hauschka. 2003. Calcium regulates the PI3K-Akt pathway in stretched osteoblasts. *FEBS letters*. 536:193-197.

Darnell Jr, J.E., I.M. Kerr, and G.R. Stark. 1994. Jak-STAT pathways and transcriptional activation in response to IFNs and other extracellular signaling proteins. *Science-AAAS-weekly paper edition-including guide to scientific information*. 264:1415-1420.

Dave, M., K.A. Papadakis, and W.A. Faubion. 2014. Immunology of inflammatory bowel disease and molecular targets for biologics. *Gastroenterology clinics of North America*. 43:405-424.

Davidson, B., I. Goldberg, W.H. Gotlieb, J. Kopolovic, B. Risberg, G. Ben-Baruch, and R. Reich. 2003. Coordinated expression of integrin subunits, matrix metalloproteinases (MMP), angiogenic genes and Ets transcription factors in advanced-stage ovarian carcinoma: a possible activation pathway? *Cancer and Metastasis Reviews*. 22:103-115.

de la Fuente, M.T., B. Casanova, J.V. Moyano, M. Garcia-Gila, L. Sanz, J. Garcia-Marco, A. Silva, and A. Garcia-Pardo. 2002. Engagement of α4β1 integrin by fibronectin induces in vitro resistance of B chronic lymphocytic leukemia cells to fludarabine. *Journal of leukocyte biology*. 71:495-502.

de Melker, A.A., D. Kramer, I. Kuikman, and A. Sonnenberg. 1997. The two phenylalanines in the GFFKR motif of the integrin α6A subunit are essential for heterodimerization. *Biochemical Journal*. 328:529-537.

De Toni-Costes, F., M. Despeaux, J. Bertrand, E. Bourogaa, L. Ysebaert, B. Payrastre, and C. Racaud-Sultan. 2010. A New alpha5beta1 integrin-dependent survival pathway through GSK3beta activation in leukemic cells. *PLoS One*. 5:e9807.

Deakin, N.O., M.D. Bass, S. Warwood, J. Schoelermann, Z. Mostafavi-Pour, D. Knight, C. Ballestrem, and M.J. Humphries. 2009. An integrin-α4–14-3-3ζ–paxillin ternary complex mediates localised Cdc42 activity and accelerates cell migration. *Journal of cell science*. 122:1654-1664.

Decca, M.B., M.A. Carpio, C. Bosc, M.R. Galiano, D. Job, A. Andrieux, and M.E. Hallak. 2007. Post-translational Arginylation of Calreticulin A NEW ISOSPECIES OF CALRETICULIN COMPONENT OF STRESS GRANULES. *Journal of Biological Chemistry*. 282:8237-8245.

Dedhar, S. 1994. Novel functions for calreticulin: interaction with integrins and modulation of gene expression? *Trends in biochemical sciences*. 19:269-271.

Den Berg, V., and E. Van. 1998. Anti-C1q receptor/calreticulin autoantibodies in patients with systemic lupus erythematosus (SLE). *Clinical & Experimental Immunology*. 111:359-364.

Denhardt, D.T., M. Noda, A.W. O'Regan, D. Pavlin, and J.S. Berman. 2001. Osteopontin as a means to cope with environmental insults: regulation of inflammation, tissue remodeling, and cell survival. *The Journal of clinical investigation*. 107:1055-1061.

Denning, G.M., K.G. Leidal, V.A. Holst, S.S. Iyer, D.W. Pearson, J.R. Clark, W.M. Nauseef, and R.A. Clark. 1997. Calreticulin biosynthesis and processing in human myeloid cells: demonstration of signal peptide cleavage and N-glycosylation. *Blood*. 90:372-381.

DiGiuseppe, J.A., S.G. Fuller, and M.J. Borowitz. 2009. Overexpression of CD49f in precursor B-cell acute lymphoblastic leukemia: Potential usefulness in minimal residual disease detection. *Cytometry Part B: Clinical Cytometry*. 76:150-155.

DiPersio, C.M., K.M. Hodivala-Dilke, R. Jaenisch, J.A. Kreidberg, and R.O. Hynes. 1997. α3β1 integrin is required for normal development of the epidermal basement membrane. *The Journal of cell biology*. 137:729-742.

Donnelly, O.G., F. Errington-Mais, L. Steele, E. Hadac, V. Jennings, K. Scott, H. Peach, R.M. Phillips, J. Bond, and H. Pandha. 2013. Measles virus causes immunogenic cell death in human melanoma. *Gene therapy*. 20:7-15.

Douma, S., T. van Laar, J. Zevenhoven, R. Meuwissen, E. van Garderen, and D.S. Peeper. 2004. Suppression of anoikis and induction of metastasis by the neurotrophic receptor TrkB. *Nature*. 430:1034-1039.

Dowling, J., Q.-C. Yu, and E. Fuchs. 1996. Beta4 integrin is required for hemidesmosome formation, cell adhesion and cell survival. *The Journal of cell biology*. 134:559-572.

Dransfield, I., C. Cabanas, A. Craig, and N. Hogg. 1992. Divalent cation regulation of the function of the leukocyte integrin LFA-1. *The Journal of cell biology*. 116:219-226.

Du, X., M. Gu, J.W. Weisel, C. Nagaswami, J.S. Bennett, R. Bowditch, and M.H. Ginsberg. 1993. Long range propagation of conformational changes in integrin alpha IIb beta 3. *Journal of Biological Chemistry*. 268:23087-23092.

Du, X.L., H. Yang, S.G. Liu, M.L. Luo, J.J. Hao, Y. Zhang, D.C. Lin, X. Xu, Y. Cai, Q.M. Zhan, and M.R. Wang. 2009. Calreticulin promotes cell motility and enhances resistance to anoikis through STAT3-CTTN-Akt pathway in esophageal squamous cell carcinoma. *Oncogene*. 28:3714-3722.

Dupuis, M., E. Schaerer, K.-H. Krause, and J. Tschopp. 1993. The calcium-binding protein calreticulin is a major constituent of lytic granules in cytolytic T lymphocytes. *The Journal of experimental medicine*. 177:1-7.

Eke, I., and N. Cordes. 2015. Focal adhesion signaling and therapy resistance in cancer. *In* Seminars in cancer biology. Vol. 31. Elsevier. 65-75.

El Azreq, M.A., D. Naci, and F. Aoudjit. 2012. Collagen/beta1 integrin signaling up-regulates the ABCC1/MRP-1 transporter in an ERK/MAPK-dependent manner. *Mol Biol Cell*. 23:3473-3484.

Elf, S., N.S. Abdelfattah, E. Chen, J. Perales-Patón, E.A. Rosen, A. Ko, F. Peisker, N. Florescu, S. Giannini, and O. Wolach. 2016. Mutant calreticulin requires both its mutant C-terminus and the thrombopoietin receptor for oncogenic transformation. *Cancer discovery*.

Eng, E.T., B.J. Smagghe, T. Walz, and T.A. Springer. 2011. Intact αIIbβ3 integrin is extended after activation as measured by solution x-ray scattering and electron microscopy. *Journal of Biological Chemistry*. 286:35218-35226.

Evans, A.L., and U. Müller. 2000. Stereocilia defects in the sensory hair cells of the inner ear in mice deficient in integrin α8β1. *Nature genetics*. 24:424-428.

Fadel, M.P., E. Dziak, C.M. Lo, J. Ferrier, N. Mesaeli, M. Michalak, and M. Opas. 1999. Calreticulin affects focal contact-dependent but not close contact-dependent cell-substratum adhesion. *J Biol Chem*. 274:15085-15094.

Fadel, M.P., M. Szewczenko-Pawlikowski, P. Leclerc, E. Dziak, J.M. Symonds, O. Blaschuk, M. Michalak, and M. Opas. 2001. Calreticulin affects beta-catenin-associated pathways. *J Biol Chem*. 276:27083-27089.

Felding-Habermann, B., T.E. O'Toole, J.W. Smith, E. Fransvea, Z.M. Ruggeri, M.H. Ginsberg, P.E. Hughes, N. Pampori, S.J. Shattil, and A. Saven. 2001. Integrin activation controls metastasis in human breast cancer. *Proceedings of the National Academy of Sciences*. 98:1853-1858.

Filshie, R., D. Gottlieb, and K. Bradstock. 1998. VLA-4 is involved in the engraftment of the human pre-B acute lymphoblastic leukaemia cell line NALM-6 in SCID mice. *British journal of haematology*. 102:1292-1300.

Finazzi, G., V. Caruso, R. Marchioli, G. Capnist, T. Chisesi, C. Finelli, L. Gugliotta, R. Landolfi, J. Kutti, and H. Gisslinger. 2005. Acute leukemia in polycythemia vera: an analysis of 1638 patients enrolled in a prospective observational study. *Blood*. 105:2664-2670.

Findley, H.W., L. Gu, A.M. Yeager, and M. Zhou. 1997. Expression and regulation of Bcl-2, Bcl-xl, and Bax correlate with p53 status and sensitivity to apoptosis in childhood acute lymphoblastic leukemia. *Blood*. 89:2986-2993.

Fornaro, M., T. Manes, and L.R. Languino. 2001. Integrins and prostate cancer metastases. *Cancer and Metastasis Reviews*. 20:321-331.

Gallay, N., C. Dos Santos, L. Cuzin, M. Bousquet, V. Simmonet Gouy, C. Chaussade, M. Attal, B. Payrastre, C. Demur, and C. Recher. 2009. The level of AKT phosphorylation on threonine 308 but not on serine 473 is associated with high-risk cytogenetics and predicts poor overall survival in acute myeloid leukaemia. *Leukemia*. 23:1029-1038.

Galluzzi, L., L. Senovilla, L. Zitvogel, and G. Kroemer. 2012a. The secret ally: immunostimulation by anticancer drugs. *Nature reviews Drug discovery*. 11:215-233.

Galluzzi, L., I. Vitale, J. Abrams, E. Alnemri, E. Baehrecke, M. Blagosklonny, T. Dawson, V. Dawson, W. El-Deiry, and S. Fulda. 2012b. Molecular definitions of cell death subroutines: recommendations of the Nomenclature Committee on Cell Death 2012. *Cell Death & Differentiation*. 19:107-120.

Garcia, S., J. Nascimento, E. Bonfa, R. Levy, S. Oliveira, A. Tavares, and A. De Carvalho. 1994. Cellular mechanism of the conduction abnormalities induced by serum from anti-Ro/SSA-positive patients in rabbit hearts. *Journal of Clinical Investigation*. 93:718.

Gardai, S.J., K.A. McPhillips, S.C. Frasch, W.J. Janssen, A. Starefeldt, J.E. Murphy-Ullrich, D.L. Bratton, P.A. Oldenborg, M. Michalak, and P.M. Henson. 2005. Cell-surface calreticulin initiates clearance of viable or apoptotic cells through trans-activation of LRP on the phagocyte. *Cell*. 123:321-334.

Garg, A.D., D.V. Krysko, T. Verfaillie, A. Kaczmarek, G.B. Ferreira, T. Marysael, N. Rubio, M. Firczuk, C. Mathieu, and A.J. Roebroek. 2012. A novel pathway combining calreticulin exposure and ATP secretion in immunogenic cancer cell death. *The EMBO journal*. 31:1062-1079.

Garg, A.D., D. Nowis, J. Golab, P. Vandenabeele, D.V. Krysko, and P. Agostinis. 2010. Immunogenic cell death, DAMPs and anticancer therapeutics: an emerging amalgamation. *Biochimica et Biophysica Acta (BBA)-Reviews on Cancer*. 1805:53-71.

Garrido, G., A. Rabasa, B. Sánchez, M.V. López, R. Blanco, A. López, D.R. Hernández, R. Pérez, and L.E. Fernández. 2011. Induction of immunogenic apoptosis by blockade of epidermal growth factor receptor activation with a specific antibody. *The Journal of Immunology*. 187:4954-4966.

Gassler, N., F. Autschbach, S. Gauer, J. Bohn, B. Sido, H. Otto, H. Geiger, and N. Obermüller. 2002. Expression of osteopontin (Eta-1) in Crohn disease of the terminal ileum. *Scandinavian journal of gastroenterology*. 37:1286-1295.

Gattei, V., P. Bulian, M.I. Del Principe, A. Zucchetto, L. Maurillo, F. Buccisano, R. Bomben, M. Dal-Bo, F. Luciano, F.M. Rossi, M. Degan, S. Amadori, and G. Del Poeta. 2008. Relevance

of CD49d protein expression as overall survival and progressive disease prognosticator in chronic lymphocytic leukemia. *Blood*. 111:865-873.
Gaynon, P.S., R.P. Qu, R.J. Chappell, M.L. Willoughby, D.G. Tubergen, P.G. Steinherz, and M.E. Trigg. 1998. Survival after relapse in childhood acute lymphoblastic leukemia. *Cancer*. 82:1387-1395.
Gelebart, P., M. Opas, and M. Michalak. 2005. Calreticulin, a Ca 2+-binding chaperone of the endoplasmic reticulum. *The international journal of biochemistry & cell biology*. 37:260-266.
Gendron, S., J. Couture, and F. Aoudjit. 2005. Collagen type I signaling reduces the expression and the function of human receptor activator of nuclear factor-κB ligand (RANKL) in T lymphocytes. *European journal of immunology*. 35:3673-3682.
Georges-Labouesse, E., M. Mark, N. Messaddeq, and A. Gansmüller. 1998. Essential role of α6 integrins in cortical and retinal lamination. *Current Biology*. 8:983-S981.
Giancotti, F.G., and E. Ruoslahti. 1999. Integrin signaling. *Science*. 285:1028-1033.
Ginsberg, M.H. 2014. Integrin activation. *BMB Rep*. 47:655-659.
Giraldo, A.M.V., M.L. Medus, M.G. Lebrero, R.S. Pagano, C.A. Labriola, L. Landolfo, J.M. Delfino, A.J. Parodi, and J.J. Caramelo. 2010. The structure of calreticulin C-terminal domain is modulated by physiological variations of calcium concentration. *Journal of Biological Chemistry*. 285:4544-4553.
Goetz, C.A., I.R. Harmon, J.J. O'Neil, M.A. Burchill, and M.A. Farrar. 2004. STAT5 activation underlies IL7 receptor-dependent B cell development. *The Journal of Immunology*. 172:4770-4778.
Goicoechea, S., A.W. Orr, M.A. Pallero, P. Eggleton, and J.E. Murphy-Ullrich. 2000. Thrombospondin mediates focal adhesion disassembly through interactions with cell surface calreticulin. *J Biol Chem*. 275:36358-36368.
Goitea, V.E., and M.E. Hallak. 2015. Calreticulin and arginylated calreticulin have different susceptibilities to proteasomal degradation. *Journal of Biological Chemistry*. 290:16403-16414.
Gold, L.I., P. Eggleton, M.T. Sweetwyne, L.B. Van Duyn, M.R. Greives, S.M. Naylor, M. Michalak, and J.E. Murphy-Ullrich. 2010. Calreticulin: non-endoplasmic reticulum functions in physiology and disease. *Faseb J*. 24:665-683.
Gold, L.I., M. Rahman, K.M. Blechman, M.R. Greives, S. Churgin, J. Michaels, M.J. Callaghan, N.L. Cardwell, A.C. Pollins, and M. Michalak. 2006. Overview of the role for calreticulin in the enhancement of wound healing through multiple biological effects. *In* Journal of Investigative Dermatology Symposium Proceedings. Vol. 11. Nature Publishing Group. 57-65.
Goldberg, I., B. Davidson, R. Reich, W.H. Gotlieb, G. Ben-Baruch, M. Bryne, A. Berner, J.M. Nesland, and J. Kopolovic. 2001. αv integrin expression is a novel marker of poor prognosis in advanced-stage ovarian carcinoma. *Clinical cancer research*. 7:4073-4079.
González-Amaro, R., M. Mittelbrunn, and F. Sánchez-Madrid. 2005. Therapeutic anti-integrin (α4 and αL) monoclonal antibodies: two-edged swords? *Immunology*. 116:289-296.
Graner, M.W. 2016. Chapter Eight-HSP90 and Immune Modulation in Cancer. *Advances in cancer research*. 129:191-224.

Graubert, T., J.R. Cook, L. Scheuttpelz, D.M. Arnold, A. Cuker, C. Neunert, K.R. McCrae, M. Ragni, S. O'Brien, and M. Arcasoy. 2013. American Society of Hematology Self-Assessment Program. American Society of Hematology.

Gray, A.J., P.W. Park, T.J. Broekelmann, G.J. Laurent, J.T. Reeves, K.R. Stenmark, and R.P. Mecham. 1995. The mitogenic effects of the Bβ chain of fibrinogen are mediated through cell surface calreticulin. *Journal of Biological Chemistry*. 270:26602-26606.

Green, D.R., T. Ferguson, L. Zitvogel, and G. Kroemer. 2009. Immunogenic and tolerogenic cell death. *Nature Reviews Immunology*. 9:353-363.

Greives, M.R., F. Samra, S.C. Pavlides, K.M. Blechman, S.M. Naylor, C.D. Woodrell, C. Cadacio, J.P. Levine, T.A. Bancroft, and M. Michalak. 2012. Exogenous calreticulin improves diabetic wound healing. *Wound Repair and Regeneration*. 20:715-730.

Guan, J.-L., L. Cary, and D. Han. 1999. Integrin-mediated signal transduction pathways. *Histology and histopathology*. 14:1001-1009.

Guo, W., and F.G. Giancotti. 2004. Integrin signalling during tumour progression. *Nature Reviews Molecular Cell Biology*. 5:816-826.

Haataja, L., V. Kaartinen, J. Groffen, and N. Heisterkamp. 2002. The small GTPase Rac3 interacts with the integrin-binding protein CIB and promotes integrin αIIbβ3-mediated adhesion and spreading. *Journal of Biological Chemistry*. 277:8321-8328.

Hanahan, D., and R.A. Weinberg. 2000. The hallmarks of cancer. *Cell*. 100:57-70.

Hanahan, D., and R.A. Weinberg. 2011. Hallmarks of cancer: the next generation. *Cell*. 144:646-674.

Hannigan, G., C. Leung-Hagesteijn, L. Fitz-Gibbon, M. Coppolino, S. Dedhar, G. Hannigan, S. Dedhar, and G. Hannigan. 1996. Regulation of cell adhesion and anchorage-dependent growth by a new. *Nature*. 379:91-96.

Harvey, R.C., C.G. Mullighan, I.-M. Chen, W. Wharton, F.M. Mikhail, A.J. Carroll, H. Kang, W. Liu, K.K. Dobbin, and M.A. Smith. 2010. Rearrangement of CRLF2 is associated with mutation of JAK kinases, alteration of IKZF1, Hispanic/Latino ethnicity, and a poor outcome in pediatric B-progenitor acute lymphoblastic leukemia. *Blood*. 115:5312-5321.

Hazlehurst, L., R. Argilagos, and W. Dalton. 2007. β1 integrin mediated adhesion increases Bim protein degradation and contributes to drug resistance in leukaemia cells. *British journal of haematology*. 136:269-275.

Hazlehurst, L., J. Damiano, I. Buyuksal, W. Pledger, and W. Dalton. 2000a. Adhesion to fibronectin via β1 integrins regulates p27 kip1 levels and contributes to cell adhesion mediated drug resistance (CAM-DR). *Oncogene*. 19.

Hazlehurst, L.A., and W.S. Dalton. 2001. Mechanisms associated with cell adhesion mediated drug resistance (CAM-DR) in hematopoietic malignancies. *Cancer metastasis reviews*. 20:43-50.

Hazlehurst, L.A., J.S. Damiano, I. Buyuksal, W.J. Pledger, and W.S. Dalton. 2000b. Adhesion to fibronectin via beta1 integrins regulates p27kip1 levels and contributes to cell adhesion mediated drug resistance (CAM-DR). *Oncogene*. 19:4319-4327.

Hidalgo, A., F. Sanz-Rodríguez, J.L. Rodríguez-Fernández, B. Albella, C. Blaya, N. Wright, C. Cabañas, F. Prósper, J.C. Gutierrez-Ramos, and J. Teixidó. 2001. Chemokine stromal cell-derived factor-1α modulates VLA-4 integrin-dependent adhesion to fibronectin and VCAM-1 on bone marrow hematopoietic progenitor cells. *Experimental hematology*. 29:345-355.

Hideshima, T., C. Mitsiades, G. Tonon, P.G. Richardson, and K.C. Anderson. 2007. Understanding multiple myeloma pathogenesis in the bone marrow to identify new therapeutic targets. *Nature Reviews Cancer*. 7:585-598.

Hoa, N., M.P. Myers, T.G. Douglass, J.G. Zhang, C. Delgado, L. Driggers, L.L. Callahan, G. VanDeusen, J.T. Pham, and N. Bhakta. 2009. Molecular mechanisms of paraptosis induction: implications for a non-genetically modified tumor vaccine. *PLoS One*. 4:e4631.

Hodge, D.R., E.M. Hurt, and W.L. Farrar. 2005. The role of IL-6 and STAT3 in inflammation and cancer. *European journal of cancer*. 41:2502-2512.

Hodkinson, P., T. Elliott, W. Wong, R. Rintoul, A. Mackinnon, C. Haslett, and T. Sethi. 2006. ECM overrides DNA damage-induced cell cycle arrest and apoptosis in small-cell lung cancer cells through β1 integrin-dependent activation of PI3-kinase. *Cell Death & Differentiation*. 13:1776-1788.

Holaska, J.M., B.E. Black, D.C. Love, J.A. Hanover, J. Leszyk, and B.M. Paschal. 2001. Calreticulin is a receptor for nuclear export. *The Journal of cell biology*. 152:127-140.

Holaska, J.M., B.E. Black, F. Rastinejad, and B.M. Paschal. 2002. Ca2+-dependent nuclear export mediated by calreticulin. *Molecular and cellular biology*. 22:6286-6297.

Howard, L., R.A. Maciewicz, and C.P. Blobel. 2000. Cloning and characterization of ADAM28: evidence for autocatalytic pro-domain removal and for cell surface localization of mature ADAM28. *Biochemical Journal*. 348:21-27.

Howard, L., Y. Zheng, M. Horrocks, R.A. Maciewicz, and C. Blobel. 2001. Catalytic activity of ADAM28. *FEBS letters*. 498:82-86.

Howlader, N., A. Noone, M. Krapcho, J. Garshell, N. Neyman, S. Altekruse, C. Kosary, M. Yu, J. Ruhl, and Z. Tatalovich. 2013. SEER cancer statistics review, 1975–2010. 2013. *Bethesda, MD: National Cancer Institute*.

Hsieh, Y.-T., E.J. Gang, H. Geng, E. Park, S. Huantes, D. Chudziak, K. Dauber, P. Schaefer, C. Scharman, and H. Shimada. 2013. Integrin alpha4 blockade sensitizes drug resistant pre-B acute lymphoblastic leukemia to chemotherapy. *Blood*. 121:1814-1818.

Huang, X., J. Wu, R. Ferrando, J. Lee, Y. Wang, R. Farese, and D. Sheppard. 2000. Fatal bilateral chylothorax in mice lacking the integrin α9β1. *Molecular and cellular biology*. 20:5208-5215.

Hughes, P.E., F. Diaz-Gonzalez, L. Leong, C. Wu, J.A. McDonald, S.J. Shattil, and M.H. Ginsberg. 1996. Breaking the integrin hinge A defined structural constraint regulates integrin signaling. *Journal of Biological Chemistry*. 271:6571-6574.

Humphries, J.D., A. Byron, and M.J. Humphries. 2006. Integrin ligands at a glance. *Journal of cell science*. 119:3901-3903.

Humphries, M. 2000. Integrin structure. *Biochemical Society Transactions*. 28:311-340.

Hunger, S.P., X. Lu, M. Devidas, B.M. Camitta, P.S. Gaynon, N.J. Winick, G.H. Reaman, and W.L. Carroll. 2012. Improved survival for children and adolescents with acute lymphoblastic leukemia between 1990 and 2005: a report from the children's oncology group. *Journal of clinical oncology*:JCO. 2011.2037. 8018.

Hutchinson, M. 2007. Natalizumab: a new treatment for relapsing remitting multiple sclerosis. *Therapeutics and clinical risk management*. 3:259.

Hynes, R.O. 2002. Integrins: bidirectional, allosteric signaling machines. *Cell*. 110:673-687.

Ignacio Arias, J., C. Sepulveda, P. Bravo, C. Hamilton-West, I. Maldonado, and A. Ferreira. 2015. Comparative effect of human and Trypanosoma cruzi calreticulin in wound healing. *Journal of tissue engineering and regenerative medicine*. 9:41-54.

Imai, C., K. Mihara, M. Andreansky, I. Nicholson, C. Pui, T. Geiger, and D. Campana. 2004. Chimeric receptors with 4-1BB signaling capacity provoke potent cytotoxicity against acute lymphoblastic leukemia. *Leukemia*. 18:676-684.

Inaba, H., M. Greaves, and C.G. Mullighan. 2013. Acute lymphoblastic leukaemia. *The Lancet*. 381:1943-1955.

Ivaska, J., L. Bosca, and P.J. Parker. 2003. PKCe is a permissive link in integrin-dependent IFN-γ signalling that facilitates JAK phosphorylation of STAT1. *Nature cell biology*. 5:363-369.

Jacamo, R., Y. Chen, Z. Wang, W. Ma, M. Zhang, E.L. Spaeth, Y. Wang, V.L. Battula, P.Y. Mak, and K. Schallmoser. 2014. Reciprocal leukemia-stroma VCAM-1/VLA-4-dependent activation of NF-κB mediates chemoresistance. *Blood*. 123:2691-2702.

Jadlowiec, J., H. Koch, X. Zhang, P.G. Campbell, M. Seyedain, and C. Sfeir. 2004. Phosphophoryn regulates the gene expression and differentiation of NIH3T3, MC3T3-E1, and human mesenchymal stem cells via the integrin/MAPK signaling pathway. *Journal of Biological Chemistry*. 279:53323-53330.

Jaiswal, S., C.H. Jamieson, W.W. Pang, C.Y. Park, M.P. Chao, R. Majeti, D. Traver, N. van Rooijen, and I.L. Weissman. 2009. CD47 is upregulated on circulating hematopoietic stem cells and leukemia cells to avoid phagocytosis. *Cell*. 138:271-285.

James, C., V. Ugo, J.-P. Le Couédic, J. Staerk, F. Delhommeau, C. Lacout, L. Garçon, H. Raslova, R. Berger, and A. Bennaceur-Griscelli. 2005. A unique clonal JAK2 mutation leading to constitutive signalling causes polycythaemia vera. *Nature*. 434:1144-1148.

Jaworski, D.C., F.A. Simmen, W. Lamoreaux, L.B. Coons, M.T. Muller, and G.R. Needham. 1995. A secreted calreticulin protein in ixodid tick (Amblyomma americanum) saliva. *Journal of Insect Physiology*. 41:369-375.

Jinawath, N., C. Vasoontara, A. Jinawath, X. Fang, K. Zhao, K.-L. Yap, T. Guo, C.S. Lee, W. Wang, and B.M. Balgley. 2010. Oncoproteomic analysis reveals co-upregulation of RELA and STAT5 in carboplatin resistant ovarian carcinoma. *PLoS One*. 5:e11198.

Johnson, S., M. Michalak, M. Opas, and P. Eggleton. 2001. The ins and outs of calreticulin: from the ER lumen to the extracellular space. *Trends in cell biology*. 11:122-129.

Jongewaard, I.N., P.M. Tsai, and J.W. Smith. 1996. The type III connecting segment of fibronectin contains an aspartic acid residue that regulates the rate of binding to integrin alpha 4 beta 1. *Cell Adhes Commun*. 3:487-495.

Joshi, M., G.P. Pogue, R.C. Duncan, N.S. Lee, N.K. Singh, C.D. Atreya, D.M. Dwyer, and H.L. Nakhasi. 1996. Isolation and characterization of Leishmania donovani calreticulin gene and its conservation of the RNA binding activity. *Molecular and biochemical parasitology*. 81:53-64.

Jovani, M., and S. Danese. 2013. Vedolizumab for the treatment of IBD: a selective therapeutic approach targeting pathogenic a4b7 cells. *Current drug targets*. 14:1433-1443.

Karska, K., L. Tuckova, L. Steiner, H. Tlaskalovahogenova, and M. Michalak. 1995. Calreticulin-the potential autoantigen in celiac disease. *Biochemical and biophysical research communications*. 209:597-605.

Kassner, P., R. Alon, T. Springer, and M. Hemler. 1995. Specialized functional properties of the integrin alpha 4 cytoplasmic domain. *Molecular biology of the cell*. 6:661-674.

Kassner, P.D., and M.E. Hemler. 1993. Interchangeable alpha chain cytoplasmic domains play a positive role in control of cell adhesion mediated by VLA-4, a beta 1 integrin. *The Journal of experimental medicine*. 178:649-660.
Kassner, P.D., S. Kawaguchi, and M.E. Hemler. 1994. Minimum alpha chain cytoplasmic tail sequence needed to support integrin-mediated adhesion. *J Biol Chem*. 269:19859-19867.
Kazama, H., J.-E. Ricci, J.M. Herndon, G. Hoppe, D.R. Green, and T.A. Ferguson. 2008. Induction of immunological tolerance by apoptotic cells requires caspase-dependent oxidation of high-mobility group box-1 protein. *Immunity*. 29:21-32.
Kepp, O., A. Gdoura, I. Martins, T. Panaretakis, F. Schlemmer, A. Tesniere, G.M. Fimia, F. Ciccosanti, A. Burgevin, and M. Piacentini. 2010. Lysyl tRNA synthetase is required for the translocation of calreticulin to the cell surface in immunogenic death. *Cell Cycle*. 9:3144-3149.
Kepp, O., A. Tesniere, L. Zitvogel, and G. Kroemer. 2009. The immunogenicity of tumor cell death. *Current opinion in oncology*. 21:71-76.
Kessenbrock, K., V. Plaks, and Z. Werb. 2010. Matrix metalloproteinases: regulators of the tumor microenvironment. *Cell*. 141:52-67.
Khalife, J., J. Liu, R. Pierce, E. Porchet, C. Godin, and A. Capron. 1994. Characterization and localization of Schistosoma mansoni calreticulin Sm58. *Parasitology*. 108:527-532.
Kim, C., T. Schmidt, E.-G. Cho, F. Ye, T.S. Ulmer, and M.H. Ginsberg. 2012. Basic amino-acid side chains regulate transmembrane integrin signalling. *Nature*. 481:209-213.
Kim, C., F. Ye, and M.H. Ginsberg. 2011. Regulation of integrin activation. *Annual review of cell and developmental biology*. 27:321-345.
Kim, M., C.V. Carman, and T.A. Springer. 2003. Bidirectional transmembrane signaling by cytoplasmic domain separation in integrins. *Science*. 301:1720-1725.
King, W.G., M.D. Mattaliano, T.O. Chan, P.N. Tsichlis, and J.S. Brugge. 1997. Phosphatidylinositol 3-kinase is required for integrin-stimulated AKT and Raf-1/mitogen-activated protein kinase pathway activation. *Mol Cell Biol*. 17:4406-4418.
Klampfl, T., H. Gisslinger, A.S. Harutyunyan, H. Nivarthi, E. Rumi, J.D. Milosevic, N.C. Them, T. Berg, B. Gisslinger, and D. Pietra. 2013. Somatic mutations of calreticulin in myeloproliferative neoplasms. *New England Journal of Medicine*. 369:2379-2390.
Knoblauch, A., C. Will, G. Goncharenko, S. Ludwig, and V. Wixler. 2007. The binding of Mss4 to α-integrin subunits regulates matrix metalloproteinase activation and fibronectin remodeling. *The FASEB Journal*. 21:497-510.
Korbelik, M., W. Zhang, and S. Merchant. 2011. Involvement of damage-associated molecular patterns in tumor response to photodynamic therapy: surface expression of calreticulin and high-mobility group box-1 release. *Cancer Immunology, Immunotherapy*. 60:1431-1437.
Kornberg, L.J., H.S. Earp, C.E. Turner, C. Prockop, and R.L. Juliano. 1991. Signal transduction by integrins: increased protein tyrosine phosphorylation caused by clustering of beta 1 integrins. *Proceedings of the National Academy of Sciences*. 88:8392-8396.
Koskela, H.L., S. Eldfors, P. Ellonen, A.J. Van Adrichem, H. Kuusanmäki, E.I. Andersson, S. Lagström, M.J. Clemente, T. Olson, and S.E. Jalkanen. 2012. Somatic STAT3 mutations in large granular lymphocytic leukemia. *New England Journal of Medicine*. 366:1905-1913.
Kralovics, R., F. Passamonti, A.S. Buser, S.-S. Teo, R. Tiedt, J.R. Passweg, A. Tichelli, M. Cazzola, and R.C. Skoda. 2005. A gain-of-function mutation of JAK2 in myeloproliferative disorders. *New England Journal of Medicine*. 352:1779-1790.

Krause, K.-H., and M. Michalak. 1997. Calreticulin. *Cell*. 88:439-443.
Kreidberg, J.A., M.J. Donovan, S.L. Goldstein, H. Rennke, K. Shepherd, R.C. Jones, and R. Jaenisch. 1996. Alpha 3 beta 1 integrin has a crucial role in kidney and lung organogenesis. *Development*. 122:3537-3547.
Kroemer, G., L. Galluzzi, O. Kepp, and L. Zitvogel. 2013. Immunogenic cell death in cancer therapy. *Annual review of immunology*. 31:51-72.
Krysko, D.V. 2013. Immunogenic Cell Death and Emission of Damps: Calreticulin and ATP. *Journal of Nanomedicine & Biotherapeutic Discovery*. 2012.
Krysko, D.V., A.D. Garg, A. Kaczmarek, O. Krysko, P. Agostinis, and P. Vandenabeele. 2012. Immunogenic cell death and DAMPs in cancer therapy. *Nature Reviews Cancer*. 12:860-875.
Krysko, O., T.L. Aaes, C. Bachert, P. Vandenabeele, and D. Krysko. 2013. Many faces of DAMPs in cancer therapy. *Cell death & disease*. 4:e631.
Kurzrock, R., M. Shtalrid, P. Romero, W.S. Kloetzer, M. Talpas, J.M. Trujillo, M. Blick, M. Beran, and J.U. Gutterman. 1987. A novel c-abl protein product in Philadelphia-positive acute lymphoblastic leukaemia.
Kwon, M.S., C.S. Park, K. Choi, J. Ahnn, J.I. Kim, S.H. Eom, S.J. Kaufman, and W.K. Song. 2000. Calreticulin couples calcium release and calcium influx in integrin-mediated calcium signaling. *Mol Biol Cell*. 11:1433-1443.
Larue, L., and A. Bellacosa. 2005. Epithelial–mesenchymal transition in development and cancer: role of phosphatidylinositol 3′ kinase/AKT pathways. *Oncogene*. 24:7443-7454.
Lau, T.-L., V. Dua, and T.S. Ulmer. 2008a. Structure of the integrin αIIb transmembrane segment. *Journal of Biological Chemistry*. 283:16162-16168.
Lau, T.-L., A.W. Partridge, M.H. Ginsberg, and T.S. Ulmer. 2008b. Structure of the Integrin β3 Transmembrane Segment in Phospholipid Bicelles and Detergent Micelles†. *Biochemistry*. 47:4008-4016.
Lau, T.L., C. Kim, M.H. Ginsberg, and T.S. Ulmer. 2009. The structure of the integrin αIIbβ3 transmembrane complex explains integrin transmembrane signalling. *The EMBO journal*. 28:1351-1361.
Leclair, P., and C.J. Lim. 2014. CD47-independent effects mediated by the TSP-derived 4N1K peptide. *PLoS One*. 9:e98358.
Legate, K.R., E. Montañez, O. Kudlacek, and R. Füssler. 2006. ILK, PINCH and parvin: the tIPP of integrin signalling. *Nature Reviews Molecular Cell Biology*. 7:20-31.
Legrand, O., G. Simonin, J.-Y. Perrot, R. Zittoun, and J.-P. Marie. 1998. Pgp and MRP activities using calcein-AM are prognostic factors in adult acute myeloid leukemia patients. *Blood*. 91:4480-4488.
Lehnert, K., Y. Yang, and G.W. Krissansen. 1998. MAdCAM-1 costimulates T cell proliferation exclusively through integrin α4β7, whereas VCAM-1 and CS-1 peptide use α4β1: evidence for "remote" costimulation and induction of hyperresponsiveness to B7 molecules. *European journal of immunology*. 28:3605-3615.
Leitinger, B., and N. Hogg. 2002. The involvement of lipid rafts in the regulation of integrin function. *Journal of cell science*. 115:963-972.
Lenartowska, M., J. Walczewski, and R. Lenartowski. 2009. [Calreticulin--the structure, cell localizations and functions in animals and plants]. *Postepy biochemii*. 55:406-415.

Leung-Hagesteijn, C.Y., K. Milankov, M. Michalak, J. Wilkins, and S. Dedhar. 1994. Cell attachment to extracellular matrix substrates is inhibited upon downregulation of expression of calreticulin, an intracellular integrin alpha-subunit-binding protein. *J Cell Sci*. 107 (Pt 3):589-600.

Levental, K.R., H. Yu, L. Kass, J.N. Lakins, M. Egeblad, J.T. Erler, S.F. Fong, K. Csiszar, A. Giaccia, and W. Weninger. 2009. Matrix crosslinking forces tumor progression by enhancing integrin signaling. *Cell*. 139:891-906.

Li, A., Q. Guo, C. Kim, W. Hu, and F. Ye. 2014. Integrin αIIb tail distal of GFFKR participates in inside-out αIIbβ3 activation. *Journal of Thrombosis and Haemostasis*. 12:1145-1155.

Li, S.S., A. Forslöw, and K.-G. Sundqvist. 2005a. Autocrine regulation of T cell motility by calreticulin-thrombospondin-1 interaction. *The Journal of Immunology*. 174:654-661.

Li, W., D.G. Metcalf, R. Gorelik, R. Li, N. Mitra, V. Nanda, P.B. Law, J.D. Lear, W.F. DeGrado, and J.S. Bennett. 2005b. A push-pull mechanism for regulating integrin function. *Proceedings of the National Academy of Sciences of the United States of America*. 102:1424-1429.

Li, Z., M.J. Calzada, J.M. Sipes, J.A. Cashel, H.C. Krutzsch, D.S. Annis, D.F. Mosher, and D.D. Roberts. 2002. Interactions of thrombospondins with α4β1 integrin and CD47 differentially modulate T cell behavior. *The Journal of cell biology*. 157:509-519.

Li, Z.W., and W.S. Dalton. 2006. Tumor microenvironment and drug resistance in hematologic malignancies. *Blood reviews*. 20:333-342.

Lim, C.J., J. Han, N. Yousefi, Y. Ma, P.S. Amieux, G.S. McKnight, S.S. Taylor, and M.H. Ginsberg. 2007. α4 Integrins are type I cAMP-dependent protein kinase-anchoring proteins. *Nature cell biology*. 9:415-421.

Lim, C.J., G.B. Spiegelman, and G. Weeks. 2001. RasC is required for optimal activation of adenylyl cyclase and Akt/PKB during aggregation. *Embo J*. 20:4490-4499.

Liu, C., P. Leclair, M. Monajemi, L. Sly, G. Reid, and C. Lim. 2016. α-Integrin expression and function modulates presentation of cell surface calreticulin. *Cell death & disease*. 7:e2268.

Liu, C.C., P. Leclair, S.Q. Yap, and C.J. Lim. 2013. The membrane-proximal KXGFFKR motif of alpha-integrin mediates chemoresistance. *Mol Cell Biol*. 33:4334-4345.

Liu, P., M. Begley, W. Michowski, H. Inuzuka, M. Ginzberg, D. Gao, P. Tsou, W. Gan, A. Papa, and B.M. Kim. 2014. Cell-cycle-regulated activation of Akt kinase by phosphorylation at its carboxyl terminus. *Nature*. 508:541.

Liu, S., D.A. Calderwood, and M.H. Ginsberg. 2000. Integrin cytoplasmic domain-binding proteins. *Journal of cell science*. 113:3563-3571.

Liu, S., S.M. Thomas, D.G. Woodside, D.M. Rose, W.B. Kiosses, M. Pfaff, and M.H. Ginsberg. 1999. Binding of paxillin to alpha4 integrins modifies integrin-dependent biological responses. *Nature*. 402:676-681.

Liu, Y., N. Chattopadhyay, S. Qin, C. Szekeres, T. Vasylyeva, Z.X. Mahoney, M. Taglienti, C.M. Bates, H.A. Chapman, and J.H. Miner. 2009. Coordinate integrin and c-Met signaling regulate Wnt gene expression during epithelial morphogenesis. *Development*. 136:843-853.

López-Ceballos, P., A.D. Herrera-Reyes, D. Coombs, and G. Tanentzapf. 2016. In vivo regulation of integrin turnover by outside-in activation. *J Cell Sci*:jcs. 190256.

Lu, C., J. Takagi, and T.A. Springer. 2001. Association of the membrane proximal regions of the α and β subunit cytoplasmic domains constrains an integrin in the inactive state. *Journal of Biological Chemistry*. 276:14642-14648.

Luo, B.-H., C.V. Carman, J. Takagi, and T.A. Springer. 2005. Disrupting integrin transmembrane domain heterodimerization increases ligand binding affinity, not valency or clustering. *Proceedings of the National Academy of Sciences of the United States of America*. 102:3679-3684.

Luo, B.-H., T.A. Springer, and J. Takagi. 2004. A specific interface between integrin transmembrane helices and affinity for ligand. *PLoS Biol*. 2:e153.

Luque, A., M. Gómez, W. Puzon, Y. Takada, F. Sánchez-Madrid, and C. Cabañas. 1996. Activated Conformations of Very Late Activation Integrins Detected by a Group of Antibodies (HUTS) Specific for a Novel Regulatory Region (355425) of the Common 1 Chain. *Journal of Biological Chemistry*. 271:11067-11075.

Margolin, J.F., C.P. Steuber, and D.G. Poplack. 1997. Acute lymphoblastic leukemia. *Principles and practice of pediatric oncology*. 3:409-462.

Martins, I., O. Kepp, F. Schlemmer, S. Adjemian, M. Tailler, S. Shen, M. Michaud, L. Menger, A. Gdoura, and N. Tajeddine. 2011. Restoration of the immunogenicity of cisplatin-induced cancer cell death by endoplasmic reticulum stress. *Oncogene*. 30:1147-1158.

Matloub, Y., B. Asselin, L.C. Stork, M. Devidas, H. Sather, J. Nachman, B. Camitta, and P.S. Gaynon. 2004. Outcome of Children with T-Cell Acute Lymphoblastic Leukemia (T-ALL) and Standard Risk (SR) Features: Results of CCG-1952, CCG-1991 and POG 9404. *Blood*. 104:680-680.

Matsunaga, T., F. Fukai, S. Miura, Y. Nakane, T. Owaki, H. Kodama, M. Tanaka, T. Nagaya, R. Takimoto, T. Takayama, and Y. Niitsu. 2008. Combination therapy of an anticancer drug with the FNIII14 peptide of fibronectin effectively overcomes cell adhesion-mediated drug resistance of acute myelogenous leukemia. *Leukemia*. 22:353-360.

Matsunaga, T., N. Takemoto, T. Sato, R. Takimoto, I. Tanaka, A. Fujimi, T. Akiyama, H. Kuroda, Y. Kawano, M. Kobune, J. Kato, Y. Hirayama, S. Sakamaki, K. Kohda, K. Miyake, and Y. Niitsu. 2003. Interaction between leukemic-cell VLA-4 and stromal fibronectin is a decisive factor for minimal residual disease of acute myelogenous leukemia. *Nat Med*. 9:1158-1165.

Mattson, M.P., F.M. LaFerla, S.L. Chan, M.A. Leissring, P.N. Shepel, and J.D. Geiger. 2000. Calcium signaling in the ER: its role in neuronal plasticity and neurodegenerative disorders. *Trends in neurosciences*. 23:222-229.

Mayer, U., G. Saher, R. Fässler, A. Bornemann, F. Echtermeyer, H. von der Mark, N. Miosge, E. Pösch, and K. von der Mark. 1997. Absence of integrin α7 causes a novel form of muscular dystrophy. *Nature genetics*. 17:318-323.

McDonald, P.C., A.B. Fielding, and S. Dedhar. 2008. Integrin-linked kinase–essential roles in physiology and cancer biology. *Journal of cell science*. 121:3121-3132.

Mcmurray, R.W., H. Tang, and H. Braley-Mullen. 1996. The role of α4 integrin and intercellular adhesion molecule-1 (ICAM-1) in murine experimental autoimmune thyroiditis. *Autoimmunity*. 23:9-23.

Meads, M.B., R.A. Gatenby, and W.S. Dalton. 2009. Environment-mediated drug resistance: a major contributor to minimal residual disease. *Nat Rev Cancer*. 9:665-674.

Meads, M.B., L.A. Hazlehurst, and W.S. Dalton. 2008. The bone marrow microenvironment as a tumor sanctuary and contributor to drug resistance. *Clin Cancer Res*. 14:2519-2526.

Meijerink, J.P., E.J. Mensink, K. Wang, T.W. Sedlak, A.W. Slöetjes, T. de Witte, G. Waksman, and S.J. Korsmeyer. 1998. Hematopoietic Malignancies Demonstrate Loss-of-Function Mutations ofBAX. *Blood*. 91:2991-2997.

Menger, L., E. Vacchelli, S. Adjemian, I. Martins, Y. Ma, S. Shen, T. Yamazaki, A.Q. Sukkurwala, M. Michaud, and G. Mignot. 2012. Cardiac glycosides exert anticancer effects by inducing immunogenic cell death. *Science translational medicine*. 4:143ra199-143ra199.

Mesaeli, N., K. Nakamura, E. Zvaritch, P. Dickie, E. Dziak, K.-H. Krause, M. Opas, D.H. MacLennan, and M. Michalak. 1999. Calreticulin is essential for cardiac development. *The Journal of cell biology*. 144:857-868.

Metcalf, D.G., D.T. Moore, Y. Wu, J.M. Kielec, K. Molnar, K.G. Valentine, A.J. Wand, J.S. Bennett, and W.F. DeGrado. 2010. NMR analysis of the αIIbβ3 cytoplasmic interaction suggests a mechanism for integrin regulation. *Proceedings of the National Academy of Sciences*. 107:22481-22486.

Michalak, M., J. Groenendyk, E. Szabo, L.I. Gold, and M. Opas. 2009. Calreticulin, a multi-process calcium-buffering chaperone of the endoplasmic reticulum. *Biochemical Journal*. 417:651-666.

Michalak, M., P. Mariani, and M. Opas. 1998. Calreticulin, a multifunctional Ca2+ binding chaperone of the endoplasmic reticulum. *Biochemistry and cell biology*. 76:779-785.

Michalak, M., R. Milner, K. Burns, and M. Opas. 1992. Calreticulin. *Biochemical Journal*. 285:681.

Misquitta, C., D. Mack, and A. Grover. 1999. Sarco/endoplasmic reticulum Ca 2+(SERCA)-pumps: link to heart beats and calcium waves. *Cell calcium*. 25:277-290.

Miyake, K., K. Medina, K. Ishihara, M. Kimoto, R. Auerbach, and P.W. Kincade. 1991. A VCAM-like adhesion molecule on murine bone marrow stromal cells mediates binding of lymphocyte precursors in culture. *The Journal of cell biology*. 114:557-565.

Miyamoto, S., H. Teramoto, O.A. Coso, J.S. Gutkind, P.D. Burbelo, S.K. Akiyama, and K.M. Yamada. 1995. Integrin function: molecular hierarchies of cytoskeletal and signaling molecules. *The Journal of cell biology*. 131:791-805.

Mizuguchi, H., Z. Xu, A. Ishii-Watabe, E. Uchida, and T. Hayakawa. 2000. IRES-dependent second gene expression is significantly lower than cap-dependent first gene expression in a bicistronic vector. *Molecular Therapy*. 1:376.

Möhle, R., S. Murea, M. Kirsch, and R. Haas. 1995. Differential expression of L-selectin, VLA-4, and LFA-1 on CD34+ progenitor cells from bone marrow and peripheral blood during G-CSF-enhanced recovery. *Experimental hematology*. 23:1535-1542.

Molica, S., G. Digiesi, G. D'Arena, R. Mirabelli, A. Antenucci, L. Conti, M. Gentile, P. Musto, A. Neri, and F. Morabito. 2016. Serum levels of soluble calreticulin predict for time to first treatment in early chronic lymphocytic leukaemia. *British journal of haematology*.

Montresor, A., M. Bolomini-Vittori, L. Toffali, B. Rossi, G. Constantin, and C. Laudanna. 2013. JAK tyrosine kinases promote hierarchical activation of Rho and Rap modules of integrin activation. *The Journal of cell biology*. 203:1003-1019.

Montresor, A., L. Toffali, M. Mirenda, A. Rigo, F. Vinante, and C. Laudanna. 2015. JAK2 tyrosine kinase mediates integrin activation induced by CXCL12 in B-cell chronic lymphocytic leukemia. *Oncotarget*. 6:34245.

Mori, Y., N. Shimizu, M. Dallas, M. Niewolna, B. Story, P.J. Williams, G.R. Mundy, and T. Yoneda. 2004. Anti-α4 integrin antibody suppresses the development of multiple myeloma and associated osteoclastic osteolysis. *Blood*. 104:2149-2154.

Morini, M., M. Mottolese, N. Ferrari, F. Ghiorzo, S. Buglioni, R. Mortarini, D.M. Noonan, P.G. Natali, and A. Albini. 2000. The α3β1 integrin is associated with mammary carcinoma cell metastasis, invasion, and gelatinase B (mmp-9) activity. *International journal of cancer*. 87:336-342.

Mudry, R.E., J.E. Fortney, T. York, B.M. Hall, and L.F. Gibson. 2000. Stromal cells regulate survival of B-lineage leukemic cells during chemotherapy. *Blood*. 96:1926-1932.

Müller, U., D. Wang, S. Denda, J.J. Meneses, R.A. Pedersen, and L.F. Reichardt. 1997. Integrin α8β1 is critically important for epithelial–mesenchymal interactions during kidney morphogenesis. *Cell*. 88:603-613.

Mullighan, C.G., S. Goorha, I. Radtke, C.B. Miller, E. Coustan-Smith, J.D. Dalton, K. Girtman, S. Mathew, J. Ma, and S.B. Pounds. 2007. Genome-wide analysis of genetic alterations in acute lymphoblastic leukaemia. *Nature*. 446:758-764.

Mullighan, C.G., J. Zhang, R.C. Harvey, J.R. Collins-Underwood, B.A. Schulman, L.A. Phillips, S.K. Tasian, M.L. Loh, X. Su, and W. Liu. 2009. JAK mutations in high-risk childhood acute lymphoblastic leukemia. *Proceedings of the National Academy of Sciences*. 106:9414-9418.

MUÑOZ, M., J. SERRADOR, M. NIETO, A. LUQUE, F. SÁNCHEZ-MADRID, and J. TEIXIDÓ. 1997. A novel region of the α4 integrin subunit with a modulatory role in VLA-4-mediated cell adhesion to fibronectin. *Biochemical Journal*. 327:727-733.

Munro, S., and H.R. Pelham. 1987. A C-terminal signal prevents secretion of luminal ER proteins. *Cell*. 48:899-907.

Murray, P.J. 2007. The JAK-STAT signaling pathway: input and output integration. *The Journal of Immunology*. 178:2623-2629.

Naci, D., M.-A. El Azreq, N. Chetoui, L. Lauden, F. Sigaux, D. Charron, R. Al-Daccak, and F. Aoudjit. 2012. α2β1 integrin promotes chemoresistance against doxorubicin in cancer cells through extracellular signal-regulated kinase (ERK). *Journal of Biological Chemistry*. 287:17065-17076.

Nakajima, K., Y. Yamanaka, K. Nakae, H. Kojima, M. Ichiba, N. Kiuchi, T. Kitaoka, T. Fukada, M. Hibi, and T. Hirano. 1996. A central role for Stat3 in IL-6-induced regulation of growth and differentiation in M1 leukemia cells. *The EMBO journal*. 15:3651.

Nakamura, K., E. Bossy-Wetzel, K. Burns, M.P. Fadel, M. Lozyk, I.S. Goping, M. Opas, R.C. Bleackley, D.R. Green, and M. Michalak. 2000. Changes in endoplasmic reticulum luminal environment affect cell sensitivity to apoptosis. *J Cell Biol*. 150:731-740.

Nakamura, K., A. Zuppini, S. Arnaudeau, J. Lynch, I. Ahsan, R. Krause, S. Papp, H. De Smedt, J.B. Parys, and W. Müller-Esterl. 2001. Functional specialization of calreticulin domains. *The Journal of cell biology*. 154:961-972.

Nakhasi, H., G. Pogue, R. Duncan, M. Joshi, C. Atreya, N. Lee, and D. Dwyer. 1998. Implications of calreticulin function in parasite biology. *Parasitology Today*. 14:157-160.

Nangalia, J., C.E. Massie, E.J. Baxter, F.L. Nice, G. Gundem, D.C. Wedge, E. Avezov, J. Li, K. Kollmann, and D.G. Kent. 2013. Somatic CALR mutations in myeloproliferative neoplasms with nonmutated JAK2. *New England Journal of Medicine*. 369:2391-2405.

Nanney, L.B., C.D. Woodrell, M.R. Greives, N.L. Cardwell, A.C. Pollins, T.A. Bancroft, A. Chesser, M. Michalak, M. Rahman, and J.W. Siebert. 2008. Calreticulin enhances porcine wound repair by diverse biological effects. *The American journal of pathology*. 173:610-630.

Nash, P.D., M. Opas, and M. Michalak. 1994. Calreticulin: not just another calcium-binding protein. *Molecular and cellular biochemistry*. 135:71-78.

Nevo, J., A. Mai, S. Tuomi, T. Pellinen, O.T. Pentikainen, P. Heikkila, J. Lundin, H. Joensuu, P. Bono, and J. Ivaska. 2010. Mammary-derived growth inhibitor (MDGI) interacts with integrin alpha-subunits and suppresses integrin activity and invasion. *Oncogene*. 29:6452-6463.

Nguyen, K., M. Devidas, S.-C. Cheng, M. La, E.A. Raetz, W.L. Carroll, N.J. Winick, S.P. Hunger, P.S. Gaynon, and M.L. Loh. 2008. Factors influencing survival after relapse from acute lymphoblastic leukemia: a Children's Oncology Group study. *Leukemia*. 22:2142-2150.

Ni, M., W. Wei, Y. Wang, N. Zhang, H. Ding, C. Shen, and F. Zheng. 2013. Serum levels of calreticulin in correlation with disease activity in patients with rheumatoid arthritis. *Journal of clinical immunology*. 33:947-953.

Nicholson-Fish, J.C., M.A. Cousin, and K.J. Smillie. 2016. Phosphatidylinositol 3-Kinase Couples Localised Calcium Influx to Activation of Akt in Central Nerve Terminals. *Neurochemical research*. 41:534-543.

Nilsson, A., L. Vesterlund, and P.-A. Oldenborg. 2012. Macrophage expression of LRP1, a receptor for apoptotic cells and unopsonized erythrocytes, can be regulated by glucocorticoids. *Biochemical and biophysical research communications*. 417:1304-1309.

Nojima, Y., M.J. Humphries, A. Mould, A. Komoriya, K. Yamada, S. Schlossman, and C. Morimoto. 1990. VLA-4 mediates CD3-dependent CD4+ T cell activation via the CS1 alternatively spliced domain of fibronectin. *The Journal of experimental medicine*. 172:1185-1192.

O'toole, T.E., Y. Katagiri, R.J. Faull, K. Peter, R. Tamura, V. Quaranta, J.C. Loftus, S.J. Shattil, and M.H. Ginsberg. 1994. Integrin cytoplasmic domains mediate inside-out signal transduction. *The Journal of cell biology*. 124:1047-1059.

O'Regan, A.W., J.M. Hayden, and J.S. Berman. 2000. Osteopontin augments CD3-mediated interferon-γ and CD40 ligand expression by T cells, which results in IL-12 production from peripheral blood mononuclear cells. *Journal of leukocyte biology*. 68:495-502.

Obeid, M. 2008. ERP57 membrane translocation dictates the immunogenicity of tumor cell death by controlling the membrane translocation of calreticulin. *J Immunol*. 181:2533-2543.

Obeid, M., A. Tesniere, F. Ghiringhelli, G.M. Fimia, L. Apetoh, J.L. Perfettini, M. Castedo, G. Mignot, T. Panaretakis, N. Casares, D. Metivier, N. Larochette, P. van Endert, F. Ciccosanti, M. Piacentini, L. Zitvogel, and G. Kroemer. 2007. Calreticulin exposure dictates the immunogenicity of cancer cell death. *Nat Med*. 13:54-61.

Octavia, Y., C.G. Tocchetti, K.L. Gabrielson, S. Janssens, H.J. Crijns, and A.L. Moens. 2012. Doxorubicin-induced cardiomyopathy: from molecular mechanisms to therapeutic strategies. *Journal of molecular and cellular cardiology*. 52:1213-1225.

Onciu, M. 2009. Acute lymphoblastic leukemia. *Hematology/oncology clinics of North America*. 23:655-674.

Opas, M., E. Dziak, L. Fliegel, and M. Michalak. 1991. Regulation of expression and intracellular distribution of calreticulin, a major calcium binding protein of nonmuscle cells. *Journal of cellular physiology*. 149:160-171.

Opas, M., M. Szewczenko-Pawlikowski, G.K. Jass, N. Mesaeli, and M. Michalak. 1996. Calreticulin modulates cell adhesiveness via regulation of vinculin expression. *The Journal of cell biology*. 135:1913-1923.

Oshita, F., Y. Kameda, N. Hamanaka, H. Saito, K. Yamada, K. Noda, and A. Mitsuda. 2004. High Expression of Integrin [beta] 1 and p53 is a Greater Poor Prognostic Factor Than Clinical Stage in Small-Cell Lung Cancer. *American journal of clinical oncology*. 27:215-219.

Païdassi, H., P. Tacnet-Delorme, M. Verneret, C. Gaboriaud, G. Houen, K. Duus, W.L. Ling, G.J. Arlaud, and P. Frachet. 2011. Investigations on the C1q–calreticulin–phosphatidylserine interactions yield new insights into apoptotic cell recognition. *Journal of molecular biology*. 408:277-290.

Pakakasama, S., G. Veerakul, D. Sosothikul, S.-o. Chainansamit, V. Laosombat, P. Thanarattanakorn, R. Lumkul, S. Wiangnon, S. Wangruangsathit, and N. Narkbunnam. 2010. Late effects in survivors of childhood acute lymphoblastic leukemia: a study from Thai Pediatric Oncology Group. *International journal of hematology*. 91:850-854.

Palazzo, A.F., C.H. Eng, D.D. Schlaepfer, E.E. Marcantonio, and G.G. Gundersen. 2004. Localized stabilization of microtubules by integrin-and FAK-facilitated Rho signaling. *Science*. 303:836-839.

Pallero, M.A., C.A. Elzie, J. Chen, D.F. Mosher, and J.E. Murphy-Ullrich. 2008. Thrombospondin 1 binding to calreticulin-LRP1 signals resistance to anoikis. *Faseb J*. 22:3968-3979.

Panaretakis, T., N. Joza, N. Modjtahedi, A. Tesniere, I. Vitale, M. Durchschlag, G. Fimia, O. Kepp, M. Piacentini, and K. Froehlich. 2008. The co-translocation of ERp57 and calreticulin determines the immunogenicity of cell death. *Cell Death & Differentiation*. 15:1499-1509.

Panaretakis, T., O. Kepp, U. Brockmeier, A. Tesniere, A.C. Bjorklund, D.C. Chapman, M. Durchschlag, N. Joza, G. Pierron, and P. van Endert. 2009. Mechanisms of pre-apoptotic calreticulin exposure in immunogenic cell death. *The EMBO journal*. 28:578-590.

Papaemmanuil, E., I. Rapado, Y. Li, N.E. Potter, D.C. Wedge, J. Tubio, L.B. Alexandrov, P. Van Loo, S.L. Cooke, and J. Marshall. 2014. RAG-mediated recombination is the predominant driver of oncogenic rearrangement in ETV6-RUNX1 acute lymphoblastic leukemia. *Nature genetics*. 46:116-125.

Papp, S., M.P. Fadel, H. Kim, C.A. McCulloch, and M. Opas. 2007. Calreticulin affects fibronectin-based cell-substratum adhesion via the regulation of c-Src activity. *Journal of Biological Chemistry*. 282:16585-16598.

Park, K.D. 2014. How do we prepare ourselves for a new paradigm of medicine to advance the treatment of pediatric acute lymphoblastic leukemia? *Blood research*. 49:3-4.

Partridge, A.W., S. Liu, S. Kim, J.U. Bowie, and M.H. Ginsberg. 2005. Transmembrane domain helix packing stabilizes integrin αIIbβ3 in the low affinity state. *Journal of Biological Chemistry*. 280:7294-7300.

Peterson, J., A. Ora, P.N. Van, and A. Helenius. 1995. Transient, lectin-like association of calreticulin with folding intermediates of cellular and viral glycoproteins. *Molecular biology of the cell*. 6:1173-1184.

Petty, J.M., C.C. Lenox, D.J. Weiss, M.E. Poynter, and B.T. Suratt. 2009. Crosstalk between CXCR4/stromal derived factor-1 and VLA-4/VCAM-1 pathways regulates neutrophil retention in the bone marrow. *The Journal of Immunology*. 182:604-612.

Pikman, Y., B.H. Lee, T. Mercher, E. McDowell, B.L. Ebert, M. Gozo, A. Cuker, G. Wernig, S. Moore, and I. Galinsky. 2006. MPLW515L is a novel somatic activating mutation in myelofibrosis with myeloid metaplasia. *PLoS Med*. 3:e270.

Platanias, L.C. 2005. Mechanisms of type-I-and type-II-interferon-mediated signalling. *Nature Reviews Immunology*. 5:375-386.

Postigo, A.A., P. Sanchez-Mateos, A. Lazarovits, F. Sanchez-Madrid, and M. De Landazuri. 1993. Alpha 4 beta 7 integrin mediates B cell binding to fibronectin and vascular cell adhesion molecule-1. Expression and function of alpha 4 integrins on human B lymphocytes. *The Journal of Immunology*. 151:2471-2483.

Pouwels, J., N. De Franceschi, P. Rantakari, K. Auvinen, M. Karikoski, E. Mattila, C. Potter, J.P. Sundberg, N. Hogg, and C.G. Gahmberg. 2013. SHARPIN regulates uropod detachment in migrating lymphocytes. *Cell reports*. 5:619-628.

Pribila, J.T., A.C. Quale, K.L. Mueller, and Y. Shimizu. 2004. Integrins and T cell-mediated immunity. *Annu. Rev. Immunol.* 22:157-180.

Prokop, A., T. Wieder, I. Sturm, F. Eβmann, K. Seeger, C. Wuchter, W. Ludwig, G. Henze, B. Dörken, and P. Daniel. 2000. Relapse in childhood acute lymphoblastic leukemia is associated with a decrease of the Bax/Bcl-2 ratio and loss of spontaneous caspase-3 processing in vivo. *Leukemia (08876924)*. 14.

Pui, C.H., M.V. Relling, and J.R. Downing. 2004. Acute lymphoblastic leukemia. *N Engl J Med*. 350:1535-1548.

Rabb, H., R. Olivenstein, T. Issekutz, P. Renzi, and J. Martin. 1994. The role of the leukocyte adhesion molecules VLA-4, LFA-1, and Mac-1 in allergic airway responses in the rat. *American journal of respiratory and critical care medicine*. 149:1186-1191.

Raghavan, M., S.J. Wijeyesakere, L.R. Peters, and N. Del Cid. 2013. Calreticulin in the immune system: ins and outs. *Trends in immunology*. 34:13-21.

Rahimi, H., K. Maurer, L. Song, E. Akhter, M. Petri, and K. Sullivan. 2013. Aberrant regulation of the integrin very late antigen-4 in systemic lupus erythematosus. *Lupus*. 22:297-306.

Rallis, C., S.M. Pinchin, and D. Ish-Horowicz. 2010. Cell-autonomous integrin control of Wnt and Notch signalling during somitogenesis. *Development*. 137:3591-3601.

Ramos, J.W., and D.W. DeSimone. 1996. Xenopus embryonic cell adhesion to fibronectin: position-specific activation of RGD/synergy site-dependent migratory behavior at gastrulation. *J Cell Biol*. 134:227-240.

Rantala, J.K., J. Pouwels, T. Pellinen, S. Veltel, P. Laasola, E. Mattila, C.S. Potter, T. Duffy, J.P. Sundberg, and O. Kallioniemi. 2011. SHARPIN is an endogenous inhibitor of [beta] 1-integrin activation. *Nature cell biology*. 13:1315-1324.

Rawlings, J.S., K.M. Rosler, and D.A. Harrison. 2004. The JAK/STAT signaling pathway. *Journal of cell science*. 117:1281-1283.

Real, P.J., A. Sierra, A. de Juan, J.C. Segovia, J.M. Lopez-Vega, and J.L. Fernandez-Luna. 2002. Resistance to chemotherapy via Stat3-dependent overexpression of Bcl-2 in metastatic breast cancer cells. *Oncogene*. 21:7611-7618.

Ren, B., G. Zou, Y. Huang, G. Xu, F. Xu, J. He, H. Zhu, and P. Yu. 2016. Serum levels of HSP70 and other DAMP proteins can aid in patient diagnosis after traumatic injury. *Cell Stress and Chaperones*:1-10.

Restrepo, I., C.S. Ortiz, and J. Camacho. 2012. Mechanisms of Therapy Resistance in Cancer. *Molecular Oncology Principles and Recent Advances*:192.

Rivera Rosado, L.A., T.A. Horn, S.C. McGrath, R.J. Cotter, and J.T. Yang. 2011. Association between alpha4 integrin cytoplasmic tail and non-muscle myosin IIA regulates cell migration. *J Cell Sci*. 124:483-492.

Robert, J., A. Ménoret, and N. Cohen. 1999. Cell surface expression of the endoplasmic reticular heat shock protein gp96 is phylogenetically conserved. *The Journal of Immunology*. 163:4133-4139.

Roderick, H.L., and S.J. Cook. 2008. Ca2+ signalling checkpoints in cancer: remodelling Ca2+ for cancer cell proliferation and survival. *Nature Reviews Cancer*. 8:361-375.

Rojiani, M.V., B.B. Finlay, V. Gray, and S. Dedhar. 1991. In vitro interaction of a polypeptide homologous to human Ro/SS-A antigen (calreticulin) with a highly conserved amino acid sequence in the cytoplasmic domain of integrin alpha subunits. *Biochemistry*. 30:9859-9866.

Romzek, N.C., E.S. Harris, C.L. Dell, J. Skronek, E. Hasse, P.J. Reynolds, S.W. Hunt, and Y. Shimizu. 1998. Use of a β1 integrin-deficient human T cell to identify β1 integrin cytoplasmic domain sequences critical for integrin function. *Molecular biology of the cell*. 9:2715-2727.

Rose, D.M., S. Liu, D.G. Woodside, J. Han, D.D. Schlaepfer, and M.H. Ginsberg. 2003. Paxillin binding to the alpha 4 integrin subunit stimulates LFA-1 (integrin alpha L beta 2)-dependent T cell migration by augmenting the activation of focal adhesion kinase/proline-rich tyrosine kinase-2. *J Immunol*. 170:5912-5918.

Roy, A., G. Ganesh, H. Sippola, S. Bolin, O. Sawesi, A. Dagälv, S.M. Schlenner, T. Feyerabend, H.-R. Rodewald, and L. Kjellén. 2014. Mast cell chymase degrades the alarmins heat shock protein 70, biglycan, HMGB1, and interleukin-33 (IL-33) and limits danger-induced inflammation. *Journal of Biological Chemistry*. 289:237-250.

Rumi, E., D. Pietra, P. Guglielmelli, R. Bordoni, I. Casetti, C. Milanesi, E. Sant'Antonio, V. Ferretti, A. Pancrazzi, and G. Rotunno. 2013. Acquired copy-neutral loss of heterozygosity of chromosome 1p as a molecular event associated with marrow fibrosis in MPL-mutated myeloproliferative neoplasms. *Blood*. 121:4388-4395.

Sambrooks, C.L., M.A. Carpio, and M.E. Hallak. 2012. Arginylated calreticulin at plasma membrane increases susceptibility of cells to apoptosis. *Journal of Biological Chemistry*. 287:22043-22054.

Sanchez, D., L. Tučková, P. Šebo, M. Michalak, A. Whelan, I. Šterzl, L. Jelınkova, E. Havrdova, M. Imramovska, and Z. Beneš. 2000. Occurrence of IgA and IgG autoantibodies to calreticulin in coeliac disease and various autoimmune diseases. *Journal of autoimmunity*. 15:441-449.

Sanderson, M.J., A.C. Charles, S. Boitano, and E.R. Dirksen. 1994. Mechanisms and function of intercellular calcium signaling. *Molecular and cellular endocrinology*. 98:173-187.

Sastry, S.K., and A.F. Horwitz. 1993. Integrin cytoplasmic domains: mediators of cytoskeletal linkages and extra-and intracellular initiated transmembrane signaling. *Current opinion in cell biology*. 5:819-831.

Sauk, J.J., K. Norris, C. Hebert, J. Ordónˆtez, and M. Reynolds. 1998. Hsp47 binds to the KDEL receptor and cell surface expression is modulated by cytoplasmic and endosomal pH. *Connective tissue research*. 37:105-119.

Schiavoni, G., A. Sistigu, M. Valentini, F. Mattei, P. Sestili, F. Spadaro, M. Sanchez, S. Lorenzi, M.T. D'Urso, and F. Belardelli. 2011. Cyclophosphamide synergizes with type I interferons through systemic dendritic cell reactivation and induction of immunogenic tumor apoptosis. *Cancer research*. 71:768-778.

Schinkel, A.H., and J.W. Jonker. 2003. Mammalian drug efflux transporters of the ATP binding cassette (ABC) family: an overview. *Advanced drug delivery reviews*. 55:3-29.

Schmidmaier, R., and P. Baumann. 2008. ANTI-ADHESION evolves to a promising therapeutic concept in oncology. *Current medicinal chemistry*. 15:978-990.

Schneider, U., H.U. Schwenk, and G. Bornkamm. 1977. Characterization of EBV-genome negative "null" and "T" cell lines derived from children with acute lymphoblastic leukemia and leukemic transformed non-Hodgkin lymphoma. *International journal of cancer*. 19:621-626.

Schrag, J.D., J.J. Bergeron, Y. Li, S. Borisova, M. Hahn, D.Y. Thomas, and M. Cygler. 2001. The structure of calnexin, an ER chaperone involved in quality control of protein folding. *Molecular cell*. 8:633-644.

Schultz, K., A. Carroll, N. Heerema, W. Bowman, A. Aledo, W. Slayton, H. Sather, M. Devidas, H. Zheng, and S. Davies. 2014. Long-term follow-up of imatinib in pediatric Philadelphia chromosome-positive acute lymphoblastic leukemia: Children's Oncology Group study AALL0031. *Leukemia*. 28:1467-1471.

Schultz, K.R., W.P. Bowman, A. Aledo, W.B. Slayton, H. Sather, M. Devidas, C. Wang, S.M. Davies, P.S. Gaynon, and M. Trigg. 2009. Improved early event-free survival with imatinib in Philadelphia chromosome–positive acute lymphoblastic leukemia: A Children's Oncology Group study. *Journal of clinical oncology*. 27:5175-5181.

Schultz, K.R., D.J. Pullen, H.N. Sather, J.J. Shuster, M. Devidas, M.J. Borowitz, A.J. Carroll, N.A. Heerema, J.E. Rubnitz, M.L. Loh, E.A. Raetz, N.J. Winick, S.P. Hunger, W.L. Carroll, P.S. Gaynon, and B.M. Camitta. 2007. Risk- and response-based classification of childhood B-precursor acute lymphoblastic leukemia: a combined analysis of prognostic markers from the Pediatric Oncology Group (POG) and Children's Cancer Group (CCG). *Blood*. 109:926-935.

Scott, L.M., G.V. Priestley, and T. Papayannopoulou. 2003. Deletion of α4 integrins from adult hematopoietic cells reveals roles in homeostasis, regeneration, and homing. *Molecular and cellular biology*. 23:9349-9360.

Seiffge, D. 1996. Protective effects of monoclonal antibody to VLA-4 on leukocyte adhesion and course of disease in adjuvant arthritis in rats. *The Journal of rheumatology*. 23:2086-2091.

Sethi, T., R.C. Rintoul, S.M. Moore, A.C. MacKinnon, D. Salter, C. Choo, E.R. Chilvers, I. Dransfield, S.C. Donnelly, R. Strieter, and C. Haslett. 1999. Extracellular matrix proteins protect small cell lung cancer cells against apoptosis: a mechanism for small cell lung cancer growth and drug resistance in vivo. *Nat Med*. 5:662-668.

Sexl, V., R. Piekorz, R. Moriggl, J. Rohrer, M.P. Brown, K.D. Bunting, K. Rothammer, M.F. Roussel, and J.N. Ihle. 2000. Stat5a/b contribute to interleukin 7–induced B-cell precursor expansion, but abl-andbcr/abl-induced transformation are independent of Stat5. *Blood*. 96:2277-2283.

Shaffer, K.L., A. Sharma, E.L. Snapp, and R.S. Hegde. 2005. Regulation of protein compartmentalization expands the diversity of protein function. *Developmental cell*. 9:545-554.
Shain, K.H., D.N. Yarde, M.B. Meads, M. Huang, R. Jove, L.A. Hazlehurst, and W.S. Dalton. 2009. Beta1 integrin adhesion enhances IL-6-mediated STAT3 signaling in myeloma cells: implications for microenvironment influence on tumor survival and proliferation. *Cancer Res*. 69:1009-1015.
Shalapour, S., J. Hof, R. Kirschner-Schwabe, L. Bastian, C. Eckert, J. Prada, G. Henze, A. von Stackelberg, and K. Seeger. 2011. High VLA-4 expression is associated with adverse outcome and distinct gene expression changes in childhood B-cell precursor acute lymphoblastic leukemia at first relapse. *Haematologica*:haematol. 2011.047993.
Shattil, S.J. 1999. Signaling through platelet integrin aIIbb3: Inside-out, outside-in, and sideways. *Thrombosis and haemostasis*. 82:318-325.
Shattil, S.J., H. Kashiwagi, and N. Pampori. 1998. Integrin signaling: the platelet paradigm. *Blood*. 91:2645-2657.
Shattil, S.J., C. Kim, and M.H. Ginsberg. 2010. The final steps of integrin activation: the end game. *Nat Rev Mol Cell Biol*. 11:288-300.
Shen, B., M.K. Delaney, and X. Du. 2012. Inside-out, outside-in, and inside–outside-in: G protein signaling in integrin-mediated cell adhesion, spreading, and retraction. *Current opinion in cell biology*. 24:600-606.
Shen, H.X., Z.F. Xia, and Y.L. Chen. 1998. [Calreticulin, a calcium binding protein]. *Sheng li ke xue jin zhan [Progress in physiology]*. 29:158-160.
Shimizu, Y., G. Van Seventer, K. Horgan, and S. Shaw. 1990. Costimulation of proliferative responses of resting CD4+ T cells by the interaction of VLA-4 and VLA-5 with fibronectin or VLA-6 with laminin. *The Journal of Immunology*. 145:59-67.
Shuai, K., J. Halpern, J. Ten Hoeve, X. Rao, and C.L. Sawyers. 1996. Constitutive activation of STAT5 by the BCR-ABL oncogene in chronic myelogenous leukemia. *Oncogene*. 13:247-254.
Simpson, C.D., K. Anyiwe, and A.D. Schimmer. 2008. Anoikis resistance and tumor metastasis. *Cancer letters*. 272:177-185.
Sirvent, N., S. Suciu, X. Rialland, F. Millot, Y. Benoit, D. Plantaz, A. Ferster, A. Robert, P. Lutz, and B. Nelken. 2011. Prognostic significance of the initial cerebro-spinal fluid (CSF) involvement of children with acute lymphoblastic leukaemia (ALL) treated without cranial irradiation: results of European Organization for Research and Treatment of Cancer (EORTC) Children Leukemia Group study 58881. *European journal of cancer*. 47:239-247.
Sjaastad, M.D., and W.J. Nelson. 1997. Integrin-mediated calcium signaling and regulation of cell adhesion by intracellular calcium. *Bioessays*. 19:47-55.
Smith, J.W., R.S. Piotrowicz, and D. Mathis. 1994. A mechanism for divalent cation regulation of beta 3-integrins. *Journal of Biological Chemistry*. 269:960-967.
Smith, M.A., S.F. Altekruse, P.C. Adamson, G.H. Reaman, and N.L. Seibel. 2014. Declining childhood and adolescent cancer mortality. *Cancer*. 120:2497-2506.
Smith, M.J., and G. Koch. 1989. Multiple zones in the sequence of calreticulin (CRP55, calregulin, HACBP), a major calcium binding ER/SR protein. *The EMBO journal*. 8:3581.
Song, G., G. Ouyang, and S. Bao. 2005. The activation of Akt/PKB signaling pathway and cell survival. *Journal of cellular and molecular medicine*. 9:59-71.

Spiro, R.G., Q. Zhu, V. Bhoyroo, and H.-D. Söling. 1996. Definition of the lectin-like properties of the molecular chaperone, calreticulin, and demonstration of its copurification with endomannosidase from rat liver Golgi. *Journal of Biological Chemistry*. 271:11588-11594.
Spisek, R., A. Charalambous, A. Mazumder, D.H. Vesole, S. Jagannath, and M.V. Dhodapkar. 2007. Bortezomib enhances dendritic cell (DC)–mediated induction of immunity to human myeloma via exposure of cell surface heat shock protein 90 on dying tumor cells: therapeutic implications. *Blood*. 109:4839-4845.
Spisek, R., and M. Dhodapkar. 2007. Towards a better way to die with chemotherapy: role of heat shock protein exposure on dying tumor cells. *Cell Cycle*. 6:1962-1965.
Springer, T.A. 1994. Traffic signals for lymphocyte recirculation and leukocyte emigration: the multistep paradigm. *Cell*. 76:301-314.
Srichai, M.B., and R. Zent. 2010. Integrin structure and function. *In* Cell-Extracellular Matrix Interactions in Cancer. Springer. 19-41.
Stephens, L.E., A.E. Sutherland, I.V. Klimanskaya, A. Andrieux, J. Meneses, R.A. Pedersen, and C.H. Damsky. 1995. Deletion of beta 1 integrins in mice results in inner cell mass failure and peri-implantation lethality. *Genes & development*. 9:1883-1895.
Strauch, U.G., A. Lifka, U. Goßiar, P.J. Kilshaw, J. Clements, and B. Holzmann. 1994. Distinct binding specificities of integrins α4β7 (LPAM-1), α4β1 (VLA-4), and αIELβ7. *International immunology*. 6:263-275.
Streuli, C.H., and N. Akhtar. 2009. Signal co-operation between integrins and other receptor systems. *Biochemical Journal*. 418:491-506.
Su, Y., W. Xia, J. Li, T. Walz, M.J. Humphries, D. Vestweber, C. Cabañas, C. Lu, and T.A. Springer. 2016. Relating conformation to function in integrin α5β1. *Proceedings of the National Academy of Sciences*. 113:E3872-E3881.
Sulova, Z., M. Seres, M. Barancik, L. Gibalova, B. Uhrik, L. Polekova, and A. Breier. 2009. Does any relationship exist between P-glycoprotein-mediated multidrug resistance and intracellular calcium homeostasis. *General physiology and biophysics*. 28 Spec No Focus:F89-95.
Szabo, E., S. Papp, and M. Opas. 2007. Differential calreticulin expression affects focal contacts via the calmodulin/CaMK II pathway. *Journal of cellular physiology*. 213:269-277.
Tadokoro, S., S.J. Shattil, K. Eto, V. Tai, R.C. Liddington, J.M. De Pereda, M.H. Ginsberg, and D.A. Calderwood. 2003. Talin binding to integrin ß tails: a final common step in integrin activation. *Science*. 302:103-106.
Takagi, J., B.M. Petre, T. Walz, and T.A. Springer. 2002. Global conformational rearrangements in integrin extracellular domains in outside-in and inside-out signaling. *Cell*. 110:599-611.
Tarr, J.M., P.G. Winyard, B. Ryan, L.W. Harries, R. Haigh, N. Viner, and P. Eggleton. 2010a. Extracellular calreticulin is present in the joints of patients with rheumatoid arthritis and inhibits FasL (CD95L)–mediated apoptosis of T cells. *Arthritis & Rheumatism*. 62:2919-2929.
Tarr, J.M., P.J. Young, R. Morse, D.J. Shaw, R. Haigh, P.G. Petrov, S.J. Johnson, P.G. Winyard, and P. Eggleton. 2010b. A mechanism of release of calreticulin from cells during apoptosis. *Journal of molecular biology*. 401:799-812.
te Loo, D.M.W., W.A. Kamps, E.R. van Wering, and S.S. de Graaf. 2006. Prognostic significance of blasts in the cerebrospinal fluid without pleiocytosis or a traumatic lumbar

puncture in children with acute lymphoblastic leukemia: experience of the Dutch Childhood Oncology Group. *Journal of clinical oncology*. 24:2332-2336.
Tefferi, A. 2010. Novel mutations and their functional and clinical relevance in myeloproliferative neoplasms: JAK2, MPL, TET2, ASXL1, CBL, IDH and IKZF1. *Leukemia*. 24:1128-1138.
Tesniere, A., L. Apetoh, F. Ghiringhelli, N. Joza, T. Panaretakis, O. Kepp, F. Schlemmer, L. Zitvogel, and G. Kroemer. 2008. Immunogenic cancer cell death: a key-lock paradigm. *Current opinion in immunology*. 20:504-511.
Tesniere, A., F. Schlemmer, V. Boige, O. Kepp, I. Martins, F. Ghiringhelli, L. Aymeric, M. Michaud, L. Apetoh, and L. Barault. 2010. Immunogenic death of colon cancer cells treated with oxaliplatin. *Oncogene*. 29:482-491.
Thinn, A.M.M., and J. Zhu. 2015. Structure and Sequence Diversity of the Membrane Distal Region of α-Cytoplasmic Tail in Integrin Activation. *Blood*. 126:3453-3453.
Titmarsh, G.J., A.S. Duncombe, M.F. McMullin, M. O'Rorke, R. Mesa, F. Vocht, S. Horan, L. Fritschi, M. Clarke, and L.A. Anderson. 2014. How common are myeloproliferative neoplasms? A systematic review and meta-analysis. *American Journal of Hematology*. 89:581-587.
Tran, H., R. Pankov, S.D. Tran, B. Hampton, W.H. Burgess, and K.M. Yamada. 2002. Integrin clustering induces kinectin accumulation. *Journal of cell science*. 115:2031-2040.
Trédan, O., C.M. Galmarini, K. Patel, and I.F. Tannock. 2007. Drug resistance and the solid tumor microenvironment. *Journal of the National Cancer Institute*. 99:1441-1454.
Tsai, B., Y. Ye, and T.A. Rapoport. 2002. Retro-translocation of proteins from the endoplasmic reticulum into the cytosol. *Nature Reviews Molecular Cell Biology*. 3:246-255.
Tseng, D., J.-P. Volkmer, S.B. Willingham, H. Contreras-Trujillo, J.W. Fathman, N.B. Fernhoff, J. Seita, M.A. Inlay, K. Weiskopf, and M. Miyanishi. 2013. Anti-CD47 antibody–mediated phagocytosis of cancer by macrophages primes an effective antitumor T-cell response. *Proceedings of the National Academy of Sciences*. 110:11103-11108.
Turner, C.E. 2000a. Paxillin and focal adhesion signalling. *Nature cell biology*. 2:E231-E236.
Turner, C.E. 2000b. Paxillin interactions. *Journal of cell science*. 113:4139-4140.
Ulmer, T.S., B. Yaspan, M.H. Ginsberg, and I.D. Campbell. 2001. NMR analysis of structure and dynamics of the cytosolic tails of integrin αIIbβ3 in aqueous solution. *Biochemistry*. 40:7498-7508.
Vacca, A., R. Ria, M. Presta, D. Ribatti, M. Iurlaro, F. Merchionne, E. Tanghetti, and F. Dammacco. 2001. α v β 3 integrin engagement modulates cell adhesion, proliferation, and protease secretion in human lymphoid tumor cells. *Experimental hematology*. 29:993-1003.
Van Der Neut, R., P. Krimpenfort, J. Calafat, C.M. Niessen, and A. Sonnenberg. 1996. Epithelial detachment due to absence of hemidesmosomes in integrin β4 null mice. *Nature genetics*. 13:366-369.
Van der Plas, D., F. Smiers, K. Pouwels, L. Hoefsloot, B. Löwenberg, and I. Touw. 1996. Interleukin-7 signaling in human B cell precursor acute lymphoblastic leukemia cells and murine BAF3 cells involves activation of STAT1 and STAT5 mediated via the interleukin-7 receptor alpha chain. *Leukemia*. 10:1317-1325.
van Hemert, M.J., H.Y. Steensma, and G.P.H. van Heusden. 2001. 14-3-3 proteins: key regulators of cell division, signalling and apoptosis. *Bioessays*. 23:936-946.

Vanhaesebroeck, B., and D.R. Alessi. 2000. The PI3K-PDK1 connection: more than just a road to PKB. *Biochem J*. 346 Pt 3:561-576.

Vardiman, J.W., J. Thiele, D.A. Arber, R.D. Brunning, M.J. Borowitz, A. Porwit, N.L. Harris, M.M. Le Beau, E. Hellström-Lindberg, and A. Tefferi. 2009. The 2008 revision of the World Health Organization (WHO) classification of myeloid neoplasms and acute leukemia: rationale and important changes. *Blood*. 114:937-951.

Vincent, E.E., D.J. Elder, E.C. Thomas, L. Phillips, C. Morgan, J. Pawade, M. Sohail, M.T. May, M.R. Hetzel, and J.M. Tavare. 2011. Akt phosphorylation on Thr308 but not on Ser473 correlates with Akt protein kinase activity in human non-small cell lung cancer. *British journal of cancer*. 104:1755-1761.

Vinogradova, O., A. Velyvis, A. Velyviene, B. Hu, T.A. Haas, E.F. Plow, and J. Qin. 2002. A structural mechanism of integrin α IIb β 3 "inside-out" activation as regulated by its cytoplasmic face. *Cell*. 110:587-597.

Waitkus-Edwards, K.R., L.A. Martinez-Lemus, X. Wu, J.P. Trzeciakowski, M.J. Davis, G.E. Davis, and G.A. Meininger. 2002. alpha(4)beta(1) Integrin activation of L-type calcium channels in vascular smooth muscle causes arteriole vasoconstriction. *Circulation research*. 90:473-480.

Walker, S.R., M. Xiang, and D.A. Frank. 2014. Distinct roles of STAT3 and STAT5 in the pathogenesis and targeted therapy of breast cancer. *Molecular and cellular endocrinology*. 382:616-621.

Walter, P., and A.E. Johnson. 1994. Signal sequence recognition and protein targeting to the endoplasmic reticulum membrane. *Annual review of cell biology*. 10:87-119.

Walther, R.F., C. Lamprecht, A. Ridsdale, I. Groulx, S. Lee, Y.A. Lefebvre, and R.J. Haché. 2003. Nuclear export of the glucocorticoid receptor is accelerated by cell fusion-dependent release of calreticulin. *Journal of Biological Chemistry*. 278:37858-37864.

Wang, L., J.E. Fortney, and L.F. Gibson. 2004. Stromal cell protection of B-lineage acute lymphoblastic leukemic cells during chemotherapy requires active Akt. *Leukemia research*. 28:733-742.

Wang, W.-A., J. Groenendyk, and M. Michalak. 2012. Calreticulin signaling in health and disease. *The international journal of biochemistry & cell biology*. 44:842-846.

Wang, Y., M. Yao, J. Zhou, W. Zheng, C. Zhou, D. Dong, Y. Liu, Z. Teng, Y. Jiang, and G. Wei. 2011. The promotion of neural progenitor cells proliferation by aligned and randomly oriented collagen nanofibers through β1 integrin/MAPK signaling pathway. *Biomaterials*. 32:6737-6744.

Ward, E., C. DeSantis, A. Robbins, B. Kohler, and A. Jemal. 2014. Childhood and adolescent cancer statistics, 2014. *CA: a cancer journal for clinicians*. 64:83-103.

Watanabe, N., L. Bodin, M. Pandey, M. Krause, S. Coughlin, V.A. Boussiotis, M.H. Ginsberg, and S.J. Shattil. 2008. Mechanisms and consequences of agonist-induced talin recruitment to platelet integrin alphaIIbbeta3. *J Cell Biol*. 181:1211-1222.

Watras, J., and B.E. Ehrlich. 1991. Bell-shaped calcium-response curves of lns (l, 4, 5) P3-and calcium-gated channels from endoplasmic reticulum of cerebellum.

Webb, D.J., K. Donais, L.A. Whitmore, S.M. Thomas, C.E. Turner, J.T. Parsons, and A.F. Horwitz. 2004. FAK–Src signalling through paxillin, ERK and MLCK regulates adhesion disassembly. *Nature cell biology*. 6:154-161.

Weisberg, E., Q. Liu, E. Nelson, A.L. Kung, A.L. Christie, R. Bronson, M. Sattler, T. Sanda, Z. Zhao, and W. Hur. 2012. Using combination therapy to override stromal-mediated chemoresistance in mutant FLT3-positive AML: synergism between FLT3 inhibitors, dasatinib/multi-targeted inhibitors and JAK inhibitors. *Leukemia*. 26:2233-2244.

Weismann, M., A.H. Guse, L. Sorokin, B. Broker, M. Frieser, R. Hallmann, and G.W. Mayr. 1997. Integrin-mediated intracellular Ca2+ signaling in Jurkat T lymphocytes. *J Immunol*. 158:1618-1627.

Weljie, A.M., P.M. Hwang, and H.J. Vogel. 2002. Solution structures of the cytoplasmic tail complex from platelet integrin αIIb-and β3-subunits. *Proceedings of the National Academy of Sciences*. 99:5878-5883.

West, K.A., J. Brognard, A.S. Clark, I.R. Linnoila, X. Yang, S.M. Swain, C. Harris, S. Belinsky, and P.A. Dennis. 2003. Rapid Akt activation by nicotine and a tobacco carcinogen modulates the phenotype of normal human airway epithelial cells. *The Journal of clinical investigation*. 111:81-90.

Wiersma, V.R., M. Michalak, T.M. Abdullah, E. Bremer, and P. Eggleton. 2015. Mechanisms of translocation of ER chaperones to the cell surface and immunomodulatory roles in cancer and autoimmunity. *Frontiers in oncology*. 5:7.

Wiest, D.L., A. Bhandoola, J. Punt, G. Kreibich, D. McKean, and A. Singer. 1997. Incomplete endoplasmic reticulum (ER) retention in immature thymocytes as revealed by surface expression of "ER-resident" molecular chaperones. *Proceedings of the National Academy of Sciences*. 94:1884-1889.

Willingham, S.B., J.-P. Volkmer, A.J. Gentles, D. Sahoo, P. Dalerba, S.S. Mitra, J. Wang, H. Contreras-Trujillo, R. Martin, and J.D. Cohen. 2012. The CD47-signal regulatory protein alpha (SIRPa) interaction is a therapeutic target for human solid tumors. *Proceedings of the National Academy of Sciences*. 109:6662-6667.

Wilson, D.W., M.J. Lewis, and H. Pelham. 1993. pH-dependent binding of KDEL to its receptor in vitro. *Journal of Biological Chemistry*. 268:7465-7468.

Winter, S.S., J.J. Sweatman, M.B. Lawrence, T.H. Rhoades, A.L. Hart, and R.S. Larson. 2001. Enhanced T-lineage acute lymphoblastic leukaemia cell survival on bone marrow stroma requires involvement of LFA-1 and ICAM-1. *British journal of haematology*. 115:862-871.

Wofford, J.A., H.L. Wieman, S.R. Jacobs, Y. Zhao, and J.C. Rathmell. 2008. IL-7 promotes Glut1 trafficking and glucose uptake via STAT5-mediated activation of Akt to support T-cell survival. *Blood*. 111:2101-2111.

Wu, L., J.A. Bernard-Trifilo, Y. Lim, S.-T. Lim, S.K. Mitra, S. Uryu, M. Chen, C.J. Pallen, N.-K. Cheung, and D. Mikolon. 2008. Distinct FAK-Src activation events promote α5β1 and α4β1 integrin-stimulated neuroblastoma cell motility. *Oncogene*. 27:1439-1448.

Wu, X., G.E. Davis, G.A. Meininger, E. Wilson, and M.J. Davis. 2001. Regulation of the L-type calcium channel by alpha 5beta 1 integrin requires signaling between focal adhesion proteins. *J Biol Chem*. 276:30285-30292.

Wu, X., J.E. Mogford, S.H. Platts, G.E. Davis, G.A. Meininger, and M.J. Davis. 1998. Modulation of calcium current in arteriolar smooth muscle by alphav beta3 and alpha5 beta1 integrin ligands. *J Cell Biol*. 143:241-252.

Xia, C.Q., and P.G. Smith. 2012. Drug efflux transporters and multidrug resistance in acute leukemia: therapeutic impact and novel approaches to mediation. *Mol Pharmacol*. 82:1008-1021.

Xia, H., R.S. Nho, J. Kahm, J. Kleidon, and C.A. Henke. 2004. Focal adhesion kinase is upstream of phosphatidylinositol 3-kinase/Akt in regulating fibroblast survival in response to contraction of type I collagen matrices via a beta 1 integrin viability signaling pathway. *J Biol Chem*. 279:33024-33034.

Xiong, J.-P., T. Stehle, B. Diefenbach, R. Zhang, R. Dunker, D.L. Scott, A. Joachimiak, S.L. Goodman, and M.A. Arnaout. 2001. Crystal structure of the extracellular segment of integrin αVβ3. *Science*. 294:339-345.

Xu, B., N. Wagner, L.N. Pham, V. Magno, Z. Shan, E.C. Butcher, and S.A. Michie. 2003. Lymphocyte homing to bronchus-associated lymphoid tissue (BALT) is mediated by L-selectin/PNAd, α4β1 integrin/VCAM-1, and LFA-1 adhesion pathways. *The Journal of experimental medicine*. 197:1255-1267.

Yabkowitz, R., V. Dixit, N. Guo, D. Roberts, and Y. Shimizu. 1993. Activated T-cell adhesion to thrombospondin is mediated by the alpha 4 beta 1 (VLA-4) and alpha 5 beta 1 (VLA-5) integrins. *The Journal of Immunology*. 151:149-158.

Yamakawa, N., K. Kaneda, Y. Saito, E. Ichihara, and K. Morishita. 2012. The Increased Expression of Integrin alpha6 (ITGA6) Enhances Drug Resistance in EVI1 Leukemia. *PLoS One*. 7:e30706.

Yanagisawa, M., K. Nakamura, and T. Taga. 2004. Roles of lipid rafts in integrin-dependent adhesion and gp130 signalling pathway in mouse embryonic neural precursor cells. *Genes to Cells*. 9:801-809.

Yang, J.T., H. Rayburn, and R.O. Hynes. 1993. Embryonic mesodermal defects in alpha 5 integrin-deficient mice. *Development*. 119:1093-1105.

Yang, J.T., H. Rayburn, and R.O. Hynes. 1995. Cell adhesion events mediated by alpha 4 integrins are essential in placental and cardiac development. *Development*. 121:549-560.

Yang, X.-D., S.A. Michie, R. Tisch, N. Karin, L. Steinman, and H.O. McDevitt. 1994. A predominant role of integrin alpha 4 in the spontaneous development of autoimmune diabetes in nonobese diabetic mice. *Proceedings of the National Academy of Sciences*. 91:12604-12608.

Yano, S., H. Tokumitsu, and T.R. Soderling. 1998. Calcium promotes cell survival through CaM-K kinase activation of the protein-kinase-B pathway. *Nature*. 396:584-587.

Ye, F., G. Hu, D. Taylor, B. Ratnikov, A.A. Bobkov, M.A. McLean, S.G. Sligar, K.A. Taylor, and M.H. Ginsberg. 2010. Recreation of the terminal events in physiological integrin activation. *The Journal of cell biology*. 188:157-173.

Yednock, T.A., C. Cannon, L.C. Fritz, F. Sanchez-Madrid, L. Steinman, and N. Karin. 1992. Prevention of experimental autoimmune encephalomyelitis by antibodies against α4βl integrin.

Young, S.A., K.E. McCabe, A. Bartakova, J. Delaney, D.P. Pizzo, R.O. Newbury, J.A. Varner, D.D. Schlaepfer, and D.G. Stupack. 2015. Integrin α4 Enhances Metastasis and May Be Associated with Poor Prognosis in MYCN low Neuroblastoma. *PLoS One*. 10:e0120815.

Zapun, A., N.J. Darby, D.C. Tessier, M. Michalak, J.J. Bergeron, and D.Y. Thomas. 1998. Enhanced catalysis of ribonuclease B folding by the interaction of calnexin or calreticulin with ERp57. *Journal of Biological Chemistry*. 273:6009-6012.

Zhang, Y., H. Li, Z. Lian, and N. Li. 2010. Myofibroblasts protect myoblasts from intrinsic apoptosis associated with differentiation via β1 integrin-PI3K/Akt pathway. *Development, growth & differentiation*. 52:725-733.

Zhou, M., L. Gu, F. Li, Y. Zhu, W.G. Woods, and H.W. Findley. 2002. DNA damage induces a novel p53-survivin signaling pathway regulating cell cycle and apoptosis in acute lymphoblastic leukemia cells. *Journal of Pharmacology and Experimental Therapeutics*. 303:124-131.

Zhu, J., B.-H. Luo, T. Xiao, C. Zhang, N. Nishida, and T.A. Springer. 2008. Structure of a complete integrin ectodomain in a physiologic resting state and activation and deactivation by applied forces. *Molecular cell*. 32:849-861.

Zhu, J., K. Motejlek, D. Wang, K. Zang, A. Schmidt, and L.F. Reichardt. 2002. β8 integrins are required for vascular morphogenesis in mouse embryos. *Development*. 129:2891-2903.

Zhu, N., and Z. Wang. 1999. Calreticulin expression is associated with androgen regulation of the sensitivity to calcium ionophore-induced apoptosis in LNCaP prostate cancer cells. *Cancer Res*. 59:1896-1902.

Zhu, Q., P. Zelinka, T. White, and M.L. Tanzer. 1997. Calreticulin-integrin bidirectional signaling complex. *Biochem Biophys Res Commun*. 232:354-358.

Appendices

Appendix A CRISPR-Cas9 Mediated Calreticulin Knockout

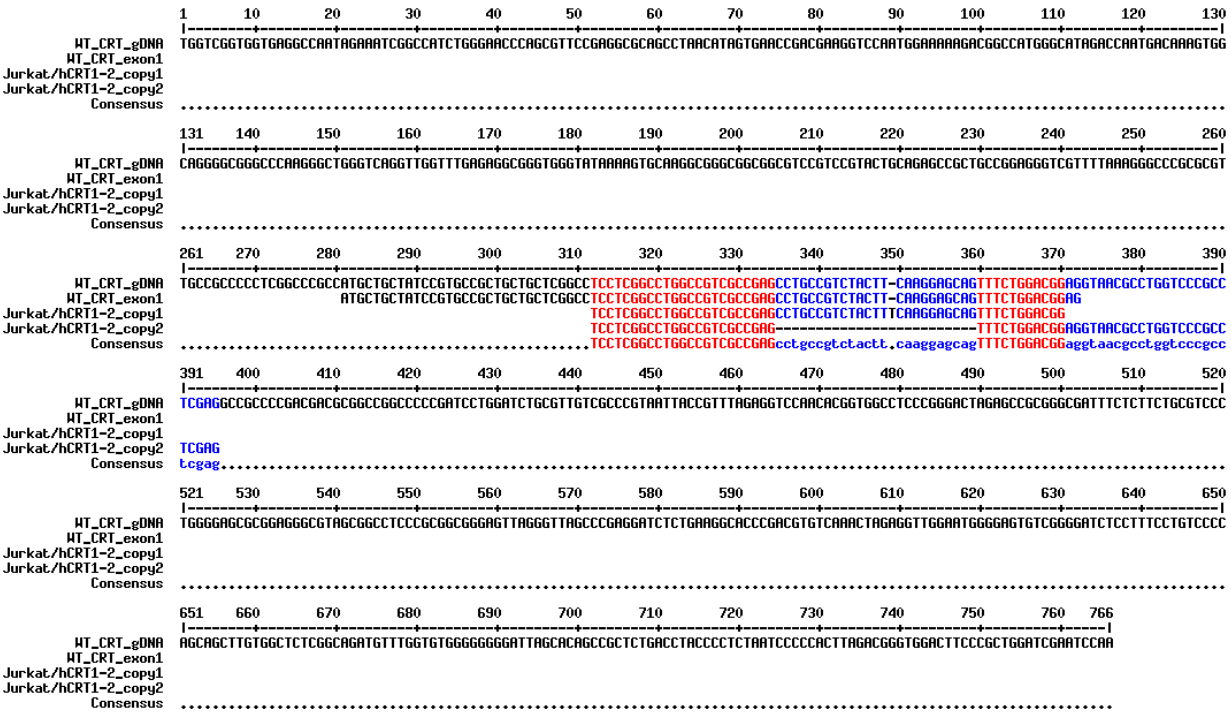

Figure A.1. CRISPR-Cas9 mediated mutation in Jurkat/hCRT1-2

Alignment analysis of Jurkat/hCRT1-2 *CALR* genomic loci sequencing result shows heterozygous mutations. *Copy 1:* Single nucleotide insertion occurs at 68 bp from the start codon and -3 bp from the PAM recognition motif. The frame shift mutated variant encodes for a predicted 58 amino acid protein product due to a premature termination codon. *Copy 2:* In frame 24 bp deletion occurs at 54 bp from the start codon.

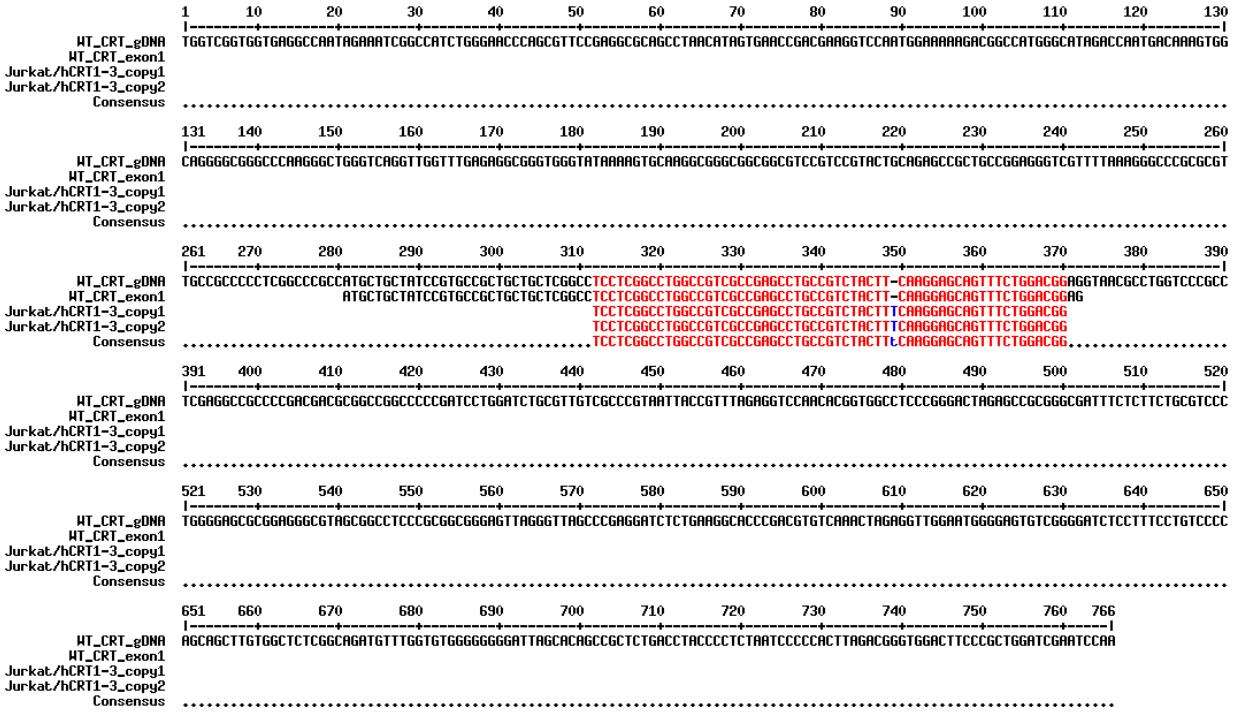

Figure A.2. CRISPR-Cas9 mediated mutation in Jurkat/hCRT1-3

Alignment analysis of Jurkat/hCRT1-3 *CALR* genomic loci sequencing result shows homozygous mutations. *Copy 1 and Copy 2:* Single nucleotide insertion occurs at 68 bp from the start codon and -3 bp from the PAM recognition motif. The frame shift mutated variant encodes for a predicted 58 amino acid protein product due to a premature termination codon. Jurkat/hCRT1-3 is referred to as $CRT^{-/-}$ in the thesis.

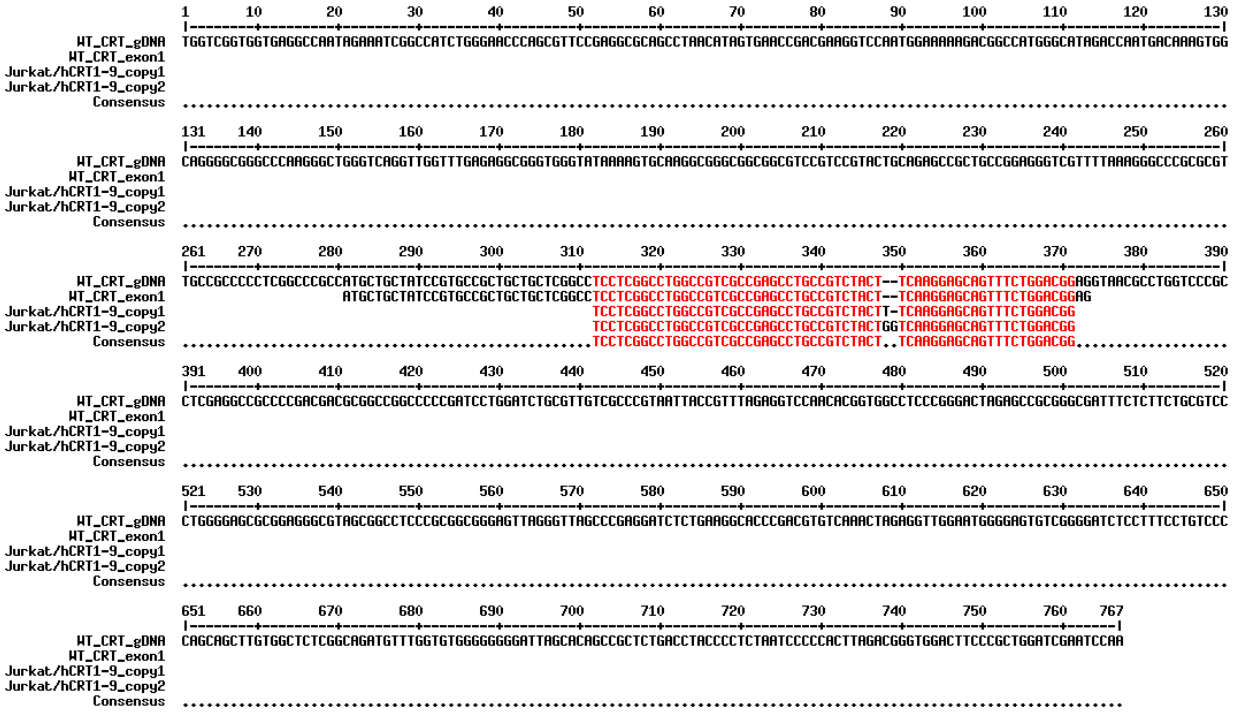

Figure A.3. CRISPR-Cas9 mediated mutation in Jurkat/hCRT1-9

Alignment analysis of Jurkat/hCRT1-9 *CALR* genomic loci sequencing result shows heterozygous mutations. *Copy 1:* Single nucleotide insertion occurs at 68 bp from the start codon and -3 bp from the PAM recognition motif. The frame shift mutated variant encodes for a predicted 58 amino acid protein product due to a premature termination codon. *Copy 2:* double nucleotide insertion occurs at 68 bp from the start codon and -3 bp from the PAM recognition motif. The frame shift mutated variant encodes for a predicted 97 amino acid protein product due to a premature termination codon.

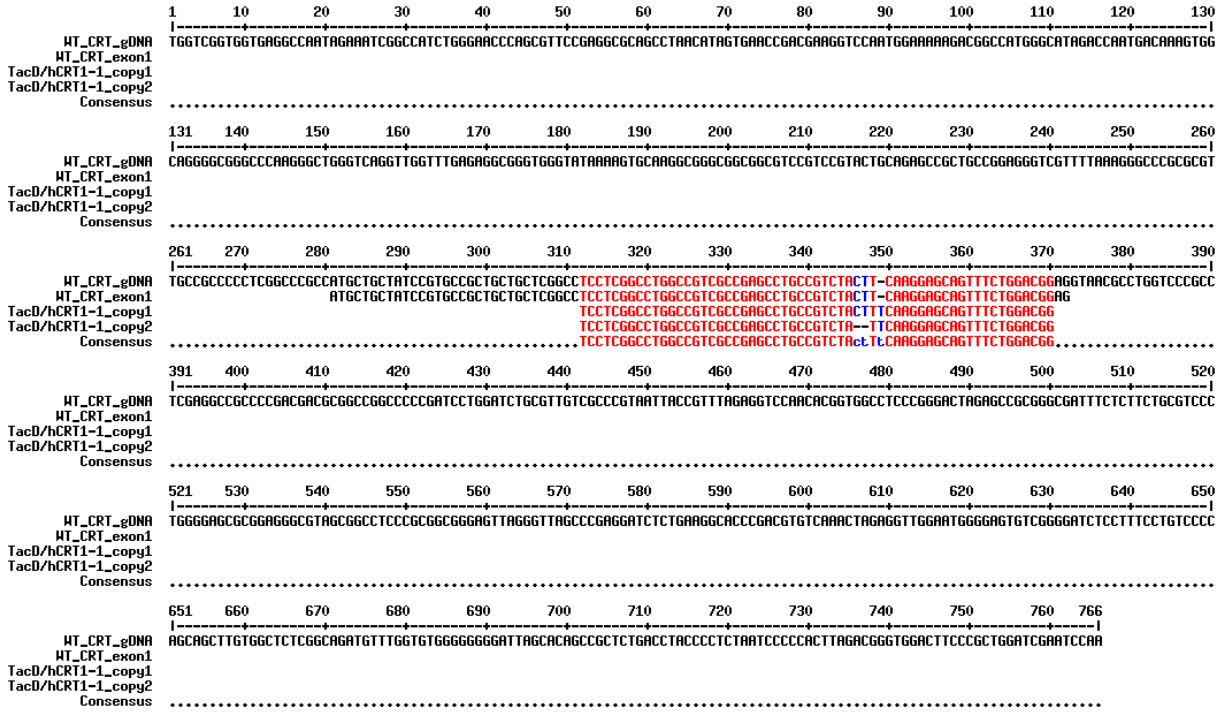

Figure A.4. CRISPR-Cas9 mediated mutation in JB4-Tacδ/hCRT1-1

Alignment analysis of JB4-Tacδ/hCRT1-1 *CALR* genomic loci sequencing result shows heterozygous mutations. *Copy 1:* Single nucleotide insertion occurs at 68 bp from the start codon and -3 bp from the PAM recognition motif. The frame shift mutated variant encodes for a predicted 58 amino acid protein product due to a premature termination codon. *Copy 2:* Single nucleotide deletion occurs at 67 bp from the start codon and -4 bp from the PAM recognition motif. The frame shift mutated variant encodes for a predicted 96 amino acid protein product due to a premature termination codon.

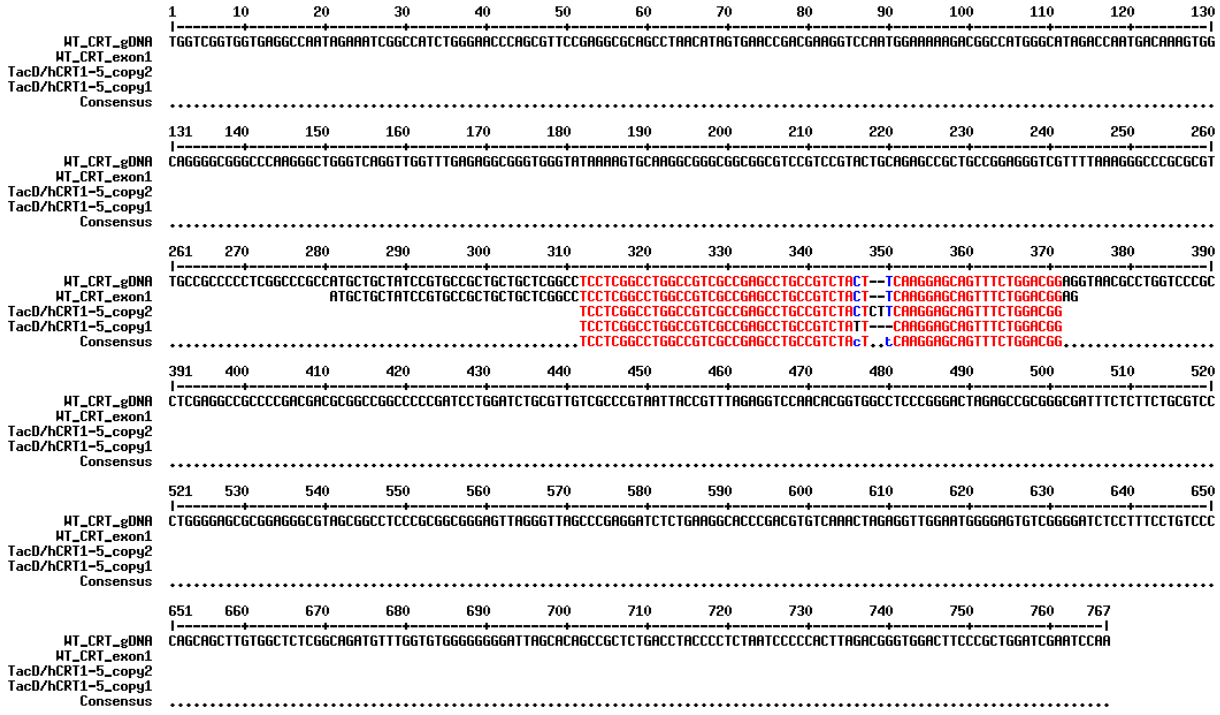

Figure A.5. CRISPR-Cas9 mediated mutation in JB4-Tacδ/hCRT1-5

Alignment analysis of JB4-Tacδ/hCRT1-5 *CALR* genomic loci sequencing result shows heterozygous mutations. *Copy 1:* Single nucleotide deletion occurs at 67 bp from the start codon and -4 bp from the PAM recognition motif. The frame shift mutated variant encodes for a predicted 96 amino acid protein product due to a premature termination codon. *Copy 2:* double nucleotide insertion occurs at 66 bp from the start codon and -5 bp from the PAM recognition motif. The frame shift mutated variant encodes for a predicted 97 amino acid protein product due to a premature termination codon.

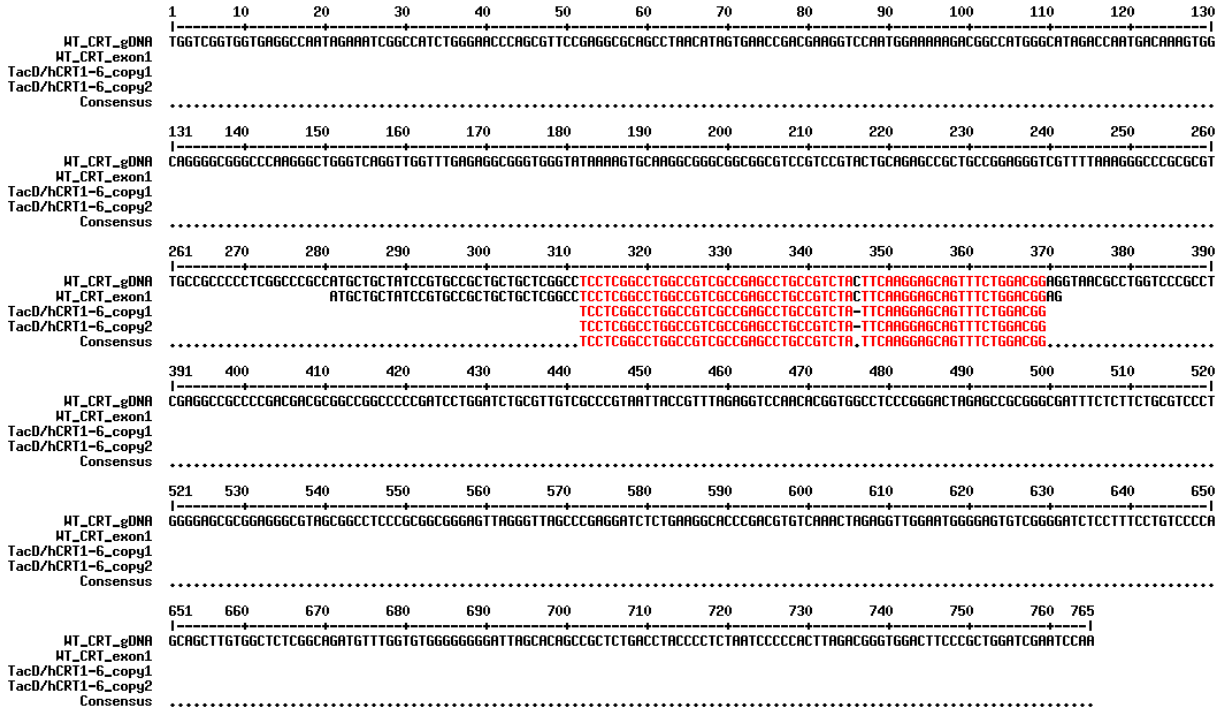

Figure A.6. CRISPR-Cas9 mediated mutation in JB4-Tacδ/hCRT1-6

Alignment analysis of JB4-Tacδ/hCRT1-6 *CALR* genomic loci sequencing result shows homozygous mutations. *Copy 1 and Copy 2:* Single nucleotide deletion occurs at 67 bp from the start codon and -4 bp from the PAM recognition motif. The frame shift mutated variant encodes for a predicted 96 amino acid protein product due to a premature termination codon. JB4-Tacδ/hCRT1-6 is referred to as Tacδ/CRT$^{-/-}$ in the thesis.

Appendix B Detection of ATP Secretion

Hallmarks of ICD include CRT cell surface presentation, ATP secretion, and HMGB1 release into the extracellular environment (Garg et al., 2010; Kroemer et al., 2013; Krysko, 2013; Krysko et al., 2012). Both ATP secretion and HMGB1 release are late apoptotic events while CRT cell surface presentation is an early apoptotic event. To determine if the time point chosen to detect CRT cell surface presentation (2 hr for oxaliplatin treatment and 4 hr for doxorubicin treatment) will also detect ATP secretion, I performed a luciferase-based ATP assay measuring the ATP released from cells treated with doxorubicin and oxaliplatin (

Table B.1). No ATP release was measurable under these conditions for WT or $CRT^{-/-}$ cells. As positive controls for ATP release, I treated the cells with lower dose ICD-inducer and for 24 hr. Both WT and $CRT^{-/-}$ cells released comparable amounts of ATP that were not significantly different from one another. Thus, the absence of CRT had no detrimental effects on ATP release due to ICD-inducers.

Cells	**Treatment**	**Extracellular ATP (M, Mean ± S.D.)**
WT	None, 4 hr	$0.6 \times 10^{-14} \pm 0.3 \times 10^{-14}$
$CRT^{-/-}$	None, 4 hr	$1.3 \times 10^{-14} \pm 1.2 \times 10^{-14}$
WT	4μg/mL doxorubicin, 4hr	$0.7 \times 10^{-14} \pm 0.5 \times 10^{-14}$
$CRT^{-/-}$	4μg/mL doxorubicin, 4hr	$0.7 \times 10^{-14} \pm 0.4 \times 10^{-14}$
WT	300μM oxaliplatin, 2hr	$4.1 \times 10^{-14} \pm 4.0 \times 10^{-14}$
$CRT^{-/-}$	300μM oxaliplatin, 2hr	$1.5 \times 10^{-14} \pm 1.0 \times 10^{-14}$
WT	None, 24 hr	$2.2 \times 10^{-10} \pm 0.7 \times 10^{-10}$
$CRT^{-/-}$	None, 24 hr	$3.5 \times 10^{-10} \pm 1.5 \times 10^{-10}$
WT	0.2μg/mL doxorubicin, 24hr	$69.3 \times 10^{-10} \pm 22.5 \times 10^{-10}$
$CRT^{-/-}$	0.2μg/mL doxorubicin, 24hr	$67.2 \times 10^{-10} \pm 15.7 \times 10^{-10}$
WT	1.5μM oxaliplatin, 24hr	$41.7 \times 10^{-10} \pm 21.7 \times 10^{-10}$
$CRT^{-/-}$	1.5μM oxaliplatin, 24hr	$35.1 \times 10^{-10} \pm 14.7 \times 10^{-10}$

Table B.1. Extracellular ATP secretion
Extracellular ATP release mediated by doxorubicin treatment was measured for WT and $CRT^{-/-}$ cells according to manufacturer's instructions (Promega ELITEN). No significant ATP release was measured for cells treated with 4 μg/mL doxorubicin for 4hr, or 300μM oxaliplatin for 2hr. As positive controls for ATP release, cells were treated with 0.2μg/mL doxorubicin, or 1.5μM oxaliplatin for 24hr. Values are mean ± S.D.; n=3.

Appendix C Expression of MHC Class I Molecule

CRT is a pleiotropic protein involved in the protein loading complex of the Major histocompatibility complex class I (MHC class I) proteins exposed on the cell surface (Colangelo et al., 2016). As such, knocking out CRT in T-ALL cells may adversely affect the proper presentation of the antigens on the surface. To determine if CRT knockout affects the presentation of MHC Class I molecule, I measured the surface MHC Class I level of WT, $CRT^{-/-}$, ssGFP-CRT and GFP-CRT cells using antibody detection and flow cytometry analysis (Figure C.1). We found that surface expression levels of MHC class I, as detected by flow cytometry of live cells, were not different when comparing WT, $CRT^{-/-}$, or $CRT^{-/-}$ cells expressing ssGFP-CRT or GFP-CRT.

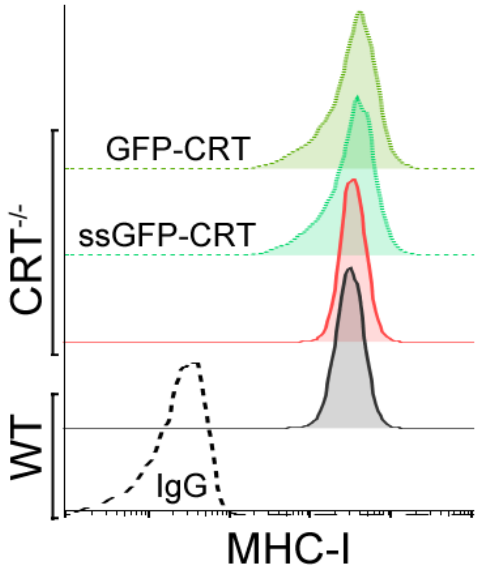

Figure C.1. CRT knockout does not affect surface expression of MHC Class I
The representative half-offset histogram overlay of MHC class I expression on live WT, $CRT^{-/-}$, and $CRT^{-/-}$ cells expressing ssGFP-CRT or GFP-CRT. Flow cytometry was used to measure surface MHC class I labeled with the α-MHC class I antibody. Plotted data is representative of 3 independently conducted replicates.

Appendix D Expression of ERp57

It has been reported that ERp57 interacts with CRT and co-translocates to the membrane in mouse cells (Obeid, 2008; Panaretakis et al., 2008). This co-translocation was found to be dependent on the expression of both ERp57 and CRT in mouse embryonic fibroblasts as the deletion of either one will result in failure of either protein to translocate to the cell surface (Obeid, 2008; Panaretakis et al., 2008). To determine if CRT knockout in human T-ALL affects the translocation of ERp57 to the cell surface, WT, $CRT^{-/-}$, ssGFP-CRT and GFP-CRT cells were treated with doxorubicin and cell surface ERp57 measured using antibody detection and flow cytometry analysis (Figure D.1). I showed robust increases in doxorubicin-treated surface ERp57 as detected by flow cytometry. I also found that ICD-induced surface ERp57 was just as robust in $CRT^{-/-}$ lymphoblasts. This result is different from what was demonstrated in murine models, where surface CRT and ERp57 exposure was found to be co-dependent on one another. Furthermore, expression of the cytosolic GFP-CRT, or the ER ssGFP-CRT, did not alter the surface exposure of ERp57, with or without ICD-inducers. Thus, our results indicate that ERp57 does not interact with the mutant CRT in a way that would affect its surface presentation in human T-lymphoblasts.

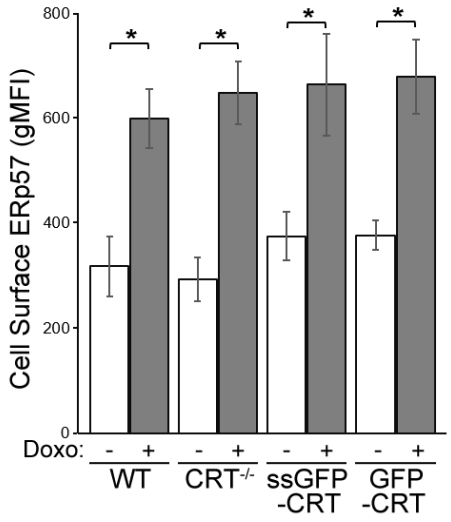

Figure D.1. CRT knockout does not affect surface translocation of ERp57 in T-ALL cells
WT, $CRT^{-/-}$, and $CRT^{-/-}$ cells expressing ssGFP-CRT or GFP-CRT were treated with or without 4 μg/mL of doxorubicin (Doxo) for 4 hours. Flow cytometry was used to measure the geometric mean fluorescence intensity (gMFI) of surface ERp57 labeled with the α-ERp57 antibody. As plotted is mean ± S.D.; n=3; *p<0.02.